Renewable Terpene-derived Polyacrylamides for Applications within the Speciality Chemistry Industry

Rhona Savin, MSci

Student Number: 4280331

Supervisors: Professor Robert Stockman, Professor Steve Howdle and Dr Jessica Gould

Thesis Submitted to the University of Nottingham for the degree of Doctor of Philosophy

Abstract

The synthesis of polymers from renewable materials is increasingly becoming of socio-economic importance; this consumer-led change has caused many industries to move away from fossil fuel based raw materials towards sustainable biobased materials. Croda Ltd is an international speciality chemicals company with a history of using sustainable biobased materials as the key raw ingredients in their products. The Stockman-Howdle collaboration has previously successfully synthesised a range of poly(acrylates) from terpenes, however to our knowledge the formation of renewable polyacrylamides from terpenes has yet to be explored. Polyacrylamides are used in a wide range of applications from drug delivery to contact lenses to wastewater treatment, and with a project market size of over 10 billion US dollars by 2024 renewable alternatives are urgently needed.

During this project, a library of renewable polyacrylamides have been synthesised in good to excellent yields on a multigram scale. The monomers have been synthesised from terpenes found in the oils of many coniferous trees, citrus peel, spearmint, caraway seeds and many other natural and waste sources. The Ritter reaction and the Overman reaction, two named reactions known for the introduction of nitrogen functionalities, were employed for the synthesis of novel the terpene-derived acrylamide monomers. These were then polymerised and copolymerised with high conversions using a variety of different free radical polymerisations to give the corresponding polyacrylamides. These polymers have then been tested for various applications in collaboration with Croda to characterise their individual properties. Hydrophilic, hydrophobic and amphiphilic polymers have been formed which have a wide range of viscosities and T_gs from 46 - 213 °C with potential applications including emulsifiers, protective hydrophobic coatings and non-ionic dispersants.

Acknowledgements

Abbreviations

AIBN – 2,2'-Azobisisobutyronitrile

AMBN - 2,2'-Azodi(2-methylbutyronitrile)

AMPS – 2-Acrylamido-2-methylpropane sulfonic acid

ATRP - Atom transfer radical polymerization

Bn – Benzyl

BMIMCl – 1-Butyl-3-methylimidazolium chloride

DBU – 1,8-Diazabicyclo(5.4.0)undec-7-ene

DCM – Dichloromethane

DDM - Dodecanethiol

DIEA – *N,N*-Diisopropylethylamine

DMA – Dynamic mechanical analysis

DMC – Dimethyl carbonate

DMDO – Dimethyl dioxirane

DMF – Dimethylformamide

DMSO – Dimethyl sulfoxide

Et - Ethyl

GC-FID - Gas chromatography flame ionization detection

GPC – Gel permeation chromatography

HATU - Hexafluorophosphate Azabenzotriazole Tetramethyl Uronium

IPA - Isopropanol

LSCT – Lower critical solution temperature

*m*CPBA – meta-Chloroperoxybenzoic acid

Me - Methyl

M_n – Number average molecular weight

M_w – Weight average molecular weight

nBuLi – n-Butyl lithium

PAM - Polyacrylamide

PET – Polyethylene terephthalate

PEG – Poly(ethylene glycol)

PLA – Poly(lactic acid)

PMMA – Poly(methyl methacrylate)

PNIPAM – Poly(N-isopropylacrylamide)

Pr – Propyl

PS - polystyrene

RAFT – Reversible addition-fragmentation chain transfer

TGA – Thermogravimetric analysis

T3P® – Propylphosphonic anhydride

TBHP – *t*-Butyl hydroperoxide

TBPB – *t*-Butyl peroxybenzoate

tBu – *t*-Butyl

T_g – Glass transition temperature

THF – Tetrahydrofuran

TLC – Thin layer chromatography

Table of Contents

10

11

1.0 Chapter 1: Introduction

1.1 Polymers

Polymers are ubiquitous to modern society as essential components of many everyday items including clothes, electrical goods and packaging.[1] However, the strain on existing resources is increasing exponentially, as the demand for polymers grows in conjunction with the increasing world population. Currently, over 99 % of commercially available monomers are derived unsustainably from hydrocarbons found in crude oil and natural gas.[2–5] The inevitable decline in fossil fuel derived monomers, as well as increasing social concerns over climate change and the increasing world population has created a strong driving force towards more environmentally friendly and sustainable monomers. Although societal concern has increased supportive policies and legislation, commercial application of novel bio derived polymers require favourable economics and material properties before industrial manufacture is economical practical.[6] This is mirrored within the policy and the literature where both the United Nations Sustainable Development Goals and the twelve principles of green chemistry and engineering, respectively, both recommend that a raw material or feedstock should be renewable rather than depleting whenever technically and economically practicable.[7–9] These social and economic pressures and the commercial interest in new monomer structures[10] have created an increased demand for cheap, novel, sustainable polymers from plant-derived feedstocks that can compete with current commercially available polymers long-term.[11–13]

Polymers are a class of materials where the unique properties of each polymer designate its application. These unique properties arise from the different monomers or co-monomers used in its synthesis. A polymer can either be a homopolymer formed of one repeating monomer unit, (Figure 1) or in the case of co-polymers at least two types of monomer units.

Figure 1: General Simplistic Scheme for the Formation of Homopolymers

There are different classifications of co-polymers depending on the monomer unit arrangement along the chain (Figure 2).[14] Random co-polymers are polymers with randomly or statistically alternating monomer units; for example ABAABABBBA, where the probability of finding a given type monomer residue at a particular point in the chain is equal to the mole fraction of that monomer residue in the chain. Block co-polymers compromise of two or more homopolymers linked by covalent bonds; for example $((AAA)_n)((BBB)_n)$. Finally, a graft macromolecule has one or more polymers/co-polymers branching off the main polymer chain as side chains.
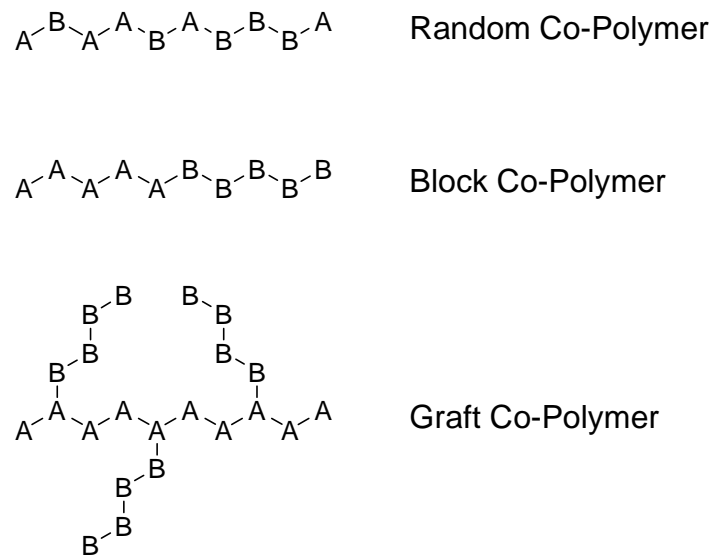
Figure 2: Examples of Varying Co-Polymer Structures

Crosslinkers connect growing polymer chains to create a 3D network with a finite and specific structure. This molecular architecture is one way of introducing properties or improving the performance of a polymer. Crosslinking can take place when a monomer has multiple reactive functional groups that can polymerise across chains or with the addition of a specific crosslinker with two or more functional groups that can link together various polymer chains.[14] (Figure 3)

14

Free Polymer Chains   Crosslinked Polymer Chains
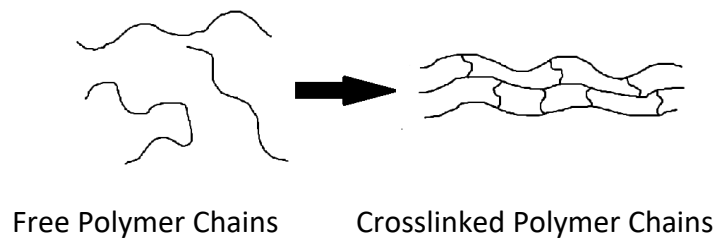
Figure 3: Structural Difference between Free and Crosslinked Polymer Chains

One of the key analytical characteristics for understanding polymer thermophysical properties is the glass transition temperature (T_g). Above the glass transition temperature, the polymer is flexible and rubbery whereas below the glass transition temperature the polymer is hard and brittle (Figure 4).[15] For example, poly(ethylene) with a low T_g of -125 °C has applications in plastic bags and bottles where flexibility is a key property. On the other hand, poly(vinyl chloride) with a higher T_g of 81 °C has applications in the building and construction industry where rigidity is often a key property.
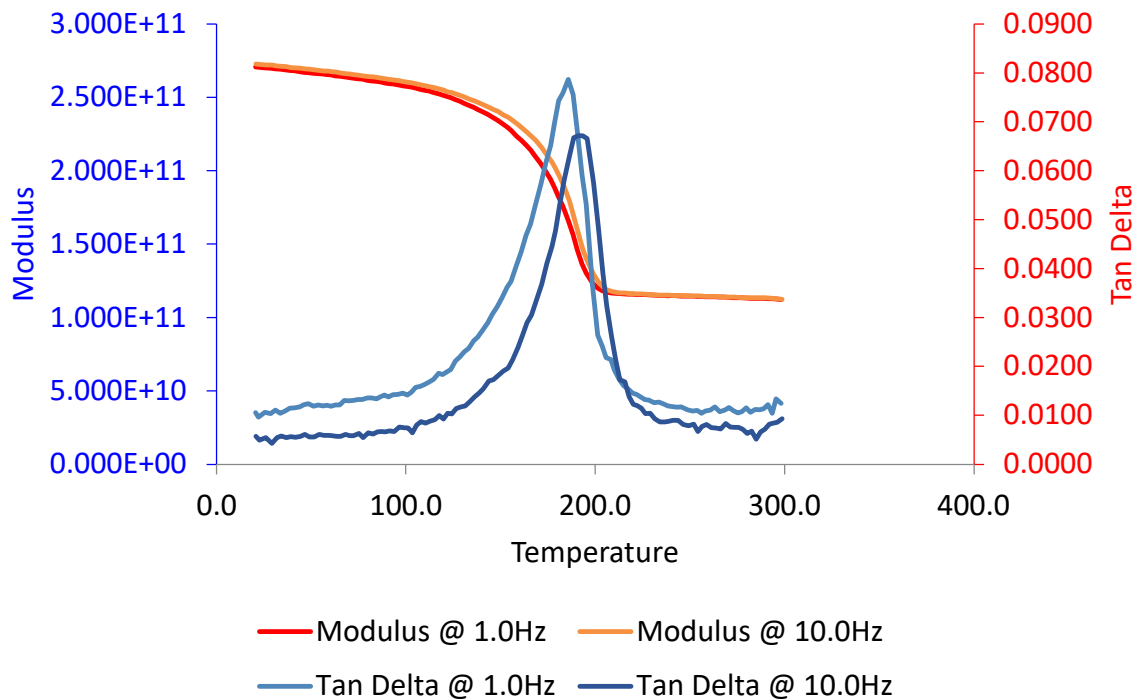
Figure 4: Dynamic Mechanical Analysis of an Amorphous Polymer

Different factors within the polymer structure, such as chain flexibility, steric bulk, symmetry, polarity and molecular weight, affect the T_g. Increasing the rigidity of the polymer, for example by adding cyclic functionalities or methyl groups to the backbone (polymethacrylates compared to polyacrylates), results in less opportunities for bond rotation which increases the T_g. Steric hindrance and the position of the substituents on the side chains along with the interactions of the substituents with the backbone all affect the rotation of the polymer backbone. The more flexible the backbone the lower the T_g. For example, if the side groups are rigid, such as *t*-butyl compared with *n*-butyl, the steric hindrance increases, which increases the T_g. Increasing the flexibility of the side groups gives a more flexible polymer, lowering the T_g (Figure 5).
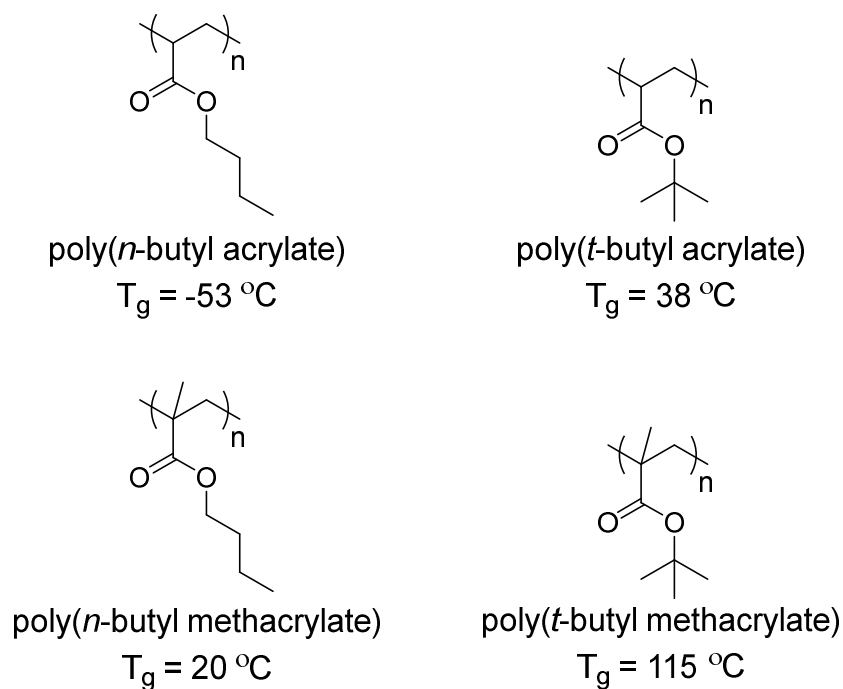
Figure 5: Changes in Glass Transition Temperature due to Polymer Backbone and Side Group Flexibility

Increased symmetry increases T_g as chains can pack closer and more thermal energy is required for chain rotation, as demonstrated by the increase in T_g due to the addition of a methyl group on the polymer backbone of poly(lactic acid) compared to polyglycolide. An increase in polarity increases T_g, as an increase in polar bonds gives stronger intermolecular interactions which restrict rotation around the backbone. The amide functionality in polycaprolactam can form hydrogen bonds between the chains, unlike the ester functionality in polycaprolactone, which restricts movement along the polymer chains and results in a higher T_g of 51 °C compared to -66 °C (Figure 6).

polyglycolide
$T_g = 39\ °C$

poly(lactic acid)
$T_g = 59\ °C$

polycaprolactone
$T_g = -66\ °C$

polycaprolactam
$T_g = 51\ °C$
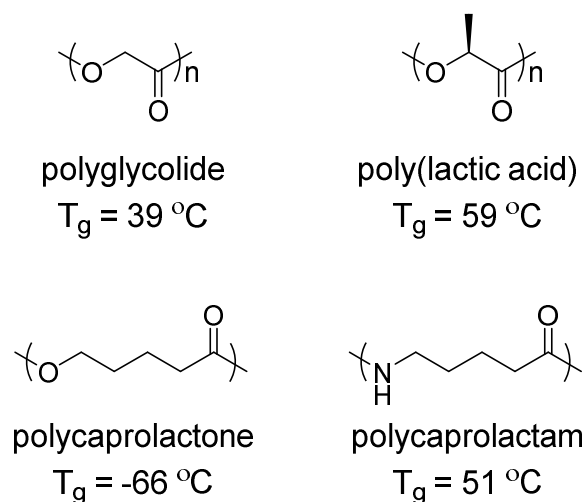
Figure 6: Changes in Glass Transition Temperature due to Polymer Symmetry and Polarity

The Flory-Fox equation (Equation 1) shows the glass transition temperature is dependent on the free movement of the polymer chains within the sample; this itself is dependent on the average molecular weight of the sample. If the sample has a low molecular weight then the samples are able to move much more freely, resulting in a lower glass transition state.

$$T_g = T_{g,\infty} - \frac{K}{M_n}$$

Equation 1: The Flory-Fox Equation[16]

1.2 Polymer Synthesis

Polymers can be synthesised through one of two methods; step-growth or chain polymerisations.[17,18] Step growth polymerisations take place during stepwise reactions between monomers, oligomers and polymers to form increasingly longer chains. Polymers such as polyesters, polyamides and polyurethanes are formed using this method. Chain growth polymerisations take place *via* of rapid repeated reactions of a free monomer continuously adding to a propagating chain to form polymers such as polyacrylates,

polyacrylamides and vinyl polymers. This method is more commonly associated with free radical polymerisations although also includes ionic polymerisations and ring-opening polymerisations. The different methods of formation give different reaction kinetics (Figure 7). In step growth polymerisations, the average molecular weight grows slowly even though the reactions between monomers proceed rapidly at the beginning. The polymers grow exponentially, with high molecular weights only attained once a high conversion is reached. On the other hand, high molecular weights are seen almost immediately in chain polymerisations and the rate of reaction depends on the solvent, the amount of initiator, and the concentration or active weight of the polymerisation.
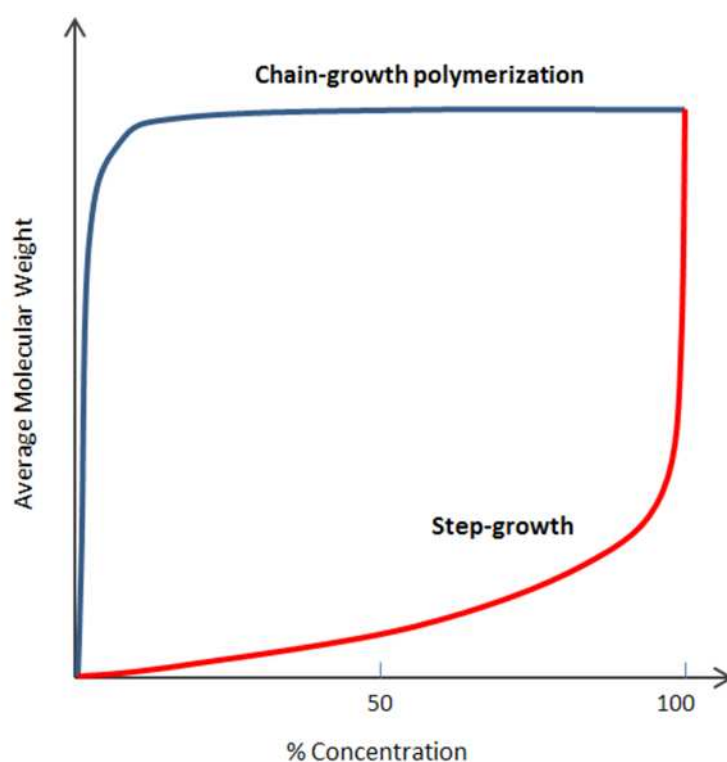
Figure 7: Step Growth Versus Chain Growth Polymerisation[17]

1.3 Free Radical Polymerisation

Free radical polymerisation is the most widely used type of chain polymerisation within the polymer industry and is suitable for solution, bulk, suspension and emulsion techniques.[19] In this thesis, solution and emulsion polymerisations will be discussed. Solution

polymerisations are the most common in industry. In solution polymerisations, the monomer, initiator and resulting polymer are all soluble in the solvent or solvent blend. In the case of free radical polymerisation, the rate of the reaction is directly proportional to the monomer concentration.[20]

The most common type of emulsion polymerisation is an oil-in-water emulsion, in which droplets of monomer (the oil) are emulsified (with surfactants) in a continuous phase of water.[21] Initially, the monomer phase consists of a dynamic equilibrium of dispersed surfactant micelles and emulsified monomer droplets within an aqueous solution. Nucleation stops when the surface area becomes large enough to absorb all the surfactant molecules. Initiator radicals formed through thermal decomposition or redox reactions, react with the in the water dissolved monomers and form soap-type free radicals then either associate with dissolved surfactant molecules or migrate into existing micelle droplets.
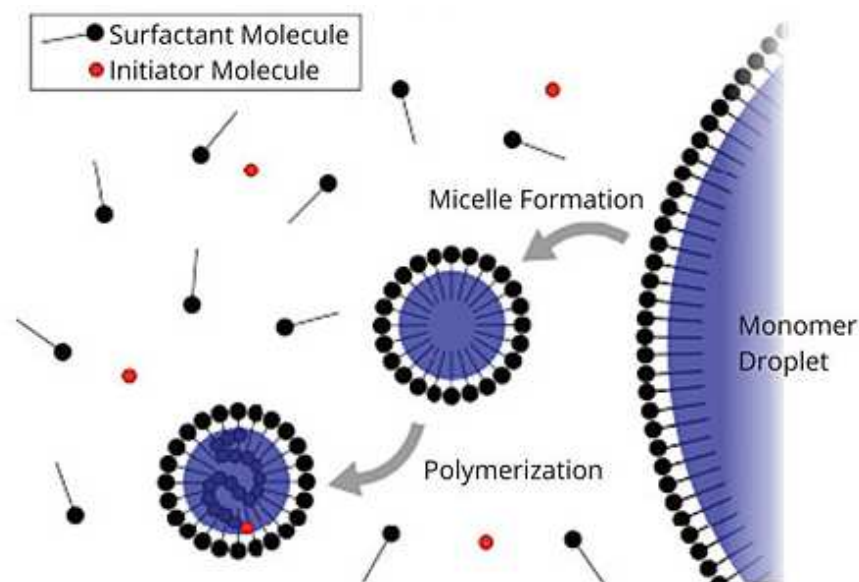
Figure 8: Emulsion Polymerisation Physical Mechanism[22]

During the next stage of emulsion polymerisation, monomers continuously migrate from the larger monomer droplets through the water phase into the surfactant micelles where they are added to the growing polymer chains. Sometimes polymerisation can also take place in the water phase depending on the solubility of the monomers and initiators. As these free polymer chains grow, they become increasingly hydrophobic and are stabilised with free surfactant molecules. The number of polymer particles and the rate of polymerization increase as long as new radicals and polymer micelles are formed. Eventually, all the surfactant in the system will have been absorbed and all the initiator molecules reacted. At this point in time, the rate of polymerization remains more or less constant. Finally, in the last stage, as the size of the monomer droplets decrease and eventually disappear, the rate of polymerisation decreases until all the monomers have reacted and termination occurs.[21]

The monomers used in free radical polymerisations ubiquitously contain alkene or alkyne bonds that can break and covalently bond with other monomers to form homopolymers or copolymers. Although a reliable technique, the standard reaction is an uncontrolled solution polymerisation and gives amorphous polymers with broad polydispersities, typically >1.3 Đ. Some progress has been made into controlled free radical polymerisation such as ATRP (atom transfer radical polymerisation) and RAFT (reversible-addition fragmentation chain transfer) polymerisation. However, uptake of these processes by industry has been slow due to the cost versus benefit trade off. ATRP involves the chain initiation of free radical polymerization by a halogenated organic species in the presence of a metal halide and RAFT involves the addition of a chain transfer agent, generally a di- or trithiocarbonylthio compound which produces the dormant form of the radical chains. One example of an industrially produced polymer using standard free radical polymerisation is poly(methyl methacrylate) (PMMA) synthesised from methyl methacrylate (Scheme 1).
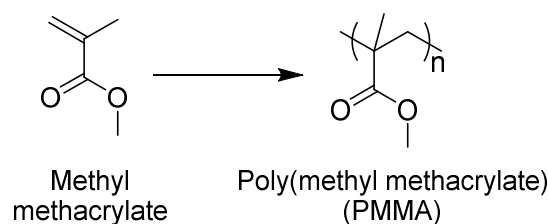
Scheme 1: Synthesis of PMMA

Free radical polymerisation takes part in four steps; radical initiation, monomer initiation, propagation and termination.[18] Radical initiations can be divided into two general categories according to the manner in which the first radical species is formed; homolytic decomposition of covalent bonds by energy absorption or electron transfer from ions or atoms containing unpaired electrons followed by bond dissociation in the acceptor molecule. During the homolytic cleavage, an initiator (e.g. azobisisobutyronitrile or AIBN) undergoes thermal decomposition to form two radicals. Redox initiation on the other hand occurs when a reducing agent and an oxidising agent produce a reactive species which decomposes to form a free radical which initiates the polymerisation. Redox initiators are useful in initiation of low temperature polymerization and emulsion polymerization, whereas thermal initiators are dependent on, generally higher, temperatures to determine their decomposition half-lives. In the initiation step, the initiator radical (I˙) will attack the carbon-carbon double bond on the monomer to form a new radical on the monomer (M˙). This monomer radical attacks the double bond on another monomer and the chain propagation continues. Termination can occur either when two radical polymer chains (P_n˙) meet (combination) or *via* hydrogen abstraction (disproportionation) resulting in dead polymer chains (Figure 9).

$$\text{Initiation} \quad \text{I}^{\bullet} + \text{M=CH}_2 \longrightarrow \text{I-CH}_2\text{-M}^{\bullet}$$

$$\text{Propagation} \quad \text{I-CH}_2\text{-M}^{\bullet} + \text{M=CH}_2 \longrightarrow \text{P}_n^{\bullet}$$

$$\text{Termination} \quad \text{P}_n^{\bullet} + \text{P}_n^{\bullet} \longrightarrow \text{P}_n$$
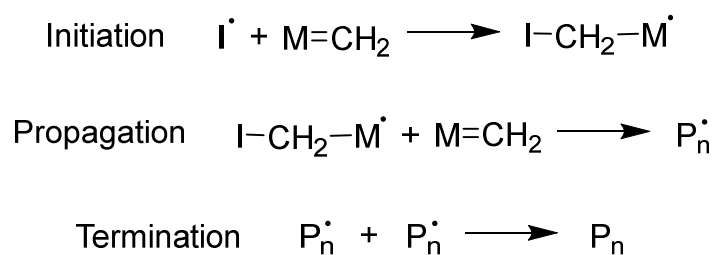
Figure 9: The Three Steps in Free Radical Polymerisation

1.4 Polymers from Renewable Sources

Biobased polymers are composed or derived in whole or in part of biological products issued from the biomass, such as poly(lactic acid) (PLA) derived from corn. A bioplastic is a biobased polymer derived from the biomass or issued from monomers derived from the biomass and which, at some stage in its processing into finished products, can be shaped by extrusion. Polymers produced from biomass are also sometimes called 'renewable polymers'. To be truly sustainable; biobased polymers also need to be environmentally friendly and green where their properties are environmentally friendly and recyclable so they adhere to the United Nations sustainable development goals and concepts of green chemistry.[9,23,24]

There is a significant economic advantage to further research in biobased polymers as the global renewable chemicals market is estimated to be £38 billion in 2015 and is projected to significantly grow to reach £65 billion by 2020 with a compound annual growth rate (CAGR) of 11 %.[25] Biobased polymers constitutes the second major segment of this market with a share of over 5 % and is projected to have a CAGR (compound annual growth rate) of 13 % during the forecasted period due to the increase in demand for eco-friendly products, changing political conditions and environmental regulations on carbon emissions as well as the fluctuating crude oil prices.[26,27]

Two examples of biobased polymers already widely used in industry are poly(lactic acid) and polyhydroxyalkanoates.[27,28] Poly(lactic acid) has been used in medical implants and

biodegradable packaging materials.[29–31] Polyhydroxyalkanoates can be used in applications such as tougher packaging material and medical equipment (Figure 10).[28,32]

Poly(lactic acid)   Poly((R)-hydroxybutyrate)
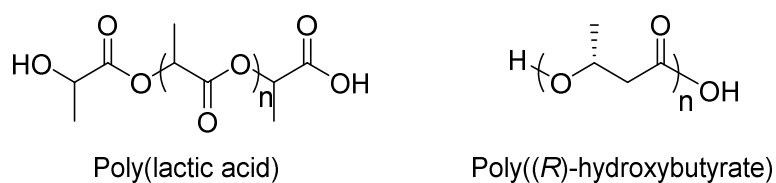
Figure 10: Examples of Commercially Produced Biobased Polymers

As well as biobased lactic acid and hydroalkanoates, other natural resources such as vegetable oils, fatty acids and terpenes have been used within the literature as naturally sourced building blocks with a wide structural range for the synthesis of renewable biobased polymers.[11,12,33]

1.5 Terpenes

A hydrocarbon rich class of compounds, terpenes are derived from isoprene units and usually contain one or more alkene bonds. They are structurally diverse with more than 30,000 naturally occurring terpenes currently known[34] which are often found in waste products in industries such as the paper making industry and the fruit juice industry.[2,10,33,35,36] They have already been used for decades in many academic research projects as a cheap method of easily accessing the chiral pool due to the numerous stereogenic centres (e.g. (+)-α-pinene and (-)-α-pinene) (Figure 11).

24

(+)-α-Pinene) (-)-α-Pinene (-)-β-Pinene

(R)-(+)-Limonene (R)-(-)-Carvone (R)-(-)-Myrtenol
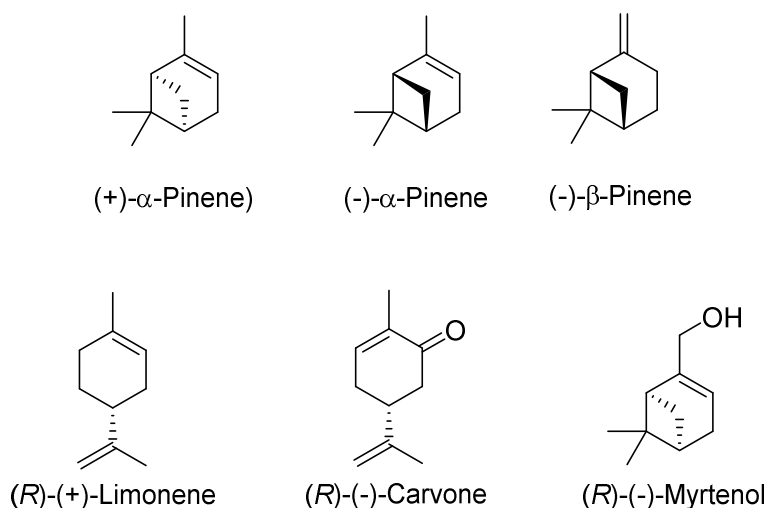
Figure 11: Examples of Common Terpenes

It has been reported that the global industry recovers 3 million tonnes of these biobased hydrocarbons per year.[37] Annual production volumes for turpentine (natural source of pinene) from pulp-industry derived pine resin stabilised in the 1980s at 330,000 tonnes per annum. Approximately 30 % of turpentine is sourced from gum rosin collected from living trees and the rest is mostly from tall oil resin, a by-product of the Kraft pulping process in the paper making industry. Limonene is also a by-product of the citrus industry, with a yearly production of 70,000 tonnes per annum.[38] As well as biobased building blocks for renewable materials, plant-derived terpenes have been considered for use in biofuels as they meet the current commercial and industrial requirements to be used directly or blended with existing fuel components for a variety of applications including jet fuel.[37] As such research is ongoing into ways to increase global terpene production via metabolic engineering of algae or genetic modification of plants.[39]

1.6 Polyterpenes

The interest in using terpenes for biobased polymers comes from their chirality and the alkene functionalities which offer the opportunity for free radical polymerisations. Robert and Day reported the first terpene based polymer, poly(β-pinene), in the 1950s which was synthesised *via* a cationic homopolymerisation of β-pinene using lewis acids (LA) (**7**) (Scheme 2).[40] However low molecular weights were reported even in the presence of a co-

25

monomer or when very low temperatures (-40 °C) were used which were not feasible on an industrial scale.[36]
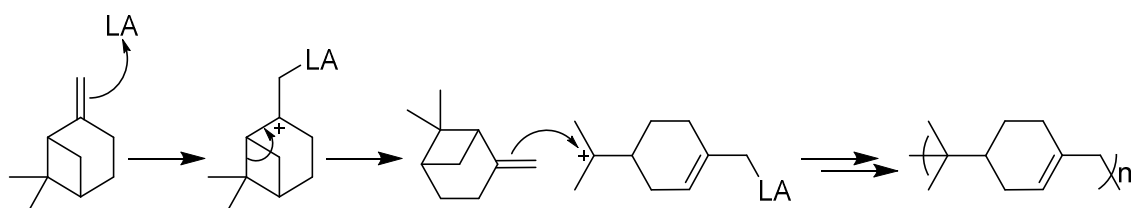
Scheme 2: Cationic Polymerisation of β-Pinene

In 1992, Keszler and Kennedy[41] successfully increased the molecular weight up to 40 kDa of the poly(β-pinene) using a conventional Lewis acid catalyst EtAlCl$_2$ and 2,6-di-*tert*-butylpyridine as the base. However, although the reaction proceeded within 6 minutes the synthesis was conducted at -80 °C, completely unfeasible on industrial scale. Analysis gave the first reported T_g of poly(β-pinene) at 65 °C and demonstrated that high molecular weight poly(β-pinene) readily yielded fibres by manual drawing from the melt.

These results were followed up almost 15 years later by Satoh *et al*. in 2006[42] who repeated the conditions reported by Keszler and Kenedy without 2,6-di-*tert*-butylpyridine and still managed to achieve molecular weights up to 25 kDa although this gave a higher T_g of 90 °C than previously reported. Investigations into alternative Lewis acid catalysts and solvents confirmed EtAlCl$_2$ to be the optimum catalyst and CH$_2$Cl$_2$-methylcyclohexane in a 1:1 ratio to be the optimum solvent system. Hydrogenation of poly(β-pinene) gave a new saturated polymer with a higher T_g of 130 °C. Hydrogenation also increased the thermal decomposition temperature from just above 300 °C for the unsaturated polymer to around 440 °C for the saturated version. These values are comparable to crude oil derived polystyrene.[42]

In 2011, Kukhta *et al*.[43] reported the synthesis of poly(β-pinene) at 20 °C with molecular weights up to 14 kDa within 0.5 minutes (Scheme 3). This was achieved by the introduction of a new co-initiator complex, described as AlCl$_3$(0.8EtOAc), with water acting as an initiator was to achieve the highest molecular weights. The ethyl acetate within the metal complex

was directly responsible for the higher molecular weights due to the inertness of ethyl acetate as a weak base toward β-H abstraction promoting chain propagation. The *in-situ* generation of a weakly nucleophilic counter anion through the interaction of [AlCl$_3$OH]$^-$ with ethyl acetate leads to the suppression of chain transfer reactions.
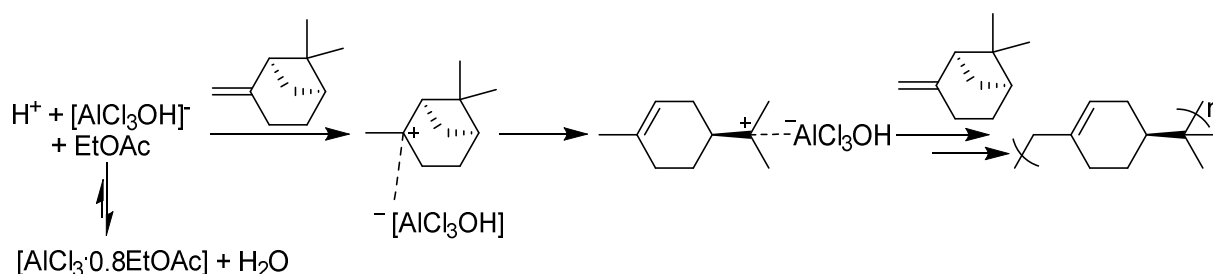
Scheme 3: Synthesis of Poly(β-pinene) using AlCl$_3$0.8EtOAc

The T_gs were comparable at around 87 °C to the previous literature value. Investigations into the solvent system revealed CH$_2$Cl$_2$/*n*-hexane (60:40) to be the best solvent system although 9 kDa was achieved in 0.5 minutes using a non-chlorinated alternative toluene. These optimised conditions using non-chlorinated solvents at room temperature are the most industrially attractive conditions to date although no further optimisation, scale up or mechanical testing has been reported.

Although other the cationic polymerisation of other terpenes has been attempted with limited success,[36] the recent literature by Sarkar and co-workers in 2014[44] reported the successful synthesis of poly(myrcene) *via* emulsion polymerisation as a potential alternative for the synthesis of some polyterpenes. Temperature, reaction time and initiator investigations gave the optimum conditions of the emulsion polymerisation at 70 °C for 20 hours using ammonium persulfate as the initiator. These optimum conditions gave a homopolymer at 93 kDa with a T_g of -73 °C and a thermal decomposition temperature of 425 °C. The reported mechanical properties of poly(myrcene) suggested potential applications as a single rubber in polymer composites, blends or adhesives however as a homopolymer it has a few draw backs such as its nonpolar nature and poor tensile strength that could inhibit industrial implementation.

1.7 Copoly(terpenes)

Uniting characteristics of two or more chemically distinct homopolymers into one renewable copolymer *via* covalent bonds allows for the combination of multiple desirable characteristics for designer applications and are ideal targets for innovation.[45] A few examples of copolymerisation of β-pinene and myrcene with other commercially available monomers have been reported.[44,46–49]

Lu and co-workers reported one of the first successful copolymers that incorporated β-pinene with styrene in 1999 (Scheme 4).[47] Poly(β-pinene) was brominated using NBS to initiate a second cationic polymerisation where styrene was grafted onto the poly(β-pinene) backbone. In a 1:1 mixture of monomers, a low molecular weight of 5300 Da was achieved with a high polydispersity for poly(β-pinene-*g*-styrene), giving a low molecular weight compared to the homopolymers.
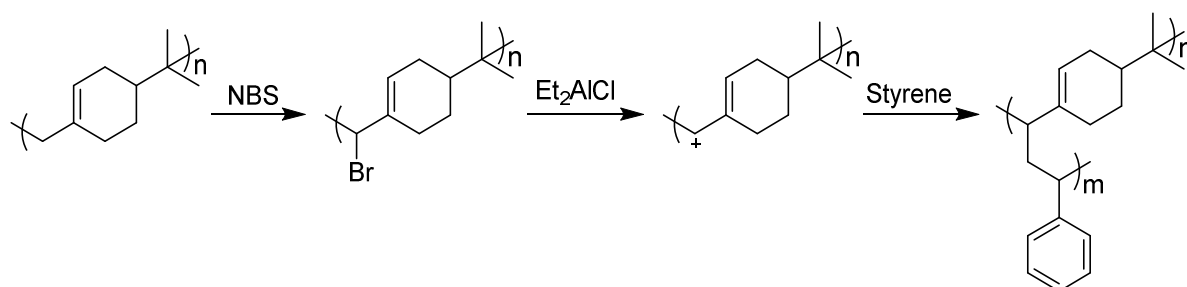
Scheme 4 : Synthesis of Poly(β-pinene-g-stryene)

Later, in 2006, Lu and co-workers attempted the radical copolymerisation of β-pinene with methyl acrylate (Figure 12).[49] However, due to the poor reactivity of β-pinene within radical polymerisations, a very low conversion, 10 %, was achieved, for polymers that were rich in methyl acrylate units and randomly alternating single β-pinene units.
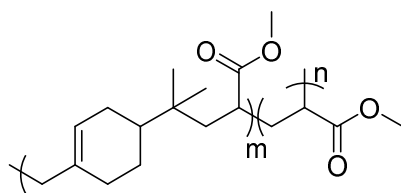
Figure 12 : Poly(β-pinene-co-methyl acrylate)

The addition of stoichiometric Et$_2$AlCl slightly increased the conversion to 35 % and the monomer fraction of β-pinene to 45 % giving a good molecular weight of 15 kDa. However, although the poor uptake of β-pinene was successfully solved with the addition of Et$_2$AlCl as a co-initiator, the poor conversion rate inhibits any industrial interest.

Despite the unpromising first results, Lu and co-workers reported a second radically initiated β-pinene copolymer using *n*-butyl acrylate in 2007 (Figure 13).[48] A moderate yield of 42 % was reported using the same Et$_2$AlCl/AIBN co-initiator method giving a remarkably high molecular weight of 50 kDa and a T_g ~ 20 °C.
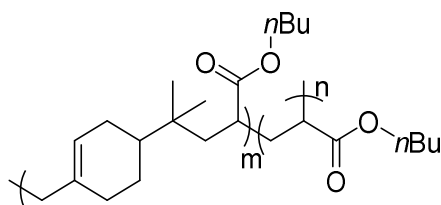
Figure 13 : Poly(β-pinene-co-butyl acrylate)

Sarkar and co-workers have reported the emulsion copolymerisation of myrcene with dibutyl itaconate and alkyl acrylates to great success (Figure 14). In 2016, Sarkar and Bhowmick[50] reported the synthesis of low T_g copolymers of myrcene and dibutyl itaconate through a persulfate-initiated emulsion polymerisation as 70 °C for 20 hours.
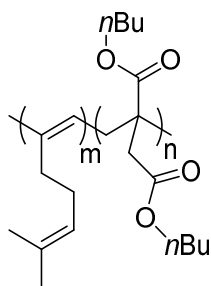
*Figure 14 : Poly(myrcene-*co-*dibutyl itaconate)*

A range of different ratios of co-monomers were investigation and resulted in high molecular weights up to 65 kDa, the best resulted from a 1:1 ratio of monomers and gave a T_g of -42 °C. Physical testing revealed elastomer like behaviours although with moderate load bearing capacities. These conditions were successfully repeated in 2017 for the emulsion polymerisations of myrcene with butyl/lauryl/stearyl acrylate (Figure 15).[51] Butyl acrylate, as the shortest carbon chain and therefore the most hydrophilic, was the most successful comonomer giving a molecular weight of 62 kDa when synthesised in a 1:1 ratio with a T_g of -30 °C. On the other hand, stearyl acrylate in a 1:1 ratio gave slightly lower molecular weights of 23 kDa giving a T_g of -59 °C. Also, unlike the high yielding polymerisation with dibutyl itaconate, co-polymerisations with alkyl acrylate only gave moderate to good yields of 50-72 %.

X = 3, 11 or 17
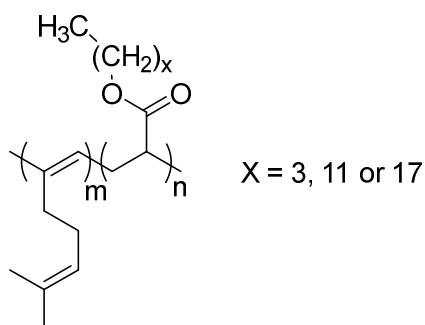
*Figure 15 : Poly(myrcene-*co-*alkyl acrylate)*

Due to the increasing demand for sustainable monomers, there has been increasing interest in terpenes as a sustainable source of monomers. However, although both homo- and co-polymerisations of β-pinene and myrcene are now theoretically industrially feasible,[43,44] the homopolymerisation of other terpenes are not, severely limiting the potential applications of this natural resource. Direct competition against fossil fuel derived poly(hydrocarbons) won't be feasible until the price of crude oil has risen exponentially therefore adding value by synthetically modifying these biobased hydrocarbons allows for applications with high-value markets to be targeted.

1.8 Derivation of Terpenes

The synthetic modification of terpenes by adding various functionalities to create novel renewable monomers not only greatly alters the properties of any resulting polymers but adds commercial value to the final product. As well as adding value to this natural resource, the influx of new monomers into the commercial polymer market has been dwindling as crude oil monomer research has been exhausted. Considering the historical issues of both cationic and radical polymerisations of unmodified terpenes, derivatisation of terpenes can result in easier polymerisations and a wider variety of more economically viable renewable polymers with different properties including renewable polyesters, polyamides and polyurethanes.[10,36,52–54]

1.8.1 Terpene-derived Polyesters

Copolymers of epoxide monomers have many uses from cosmetics to lubricants to engineering plastics. The first terpene-derived epoxide monomer (**1**) was reported in 2004 by Byrne *et al* (Scheme 5).[55] Limonene epoxide (**1**) was successfully copolymerised with carbon dioxide using a catalytic zinc complex to give a novel regioregular polycarbonate (**2**) with molecular weights of up to 25 kDa with a T_g of 110 °C. However, as the commercially available limonene oxide consists of 45 % of the *cis* isomer, selectively polymerising only the *trans* isomer is uneconomical and wasteful.
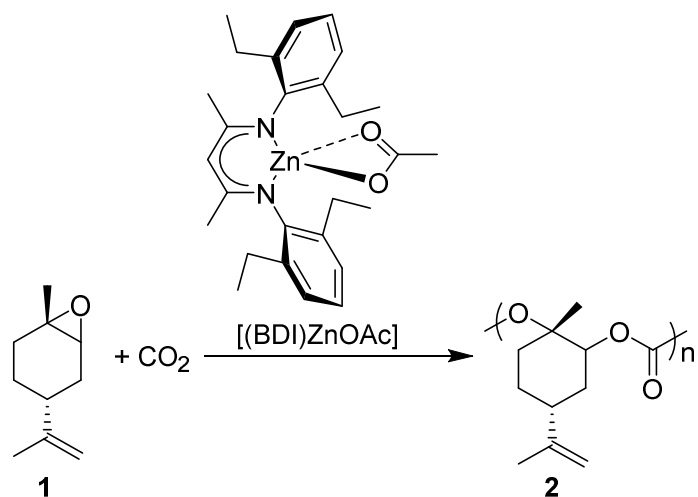
Scheme 5: Synthesis of Renewable Regioregular Polycarbonate

Further optimisation, scale up and properties testing of poly(limonene carbonate) was conducted by Hauenstein *et al*. in 2016.[56] The reported properties of this potentially biodegradable polymer were very promising, a high T_g of 130 °C and a thermal decomposition temperature of 265 °C are comparable to the fossil fuel derived bisphenol A polycarbonate. The polymer also exhibited good aesthetic properties with high transmission and high clarity suggesting potential applications in protective coatings.

In 2010, Lowe *et al*. used modified carvone to produce novel polyesters *via* a ring-opening polymerisation similar to commercially available polycaprolactone.[57] (Scheme 6) Carvone is a naturally occurring terpene found in spearmint and caraway oils, 10,000 tonnes of which are commercially produced annually.[58]

Hydrogenation of carvone (**3**) produced dihydrocarvone (**4**) and further hydrogenation produced carvomethone (**5**). Both of these products were subjected to a Baeyer-Villiger oxidation resulting in a ring expansion to lactones (**6** and **7**). Ring opening polymerisations catalysed by ZnEt₂ formed polyesters; polydihydrocarvide (**8**) and polycarvomethide (**9**) respectively (Scheme 6). The alkene moiety on polydihydrocarvide can be modified post-polymerisation to expand the range of potential polymers, as by the Hillmyer group in 2013.[59]
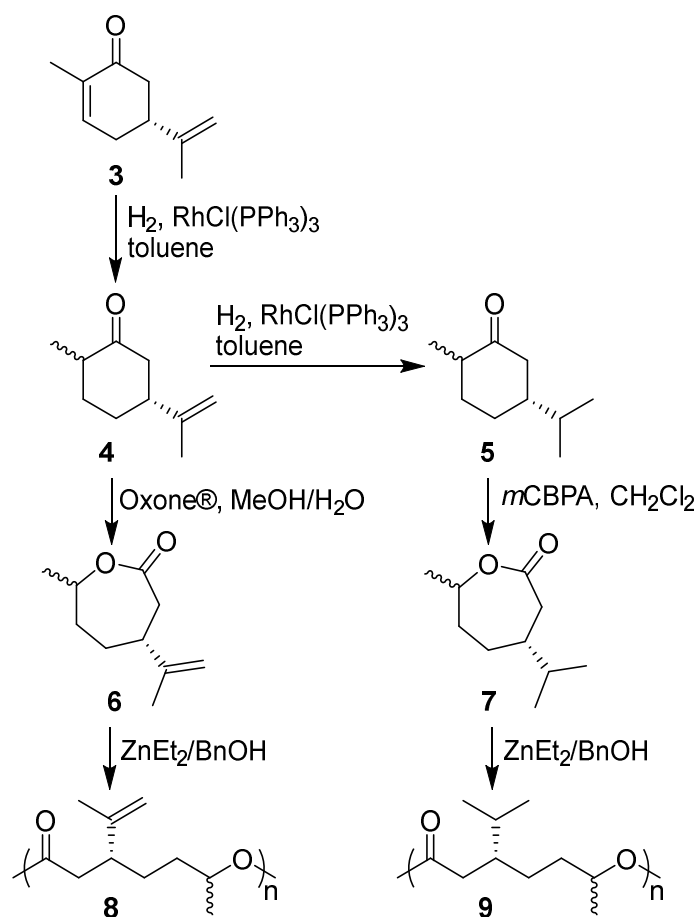
Scheme 6: Synthesis of Polyhydrocarvide and Polycarvomethide by Lowe et al.[57]

In 2017, Quilter *et al.* reported the synthesis of a β-pinene derived lactone (**14**) as another bio-based alternative to polycaprolactone (Scheme 7).[60] β-Pinene (**10**) has a higher annual production than carvone at around 120,000 tonnes per annum. However, the synthesis of the lactone monomer (**14**) required four steps compared to the two reported by Lowe *et al.* Investigations into initiator, time and temperature of the reaction gave good molecular weights up to 32 kDa and conversions between 14 – 99 %. The polymers had low glass transition temperatures around -50 °C. Co-polymerisations were then attempted between the lactone and lactide. Optimisations of the initiator, monomer ratio and temperature gave moderate molecular weights up to 9 kDa and conversions between 31 – 91 %. Despite initial comparison to polycaprolactone, no analytical comparisons between the monomers or the

corresponding polymers were made. Also, the complex monomer synthesis is currently not economically viable for industry with no obvious application.
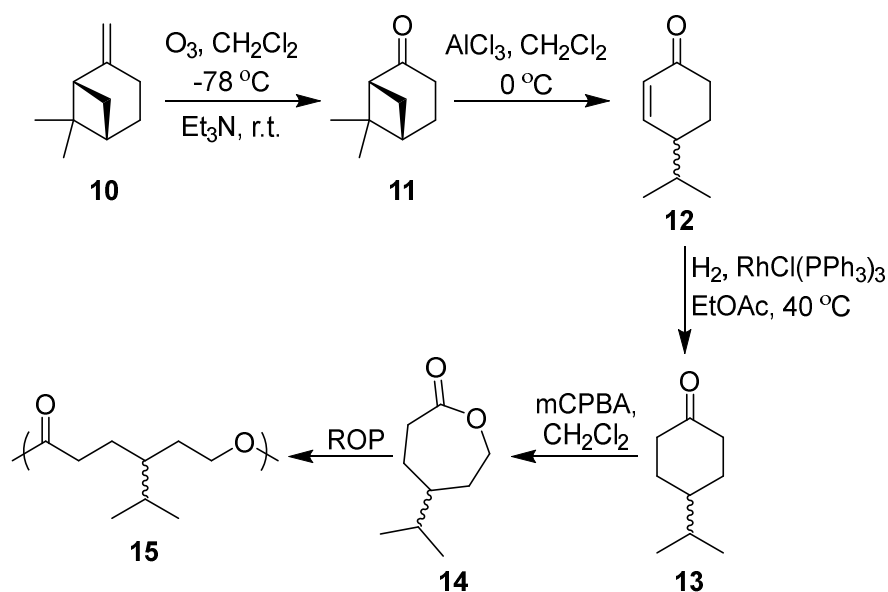
Scheme 7: Synthesis of Biobased Poly(4-isopropylcaprolactone)

In 2019, Thomsett *et al.* reported the synthesis of limonene derived polyesters using condensation polymerisations (Scheme 8).[52] Double hydroboration oxidation of limonene (**16**) resulted in the corresponding diol (**17**) in an excellent 97 % yield. This diol (**17**) was then copolymerised with renewable succinic acid (**18**) to give a renewable polyester (**19**) with molecular weights up to 30 kDa. A catalyst screen found Ti(OBu)$_4$ at 230 °C for 3 hours to give the highest molecular weight of 30 kDa, with a corresponding T_g of 16 °C. This polymer (**11**) was subjected to a mixture of THF and NaOH (3M) at 95 °C for 10 days. This resulted in the complete degradation of the novel polymer (**19**) and full recovery of the starting monomer (**16**). In an attempt to make a homopolyester completely from a limonene derived monomer, the tertiary alcohol on the diol (**9**) was selectively oxidised to form the respective hydroxy acid (**20**). However, due to a competing intramolecular ring closing reaction to form an 8-membered lactam, low molecular weights up to 3 kDa were achieved. The successful formation of a completely recyclable renewable polyester with good molecular weight is an excellent start towards a sustainable circular economy, however oxidation *via*

hydroboration oxidation using borane is too hazardous for use on an industrial scale and alternative routes would have to be investigated along with further mechanical testing to determine a suitable application.
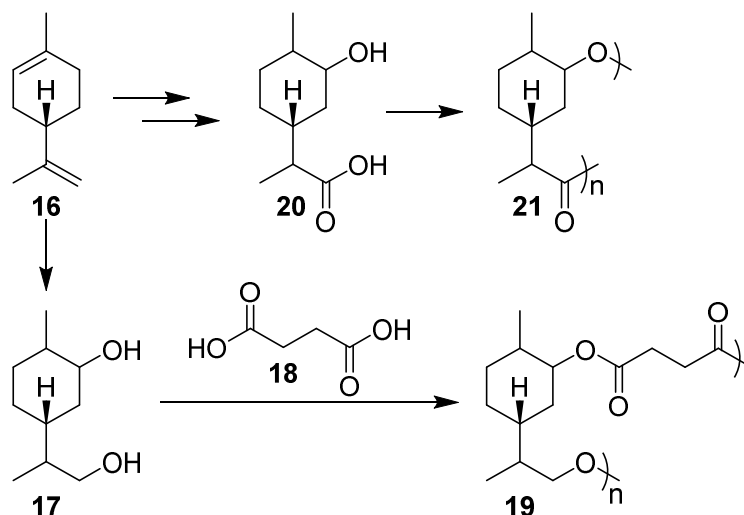
Scheme 8: Synthesis of Limonene-derived Polyesters via Oxidation Chemistry

1.8.2 Terpene-derived Polyamides

In 2014, Winnacker and co-workers used menthone (**22**), a naturally occurring terpene found in peppermint and geranium oil, to form novel polyamides (Scheme 9).[61] Menthone (**22**) was reacted with hydroxylamine to give a mixture of both oximes **23** and **24**. These were separated and transformed *via* the Beckmann rearrangement using poly(phosphoric acid) to the corresponding lactams **25** and **26** respectively. However, mixtures of the two lactams were obtained even when a single oxime isomer was charged. In 2015, Winnacker and co-workers successfully synthesised lactam **26** directly and regioselectively from carvone using hydroxyl-*O*-sulfonic acid.[53] Anionic ring opening polymerisation using potassium as the initiator and benzoyl chloride as the co-initiator gave oligoamide **27** in 58 % yield and oligoamide **28** in 53 % yield.
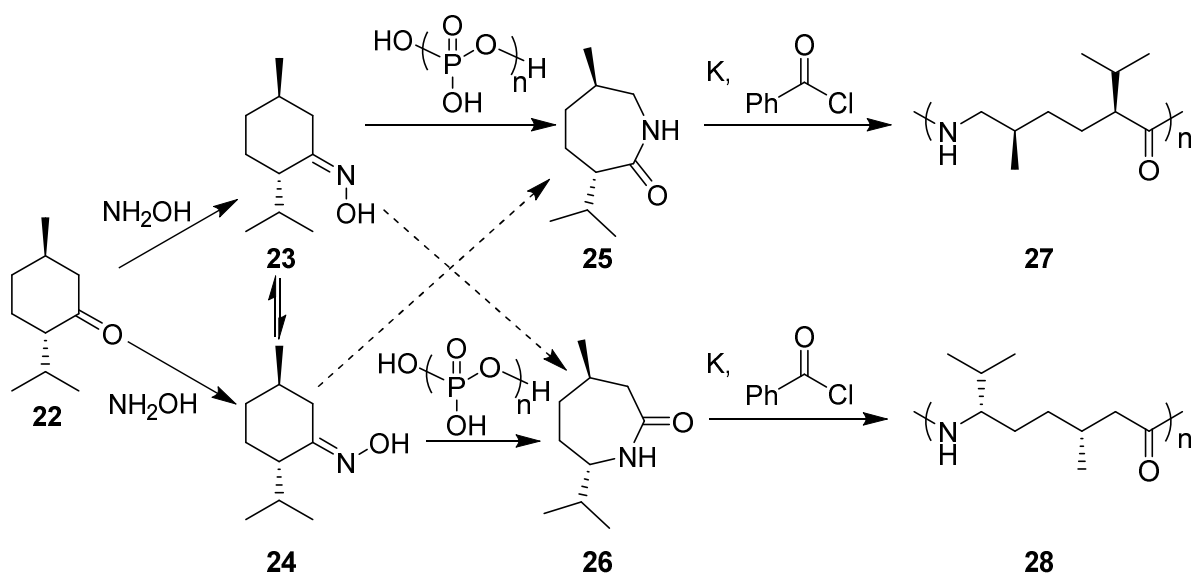
Scheme 9: Synthesis of Polyamides by Winnacker and co-workers in 2014[61]

Winnacker and Sag extended this work in 2018 reporting a new renewable polyamide derived from β-pinene (Scheme 10).[62] β-Pinene **10** is one of the most abundant terpenes found in turpentine oil. The monomer **31** was formed firstly by oxidising the exocyclic alkene to ketone **29** then secondly the Beckman rearrangement was employed. A different anionic polymerisation procedure was used which boosts a more controlled dosage and reaction facilitating upscaling. For the anionic ring opening polymerisation, sodium hydride and potassium *tert*-butoxide were used as initiators along with the benzoylated lactam **32** as a co-initiator. The innovative polymer **33** has been reported to have good thermal properties with some similarities to conventional Nylon-6. The thermal decomposition temperature of above 400 °C and a T_g of around 150 °C suggest a use as a high-performance polymer although it was stated that further research into applications is ongoing.
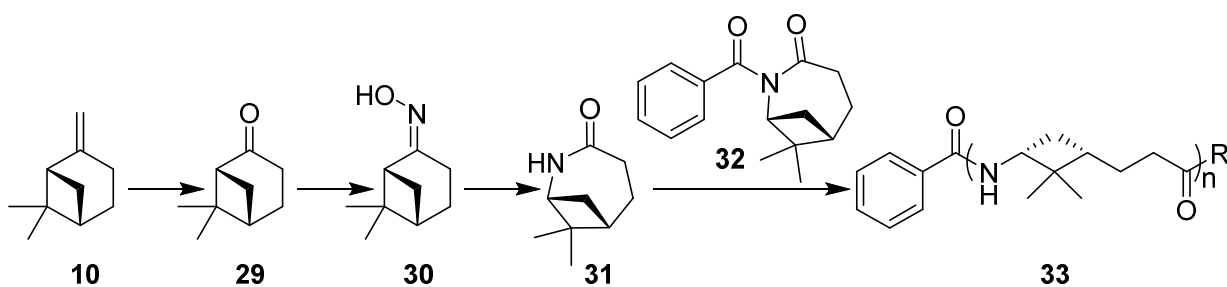
*Scheme 10: Polyamide **44** derived from β-Pinene by Winnacker and Sag[62]*

Stockmann *et al.* reported the synthesis of novel polyamides derived from α-pinene and 3-carene in 2019 (Scheme 11).[63] The synthesis of both δ-lactam monomers (**35** and **38**) follows the same reaction pathway to that of Winnacker and Saag's monomer synthesis. Both alkali-initiated anionic ring-opening polymerisations and HCl-initiated cationic ring-opening polymerisations were investigated. Most of the novel lactams gave low molecular weight apart from the δ-lactam derived from 3-carene which gave good molecular weights up to 33 kDa with 77 % conversion and a T_g of 120 °C. An application requiring transparency as well as thermal resistance was suggested due to the high T_g and thermal decomposition temperature of 400 °C.
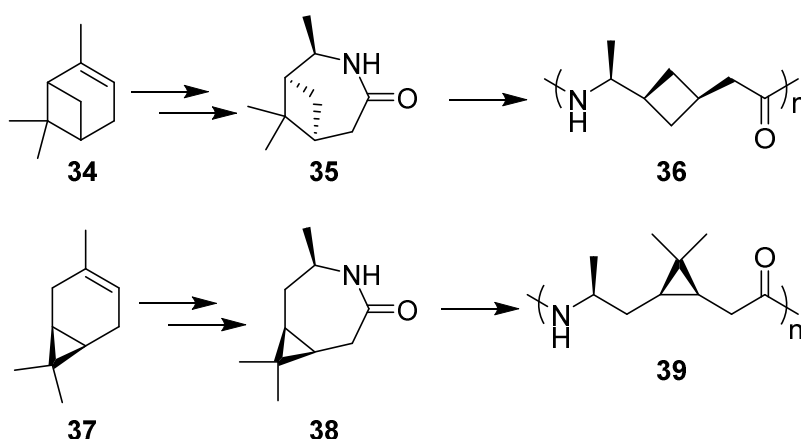
Scheme 11: Terpene-derived Polyamides reported by Stockmann et al.[63]

1.8.3 Terpene-derived Polymers *via* Thiol-ene Click Chemistry

As well as the use of modified terpenes in ring opening polymerisations to form polyesters and polyamides, the ubiquitous alkene moieties within terpenes lends themselves to thiol-ene click chemistry. Firdaus and Meier have reported the synthesis of a range of polyesters **41** and **42**, polyamides **43** and polyurethanes **44** *via* thiol-ene additions to (*R*)-(+)-limonene and (*S*)-(-)-limonene (**16**) in 2011 and 2014.[64,65]

In 2011, Firdaus, Montero de Espinosa and Meier had used similar chemistry to synthesise polyesters **41** and **42** from limonene (**16**) (Scheme 12).[64] Then in 2014, they furthered this work with the formation of polyamides **43** and polyurethanes **44** from limonene **16** (Scheme 12).[65] A range of thiols were used *via* thiol-ene click chemistry to form a variety of monomers **40a-d** with a range of functionalities in the R groups. These were polymerised *via* condensation polymerisations to form both amorphous and semi crystalline polymers. The polyesters generally had a M_n up to 25 kDa and glass transition temperature of -45 °C. The polyamides had a M_n up to 12 kDa and T_g around 42 °C and the polyurethanes had a M_n up to 12.6 kDa and T_g around 16 °C.
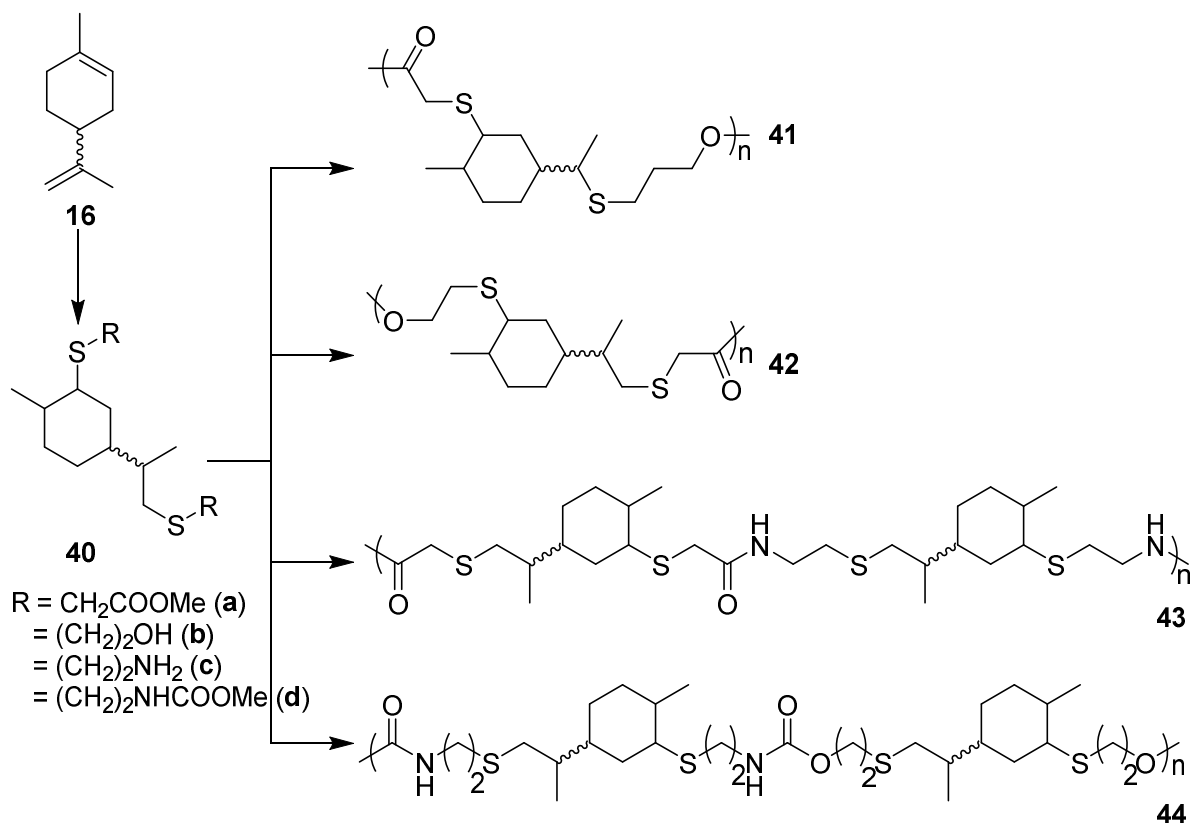
Scheme 12: Synthesis of Limonene derived Polyesters, Polyamides and Polyurethanes through the use of Thiol-ene Click Chemistry

1.8.4 Terpene-derived Epoxy-Amine Oligomers

In 2019, O'Brien *et al*. reported the synthesis of epoxy-amine oligomers **47** for synergistic anti-fungal treatments (Scheme 13).[66] Independently, carvone **3** is known to have anti-fungal activity[58] so this terpene was bis-epoxidised to form a new renewable monomer **45** using Oxone® in a good 83 % yield. This renewable bis-epoxide monomer **45** was copolymerised in neat conditions at 70 °C for 7 days resulting in oligomers up to 500 Da. The oligomer was found to work in synergy with known fungicide IPBC and the antifungal drug amphotericin B against *Trichoderma virens* and *Candida albicans* respectively. These positive results indicate the future use of these oligomers in antifungal treatments to reduce the use of fungicides and the increasing resistance to them.
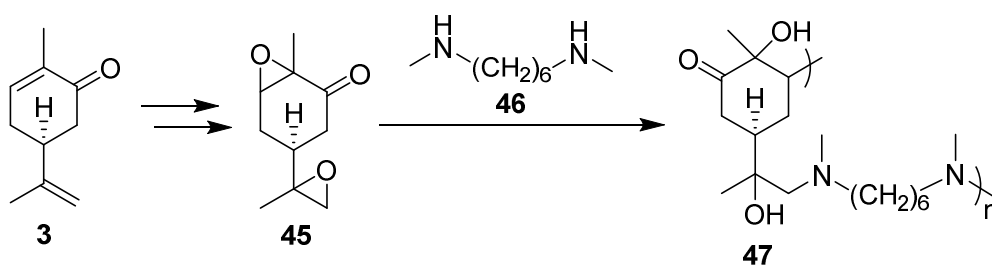
Scheme 13: Synthesis of Terpene-derived anti-Fungal Oligomers

1.8.5 Terpene-derived Polyacrylates and Polymethacrylates

In 2012, Sainz *et al*. reported the formation of acrylate and methacrylate monomers from the four most commercially available terpenes, (+)-α-pinene, (-)-β-pinene, (*R*)-(+)-limonene and (*R*)-(-)-carvone (Scheme 14).[67] Free radical polymerisation yielded a range of novel polymers with very different properties and potential applications.
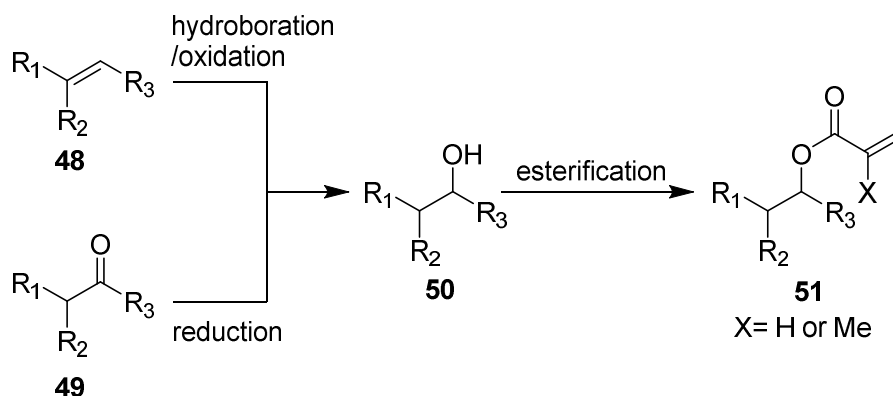
Scheme 14: General Synthesis of Terpene-derived (Meth)acrylates

Terpenes **48** (α-pinene, β-pinene and limonene) underwent hydroboration then oxidation to the corresponding alcohol in single diastereomers, the ketone functionality on carvone **49** was reduced using lithium aluminium hydride to the corresponding alcohol in a 1:1 mixture of diastereomers. The alcohol **39** was esterified using acryloyl or methacryloyl chloride to form a range of monomers **51** (Figure 16).
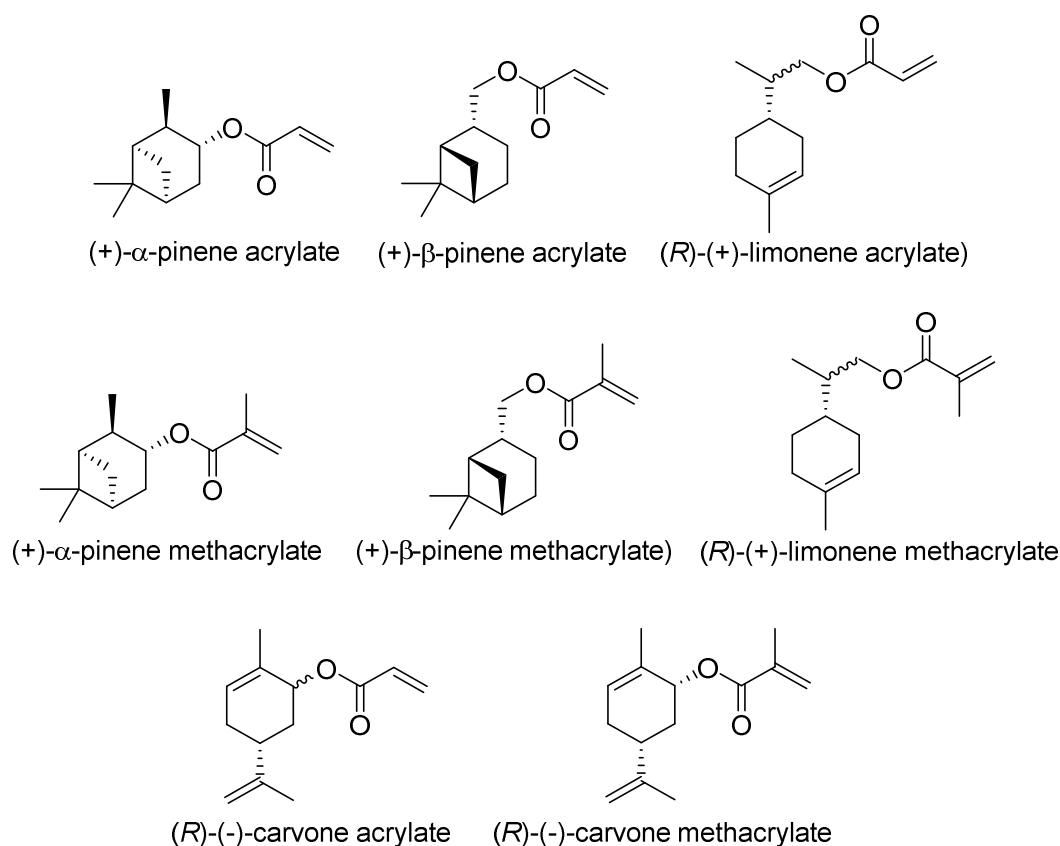
Figure 16: Range of Terpene-derived Acrylate and Methacrylate Monomers

To improve the sustainability of the monomer synthesis the esterification conditions were replaced with acrylic acid and methacrylic acid alongside propylphosphonic anhydride (T3P®). Using T3P® gives an environmentally benign water-soluble triphosphate by-product which is considerably greener than waste chloride.[33] Most of the terpene-derived acrylate and methacrylate monomers were polymerised in cyclohexanone using AIBN. The different polymers synthesised gave a range of properties due to the variations in their structure which affected the backbone and side chains in the polymers which lower or increase the T_g of the polymer. The application of high quality, glossy, biobased coatings was explored for poly(carvone methacrylate) where the exocyclic double bond was reacted with the commercial cross-linker Thiocure®. Although an excellent high value application was found for these materials, alternate syntheses would have to be considered for safe, economically viable industrial scale up.

In 2018, Lima *et al.* reported the syntheses of poly(sobrerol acrylate) and poly(sobrerol methacrylate) as potential renewable substitutions for polystyrene (Scheme 15).[68] Unsaturated polyester resins, (widely used thermoset polymers), are obtained from the free radical polymerisation of unsaturated polyesters with an unsaturated monomer which has the role of both reducing the viscosity of the unsaturated polyester and acting as a crosslinking agent. Styrene is commonly used as the unsaturated monomer as it provides high tensile and flexural strength. The two monomers **54** and **55** were synthesised in two steps from α-pinene oxide **52** in only moderate overall yields of 44 % and 52 % respectively.
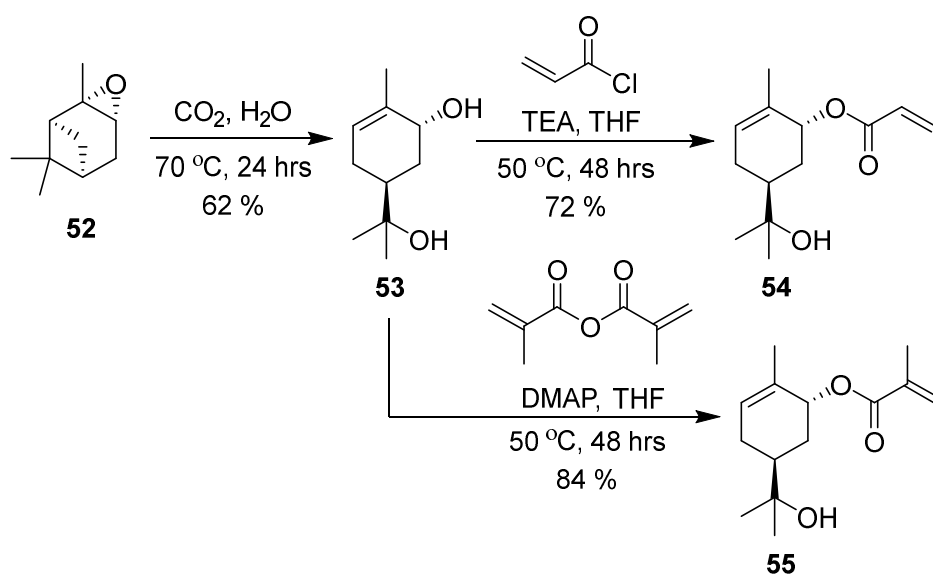
Scheme 15: Synthesis of trans-Sobrerol Acrylate and Methacrylate derived from α-pinene

The monomers, along with styrene as a control were incorporated into three different unsaturated polyesters. Styrene performed significantly better that sobrerol acrylate or methacrylate at lowering the viscosity of all three unsaturated polyester resins. The sobrerol monomers had little difference in their effect on the viscosity when compared and lowered the viscosity enough for the molding process to be successful. The gel content of all three unsaturated monomers was excellent showing good crosslinking abilities. The sobrerol monomers both imparted a similar double degradation pathway initiating at about 200 °C compared to the singular degradation pathway of styrene initiating at around 300 °C. The T_g's for sobrerol acrylate and styrene were comparable however, sobrerol methacrylate was

reported to unusually have two T_g peaks. This was theorised to be due to the presence of two immiscible phases within the crosslinked network, one for the polyester section and one for the poly(*trans*-sobrerol methacrylate). Overall sobrerol acrylate and methacrylate have demonstrated to be viable replacements to styrene in unsaturated polyester resins although further work is needed to investigate viscosity modifiers to lower the viscosity of the unsaturated polyester resins containing the sobrerol monomers. Also due to the low cost of styrene compared to the novel monomers further work is needed to demonstrate superior performance, or to increase the overall yields of the monomer syntheses to make them economically viable.

In 2019, Stamm *et al*. introduced the chemoenzymatic synthesis of *trans*-sobrerol in one step from α-pinene **34** using P450-BM3/2M enzymes (Scheme 16). Sobrerol methacrylate **55** was produced via both a synthetic Shotten Bauman reaction and an enzymatic lipase reaction. This renewable monomer **55** was polymerised *via* enzymatic, free radical, ATRP and RAFT polymerisations.[69]
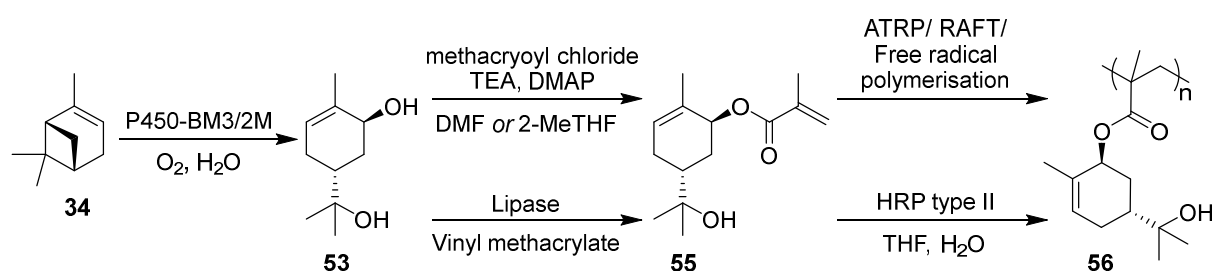
Scheme 16: Three Step Synthesis of Poly(trans-Sobrerol Methacrylate)

RAFT polymerisation of *trans*-sobrerol methacrylate **55** followed first order kinetics with respect to monomer conversion (Figure 16). A linear evolution of molecular weight was also seen with respect to monomer conversion demonstrating good polymerisation control and achieving close-to-target molecular weights up to 32 kDa and polydispersities of 1.2.

43
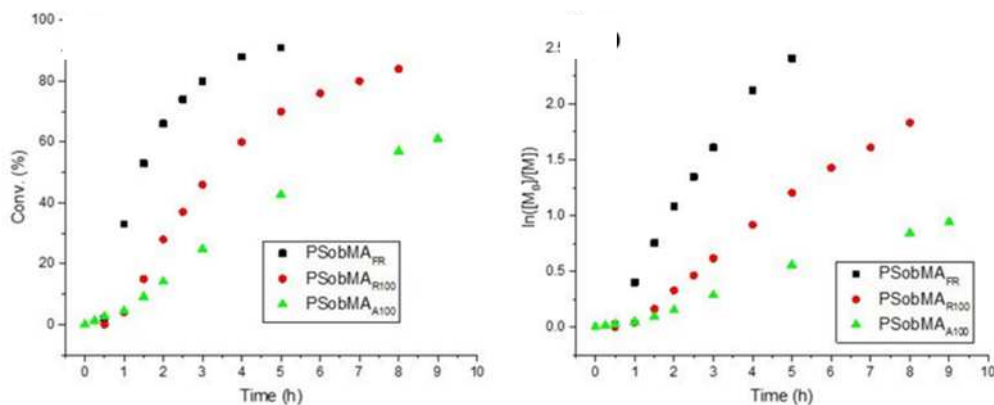
Figure 17: trans-Sobrerol Methacrylate Polymerisation Kinetics with Respect to Monomer Conversion and ln(M_n/[M]) Taken from Source Material[70]

ATRP was investigated as an alternative method of controlled polymerisation with equally good results and control. Comparatively, an uncontrolled free radical polymerisation was also attempted giving a high molecular weight of 48 kDa and high polydispersity of 2.4. In addition to the traditional free radical techniques, Stamm *et al*. polymerised *trans*-sobrerol methacrylate using horseradish peroxidase (HRP) in high conversion to give a high molecular weight of 40 kDa and high polydispersity of 1.9. T_gs of 116 to 154 °C were reported depending on the molecular weight and T_ds (decomposition temperatures) were reported at around 70 °C higher than their respective T_gs. As each repeating unit of poly(*trans*-sobrerol methacrylate) contains both a tertiary alcohol and a substituted alkene, post-polymerisation cross-linking was investigated to form novel coatings. The polymer was cross-linked using thiol-ene click chemistry and *trans*-esterification with great success demonstrating potential applications in biobased coatings.

In 2019, Droesbeke and Du Prez reported the sustainable synthesis of renewable terpenoid-based (meth)acrylates using the CHEM21 green metrics toolkit (Figure 18).[71] The CHEM21 green metrics toolkit consists of four stages called; zero, first, second and third pass. First, an initial screening of different procedures is carried out using the Zero Pass. At this level, concerns of the use of highly hazardous solvents and chemicals with regard to health and safety are assessed, as well as the efficiency of the reaction in terms of conversion, yield, selectivity, and so forth. The routes with the most promising results are further investigated

44

at the First Pass where the process mass intensity (PMI) is calculated and the concerns in health, safety and ecology are elaborated. The two last passes are "industrial" toolkits and foresee a more thorough analysis of reactions or pathways at pilot scale and beyond. They typically include some key parameters, such as, a detailed energy investigation, the costs, the renewable intensity, and the resulting waste. This toolkit was used to investigate five different synthetic routes for the formation of terpene-derived acrylate derivatives.

R = H, Me

Tetrahydrogeraniol (meth)acrylate

Geranyl (meth)acrylate

Citronellyl (meth)acrylate

L-menthyl (meth)acrylate
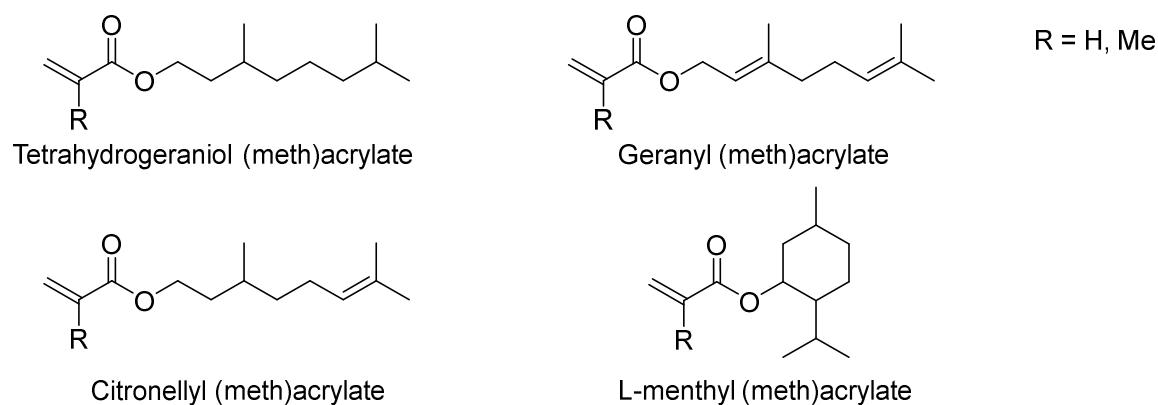
Figure 18: Range of Terpene-derived Acrylate and Methacrylate Monomers

After analysis using the CHEM21 green metrics toolkit, it was found that the method combining the use of a drying agent and a catalyst without using additional solvents was preferred. In the case of acid/base sensitive reagents, such as geraniol, an enzymatic pathway is advised. In the future, this could be a useful methodology when confronted with several alternative synthetic pathways in order to choose the best suitable and sustainable pathway with the intention of transferring this knowledge to an industrial scale although currently it has only been used on a laboratory scale and further development needs to occur before it could be used generically.

1.9 Polyacrylamides

Whilst a wide variety of renewable terpene-derived polymers including polyacrylates, polyesters, polyamides, polyurethanes and polycarbonates, have been reported, one class of polymers, polyacrylamides have yet to be explored. Petroleum-based polyacrylamides as both homopolymers and copolymers have a wide range of applications spanning a number

of different industries. The acrylamide monomer itself has been widely used in different chemical industries, such as in dyes, thickening agents and pesticide formation.[72–77] Polyacrylamide, Poly(AMPS) and Poly(N-isopropylacrylamide) are the three most commercially used polyacrylamides however all three are derived from petroleum based sources.[74]

Polyacrylamide (PAM) (Figure 19) is a non-ionic, watersoluble, and bio-compatible polymer that can be tailored to meet a broad range of applications. The polymer can be synthesized as a simple linear chain or as a cross-linked structure.[74]
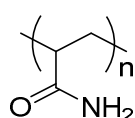
Figure 19: Polyacrylamide

Polyacrylamide increases the viscosity of water and encourages the flocculation of particles present in water. The cross-linked polymer can absorb and retain extremely large amounts of water because the amide groups form strong hydrogen bonds with water molecules. Poly(acrylamide-co-acrylic acid) (Figure 20) and its sodium salts, for example, are widely used as thickening agents, flocculating agents in waste water treatment and as the gel in gel electrophoresis.[74]
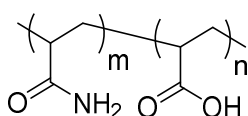
Figure 20: Poly(acrylamide-co-acrylic acid)

Acrylamides have also been used as the anionic comonomer, 2-acrylamido-2-methylpropane sulfonic acid (AMPS) (Figure 21) was a commercial product from Lubrizol. Made by the Ritter reaction between acrylonitrile and isobutylene in the presence of

sulfuric acid and water, AMPS is a reactive, hydrophilic, sulfonic acid acrylamide monomer used to alter the chemical properties of wide variety of anionic polymers. The earliest patents, in the 1970s using this monomer were filed for acrylic fibre manufacturing. Today, there are over several thousand patents and publications involving use of AMPS, again in a wide range of applications, including water treatment, oil field, construction chemicals, hydrogels for medical applications, personal care products, emulsion coatings, adhesives, and rheology modifiers. [74,76,78,79]
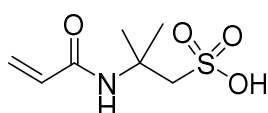
Figure 21: AMPS (2-acrylamido-2-methylpropane sulfonic acid)

Poly(*N*-isopropylacrylamide) (PNIPAM) (Figure 22) is another well-known polyacrylamide in the literature first synthesised in the 1950s.[34] PNIPAM is known for being a thermosensitive water-soluble polymer with hydrophobic moieties that is able to reversibly change its structure due to external temperature changes.[35] Cross-linked PNIPAM forms a 3-D hydrogel that can be used in a variety of applications, from biomaterials to drug delivery to soil erosion control.[36–42] However, PNIPAM and other polyacrylamides are industrially synthesised from staring materials derived acquired from crude oil.[43]
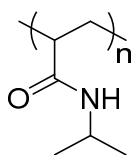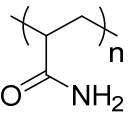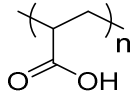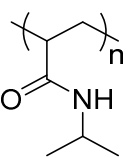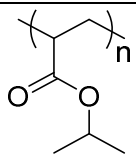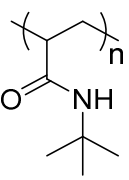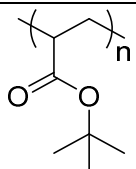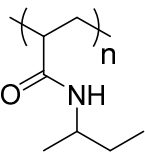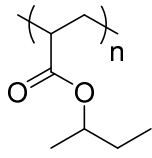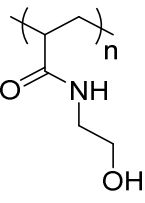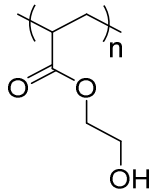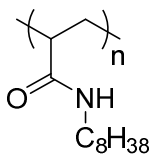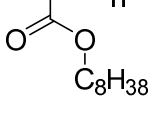
Figure 22: Poly(N-isopropyl acrylamide)

The interesting and unique properties that PNIPAM, PAM and other polyacrylamides exhibit are due to the hydrogen bonds formation between amide side chains. This increased

polarity gives all polyacrylamides consistently higher T_gs than the equivalent polyacrylates (Table 1).[80]

Table 1: Comparison between the glass transition temperatures of polyacrylamides and polyacrylates

Polyacrylamide	T_g (°C)	Polyacrylate	T_g (°C)
Poly(acrylamide)	165	Poly(acrylic acid)	105
Poly(*N*-isopropyl acrylamide)	130	Poly(isopropyl acrylate)	-2
Poly(*N-tert*-butyl acrylamide)	128	Poly(*tert*-butyl acrylate)	38
Poly(*N-sec*-butyl acrylamide)	117	Poly(*sec*-butyl acrylate)	-20
Poly(*N*-hydroxyethyl acrylamide)	118	Poly(2-hydroxyethyl acrylate)	-14

	-53		-65
Poly(*N*-octyl acrylamide)		Poly(octyl acrylate)	

A high T_g is essential for materials that aspire to replace any incumbent commodity plastics employed in the amorphous state.[81] Current commercially available biopolymers, include PLA (T_g = 55 °C), PET (T_g = 74 °C) and PEF (T_g = 86 °C). At the moment, corn-based PLA is arguably the most successful biopolymer, however it suffers from brittleness, poor barrier properties and slow degradation under typical environmental conditions. All of which inhibit its uptake in replacing all the commercially available fossil fuel-based plastics. Considering the volume and range of fossil fuel-based plastics currently produced annually, it is unreasonable to expect one bioplastic to replace them all. The low T_g of PLA in particular has especially limited its market expansion to replace higher T_g materials such as PET and PS.[82] The lack of commercially available, high glass transition temperature biopolymers has created an opportunity in academia and industry to fill this market void.

This is where renewable polyacrylamides could present a solution; with traditionally high glass transition temperatures and wide-ranging applications, renewable polyacrylamides could be viable replacements for the high T_g fossil fuel-based plastics that we are reliant on.[44]

1.10 Renewable Polyacrylamides

The renewable polyacrylamides currently published in literature mostly consist of *N*-isopropylacrylamide (**60**) grafted to a renewable materials such as cellulose, chitosan, lignin, guar gum and barley.[83–88] These poly(*N*-isopropylacrylamide) materials have the same properties as the homopolymers but a higher renewable content. Proposed applications for these materials are similar to the homopolymers in drug delivery, wastewater treatment and flocculants.

A good example of grafted poly(N-isopropylacrylamide) was reported in 2014 by the Meier group using cellulose (**57**) to form RAFT agent (**59**) (Scheme 17).[43] This is then polymerised with *N*-isopropylacrylamide to form thermoresponsive polyacrylamide **61** with proposed applications in drug delivery systems**.**
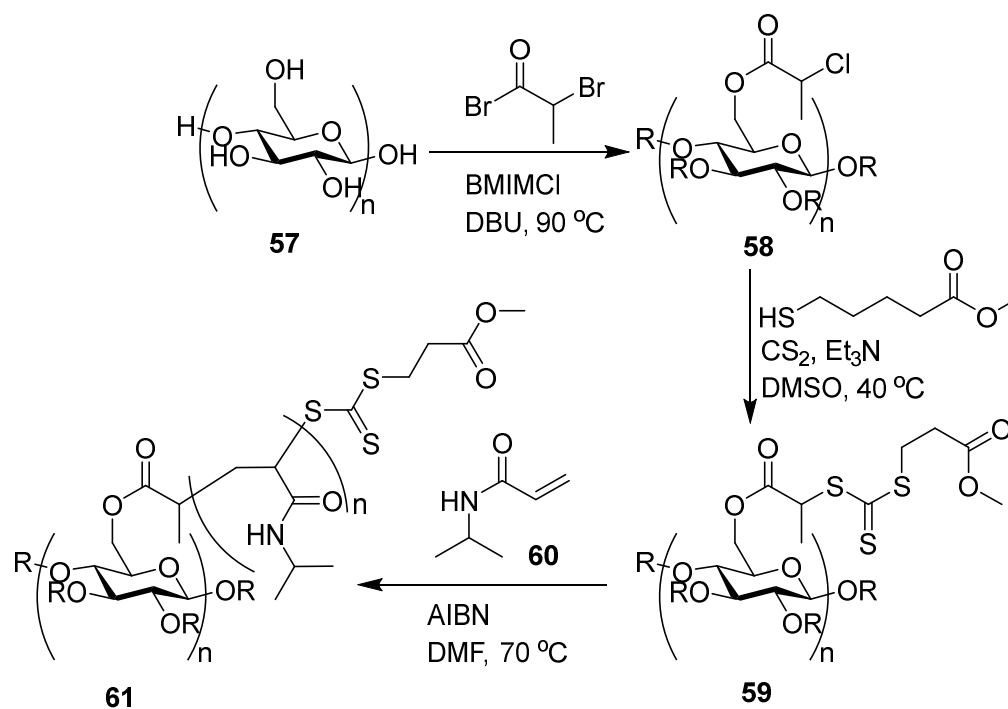
Scheme 17: RAFT Polymerisation of Polyacrylamide onto Cellulose

Although grafting PNIPAM onto renewable materials such as cellulose (**57**) is a good way of increasing the renewable content within existing polymer material applications, the acrylamide itself, poly(*N*-isopropylacrylamide), is still non-renewable.

Some advances have been made into synthesising novel renewable acrylamides from sustainable materials.

Dopamine is an extensively studied major component of the adhesion properties in mussels and is known to universally enhance polymeric adhesion properties even in the presence of water. Several research groups have capitalised on this natural material to form new renewable polyacrylamides for adhesives and coatings applications (Scheme 18).

In 2013, Nishida *et al*. used dopamine acrylamide along with two crude-oil based acrylamides to form a random triblock copolymer with applications as a synthetic adhesive for use both in air and water environments.[89] The renewable dopamine acrylamide was synthesised using a simple base-catalysed Schotten Baumann amidation with triethylamine in a good 65 % yield. In 2016, Yang *et al*. also used a Schotten Baumann amidation with sodium tetraborate decahydrate and sodium bicarbonate to form the desired dopamine acrylamide in a 54 % yield.[90] Free radical copolymerisation with crude oil-based 2-aminoethyl methacrylamide hydrochloride gave a pH-sensitive random diblock copolymer with proposed applications in waterborne paints. The use of dopamine acrylamide in block copolymers continued in 2018 when Lamping *et al*. reported its potential as a carbohydrate responsive and reusable glue with potential applications in responsive biomedical adhesion methods *in vivo*.[91] Using a similar synthesis to Nishida *et al.,* the desired dopamine acrylamide in this case was synthesised in an excellent quantitative yield. This was then polymerised *via* ATRP with hydroxyethyl acrylate to form a strong, water-resistant adhesive polymer. Finally, the same dopamine acrylamide synthesis was used by Gang *et al*. in 2019 in the formation of a novel robust self-healing magnetic double-network hydrogel with magnetic Fe_3O_4.[92]
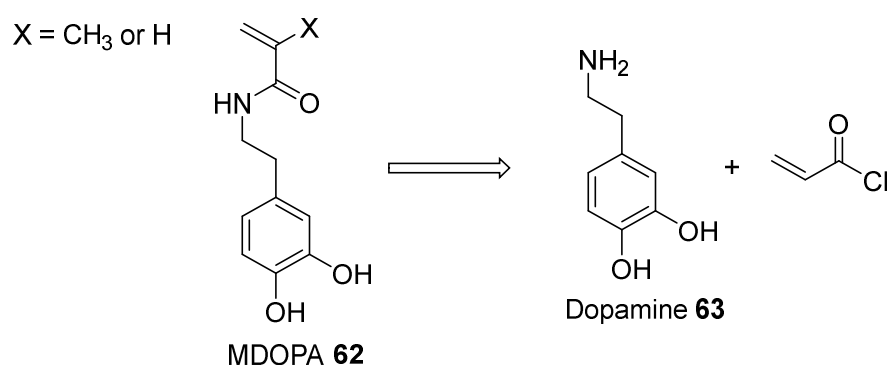
Scheme 18: Retrosynthesis of Dopamine (Meth)acrylamide

In 2017, Kim and Chung reported the use of *N*-methacryloyl-3,4-dihydroxyl-*L*-phenylalanine **62** (MDOPA) within new photo-responsive bio-inspired adhesives (Scheme 19).[93] MDOPA **62** was synthesised *via* a base-catalysed Schotten-Baumann reaction on a multi-gram scale

(~3.5 g). Along with MDOPA, a photocleavable crosslinker and a zwitterionic monomer where polymerised *via* free radical polymerisation to form a photo-responsive random terpolymer adhesive with a high adhesion strength of 341 kPa.
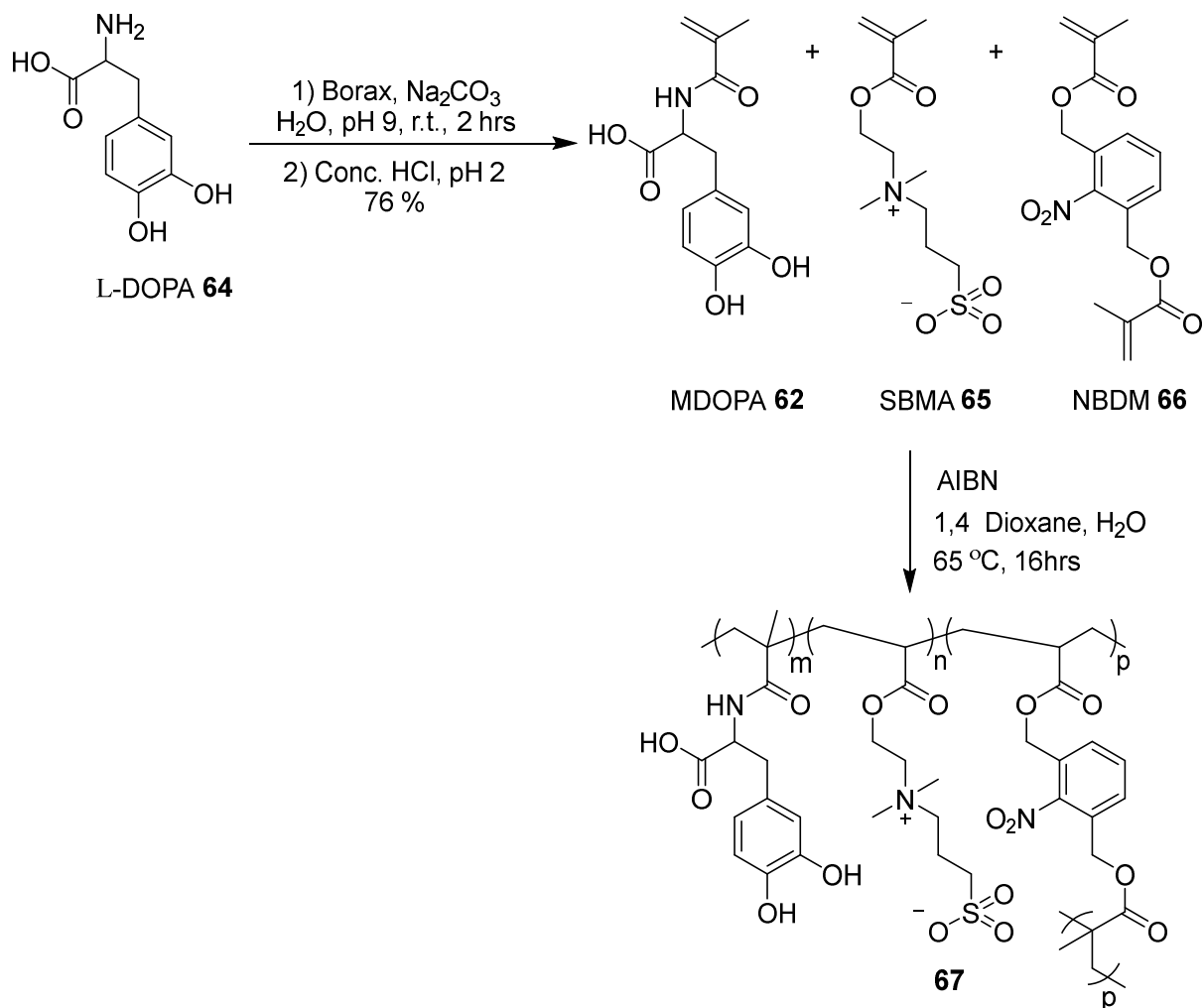
Scheme 19: Synthesis of Triblock Copolymer Containing Renewable MDOPA

In 2020, Li *et al*. used galactose **68**, a naturally occurring sugar, to synthesise a renewable polyacrylamide for co-polymerisation with PNIPAM to form a drug delivery system for the anti-cancer drug, doxorubicin hydrochloride (Scheme 20).[94] The desired acrylamide **70** was synthesised over three steps with a good overall yield of 63 %. Selective S_N2 amination using ammonium carbonate gave a stable amine intermediate **69** which was telescoped onto the amidation step. The amidation step was a good yielding, Schotten Baumann amidation using

acryloyl chloride and sodium carbonate which gave the sugar-based acrylamide **70** in 72 % yield. The alcohol groups were then protected using acetyl moieties before use in a RAFT polymerisation with PNIPAM although no GPC data was reported to indicate successful control of the polymerisation.
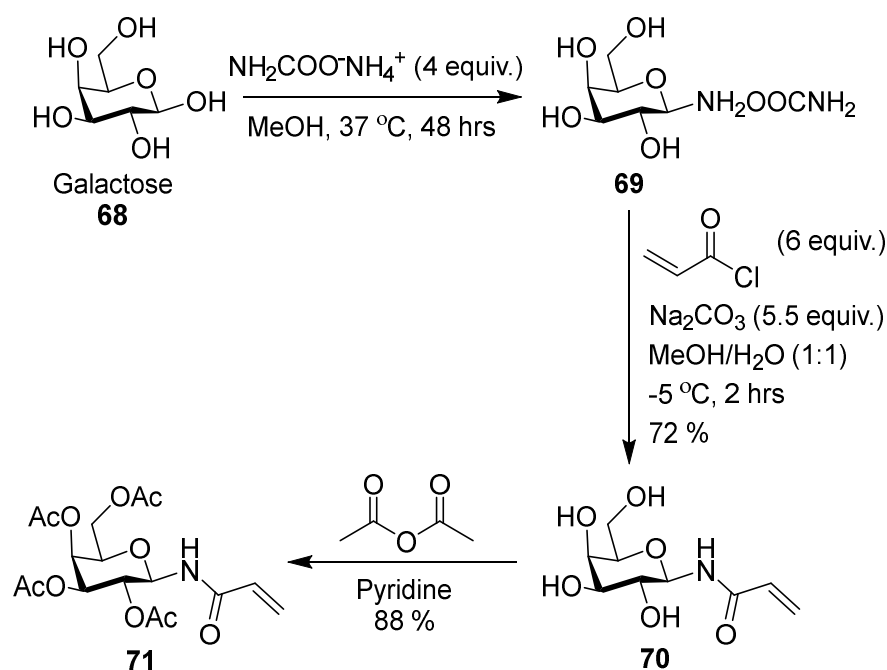
Scheme 20: Synthesis of Acyl Protected Galactosyl Acrylamide

In 2011, H. Liu *et al*. reported the synthesis of a new guaiacol-based polyacrylamide **74** with promising anti-bacterial properties (Scheme 21).[95] Guaiacol **72** is a cheap natural product isolated from the guaiac resin obtained from beechwood. Initial synthesis of the novel monomer *via* a Friedel-Crafts alkylation of N-hydroxymethylacrylamide **73** (non-renewable) and guaiacol **72** gave the monomer **74** in a low 31 % yield over 4 days.
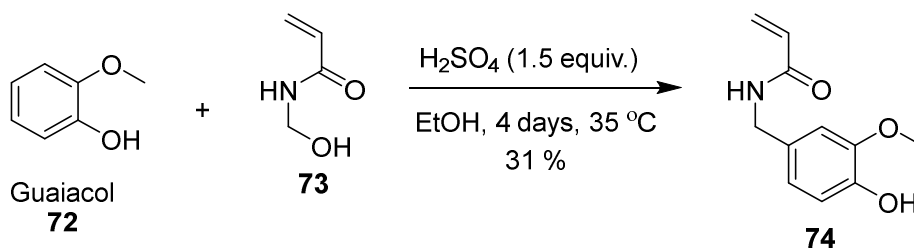
Scheme 21: One-Pot Synthesis of Guaiacol-based Polyacrylamide

This long, low yielding reaction led to the investigation of an alternative route from vanillin (Scheme 22). Vanillin is another cheap natural product, which can be sourced directly from vanilla pods or synthetically from other natural products. Condensation of vanillin **75** with hydroxylamine gave the corresponding oxime **76** which was reduced *via* hydrogenation to give the amine **77**. The amine **77** then formed the desired acrylamide **78** through a Schotten-Baumann reaction with an overall yield of 28 %. Although this route takes half the time of the Friedel-Crafts alkylation, it is similarly low yielding and less sustainable over the three steps.
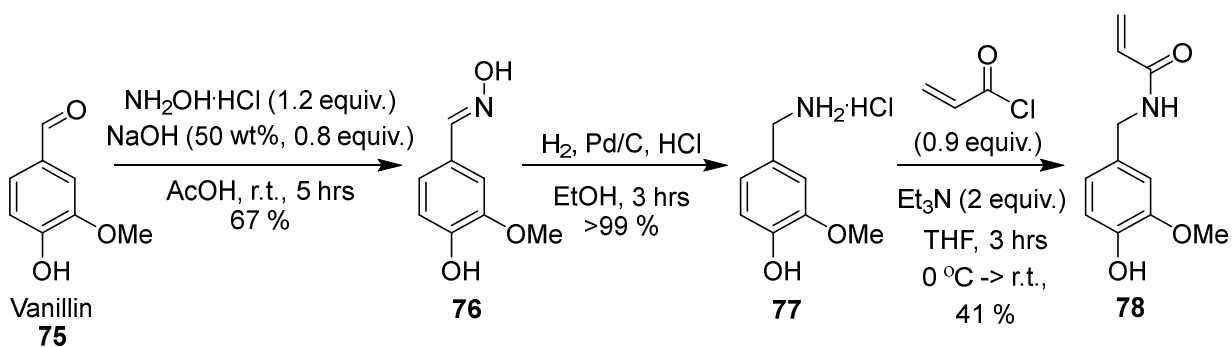
Scheme 22: Three-Step Synthesis of Guaiacol-Based Acrylamide

Polymerisation investigations into the novel monomer **79** looked into the influence of reaction times and initiator concentrations on the molecular weight and polydispersity of

the corresponding polymer **80** (Scheme 23). Overall, the molecular weights averages were relatively low for a free radical polymerisation, 3.6-6.6 kg mol^{-1}.

AIBN (1 wt%)

Toluene/DMF (1:1)
70 °C, 24 hrs
78 % conversion

79

80
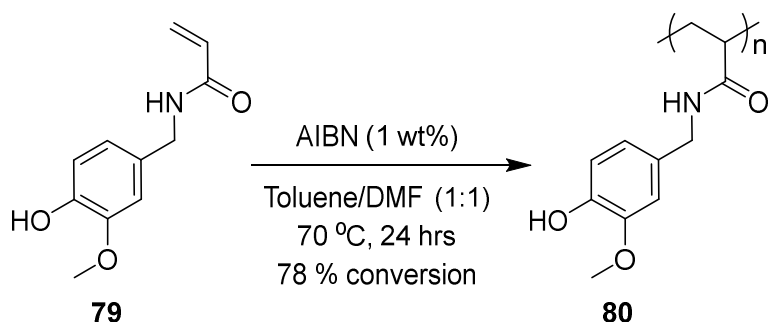
Scheme 23: Free Radical Polymerisation of Guaiacol-based Polyacrylamide

As phenolic compounds and polymers containing phenols have previously been shown to have antimicrobial properties, this application was investigated by Hui *et al*. for their novel polymer.[95] The novel polymer exhibited potential activity against Bacillus subtilis using anti-adhesion and anti-biofilm tests. After an adhesion time of 3 hours compared to a non-coated glass slide, there was a decrease of bacteria of 99 % on the polymer coated glass slide.

1.11 Project Aims

The challenge of synthesising a biobased polymer with favourable economics and material properties from a novel, sustainable monomer using green chemistry, which is then industrial manufactured and sold as a commercial product is huge. This is clearly demonstrated by the large number of biobased monomers within the literature from renewable resources such as terpenes, vegetable oils and polysaccharides, yet the incredibly small number of commercially available biobased polymers such as poly(lactic acid).

Terpenes are an abundant natural resource derived most often from non-food or waste biomass with the potential to match the industrial scale of poly(lactic acid). Already approved by the FDA for use in food and food packaging, terpenes are already widely used in the food and fragrance industry, making their expansion into the polymers and plastics market feasible. Unfortunately, to this date, unmodified terpenes have proven difficult to polymerise requiring expensive and/or high energy processes with poor low molecular weight results. Recent literature precedent concerning the derivation of terpenes has been extensive with the synthesis of novel polyamides, polyesters, polyurethanes, polycarbonates and polyacrylates have been reported. However, one class of polymers, polyacrylamides, has yet to be explored. Other renewable polyacrylamides in the literature have been synthesised from sugar and phenolic compounds such as galactose, dopamine derivatives and vanillin producing interesting properties and applications in biobased coatings, adhesives and drug delivery systems. Exploiting terpenes to form renewable polyacrylamides could produce some novel, commercially feasible renewable polyacrylamides with high value applications as alternatives to fossil/petroleum-based polymers.

The biggest hurdle for novel renewable monomers is the step from academia to industry for commercialisation. If there is no demand for the product or if the cost to benefit ratio is too high then the likelihood of commercialisation is very low no matter how green, sustainable or ground-breaking the biobased polymer is. This is where the United Nations Sustainable Development Goal 17 (Partnerships for the goals - the means of implementation and revitalize the global partnership for sustainable development) plays a vital role in the development of successful new technologies.

57

Croda Europe Ltd is the European branch of Croda International Ltd, an international business-to-business speciality chemicals company that delivers real benefits to a range of diverse products including health and beauty, engine lubricants, plastics and many more. In order to meet the needs of their customers, address market trends and continually grow; they have a commitment to sustainable innovation that runs through every aspect of their business including the use of natural raw renewable materials, the production of sustainable ingredients and ethical business operations.[96] Croda International Plc has aligned themselves with the United Nations Sustainable Development Goals and aims to have, by2030, over 75% of their organic raw materials by weight as bio-based, absorbing carbon from the atmosphere as they grow. This has been deeply imbedded within their history as their very first product was Lanolin, a natural and sustainable ingredient created as a result of processing sheep's wool for textile industries.

The aim of this project is to synthesise a library of renewable polyacrylamides in good to excellent yields on a multigram scale. In terms of this partnership and in alignment with their sustainable innovation objective to accelerate the transition to biobased products by moving away from fossil/petrochemical feedstocks, the polymers will be synthesised from terpenes in three steps or less and contain a renewable content of 75 % in line with Croda's carbon positive goal and the 12th United Nations Sustainable Development Goal. Thermally-initiated solution polymerisations, redox-initiated solution polymerisations and redox-initiated emulsion polymerisation methods will be investigated to determine the optimum polymerisation methods with regards to sustainability so it can be easily commercialised on an industrial scale. Both homopolymers and copolymers, with a library of functional groups targeting alternative properties, will be synthesised to give a wide range of properties, increasing the chance of developing a competitive commercial product suitable for one of Croda's targeted markets. The monomers and polymers will be fully characterised, the polymer properties tested (e.g. viscosity, hydrophobicity, hydrophilicity), and potential applications (e.g. dispersants, surfactants, coatings) investigated in collaboration with Croda Europe Ltd.

2.0   Chapter 2: Monomer Synthesis

To reach our aim of synthesising a library of renewable terpene-based polyacrylamides, a series of novel monomers must be produced. In order to synthesis acrylamides from the alkene and alcohol functionalities ubiquitous to terpenes, two well-established syntheses, the Overman rearrangement and the Ritter reaction were considered.[97,98] Although amides are a ubiquitous functional group in natural products and synthetic materials across every chemical industry, the ACS Green Chemistry Institute Pharmaceutical Round table identified amide formations as one of the most problematic syntheses in the pharmaceutical industry.[99,100] Our aim is to synthesis a range of novel terpene-based acrylamides in two steps or less with good to excellent yields on a multigram scale.

2.1   Overman Reaction

First reported in 1974, the Overman rearrangement is the 1,3-transposition of alcohol and amine functionalities *via* the [3,3]-sigmatropic rearrangement of allylic trichloroacetimidates (Scheme 24).[97,101]
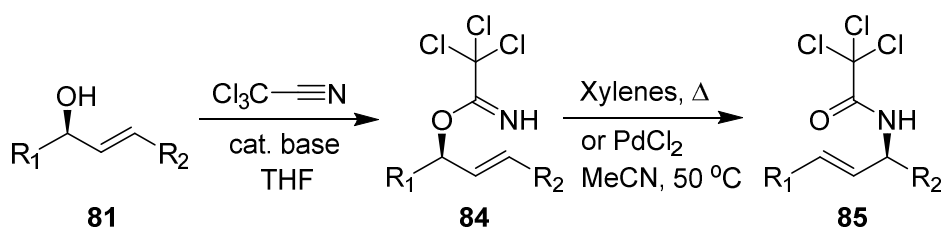
Scheme 24: General Scheme for the Overman Rearrangement

First allylic alcohol **81** is deprotonated under basic conditions (Scheme 25). The deprotonated alcohol **82** nucleophilically attacks trichloroacetonitrile to give trichloroacetimidate anion **83**. This intermediate deprotonates the starting alcohol which propagates the reaction and forms trichloroacetimidate **84**.

59
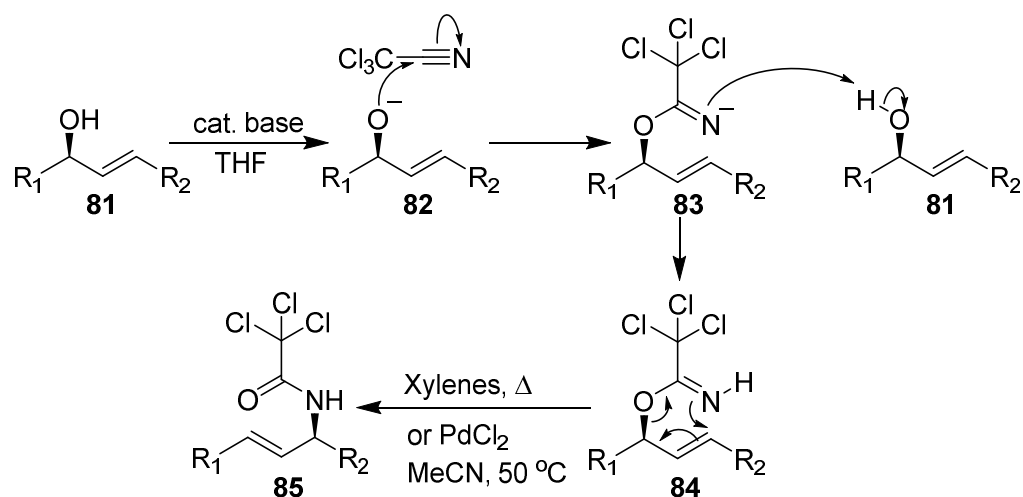
Scheme 25: Overman Rearrangement Mechanism

Heating trichloroacetimidate **84** at reflux in a solvent (commonly xylenes) for several hours or exposing to certain transitional metal catalysts, such as PdCl$_2$, results in a thermal [3,3]-sigmatropic rearrangement which proceeds *via* a chair-like transition state resulting in the corresponding allylic trichloroacetamide **85** in high yields (Scheme 26).
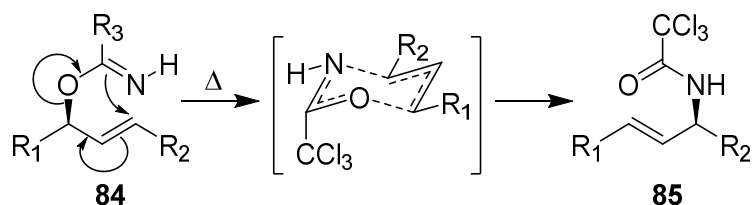
Scheme 26: Overman [3,3]-Sigmatropic Rearrangement Mechanism

The rearrangement is irreversible and completely regiospecific. It is known that this [3,3]-sigmatropic rearrangement is suprafacial and stereospecific with secondary allylic alcohols preferentially forming (*E*)-alkenes, retaining the stereochemistry of the starting material. The allylic trichloroacetamides can be hydrolysed in basic conditions to afford the corresponding amines.

There is already precedent for the use of the Overman rearrangement on terpenes; two examples have been reported by Valeev *et al*. in 2009[102] (Scheme 27) and Csillag *et al*. in 2012 (Scheme 28).[103]

During investigations into possible synthetic transformations of (*R*)-(-)-carvone in 2009, Valeev *et al*. reported the formation of *N*-carvyltrichloroacetamide (**87**) in a low overall yield of 28 % *via* an Overman rearrangement in xylene.[102]
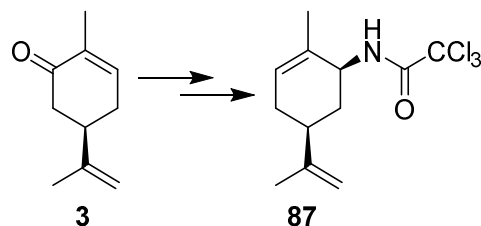
Scheme 27: (R)-(-)-Carvone Derived Trichloroacetamide Synthesised by Valeev et al.[102]
i) LiAlH4 (0.25 equiv.), Et2O, -78 °C; ii) DBU (2 equiv.), CCl₃CN (2 equiv.), CH₂Cl₂, r.t.; iii) xylene, reflux

In 2012, Csillag *et al*. reported the synthesis of a library of chiral pinane-based aminodiols from (*R*)-(-)-myrtenol (**88**) *via* allyl trichloroacetamide **89**. Allyl trichlorochloroacetamide **89** was synthesised in two steps with an excellent overall yield of 92 % (Scheme 28).[103]
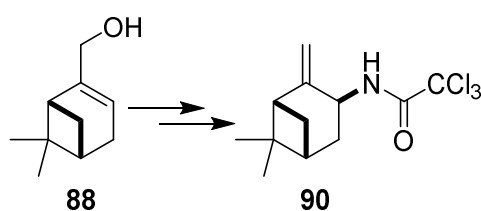
Scheme 28: Myrtenol Derived Trichloroacetamide Synthesised by Csillag et al.[103]
i) CCl₃CN (1.8 equiv.), DBU (1.5 equiv.), DCM, 0 °C; ii) anhydrous K₂CO₃, dry xylene, reflux

2.1.1 *N*-Pinocarveol Acrylamide

Taking inspiration from the procedure by Csillag *et al.*[103], a myrtenol derived acrylamide **92** was synthesised in 4 steps *via* trichloroacetamide **90** (Scheme 29). Analysis of the *J* values and coupling interactions within a range of NMR techniques (^{1}H, ^{13}C, COSY, HSQC, HMBC) determined the stereochemistry which was confirmed within literature.[103]
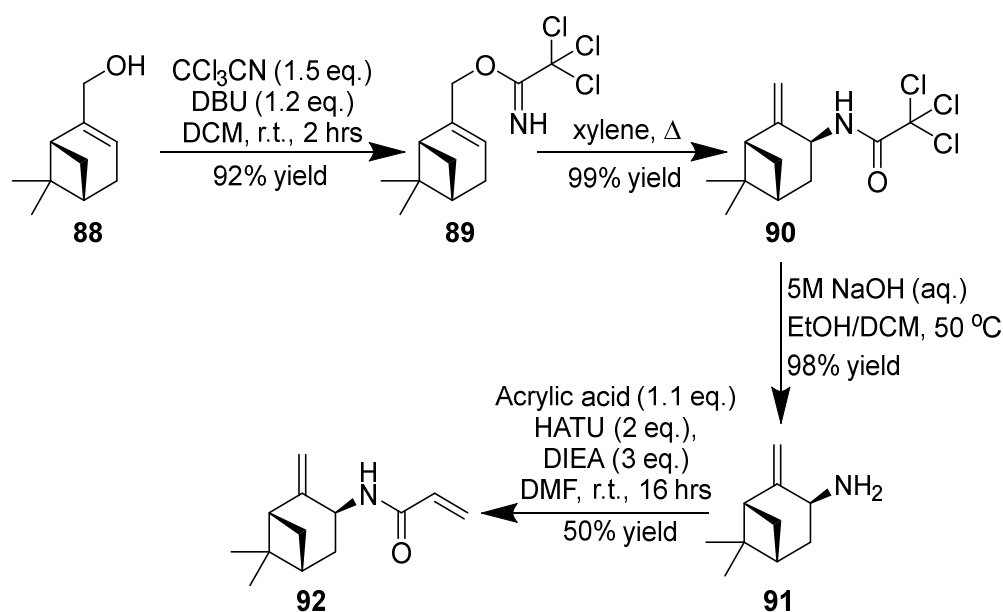
Scheme 29: Synthesis of N-Pinocarveol Acrylamide from Myrtenol

The mechanism proceeds *via* the base-mediated Overman rearrangement (Scheme 30) as previously discussed ending in a [3,3]-sigmatropic rearrangement to form *N*-pinocarveol trichloroacetamide **90** *via* myrtenyl trichloroacetimidate **89** with a comparable overall yield of 91 %. This was then hydrolysed using sodium hydroxide with an excellent yield of 98 % to amine **91**. Without further purification of amine **91**, amide **82** was formed using stoichiometric equivalents of HATU and acrylic acid in DMF. The HATU amidation gave a moderate yield of 50%, dropping the overall yield of the 4-step synthesis to 45 %. The reagent T3P® was also investigated as an alternative, more sustainable coupling reagent but only gave trace amounts of the desired acrylamide product.
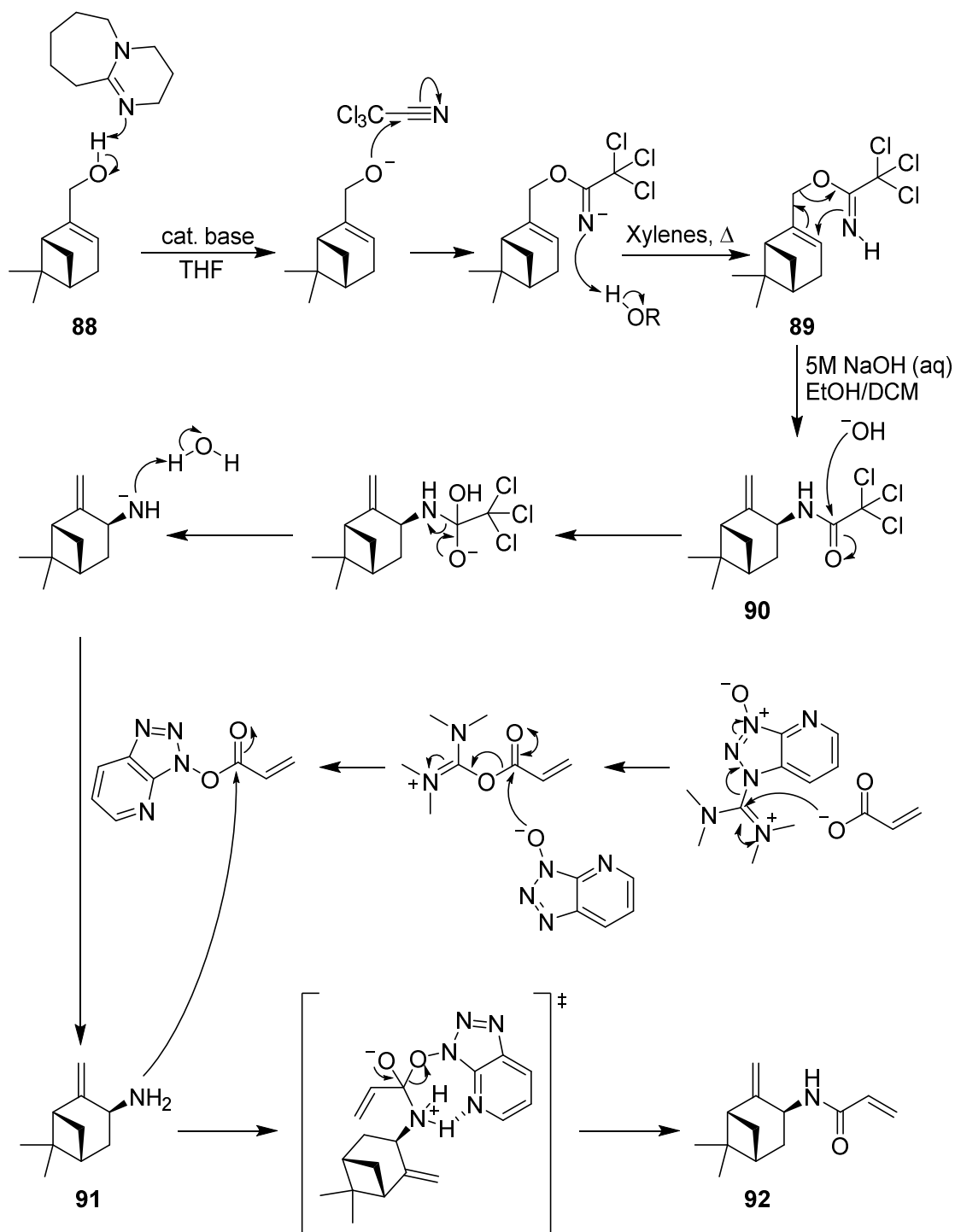
Scheme 30: Full Mechanism for the synthesis of N-Pinocarveol Acrylamide

2.1.2 *N*-Myrtenyl Acrylamide

As α-pinene is the most commercially available terpene, the synthesis of a novel α-pinene derived acrylamide monomer was investigated. As α-pinene **34** doesn't have the required allylic alcohol functionality, known terpenoid pinocarveol **93** was formed *via* epoxidation then subsequent base-catalysed ring opening. A telescoped Overman rearrangement of **94** followed by an amide hydrolysis under basic conditions formed the primary amine **96**, myrtenylamine, in a good overall yield of 77 % across 3 steps (Scheme 31). Without purification myrtenylamine as used in a Schotten-Bauman amidation to form the desired myrtenyl acrylamide **97** in a 56 % yield.
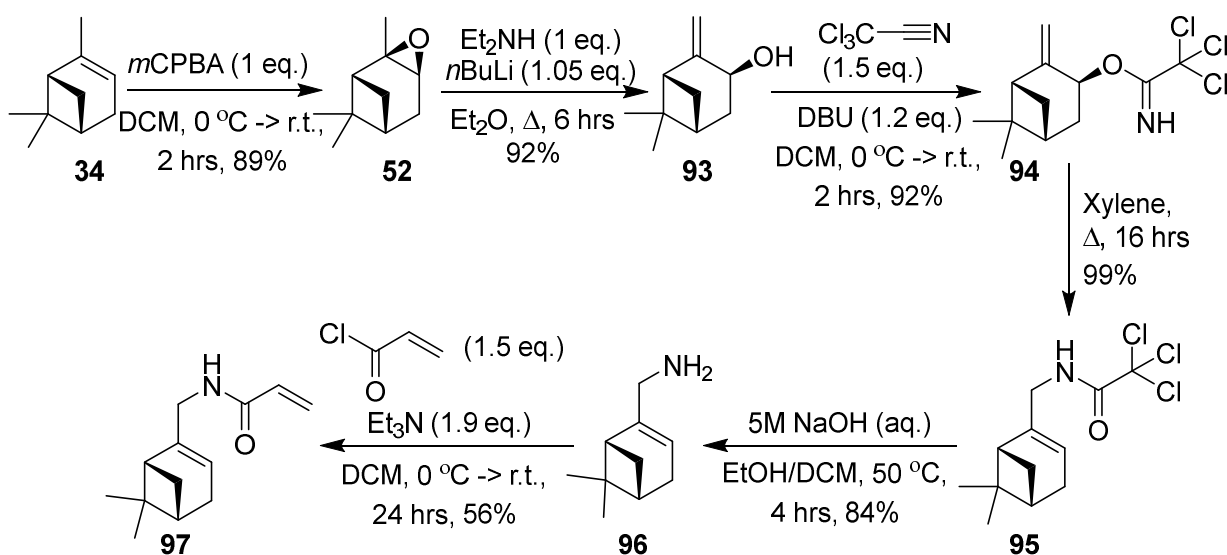
Scheme 31: Synthesis Route to N-Myrtenyl Acrylamide

The full mechanism for the synthesis of *N*-myrtenyl acrylamide initiates with the epoxidation of (-)-α-pinene (Scheme 32). (-)-α-Pinene **34** was diastereoselectively epoxidised using *m*CPBA with retention of stereochemistry due to steric hindrance of the bulky *gem*-dimethyl group during the concerted mechanism directing the face of attack. α-Pinene oxide **52** underwent a base-promoted epoxide isomerisation using stoichiometric amounts of *n*-butyl lithium and diethylamine to form lithium diethylamide as the base resulting the formation of pinocarveol **93**. Deprotonated pinocarveol nucleophilically attacks trichloroacetonitrile to

form pinocarveol trichloroacetimidate **94** which undergoes a thermally induced [3,3]-sigmatropic rearrangement to form myrtenyl trichloroacetamide **95**. Base-catalysed amide hydrolysis forms myrtenyl amine **96** which nucleophilically attacks acryloyl chloride under basic conditions to form myrtenyl acrylamide **97**.
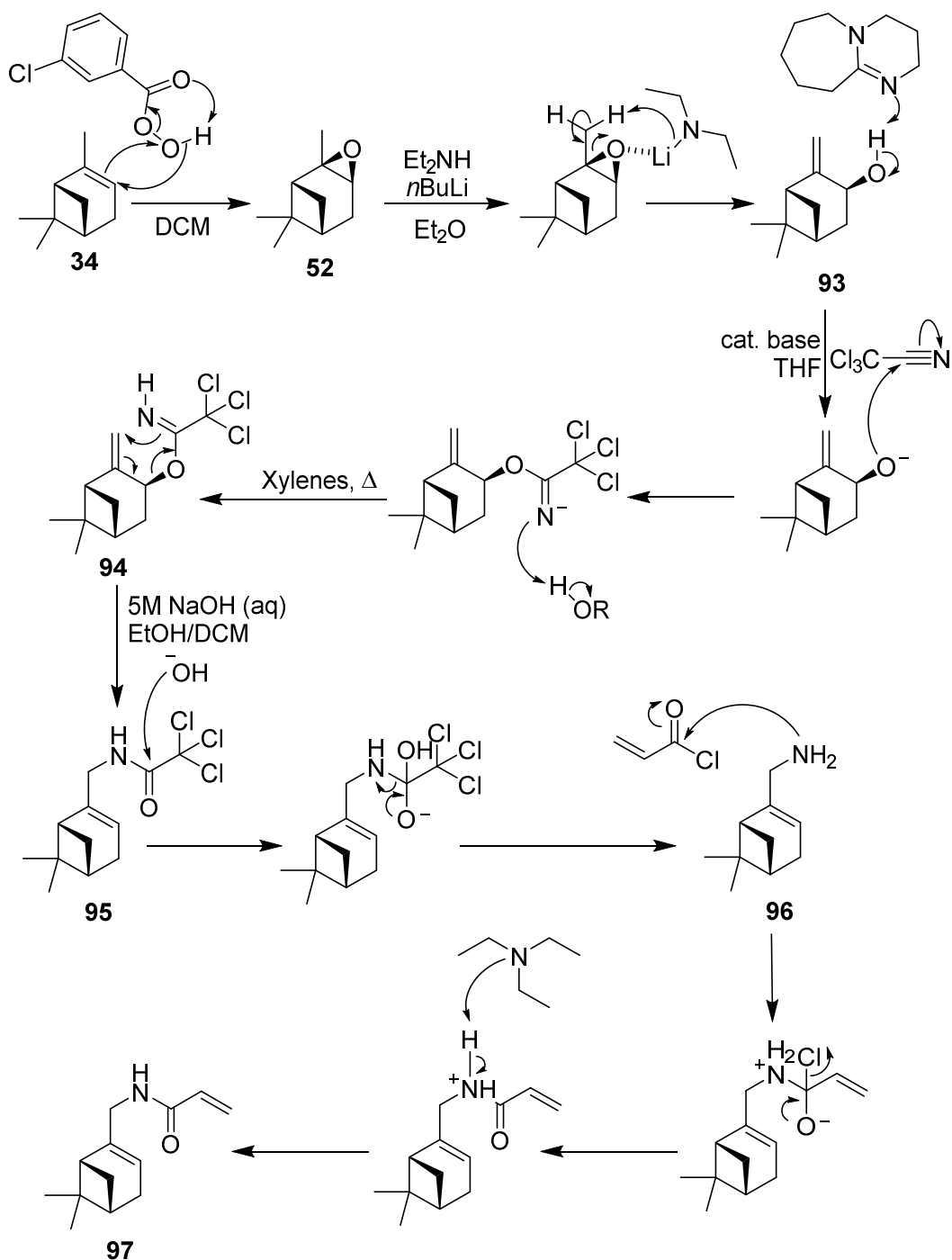
Scheme 32: Full Mechanism for the Synthesis of N-Myrtenyl Acrylamide

Within industry, the formation of an amide using either a commercially available acid chloride as the acylating reagent or the *in situ* generation of one using a low-cost chlorinating agent, is still by far the most popular according to the data collected by Sabatini *et al*.[104] This is due to the low waste output of the reaction, although the sustainability and safety of this traditional reaction has led to an increase in the use of amide coupling reagents. In both literature and industry, Sabatini *et al*. reported T3P® and HATU to be the preferred options.[104] Investigations into alternative acylating and coupling reagents between acrylic acid and myrtenylamine found T3P® to be the optimum coupling reagent forming myrtenyl acrylamide in an 84 % yield (Scheme 33 Route **C**). Fortunately, T3P® was also the most sustainable route out of the three as although a large amount of reagent waste was produced, the reagents and solvents were the safest and most sustainable.
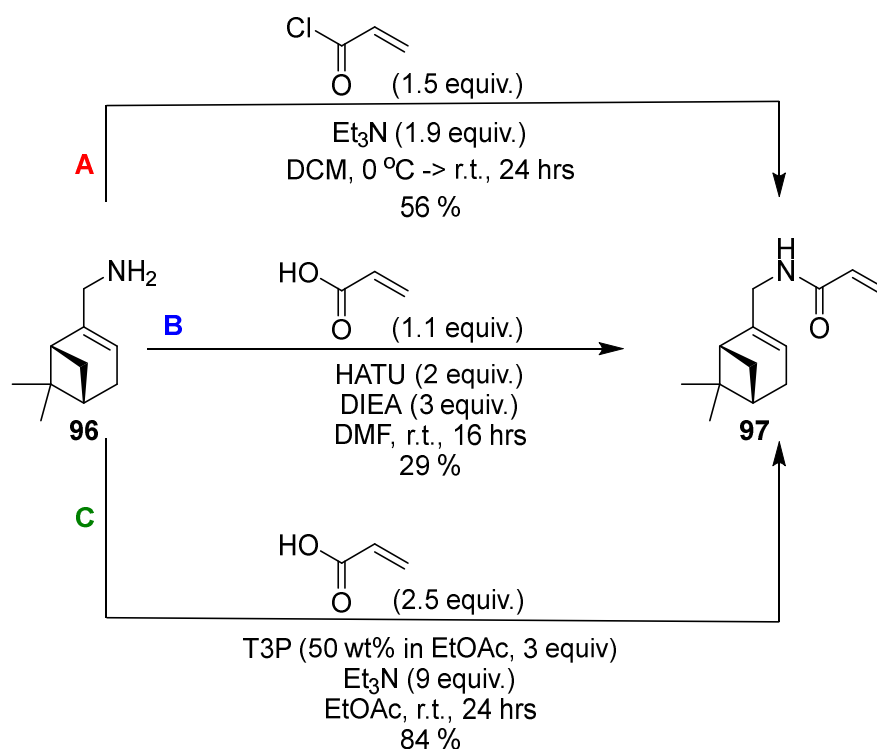
Scheme 33: Comparison of Amidation Reactions in the Synthesis of N-Myrtenyl Acrylamide

Although the successful synthesis of novel acrylamide monomers have been achieved *via* the Overman rearrangement. Shorter, more sustainable routes of three or less steps are

desirable commercially for the synthesis of new monomers to be economically viable. However, the current route *via* the Overman rearrangement requires several hazardous reagents including toxic and expensive trichloroacetonitrile. If these novel monomers are to be considered commercially, a shorter alternative route with more environmentally friendly reagents is needed. Investigations into replacing the Overman rearrangement to synthesis myrtenylamine followed two different routes. A two-step synthetic route starting with the tosyl protection of myrtenol **88** (Scheme 34) was initially proposed. Inspired by a similar route by Hajjaj *et al*. in 2016,[105] the tosyl alcohol would theoretically be a strong leaving group in a displacement reaction using ammonium hydroxide to form primary amine **96**. This could then be coupled with acrylic acid using the previously reported conditions to form the desired monomer. However, the tosylation step was unsuccessful with recovery of the myrtenol starting material. This was due to the poor nucleophilicity of the unsaturated alcohol preventing the desired S_N1 reaction with tosyl chloride. In the future, the deprotonation of the alcohol with a strong base such as *n*-butyllithium could be investigated to activate the alcohol.[106]
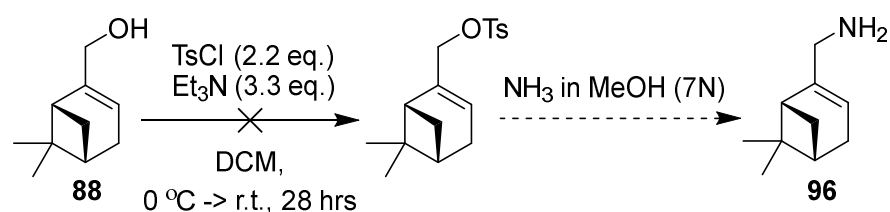
Scheme 34: Tosyl Protection Route to N-Mrytenyl Acrylamide

Next, the reductive amination of myrtenal was proposed. Myrtenal is a commercially available terpenoid which is synthesised commercially *via* the oxidation of myrtenol based on the work by Dangerfield *et al*. in 2010 (Scheme 35).[107] However, initial investigations showed the formation of numerous side products during the reductive amination, potentially due to competing 1, 4-Michael additions.

67
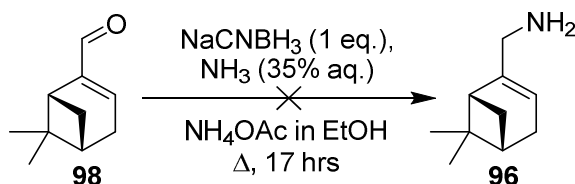
Scheme 35: Reductive Amination Route to N-Mrytenyl Acrylamide

Finally, in collaboration with Chris Peel and Freya Taday we turned to an alternative enzymatic route for the reductive amination using modified transaminase enzymes, ATA-113 and ATA-256. These two enzymes were selected due to their wide substrate acceptance profile and their ability to accept o-xylene diamine (OXYL); a powerful equilibrium driving 'smart' diamine donor system that doubles as a colorimetric screen.[108]

Small scale biotransformations (1 mL) utilising ATA-113 and ATA-256 (2.5mg/mL) were carried out on a 10 mM scale using excess OXYL as the amine donor. GC-FID analysis of the biotransformations after 24 hours at 30°C indicated the reactions had proceeded with quantitative conversion for both ATA-113 and ATA-256. Due to the better active site moiety and generally higher associated with ATA-256, this enzyme was selected for this study. Also, having used OXYL to identify the optimum transaminase, high concentrations of a cheaper amine donor, isopropylamine, was used subsequently.

Small scale biotransformations were set up with ATA-256 and isopropylamine using 50, 100, 150 and 200 mM of substrate aldehyde. GC-FID analysis of the resulting biotransformations after 24 hours at 30 °C revealed the maximum concentration to still achieve quantitative conversion was 50 mM for myrtenal. However, when these conditions were scaled up to 1 mmol, the reactions appeared to stall after achieving around 15 % conversion. Visual examination of the reaction mixtures appeared to indicate the problem may be due to poor substrate solubility, with the mixtures appearing cloudy and non-homogenous. Until this point 20% v/v DMSO had served as a co-solvent to solubilise the substrate into the aqueous reaction mixture.

To examine if this was the case, water soluble organic solvents; THF, acetonitrile, DMF and DMSO were tested for their ability to solubilise the desired substrate into the aqueous reaction media. These were examined visually for each solvent, ranging from 10 – 50 % in 10 % increments. In HEPES buffer, 20% v/v DMF was found to form a non-cloudy homogenous solution with the desired aldehyde substrate and the resulting biotransformation was achieved in quantitative conversion *via* GC-FID and an 83 % isolated yield.

As previously discussed, myrtenyl amine **96** was taken forward to form myrtenyl acrylamide **97** using T3P® as the coupling agent. This gave the renewable monomer in two steps with a good overall yield of 70 % (Scheme 36). Comparatively to the Overman rearrangement, this biotransformation route is sustainable and viable for industrial scale up.
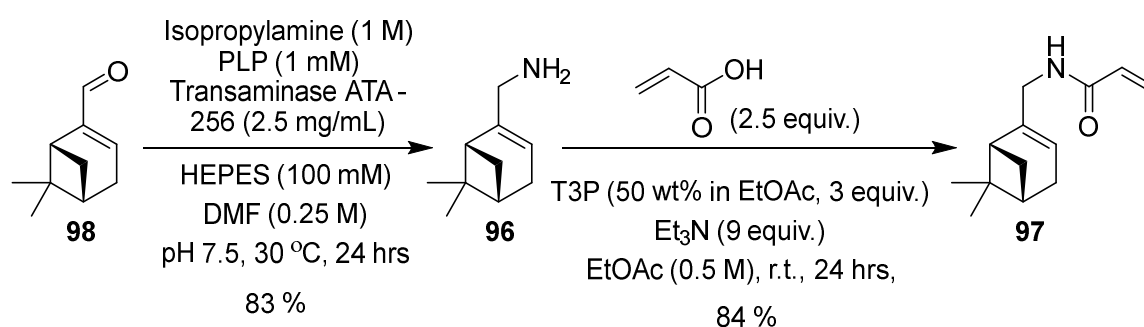
Scheme 36: Synthesis of N-Myrtenyl Acrylamide via Biotransformation

In conclusion, two novel acrylamide monomers, *N*-pinocarveol acrylamide and *N*-myrtenyl acrylamide, have been synthesised using an Overman rearrangement, from α-pinene and β-pinene derived terpenoids in 45 % and 55 % respectively. *N*-Myrtenyl acrylamide was then optimised further by replacing the Overman rearrangement with a single step biotransformation. There is an ongoing debate within industry about the large scale use of enzymes due to the high capital cost and concerns over the disposal of biological waste.[109] In this case, switching the synthesis of myrtenylamine to a biotransformation decreases both the overall energy consumption and the amount of generated waste thereby

improving the sustainability and industrial viability.[110,111] Along with the sustainable T3P®
amidation, *N*-myrtenyl acrylamide was formed in a good 70 % yield.

2.2 Ritter Reaction

The Ritter reaction is an atom economical reaction first reported in 1950, which produces amides through the reaction of nitriles with alcohols or alkenes in the presence of acid (Scheme 37).[98,112] Due to the excess use of acid the reaction scope was limited to the substrates with acid tolerant functionalities only. Several important advances have been achieved in recent years with respect to substrates, the variety of catalysts, the reaction media and the diversity of products.[113,114]
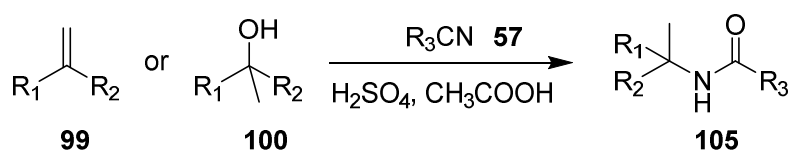
Scheme 37: The Ritter Reaction

Initially, a carbocation (**102**) is generated from an alcohol (**100**), an alcohol derivative, or an alkene (**99**) using an acid (usually concentrated sulfuric acid) (Scheme 38). The carbocation (**102**) then undergoes a nucleophilic attack from the nitrile to produce a nitrilium species (**103**), which hydrates to form an amide (**105**).
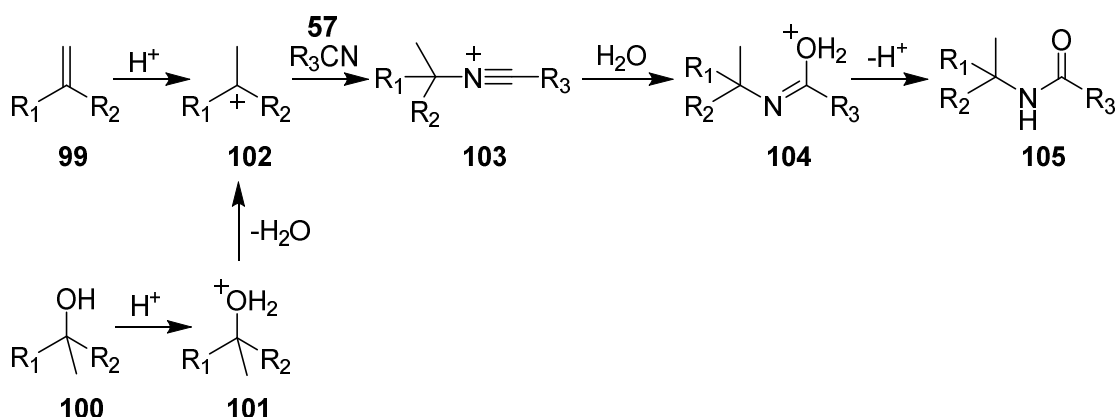
Scheme 38: Accepted Mechanism of the Ritter Reaction

The one-step Ritter reaction potentially has a high sustainability factor, due to the high atom economy and low E factor (total waste/product), especially when run solvent-free. In addition, the reagents, alkenes, and alcohols, are ubiquitous, cheap, commercially available materials including naturally occurring materials such as terpenes and terpenoids. The Ritter reaction has already been used in the large-scale industrial synthesis of several drugs, including amantadine, an anti-Parkinson's drug, and Indinavir, a protease inhibitor used to treat HIV/AIDS (Figure 23).[115,116]
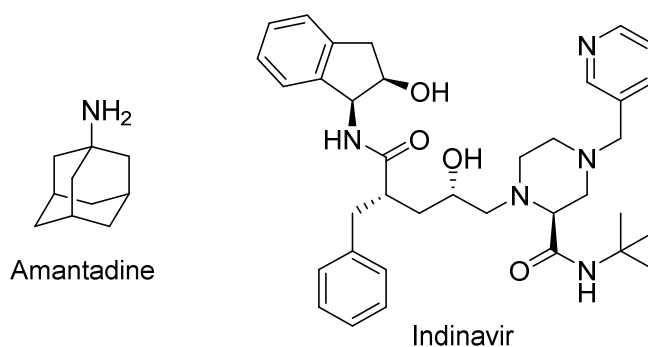
Figure 23: Examples of Substrates Synthesised Using the Ritter Reaction

The recent progress made towards the Ritter reaction has produced good yields in a wide range of reactants during a short reaction time under solvent-free conditions with low metal catalyst loadings. The most promising developments in the Ritter reactions are the reported methods using microwave technology.[55–57]

Terpenes are often used as cheap chiral reagents in substrate scopes to test the robustness of new methodologies, including new developments in the Ritter reaction. Ritter and co-workers themselves used camphene in his original reaction with sulfuric acid (Scheme 39).[98] Naturally found in coniferous trees, camphene (**106**), is industrially produced by the catalytic isomerisation of α-pinene (**34**).[117] Few details were given about the reaction conditions surrounding the synthesis of *N*-isobornyl acrylamides.

72
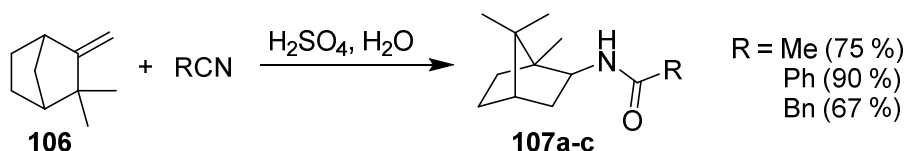
Scheme 39: Synthesis of N-Isobornyl Acetamide/Phenylamine/Benzylamine by Ritter and co-workers

2.2.1 *N*-Isobornyl Acrylamide

Closely related to the commercially available isobornyl acrylate and methacrylate, *N*-isobornyl acrylamide is the most targeted terpene-derived acrylamide in the literature and therefore its commercial synthesis was investigated first. The synthesis of *N*-isobornyl acrylamide has been previously reported *via* the Wagner-Meerwein rearrangement and subsequent Ritter reaction of camphene or *L*-borneol with acrylonitrile using a variety of Brønsted and Lewis acid catalysts.

The Wagner-Meerwin rearrangement was first discovered in bicyclic terpenes and has since been utilised in the large-scale synthesis of many drugs and anti-tumour agents. The mechanism includes the generation of the 2-norbornyl cation in the [1,2]-shift of an adjacent carbon-carbon bond to generate a new carbocation in a thermodynamically more stable structure. (Scheme 40) In accordance, with the Woodward-Hoffman rules the stereochemistry of the migrating group is maintained although depending on the structure and stereochemistry of the substrate the mechanism of the rearrangement can vary.[118–121]
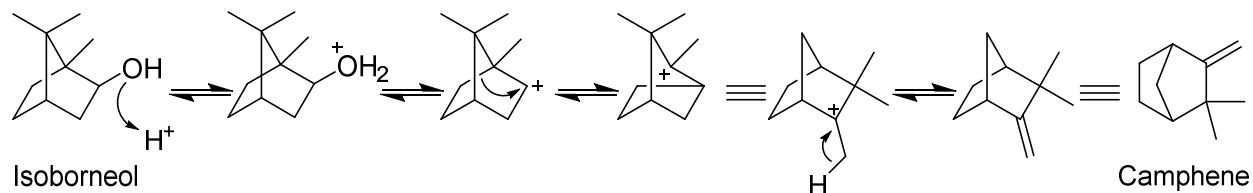
Scheme 40: Mechanism of the Wagner-Meerwein Rearrangement

While the formation of *N*-isobornyl acrylamide was first hypothesised in 2002 by Kazahov, Kazantsev and Malyshev, it was not characterised until 2012 by Hanzawa *et al*. Synthesised under solvent free conditions using catalytic iodine in the presence of water *N*-isobornyl acrylamide **108** was isolated in an 83 % yield (Scheme 41).[122] However, attempting to expand this methodology to other terpenes including α-pinene, β-pinene and limonene, was unsuccessful giving either no reaction or complex mixtures.
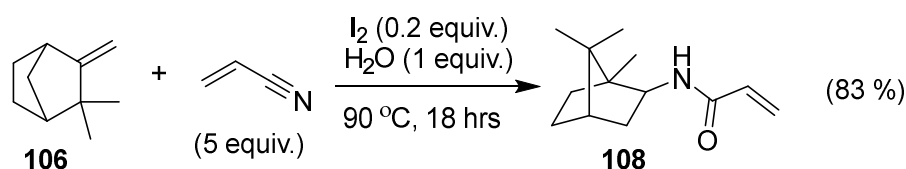
Scheme 41: Synthesis of N-Isobornyl Acrylamide by Hanzawa et al.[122]

Four years later, Posevins, Suta and Turks reported the synthesis of racemic *N*-bornyl acrylamides *via* an indium triflate catalysed Ritter reaction in liquid sulfur dioxide (Scheme 42).[123] In this case, *L*-(-)-borneol **109** was used as the starting material which underwent a 6, 2-hydride shift of the intermediate carbenium ion to form the products in a 68 % yield. More conventional conditions for the Ritter reaction of *L*-(-)-borneol **109** with acetonitrile, stoichiometric H_2SO_4 (10 equiv.) and acetic or trifluoroacetic acid resulted in a 55 % yield.
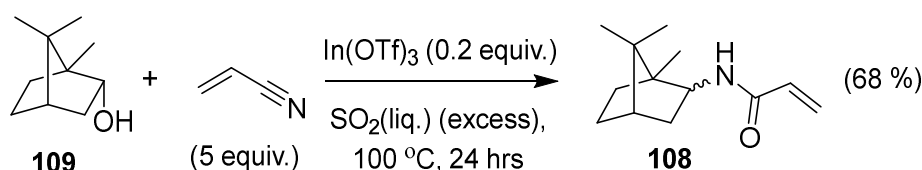
Scheme 42: Synthesis of N-Bornyl Acrylamides by Posevins, Suta and Turks[123]

In 2019, a patent CN109810011A reporting the novel synthesis of *N*-isobornyl acrylamide **108** for the application of high molecular polymerisations was published (Scheme 43).[124] A screen of Lewis acid catalysts gave $FeCl_3$ (18 mol%) at 120 °C for 12 hours as the optimum conditions with a yield of 90 % and a reaction selectivity of 97.8 %. Although polymerisation

74

conditions were not given, it was reported that the unique scaffold structure of poly(*N*-isobornyl acrylamide) gives good water resistance, thermal stability and a high glass transition temperature. Properties that are compatible with various resins, solvents, pigments and fillers.
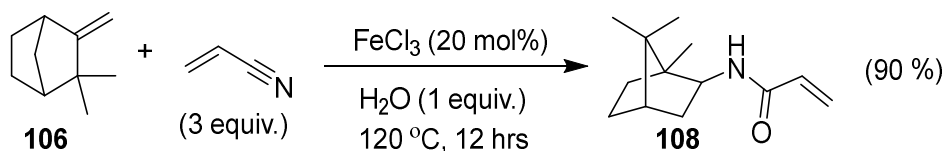
Scheme 43: Synthesis of N-Isobornyl Acrylamide within Patent CN109810011A[124]

Our initial investigation was inspired by the original Ritter paper by using only inexpensive sulfuric acid as a Brønsted acid catalyst (Scheme 44). Although water was stated on the original reaction scheme, we decided to conduct the reaction in neat conditions with acrylonitrile acting as both a reagent and the solvent. Water was added after 2 hours once full conversion was reached *via* TLC to give *N*-isobornyl acrylamide as clear crystals in 72 %. Analysis of the *J* values and coupling interactions within a range of NMR techniques (^{1}H, ^{13}C, COSY, HSQC, HMBC) determined the stereochemistry which was confirmed within literature.[122]
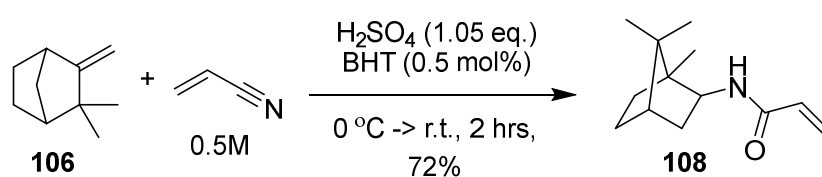
Scheme 44: Initial Synthesis of N-Isobornyl Acrylamide

As previously stated, under acidic conditions, camphene rearranges *via* the Wagner-Meerwein rearrangement to form the isobornyl carbocation. This allows for nucleophilic attack by the nitrile forming the nitrilium ion. This was then hydrated to form *N*-isobornyl acrylamide (**108**) (Scheme 45).
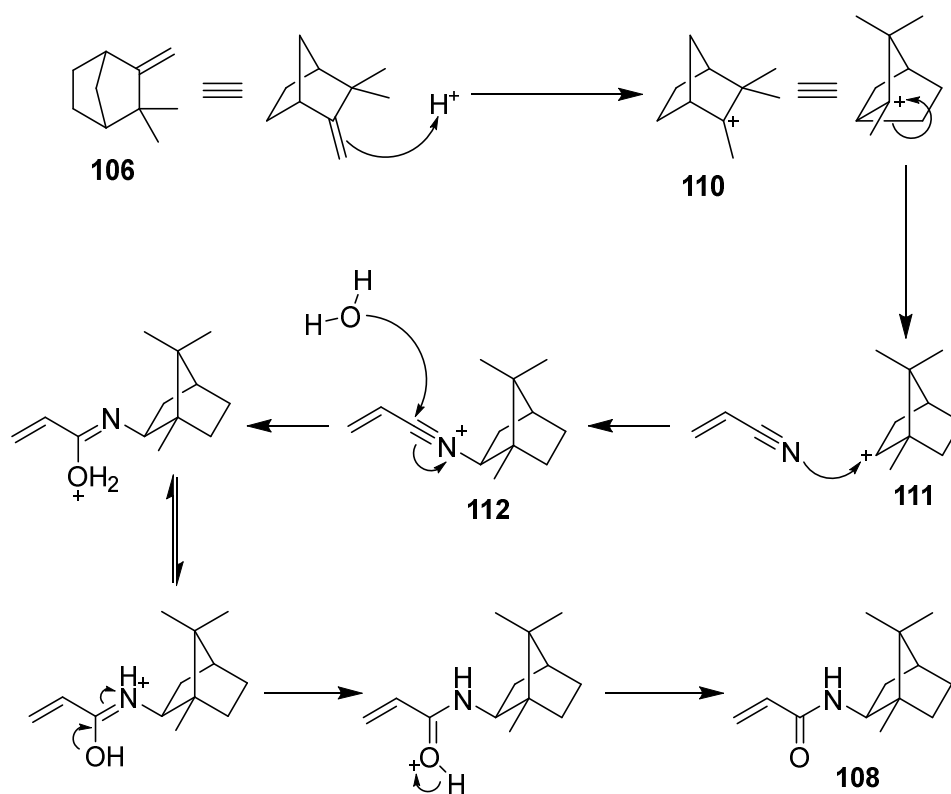
Scheme 45: Mechanism of the Ritter reaction on Camphene

Stereospecific nucleophilic attack of acrylonitrile to the norbornyl cation **111** gives a nitrilium ion **112** as the *exo*-isomer. This rearrangement is both diastereo- and enantioselective due to the transition state favouring an antiperiplanar attack by the nitrile to form the *exo*-isomer (Scheme 46).
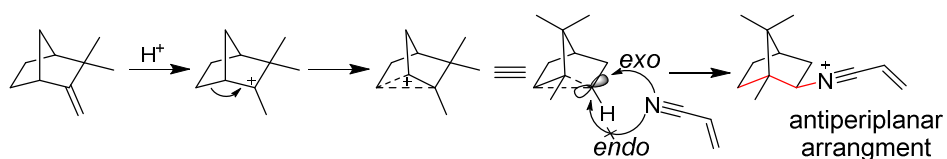
Scheme 46: Simplified exo vs endo diagram for bicyclic systems

This is then hydrated to form *N*-isobornyl acrylamide selectively as one stereoisomer. This was confirmed by the X-Ray crystal structure of *N*-isobornyl acrylamide after hot recrystallization in methanol. (Figure 24)
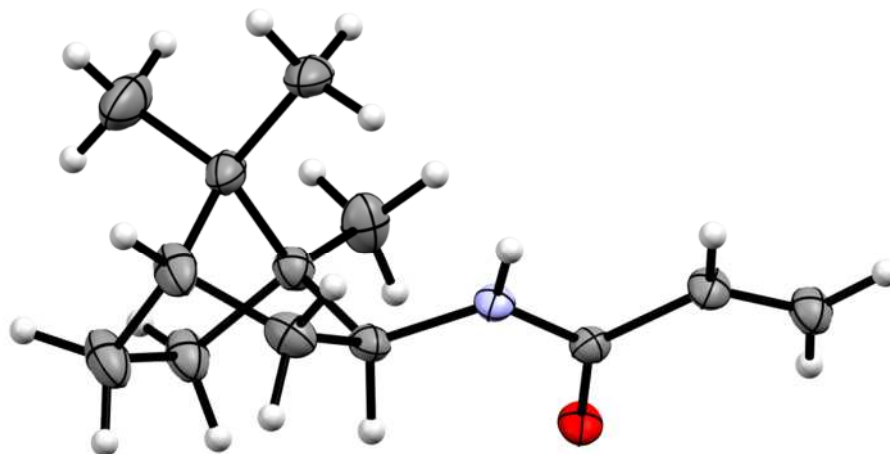
Figure 24 : Crystal Structure of N-Isobornyl Acrylamide

Isoborneol **113** and *L*-borneol **109** were used also investigated briefly as alternative starting materials for the Wager-Meerwein rearrangement. *N*-Isobornyl acrylamide **108** was successfully formed from isoborneol in a 72 % yield. However, after several attempts varying the concentration of acid and reaction time, no acrylamide was observed from *L*-borneol (Scheme 47).
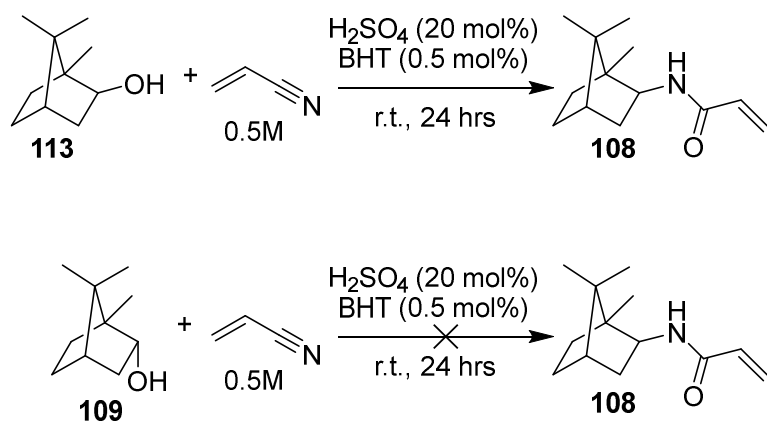
Scheme 47: Route to N-Isobornyl Acrylamide from Isoborneol and L-(-)-borneol respectively

The failure of *L*-borneol as a starting material is due to *trans-anti-peri*-planar arrangements, the *exo*-isomer would give the bridged cation that we know but the *endo*-isomer should give the more strained, unfavourable bridged cation (Figure 25).[125]
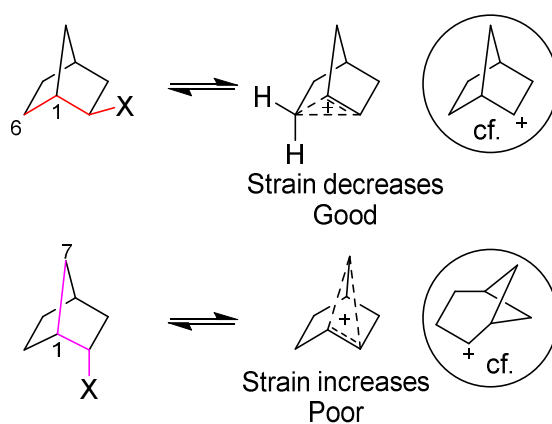
Figure 25 : Diagram showing Endo/Exo differences in a Generalised Bicyclic Structure

Although both camphene **106** and isoborneol **113** can be used as starting materials in the formation of *N*-isobornyl acrylamide, camphene is commercially cheaper and so was used as the starting material for the investigations into optimisation and scale up.

The initial yield on a 1 mmol scale (0.15 g) for the Ritter reaction between camphene and acrylonitrile was 72 %. However, when the scale of the reaction was increased to 10 mmol

(1.5 g), there was a slight exotherm (4 °C) during the addition of sulfuric acid and after 24 hours a poor yield of 29 % was isolated (Table 2 Entry 1). Optimisation of the synthesis of *N*-isobornyl acrylamide was conducted with a range of acid concentrations, solvents, and reaction times investigated. (Table 2)

By monitoring the reaction by TLC it was determined that the reaction had reached completion after 2 hours giving a comparable yield of 28 % (Table 2 Entry 2). In order to improve the safety and the control of the reaction, especially on larger scales, sulfuric acid was added at 0 °C, after which the reaction was warmed to room temperature, this gave a comparable isolated yield of 28 % so this methodology was subsequently used for all future reactions.

Table 2: Optimisation of N-Isobornyl Acrylamide
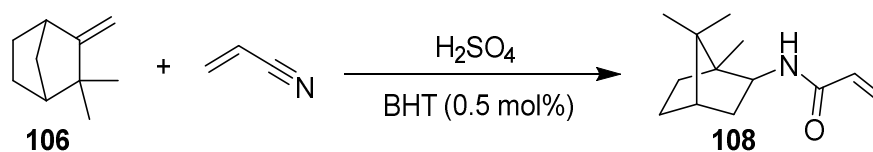
Entry	[H_2SO_4] (equiv.)	Acrylonitrile (M)	Time (hours)	Addition Temperature (°C)	Isolated Yield (%)
1	1.05	0.5	24	20	29
2	1.05	0.5	2	20	28
3	1.05	0.5	2	0	28
4	0.5	0.5	2	0	21
5	1.5	0.5	2	0	33
6	2.1	0.5	2	0	42
7	2.1	1	2	0	64
8	2.1	2	2	0	54

Next, we looked to improve the yield by investigating the acid catalyst loading at 0.5, 1.5 and 2.1 equivalents in comparison to the previously used 1.05 equivalents (Table 2 Entries 4-6). As the acid catalyst loading increased, the yield increased proportionally to 42 %. The acid catalyst loading was not taken further than 2.1 equivalents for safety reasons as quenching higher quantities of strong acid with saturated sodium bicarbonate on a large scale would have been unsafe.

The chart shows Yield (%) on the y-axis (0 to 50) versus [H$_2$SO$_4$] (equiv.) on the x-axis (0 to 2.5). The fitted line is labelled:

$$y = 12.99x + 14.276$$
$$R^2 = 0.9964$$
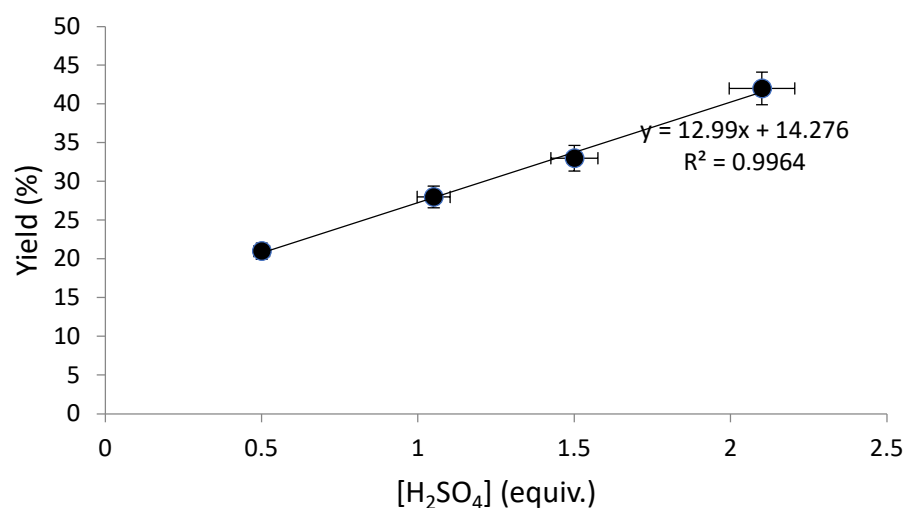
Figure 26: Graph Showing the Effect of Acid Loading on the Isolated Yield

Finally, the concentration of the reaction was investigated with acrylonitrile as both a reagent and the solvent added at 1 and 2 M (Table 2 Entries 7 & 8). Comparatively to the 0.5 M reaction giving a yield of 42 %, increasing the concentration, increased the yield. Interestingly however, 1 M was the optimum concentration giving a yield of 64 % compared to 54 % at 2 M. This was potentially due to degradation of camphene in the concentrated acidic mixture.

Once the optimum conditions of 2.1 equivalents of sulfuric acid with 1 M acrylonitrile were determined, the synthesis of *N*-isobornyl acrylamide was scaled up 100 fold to form over 200 g of product (Table 3). Fortunately, as the scale increase so did the yield, up to a good 81 %.

Table 3: Scale Up of N-Isobornyl Acrylamide Synthesis
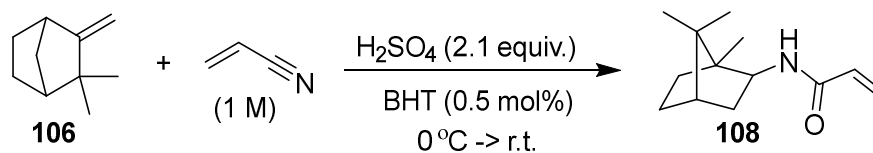
Scale (mmol)	Reaction time (hrs)	Isolated Yield (g)	Isolated Yield (%)
10	2	1.0/1.3	64
50	16	5.9	58
250	24	41.5	81
1250	24	207.5	81

As well as being high yielding, this one-step reaction is facile; quenching the reaction with sodium bicarbonate gives the product as an easily filtered white solid. The waste output is also low as the acrylonitrile can be partially recovered, reducing reaction costs. *N*-isobornyl acrylamide was determined to be an air stable solid at room temperature. When left in the crude solution at 5 °C for 1 month before isolation the yield dropped from 64 % to 41 %, representing a less than 1 % drop in yield per day, demonstrating good stability for industrial transport, storage and use.

Although the formation of *N*-isobornyl acrylamide using sulfuric acid and acrylonitrile is cheap, industrially viable and high yielding, the reagents themselves have many hazards associated with them (flammable, corrosive, irritant and toxic). Ideally, these reagents would be exchanged for less harmful reagents that are still cheap, industrially viable and high yielding.

Initially, Amberlyst® 15 was investigated as a replacement for sulfuric acid. Amberlyst® 15 is a non-hazardous, heterogeneous acid catalysis consisting of a polystyrene based ion exchange resin with strongly acidic sulfonic group. It has already been used successfully as a

replacement for sulfuric acid in Ritter-type reaction by Das *et al.* in 2006[126] and Mokhtary and Goodarzi in 2012.[127]

Here, the equivalents of Amberlyst® 15, acetic acid and acrylonitrile were investigated, along with the reaction temperature and time. Starting with the conditions reported by Mokhtary and Goodarzi in 2012,[127] *t*-butyl acetate **114** was reacted with acrylonitrile with a large excess of Amberlyst® 15 at 70 °C, also demonstrating good recyclability of the catalyst (Scheme 48).
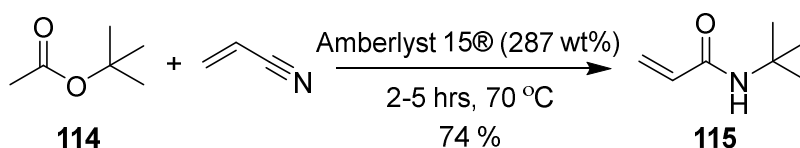
Scheme 48: Amberlyst® 15 in the Ritter reaction of t-Butyl Acetate and Acrylonitrile

The paper in 2012 used an equal ratio of ester (instead of the traditional alcohol or alkene) and nitrile. However due to stirring constraints, in our reaction 2 M acrylonitrile was used (Table 4 Entry 1). These conditions unfortunately gave a poor isolated yield of 5 % due to a low conversion rate. In order to improve the conversion rate, acetic acid was added as a co-catalyst, as in the historical Ritter reaction.[98] This did slightly improve the isolated yield although it was still a poor 13 % (Table 4 Entry 2). The premise behind using Amberlyst® 15 as a heterogeneous substitute for sulfuric acid, as well as to reduce the number of hazardous reagents, was to improve the recyclability of the acrylonitrile by simply filtering off the solid catalyst and product. As the addition of acetic acid didn't dramatically improve the reaction, it was decided it would not be included in further optimisations. Next the relevance of the reaction temperature was investigated by repeating the original reaction at room temperature (Table 4 Entry 3). This gave a poor but comparable yield suggesting that temperature was not a major factor in the high conversion of this reaction. The low conversion was suggested to be due to the poor mixing of the reaction with the excess of Amberlyst® 15. Therefore the concentration of acrylonitrile was decreased to 1 M, with the possibility of solvent recyclability negating waste concerns (Table 4 Entry 4). Although, the reaction at 6 hours gave a comparable yield, leaving the reaction for 24 hours gave a

significant improvement to 28 % yield (Table 4 Entry 5). After 24 hours, the reaction degraded giving a lower isolated yield, 14 %, after 72 hours (Table 4 Entry 6). The simultaneous use of a lower volume of Amberlyst® 15 gave lower conversions and a lower isolated yield at 11 % (Table 4 Entry 7).

Table 4: Synthesis of N-Isobornyl Acrylamide using Amberlyst® 15
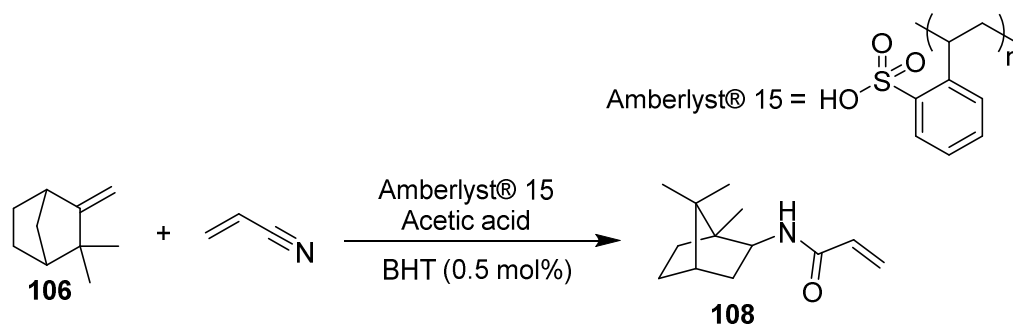
Entry	Amberlyst® 15 (equiv.)	Acetic acid (equiv.)	Acrylonitrile (M)	Temperature (°C)	Time (hrs)	Isolated Yield (%)
1	15	-	2	70	6	5
2	15	1.1	2	70	6	13
3	15	-	2	r.t.	6	5
4	15	-	1	r.t	6	6
5	15	-	1	r.t.	24	28
6	15	-	1	r.t.	72	14
7	5	-	1	r.t.	72	11

In conclusion, *N*-isobornyl acrylamide has been synthesised *via* the Ritter reaction between acrylonitrile and both camphene and isoborneol with either concentrated sulfuric acid or Amberlyst® 15. One of Croda's sustainability aims is to have over 75 % by weight of biobased material in their organic raw materials by 2030; synthesising *N*-isobornyl

acrylamide from camphene or isoborneol means that 82 % of the monomer is biobased, achieving this aim. Successful recovery of excess acrylonitrile was also achieved. The optimum conditions using camphene, acrylonitrile and concentrated sulfuric acid were scaled up to a hundred gram scale in a reliable, facile, one-step reaction with a simple filtration purification to form *N*-isobornyl acrylamide as an air-stable white powder in a very good 81 % yield.

2.2.2 *N-trans* Sobrerol Acrylamide

Already reported as the starting material for several novel renewable polymers within the literature,[68,69] *trans*-Sobrerol (**53**) is a terpenoid synthesised commercially from α-pinene; *via* oxidation then rearrangement of the bicyclic terpene to form the terpenoid diol in an overall yield of 56 % (Scheme 49).[128]
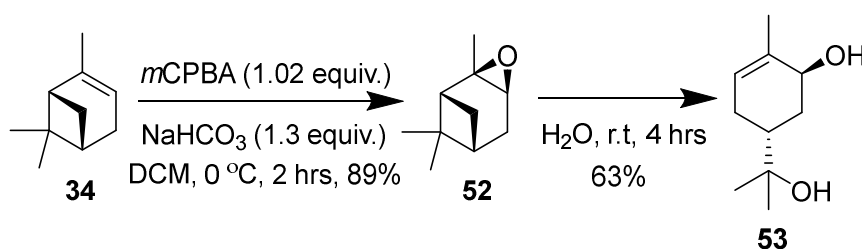
Scheme 49: Synthesis of trans-Soberol from α-Pinene

α-Pinene oxide was formed using the epoxidation of α-pinene **34** using *meta*-chloroperoxybenzoic acid (*m*CPBA). This concerted mechanism happens with retention of stereochemistry and high enantioselectivity to form α-pinene oxide **52** in 89 % yield (Scheme 50).
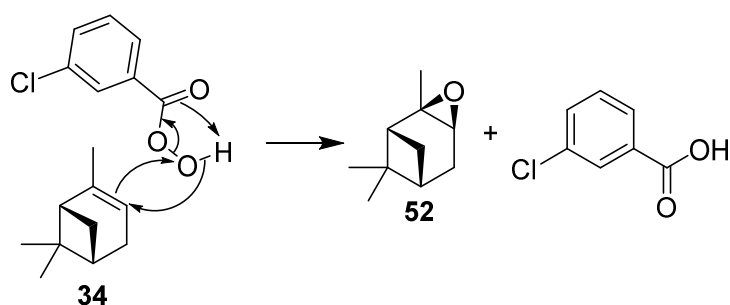
Scheme 50: Mechanism for the Epoxidation of α-Pinene

α-Pinene oxide **52** underwent acid-catalysed ring-opening and rearrangement during hydrolysis at room temperature and was first reported by Xu and Qu[129] to form the corresponding enantiomerically pure *trans*-sobrerol **53** in 63 % yield (Scheme 51).
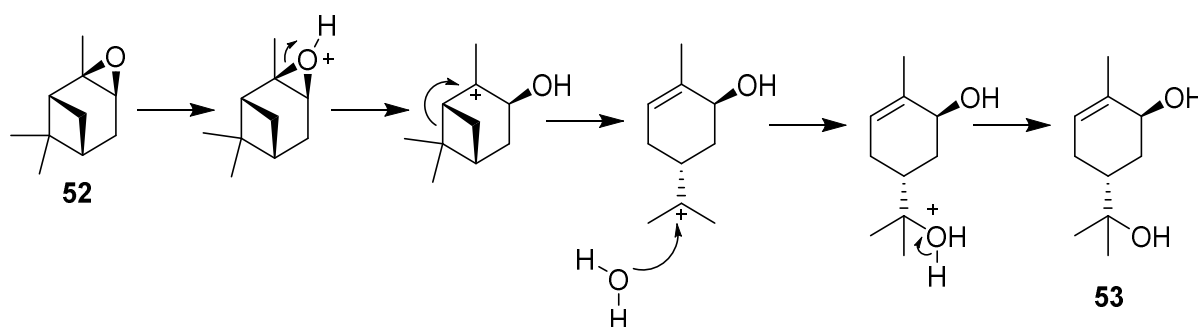
Scheme 51: Ring Opening Mechanism of α-Pinene Oxide

As a potentially explosive peroxide, *m*CPBA is problematic on a large scale and chlorinated solvents such as dichloromethane have significant health and environmental issues, so an alternative route was investigated for the formation of α-pinene oxide. An epoxidation using the *in situ* formation of dimethyldioxirane (DMDO) was employed (Scheme 52).
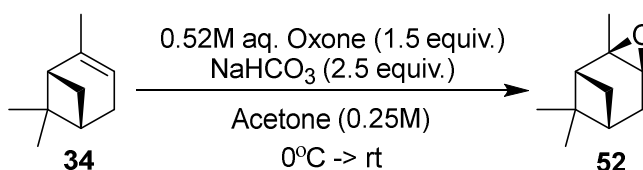
Scheme 52: Initial investigations into the Formation of α-Pinene Oxide using Oxone®

The peroxymonosulfate anion reacts with acetone in a base-catalysed nucleophilic addition reaction (Scheme 53). The sulfate, as a good leaving group, facilitates the base-catalysed ring closure to dimethyldioxirane. Dimethyldioxirane, also referred to as Murray's reagent, is a powerful epoxidising agent and epoxidises α-pinene in a concerted mechanism to form α-pinene oxide.
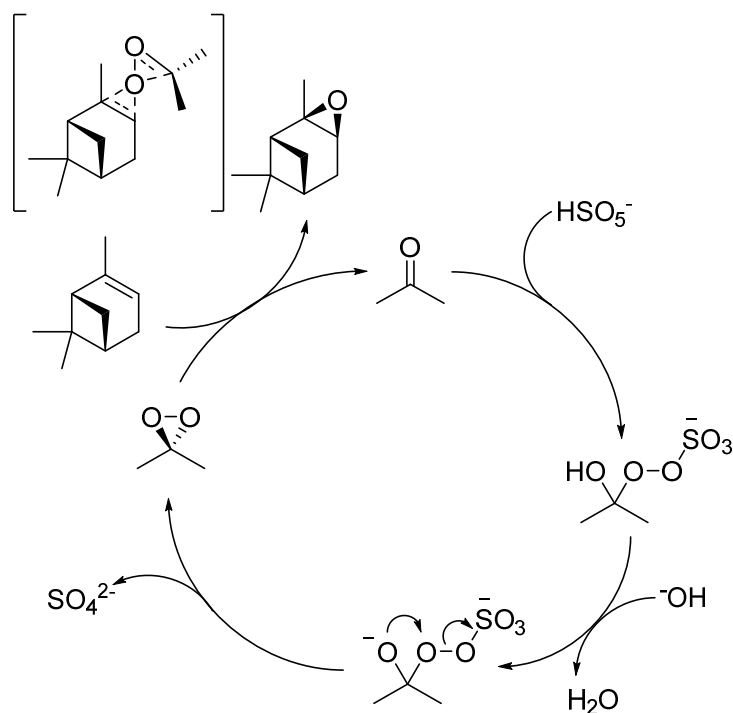
Scheme 53: DMDO Epoxidation Mechanism of α-Pinene Oxide

Initially the crude biphasic mixture was taken forward and reacted as previously reported with CO_2 in water to give *trans*-sobrerol in a 47 % yield (Scheme 54). However, when the biphasic crude was left to stand in air clear crystals formed, after washing with cold DCM these were identified as *trans*-sobrerol. It was proposed α-pinene oxide can ring opening in the aqueous environment of the dimethyldioxirane reaction to form *trans*-sobrerol. The stereochemistry was determined by COSY, HSQC and HMBC NMR and confirmed against literature.[129]
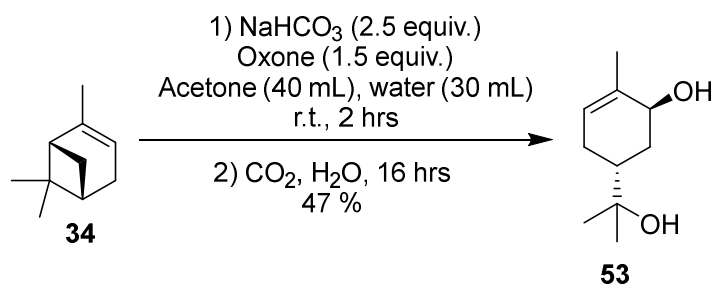
Scheme 54: Initial Investigations into the One-Pot Synthesis of trans-Sobrerol

The synthesis of *trans*-sobrerol in one-step from α-pinene was investigated with optimisation of the reaction time, temperature and reagents. The ring opening reaction is difficult to monitor due to the affinity of *trans*-sobrerol to water. As the epoxidation of α-pinene rapidly reaches full conversion as suggested by NMR and TLC, the suspected rate limiting step is the intermolecular epoxide ring opening step, which requires optimisation. Initially the reaction temperature was investigated with a screen at 5 °C, room temperature (~20 °C), 40 °C and 60 °C (Table 5 Entries 1-4). As the temperature increased the yield decreased significantly, showing temperature to be a key factor. Next, the volume of solvent was investigated with the volume of acetone decreased to 5 mL and the volume of water increased from 30 mL to 120 mL, to promote the ring opening step to *trans*-sobrerol (Table 5 Entries 5-7). However, the reduction of acetone from 40 mL to 5 mL drastically decreased the yield to trace amounts where the volume of water was inconsequential. This could potentially be due to the consequently low concentration of DMDO. Next the equivalents of NaHCO$_3$ and Oxone® were screened (Table 5 Entries 8-10). Altering the equivalents of NaHCO$_3$ showed that more equivalents resulted in a slightly higher yield of *trans*-sobrerol. This is due to the pH change associated with higher equivalents of base. When Bleier and Elrod reported the kinetics and thermodynamics of aqueous phase reactions of α-pinene oxide in 2013, they reported lower pH conditions favoured the competing formation of campholenic aldehyde.[130] The equivalents of Oxone® seemed to be non-proportional to the yield. Finally, as the reaction was difficult to monitor, the reaction time was investigated by stopping the reaction after 1, 2.5, 16 and 72 hours (Table 5 Entries 11-14). Surprisingly, the reaction gave a high yield of 35 % after one hour, this yield was stable until 38 % at 16 hours, after which the yield halved at 24 hrs and stayed low at 72 hours. This suggested *trans*-sobrerol is unstable in the aqueous environment, decomposing to a mixture of other terpenoids.

Table 5: Optimisation of a One-Pot Synthesis of trans-Sobrerol
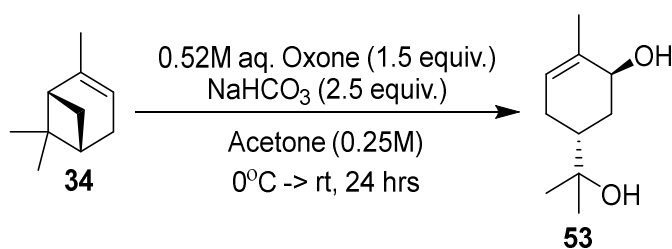
Entry	Oxone® (equiv.)	Acetone (mL)	NaHCO₃ (equiv.)	Water (mL)	Temperature (°C)	Time (hrs)	Yield (%)
1	1.5	40	2.5	30	5	24	31
2	1.5	40	2.5	30	r.t	24	19
3	1.5	40	2.5	30	40	24	3
4	1.5	40	2.5	30	60	24	3
5	1.5	5	2.5	30	r.t.	24	1
6	1.5	5	2.5	90	r.t	28	5
7	1.5	5	2.5	120	r.t.	24	3
8	1.5	40	1.5	30	r.t.	24	5
9	1.5	40	5	30	r.t.	24	26
10	3.0	40	2.5	60	r.t.	24	18
11	1.5	40	2.5	30	r.t.	72	14
12	1.5	40	2.5	30	r.t.	16	38
13	1.5	40	2.5	30	r.t.	2.5	35
14	1.5	40	2.5	30	r.t.	1	35

Next, the use of catalysts that have been previously used in the various reported syntheses of *trans*-sobrerol from α-pinene oxide were investigated. Initially, the Brønsted acid catalyst H_2SO_4 was investigated (Table 6 Entry 1) to both promote the acid catalysed epoxide ring opening and provide a sulfate counter ion to promote the formation of *trans*-sobrerol over campholenic aldehyde as discussed by Bleier and Elrod in 2013.[130] The pH was carefully lowered to pH 5 using H_2SO_4 as with the previous CO_2 reaction, lower pH values shown to favour the competing campholenic aldehyde pathway. However, the addition of H_2SO_4 did not have any effect on the yield overall. The addition of CO_2 was also investigated to create a one-pot reaction based on the previous used strategy reported by Lima *et al*. in 2018.[68] CO_2 was bubbled through with both the original volume of water, 30 mL, and higher volume of 90 mL to produce carbonic acid and promote the formation of *trans*-sobrerol (Table 6 Entries 2 & 3). However, the addition of CO_2 in both cases lead to a decrease in yield when used in a one pot reaction. In 2011, Costa *et al*. reported the use of SiO_2 as a Lewis acid in the synthesis of *trans*-sobrerol from α-pinene oxide in a 69 % yield.[131] When an excess of SiO_2 was added to the reaction, the yield was comparable to the non-catalysed reaction (Table 6 Entry 4). Another Lewis acid catalyst, $RuCl_3$, was used by Rothenberg *et al*. in 1998 to form *trans*-sobrerol from α-pinene oxide in an excellent 94 % yield.[132] However, when $RuCl_3$ was added to the Oxone® epoxidation the yield was comparable to the non-catalysed reaction (Table 6 Entries 5 & 6). The third Lewis acid investigated was the heteropoly acid catalyst $H_3PW_{12}O_{40}$. 0.0075 mM $H_3PW_{12}O_{40}$ in acetone was used by Da Silva Roche *et al*. to form *trans*-sobrerol from α-pinene oxide in a 71 % yield.[133] The Lewis acid catalyst was added for both 16 and 24 hours to the Oxone® reaction (Table 6 Entries 7 & 8). However, again the addition of the catalyst gave a comparable yield to the non-catalysed reaction. Finally, the addition of a counter ion to stabilise the *para*-menthenic cation precursor to *trans*-sobrerol was investigated. NBu_4PF_6 was chosen as Yaragorla *et al*. reported successfully using PF_6^- as a counter ion to the tertiary carbocation formed during a microwave assisted, Ca(II)-catalysed Ritter reaction.[134] However, in this case, the addition of a counter ion resulted in a reduction in the yield to 10 % (Table 6 Entry 9).

Table 6: Investigations into the Effect of a Catalyst on the Synthesis of trans-Sobrerol
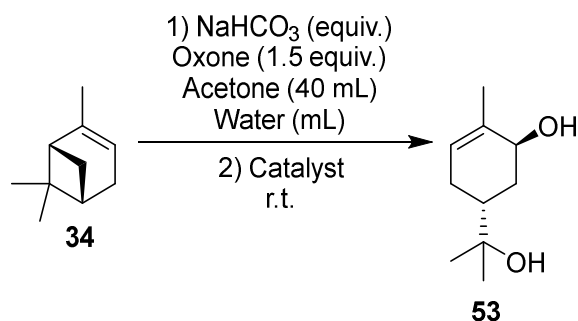
Entry	NaHCO₃ (equiv.)	Water (mL)	Catalyst	Time (hrs)	Yield (%)
1	1.5	30	H_2SO_4 (pH 5)	24	20
2	2.5	30	CO_2 (excess)	4	16
3	2.5	90	CO_2 (excess)	24	6
4	2.5	30	SiO_2 (28 eq.)	24	17
5	2.5	30	$RuCl_3$ (0.1 mol%)	16	24
6	2.5	30	$RuCl_3$ (0.1 mol%)	1	33
7	2.5	30	$H_3PW_{12}O_{40}$ (0.005 mol%)	24	23
8	2.5	30	$H_3PW_{12}O_{40}$ (0.005 mol%)	16	35
9	2.5	30	$NBu4^+PF6^-$	24	10

During their investigations into the $H_3PW_{12}O_{40}$ catalysed isomerisation of α-pinene oxide **52**, Da Silva Roche *et al*. reported the effects of different solvents on the potential reaction pathways.[135] The increase in both solvent basicity and polarity strongly prejudices route **B** to

form campholenic aldehyde **116**, and favours the *para*-menthenic route **A** to form *trans*-sobrerol **53**. However, if the solvent is too basic the direct deprotonation of the *para*-menthenic cation **117** is favoured over the nucleophilic addition of water to form *trans*-carveol **118** (Scheme 55).[133]
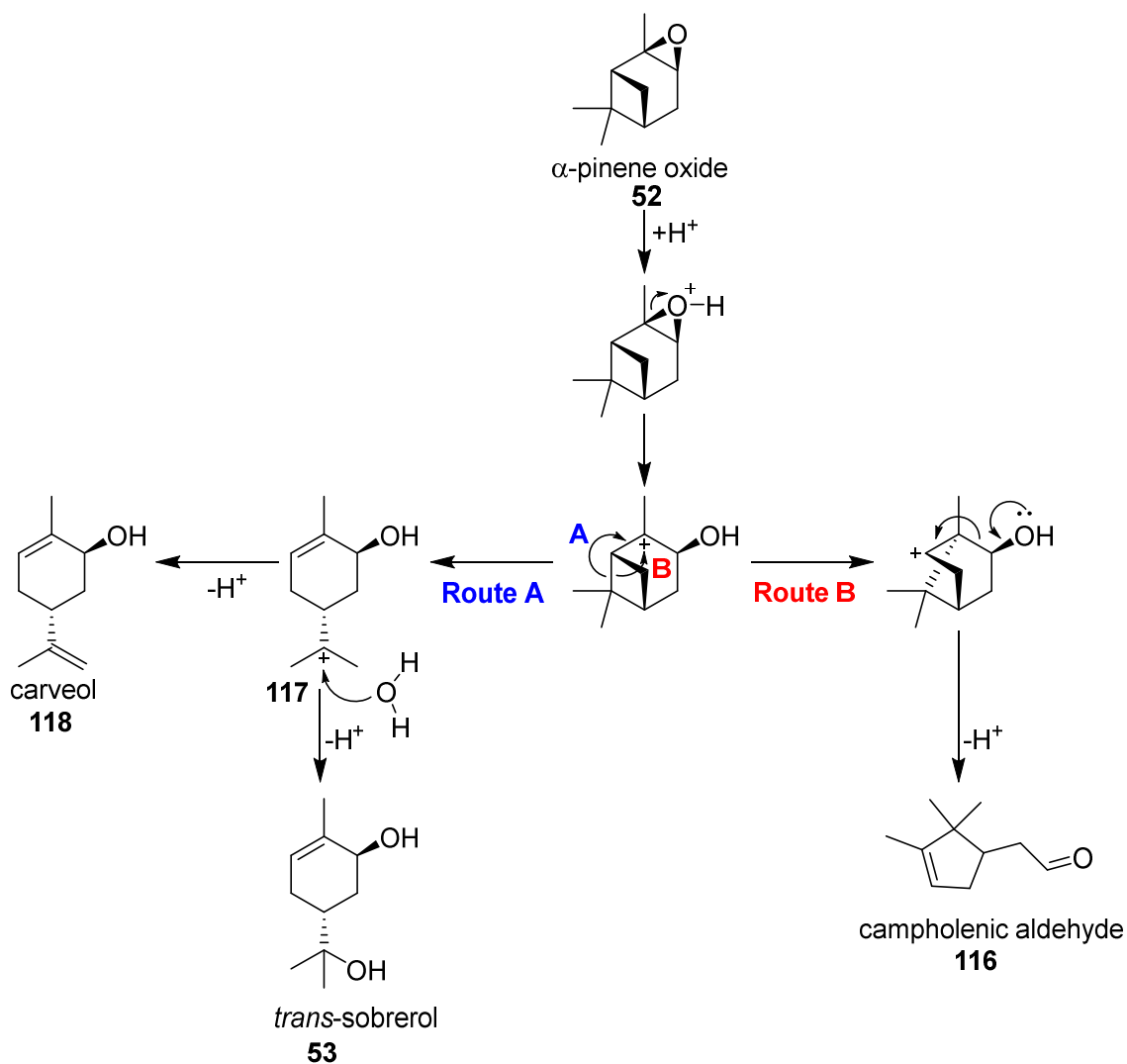
Scheme 55 : Acid-catalysed rearrangements of α-pinene oxide

A small solvent screen was conducted with a range of dielectric constants and basicity's to investigate the effect of solvent on the one-step Oxone® procedure (Table 7). Similarly to the previously reported literature, solvents with high dielectric constants favoured the *para*-menthenic route **A** although the yield was comparable to the original acetone/water

reaction. THF with a dielectric constant of 7.6 gave a trace yield of *trans*-sobrerol **53** at 2 % (Table 7 Entry 4) and DMC with the lowest dielectric constant appeared to inhibit the *para*-menthenic route completely giving a 52 % yield of α-pinene oxide **52** (Table 7 Entry 5).

Table 7: Investigations into the Effect of a Co-solvent on the Synthesis of trans-Sobrerol
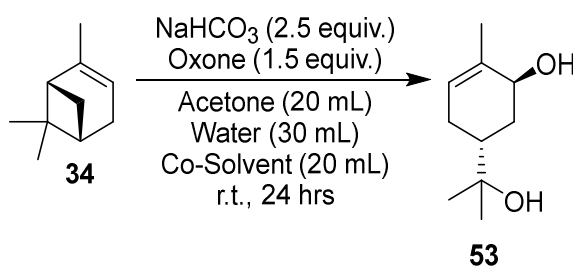
Entry	Co-Solvent (20 mL)	Dielectric Constant $(\varepsilon)^{133,136}$	Approx. pKa (rel. to $H_2O)^{133,137}$	Yield (%)
1	Acetone	20.7	-7	19
2	EtOH	25.3	-2	16
3	MeCN	37.5	-10	21
4	THF	7.6	-3.5	2
5	DMC	3.8	-5.5	0*

*(52% α-pinene oxide)

Comparing the three alternative routes to *trans*-sobrerol (Scheme 56) shows the two greener alternative routes (**B** and **C**) give comparable yields to the original syntheses (**A**) whilst avoiding the use of potentially explosive *m*CPBA and potential carcinogen DCM satisfying some of the green chemistry principles.[7] Alternatively, routes **B** and **C** have minimal hazards associated whilst using a cheaper oxidizing reagent. Future investigations will look at improving the one-pot synthesis further by investigating the scale up and industrial feasibility of the reaction.

93
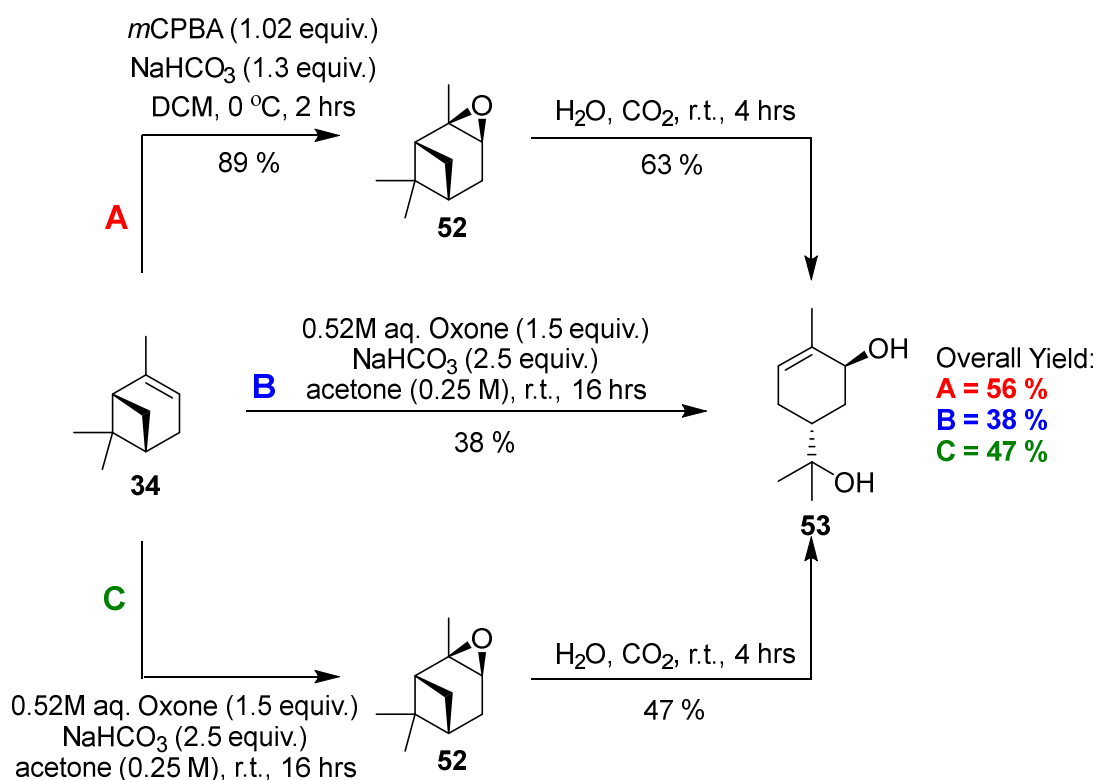
Scheme 56: Comparison of the Three Routes Employed in the Formation of trans-Sobrerol

Trans-sobrerol acrylamide (**2c**) is of particular interest as a novel monomer as the additional functional groups could be further modified either pre- or post-polymerization to further tune the polymer properties. Stamm *et al*. produced biobased coatings through the post-polymerisation thiol-ene click and transesterification reactions with the endocyclic alkene and tertiary alcohol on *trans*-sobrerol methacrylate (Scheme 57).[69] This could be potentially repeated using our poly(*N-trans* sobrerol acrylamide).
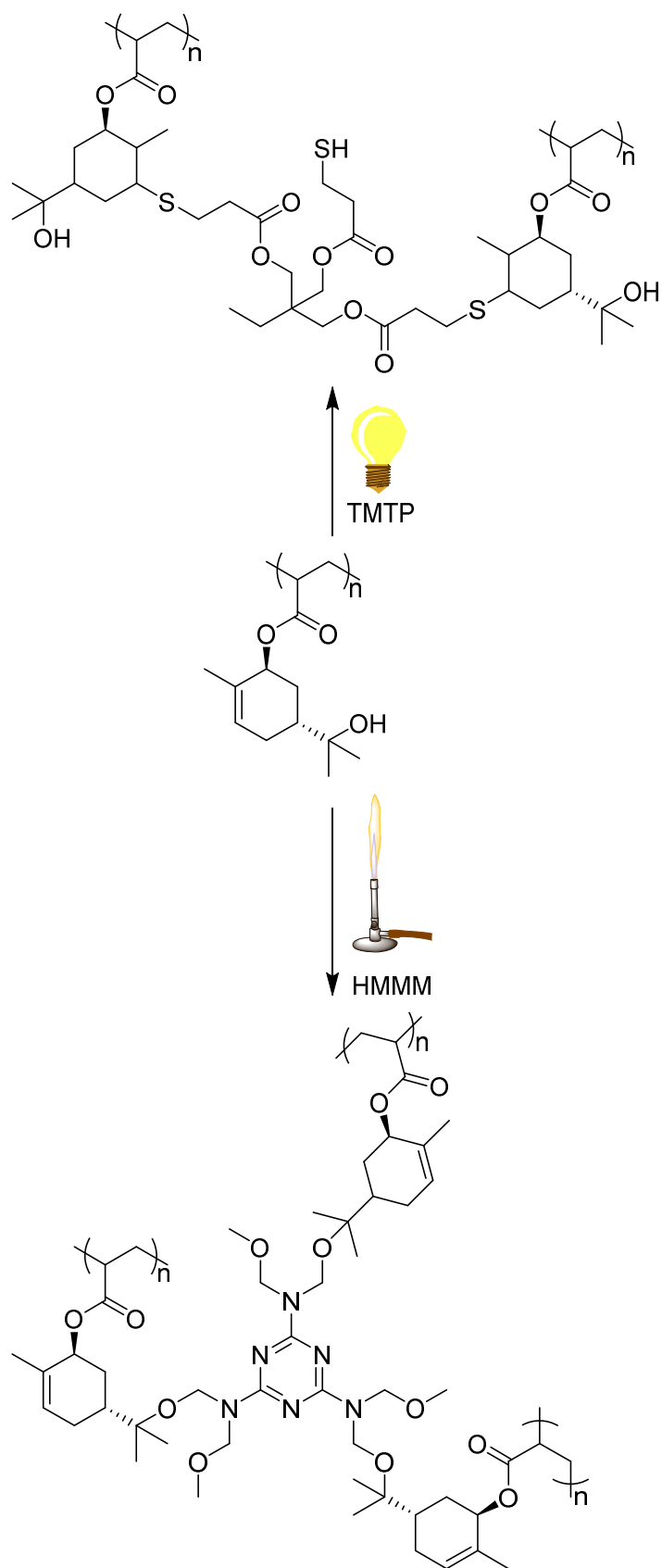
Scheme 57: Formation of biobased coatings using Poly(trans-Sobrerol Methacrylate) and cross-linkers TMTP or HMMM by Stamm et al.[69]

Again, the Ritter reaction using acrylonitrile was employed in the synthesis of *N-trans-*sobrerol acrylamide from starting terpenoid *trans*-soberol. An initial reaction using 1.05 equivalents of sulfuric acid and 0.5 M acrylonitrile gave a moderate yield of 37 %. (Scheme 58)
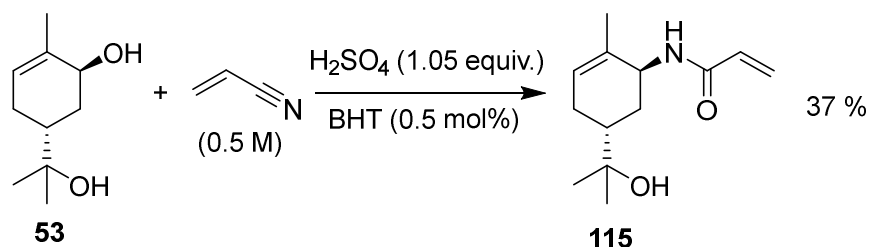
Scheme 58: Initial Synthesis of N-trans-Sobrerol Acrylamide using the Ritter Reaction

As previously discussed, the mechanism for the Ritter reaction on *trans*-sobrerol **53** proceeded *via* the initial formation of an allylic carbocation **119** from the hydrolysis of *trans*-sobrerol **53** under acidic conditions. Acrylonitrile nucleophilically attacks the allylic carbocation (**119**) to form a nitrilium ion intermediate (**120**). Finally, irreversible hydration of the nitrilium ion forms the desired acrylamide **121**, *N-trans* sobrerol acrylamide (Scheme 59).
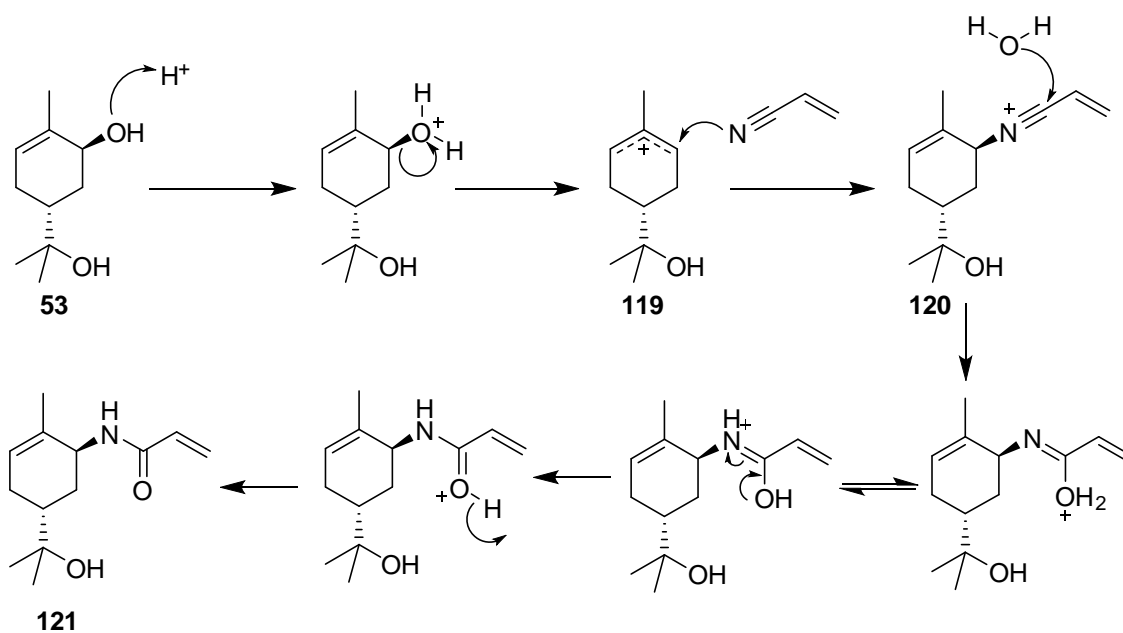
Scheme 59: Mechanism for the Synthesis of N-trans-*Sobrerol Acrylamide* via *the Ritter Reaction*

Analysis of the *J* values and coupling interactions within a range of NMR techniques (^{1}H, ^{13}C, COSY, HSQC, HMBC) and isolating the crystal structure of the sobrerol acrylamide confirmed that the Ritter reaction was diastereoselective towards the formation of the *trans* isomer with no evidence of the *cis* isomer (Figure 27).
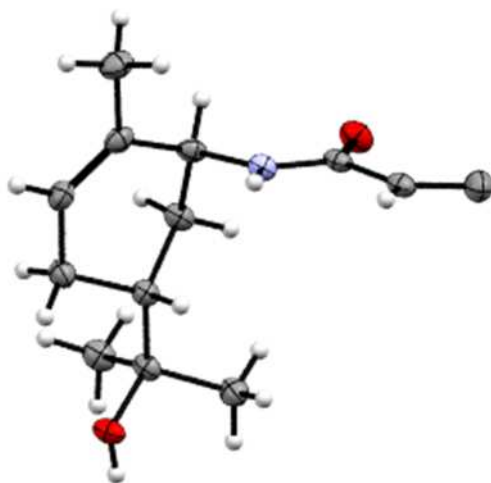
Figure 27: Crystal Structure of N-trans-Sobrerol Acrylamide

Similar to the *exo-* selectivity in the formation of *N*-isobornyl acrylamide, the diastereoselectivity of the Ritter reaction in this case was also proposed to be due to steric hindrance. In an S_N1-type reaction under acidic conditions, an allylic carbocation is generated, which undergoes diastereoselective nucleophilic attack to avoid the 1, 3-diaxial strain caused by the steric hindrance of the *tert*-butanol substituent. This resulted in the retention of stereochemistry to give *trans*-sobrerol acrylamide (**121**) (Scheme 60). Although diastereoselective, the reaction was not enantioselective as the allylic carbocation could undergo nucleophilic attack from either side of the molecule.
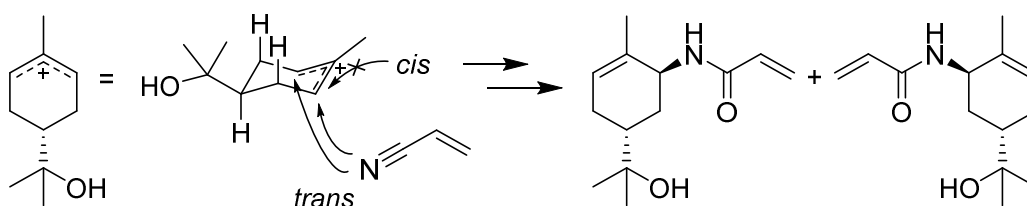
Scheme 60: Diastereoselectivity vs *Enantioselectivity of the Ritter reaction due to Steric Hindrance*

Investigations into the acid catalyst loadings and reaction concentration were conducted to optimise the reaction (Table 8). The acid loading was decreased from 1.05 equivalents to 5 mol%, the optimum loading being 10 mol%, as 5 mol% struggled to reach full conversion. At each acid catalyst loading, the reaction concentration was investigated with acrylonitrile acting as both a reagent and the solvent.

Table 8: Optimisation of N-trans-Sobrerol Acrylamide
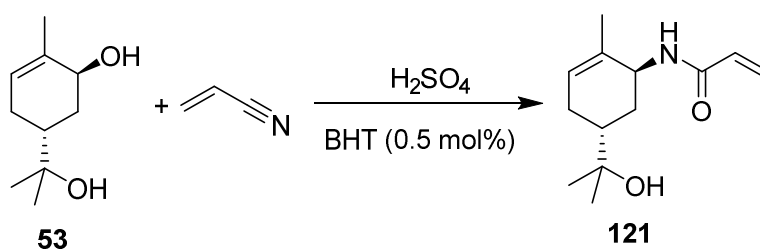
Entry	H_2SO_4 (mol%)	Acrylonitrile (M)	Yield (%)
1	105	0.5	37
2	25	0.5	35
3	25	0.2	73
4	25	0.1	77
5	10	1.0	15
6	10	0.5	47
7	10	0.2	76
8	10	0.1	83
9	5	0.1	44
10	5	0.2	47

An acrylonitrile concentration of 0.1 M with 10 mol% of sulfuric acid gave the highest yield, 83 %, with the yield inversely proportionally to the increasing concentration (Figure 28). Although 0.1 M of acrylonitrile gave the highest yield, a compromise was made between the yield and the ease of scale up by conducting further reactions at 0.2 M, a loss of 5 % yield for 50 % less acrylonitrile. This also improves the sustainability of the reaction as although, theoretically, the acrylonitrile can be recycled and reused in another reaction, it was safer and more economical to use less acrylonitrile.
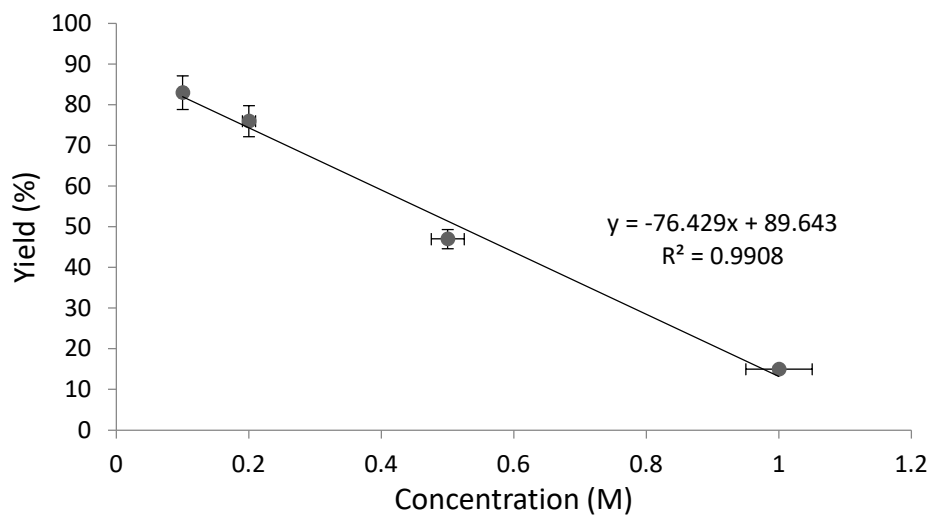
Figure 28: Graph Showing the Effect of Reaction Concentration on the Isolated Yield

It was discovered that at higher concentrations of acrylonitrile and acid catalyst loadings the major side product, pinol, was favoured. This side product was proposed to be forming during a competing intramolecular S_N1 nucleophilic attack from the tertiary alcohol to the allylic carbocation (Scheme 61 Route **B**).
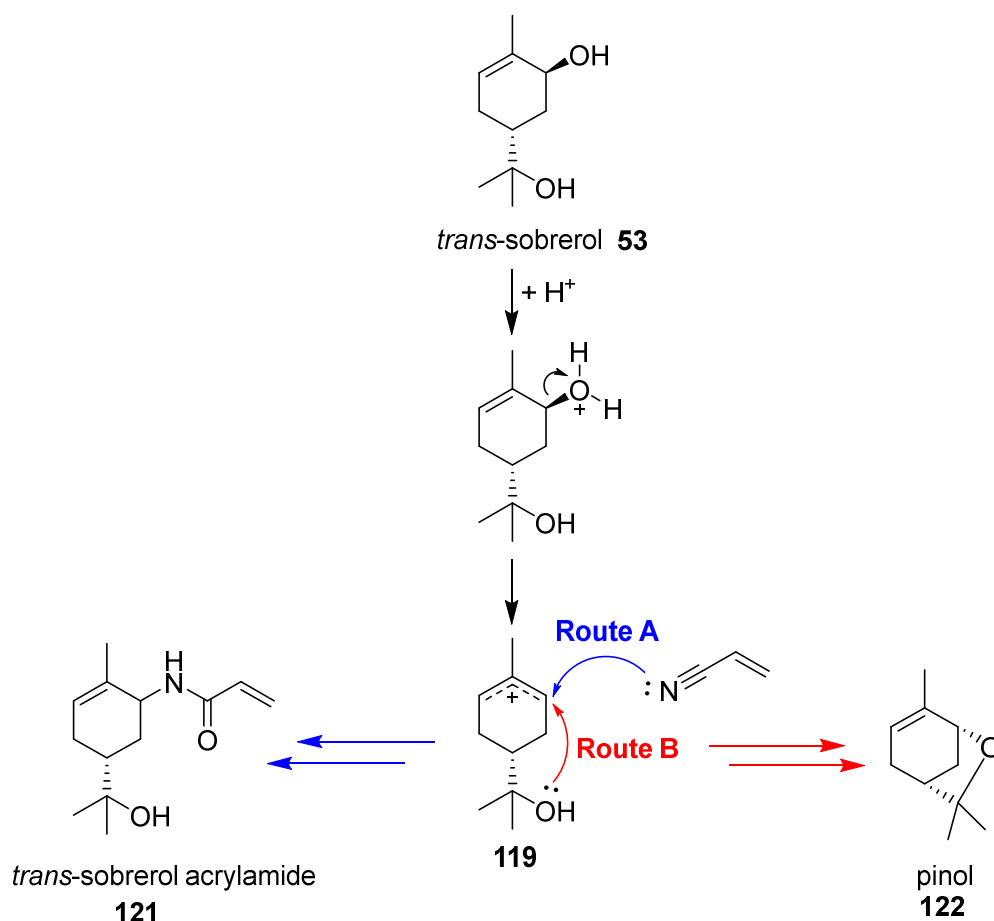
Scheme 61: Mechanism to Show Competing Inter- and Intra-Molecular Pathways

Therefore, by reducing the acid catalyst loading and reaction concentration and limiting the influence of this side reaction, the desired acrylamide was formed in a good yield of 83 %. With the optimum conditions and procedure in hand, the synthesis of *N-trans*-sobrerol acrylamide was successfully scaled up by factors of 3-5 up to a 130 g reaction with an overall 10 % decrease in yield (Table 9). *N-trans* sobrerol acrylamide is an air stable solid at room temperature. Even when left in a crude state at 5 °C for 1 month before purification, the yield was comparable, demonstrating good stability for industrial transport, storage and use.

101

Table 9: Scale Up of N-trans-Sobrerol Acrylamide Synthesis
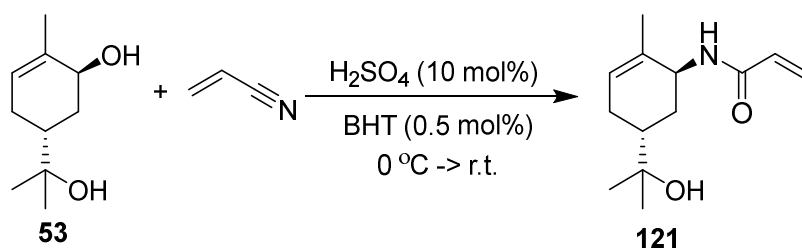
Entry	Scale (mol)	Starting Material Mass (g)	Yield (%)
1	0.01	1.7	76
2	0.25	43.1	61
3	0.75	129.2	66

In conclusion, a novel acrylamide monomer, *N-trans* sobrerol acrylamide was synthesised in a two-step synthesis from α-pinene, the most abundant natural terpene. Both the synthesis of *trans*-sobrerol and the synthesis of *N-trans*-sobrerol acrylamide have been conducted on a hundred gram scale in facile reactions to give an air-stable novel monomer with additional functionalities for post-polymerisation modifications and potential applications in protective coatings.

2.2.3   *N-trans* Carveol Acrylamide

Similarly to *trans*-sobrerol, the allylic alcohol on (-)-carveol is also reactivity under Ritter reaction conditions. Carveol acrylamide has been previously synthesised as a by-product in the formation of carveol bisacrylamide by V. Nair *et al*. in 2002.[138] *N-trans*-Carveol acrylamide was formed from α-pinene using stoichiometric cerium(IV) ammonium nitrate (CAN) and acrylonitrile in 9 % yield (Scheme 62).
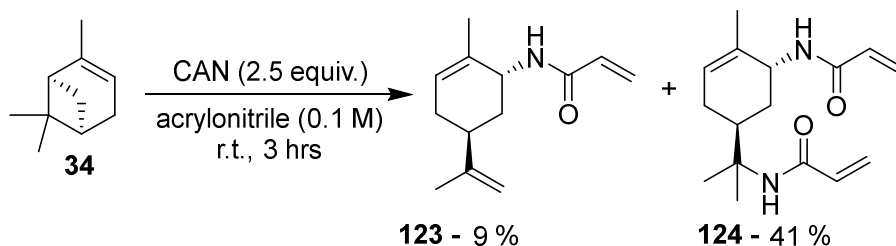
Scheme 62: CAN-mediated Synthesis of N-trans-Carveol Acrylamide by V. Nair et al.[138]

Using the Ritter reaction, *N-trans*-carveol acrylamide **123** was initially formed in a moderate yield, 33 %, using stoichiometric equivalents of sulfuric acid and 0.5 M acrylonitrile (Scheme 63). Analysis of the *J* values and coupling interactions within a range of NMR techniques (^{1}H, ^{13}C, COSY, HSQC, HMBC) determined the stereochemistry which was confirmed within literature.[138]
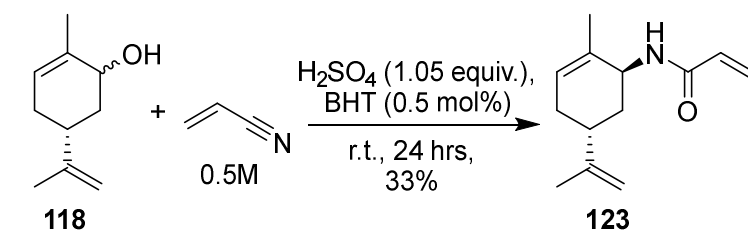
Scheme 63 : Optimised Reaction Condition for the formation of N-trans-Carveol Acrylamide

103

As previously discussed, the mechanism for the formation of *N-trans*-carveol acrylamide *via* the Ritter reaction proceed first *via* the protonation and hydrolysis of alcohol **118** under acidic conditions to form an allylic carbocation **125**. Nucleophilic attack of acrylonitrile on the allylic carbocation **125** forms a nitrilium ion **126**, which is then hydrated to form the desired acrylamide **123** (Scheme 64).
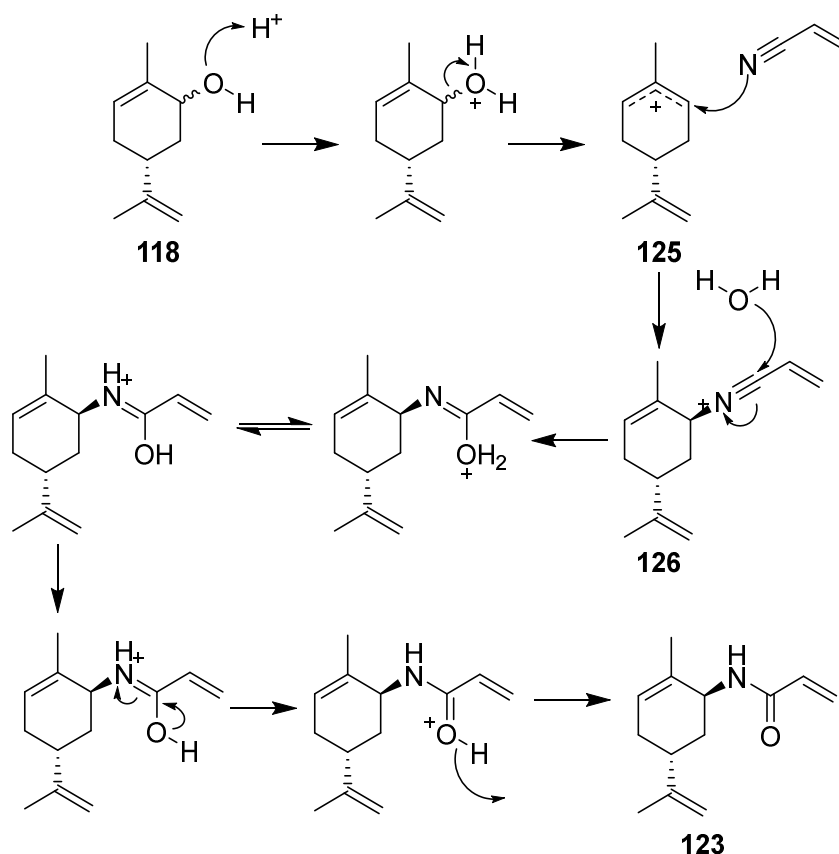
Scheme 64 : Mechanism for the Synthesis of N-trans-Carveol Acrylamide

Again, similar to the two previous Ritter-derived monomers the formation of *N-trans*-carveol acrylamide is diastereoselective due to the steric hindrance from the exocyclic alkene enforcing a preference for *N-trans*-carveol acrylamide (Figure 29), but not enantioselective as the acrylonitrile is not directed and can nucleophilically attack the allylic carbocation at either end.
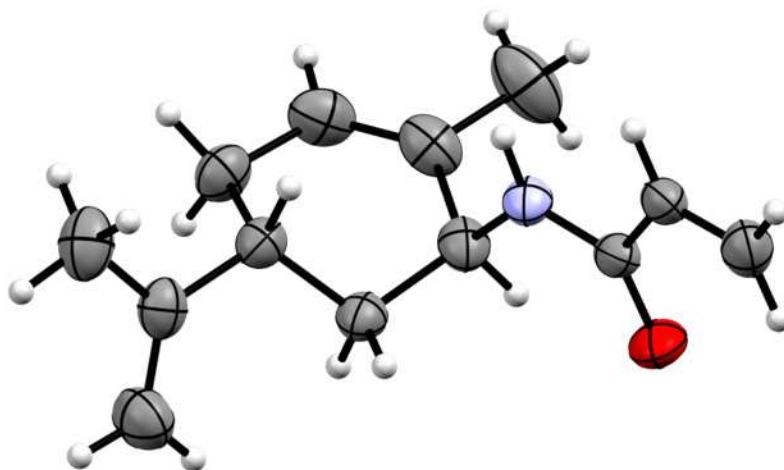
Figure 29 : Crystal Structure for N-trans-Carveol Acrylamide

Initial analysis showed a mixture of mono and bis-substituted *N-trans*-carveol acrylamides due to the reactivity of the exocyclic alkene under Ritter reaction conditions. Therefore, optimisation reactions investigating reaction time, amount of acid catalyst and its charging temperature were conducted. It was discovered that overreaction, often in higher concentrations of acid, formed *N*-carveol bisacrylamide through the formation of a tertiary carbocation at the exocyclic alkene (Scheme 65).
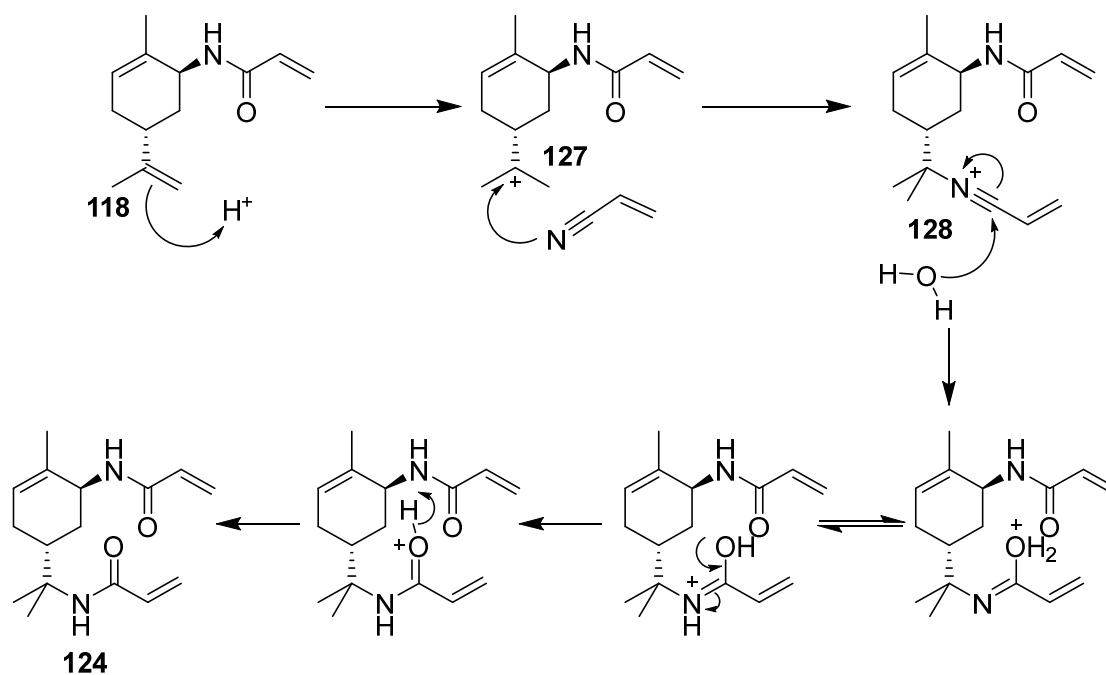
Scheme 65: Mechanism for the Synthesis of N-trans-Carveol Bisacrylamide

During optimisation, a good 69 % yield was initially achieved by reducing the reaction time through monitoring *via* TLC (Table 10 Entry 2). However when the scale of the reaction was increased by a factor of 10, an exotherm was observed upon addition of the acid at room temperature which caused the product to decompose (Table 10 Entry 3). Cooling the reaction to 0 °C during the addition of sulfuric acid restored the yield to 67 % (Table 10 Entry 4). Analysis from mass spectrometry and NMR could not identify any of the products within the resulting complex mixture. In order to reduce the formation of the side product, *N*-carveol bisacrylamide, the acid loading was decreased to 50 and 25 mol% (Table 10 Entries 5 & 6). This successfully limited the side-reaction forming the corresponding *N-trans*-carveol acrylamide in an excellent yield of 97 %.

Table 10 : Optimisation of N-trans-Carveol Acrylamide Synthesis
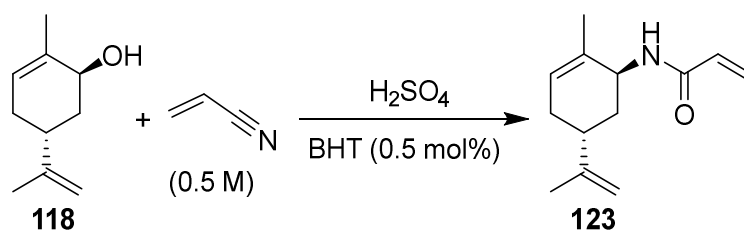
Entry	Scale (mmol)	[H_2SO_4] (equiv.)	Time (hrs)	Addition Temperature (°C)	Yield (%)
1	1	1.05	24	20	33
2	1	1.05	2	20	69
3	10	1.05	2	20	-
4	10	1.05	2	0	67
5	10	0.5	2	0	79
6	10	0.25	2	0	97

With the optimum conditions and procedure in hand, the reaction was scaled up in factors of 5 to a decigram scale. Increasing the scale of the reaction minimally affected the yield which dropped slightly to 86 % (Table 11).

Table 11: Scale Up of N-trans-Carveol Acrylamide Synthesis
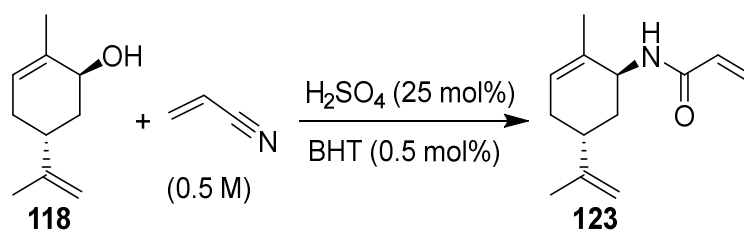
Entry	Scale (mmol)	Scale (g)	Time (hours)	Yield (%)
1	10	1.5	2	97
2	50	7.6	2	90
3	250	38.1	6	86

This facile, one step reaction is conducted in air with a straightforward quench and filter to remove the desired product once full conversion has been reached. *N-trans*-Carveol acrylamide was also determined to be an air stable solid at room temperature and when left in the crude solution at 5 °C for 1 month before isolation the yield dropped from 97 % to 81 %, a less than 1 % drop in yield per day, demonstrating good stability for industrial transport, storage and use.

2.2.4 *N*-Carvone Acrylamide

A similar structure to carveol, carvone (**3**) is another naturally occurring terpene found in spearmint and caraway essential oils. Interestingly to us, it contains the same exocyclic alkene susceptible to the Ritter reaction as seen in carveol. An initial Ritter reaction of carvone was conducted using stoichiometric acid and 1 M acrylonitrile as both a reagent and the solvent to give the desired *N*-carvone acrylamide (**131**) in a moderate 38 % yield (Scheme 66).
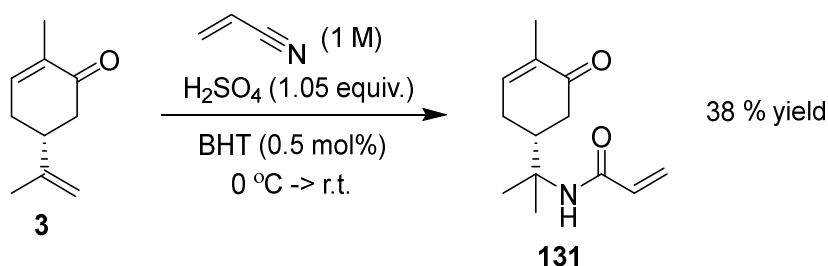
Scheme 66: Initial Synthesis of N-Carvone Acrylamide

As previously discussed, the mechanism for the formation of *N*-carvone acrylamide *via* the Ritter reaction proceed first via the protonation the exocyclic alkene on carvone **3** under acidic conditions to form an tertiary carbocation **129**. Nucleophilic attack of acrylonitrile on the tertiary carbocation **129** forms a nitrilium ion **130,** which is then hydrated to form the desired acrylamide **131** (Scheme 67).
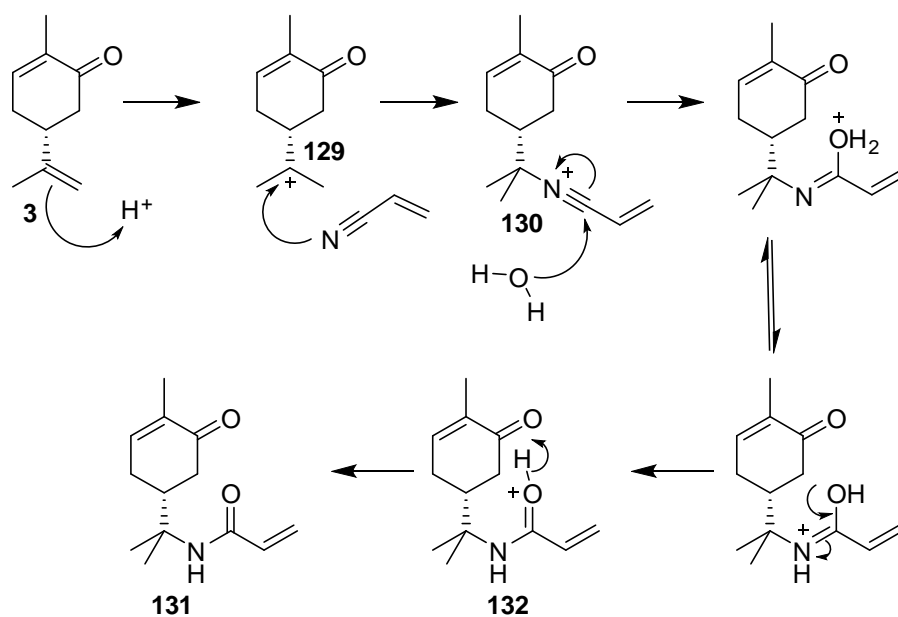
Scheme 67: Mechanism for the Ritter reaction of Carvone and Acrylonitrile

The Ritter reaction proceeded with retention of stereochemistry to form a singular enantiomer as formation of the carbocation retained the chiral centre in *R*-(-)-carvone. This was confirmed by X-ray crystallography of recrystallized *N*-carvone acrylamide (Figure 30).
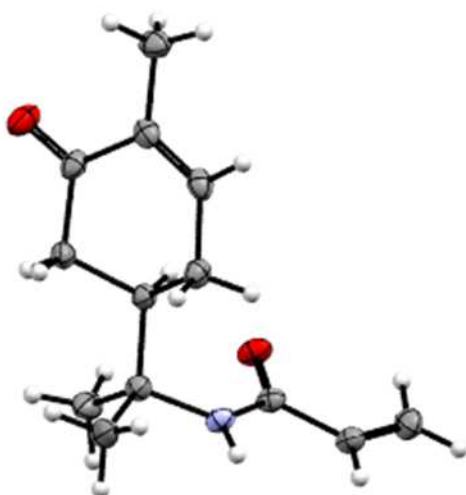
Figure 30: X-Ray Crystal Structure of N-Carvone Acrylamide

The reaction was then optimised by investigating the acid loading and reaction concentration. Both lower and higher acid loadings and reaction concentrations were screened showing that both variables were key to reaction success (Table 12 Entries 1-3).

Table 12: Optimisation of N-Carvone Acrylamide Synthesis
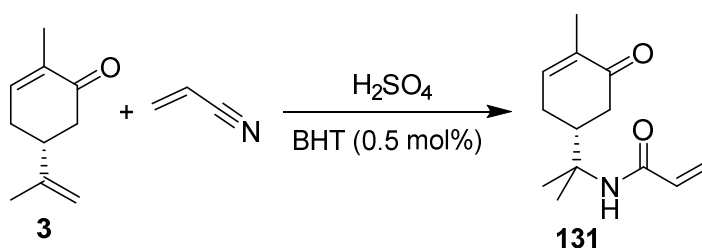
Entry	H_2SO_4 (equiv.)	Acrylonitrile (M)	Isolated Yield (%)
1	1.05	1	38
2	0.5	1	24
3	2.1	1	77
4	2.1	0.5	53
5	2.1	2	61

Increasing the acid loading proportionally increased the isolated yield with 2.1 equivalents of sulfuric acid resulting in a good 77 % (Table 12 Entry 3). Higher equivalents of acid were not considered, despite the potentially higher yielding results, due to safety concerns when scaling up.

111
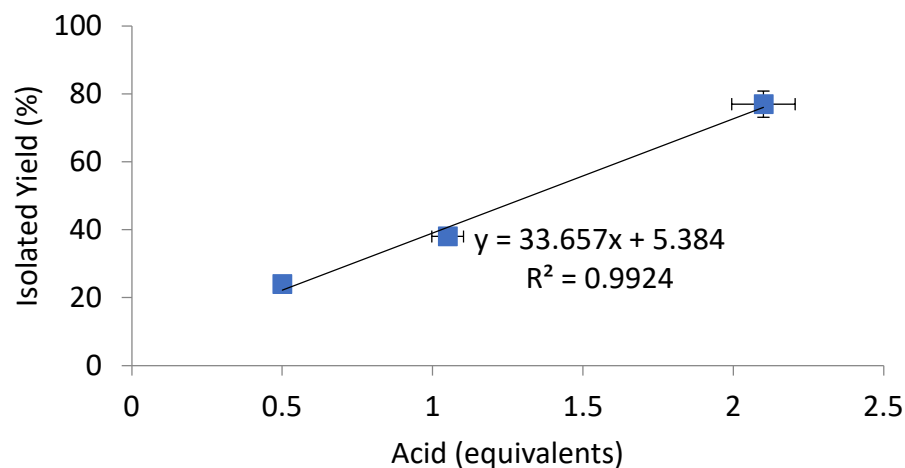
Figure 31: Graph Showing Acid Catalyst Loading versus Isolated Yield

Next, the reaction concentration was investigated targeting both higher and lower concentrations (Table 12 Entries 4 & 5). Increasing and decreasing the reaction concentration decreased the isolated yield. Increasing the concentration resulted in degradation of the starting material due to the increased acidity; decreasing the concentration decreased the reaction conversion also lowering the yield.

The optimum conditions of 2.1 equivalents of sulfuric acid and 1 M acrylonitrile were taken forward into the reaction scale up. The Ritter reaction of carvone was scaled up in factors of 5 to a large 188 g scale. An initial yield drop was seen during the first scale up but from 50 mmol onwards the yields were comparable around a good 60 % yield (Table 13). This facile, one step reaction is conducted in air with a simple quench and filtration to remove the desired product once full conversion has been reached.

Table 13: Scale Up of N-Carvone Acrylamide Synthesis
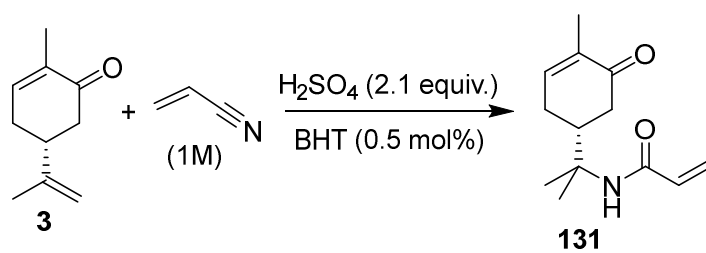
Entry	Scale (mmol)	Scale (g)	Yield (%)
1	10	1.5	77
2	50	7.5	63
3	250	37.5	57
4	1250	187.5	60

2.2.5 *N*-Pulegone Acrylamide

N-Pulegone acetamide was previously synthesised in 2015 by Kozlov *et al.* using a simple Ritter reaction procedure (Scheme 68).[139] Three equivalents of sulfuric acid in excess acetonitrile were used to form the product in a moderate 56 % yield. The reaction proceeded as expected through a tertiary carbocation to form the amide stereoselectively with the methyl and isopropylamide in the equatorial positions.
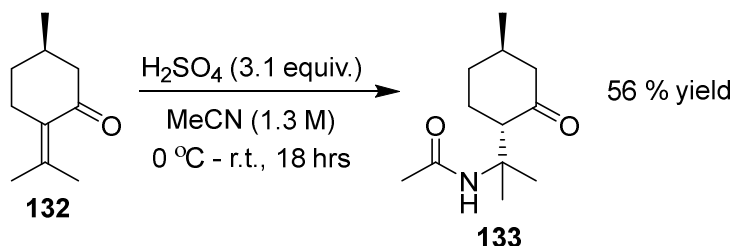
Scheme 68: Synthesis of N-Pulegone Acetamide by Kozlov et al.[139]

Building on Kozlov's success, we targeted the synthesis of *N*-pulegone acrylamide. Pulegone is another terpene found in the mint family from the essential oils of catnip and pennyroyal. An initial investigation using 1 M acrylonitrile and 1.05 equivalents of sulfuric acid gave the desired *N*-pulegone acrylamide in a moderate yield, 34 % (Scheme 69). Analysis of the *J* values and coupling interactions within a range of NMR techniques (^{1}H, ^{13}C, COSY, HSQC, HMBC) determined the stereochemistry which was confirmed within literature.[139]
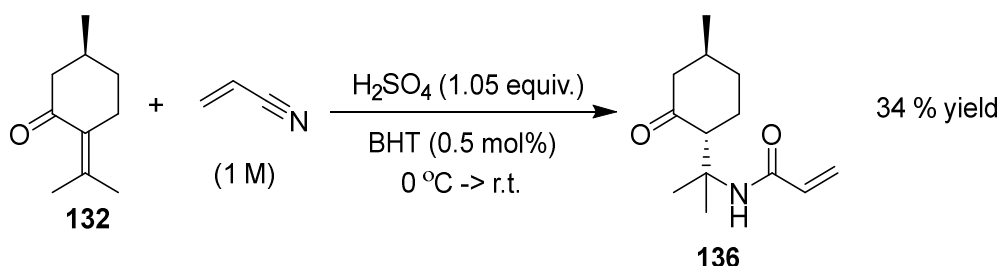
Scheme 69: Initial Synthesis of N-Pulegone Acrylamide

This structure is of particular interest due to its additional unsaturated ketone functionality which could be targeted in post-polymerisation functionalisations or as a moiety for drug attachment. The structure and stereochemistry was confirmed *via* recrystallization and X-ray crystallography along with the standard analysis (Figure 32).
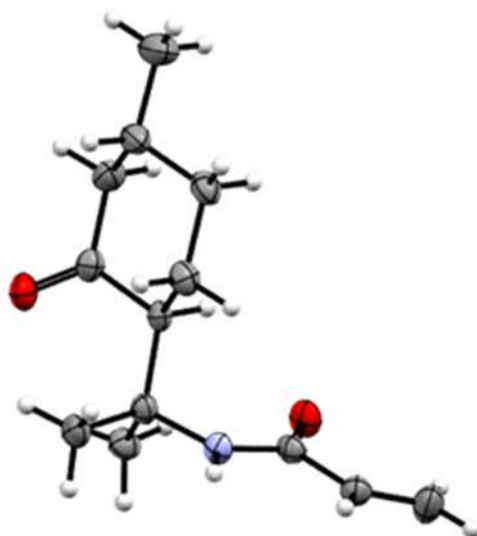
Figure 32: X-Ray Crystallography Structure of N-Pulegone Acrylamide

The Ritter reaction of pulegone and acrylonitrile is proposed to proceed *via* the traditional mechanism. First, the alkene **132** is protonated under acidic conditions to form a tertiary carbocation **134**. Nucleophilic attack from acrylonitrile forms the corresponding nitrilium ion **135** which is hydrated in the reaction quench to form the desired *N*-pulegone acrylamide **136**.
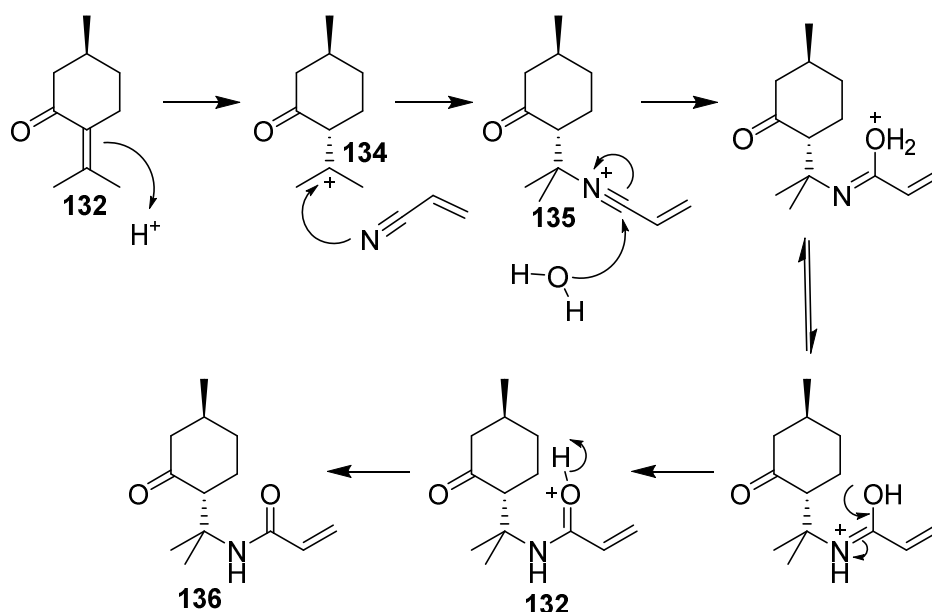
Scheme 70: Mechanism for the Ritter Reaction of Pulegone and Acrylonitrile

Optimisation reactions investigating acid catalyst loadings and reaction concentration were conducted to improve the yield. Decreasing the acid catalyst loading to 0.5 equivalents gave a comparable yield to the initial reaction (Table 14 Entry 1). Increasing the acid catalyst loading to 2.1 equivalents increased the isolated yield to a moderate 54 % (Table 14 Entry 3), comparable to the previous synthesis of *N*-pulegone acetamide by Kozlov *et al.*[139] Higher equivalents of acid were not considered, despite the potentially higher yielding results, due to safety concerns when scaling up. Investigations into higher and lower reaction concentrations gave lower isolated yields (Table 14 Entries 4 & 5). Lower concentrations lowered the acid concentration and decreased conversion, higher concentrations with increased acid concentration caused the starting material to degrade.
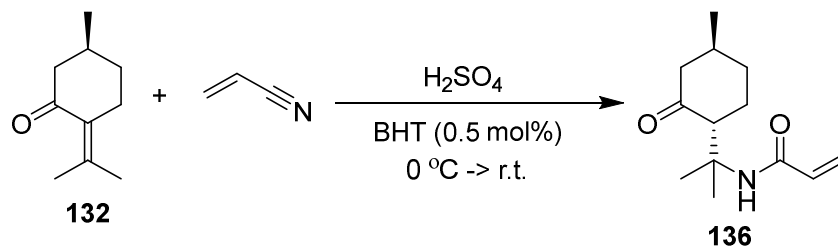
Entry	H_2SO_4 (equiv.)	Acrylonitrile (M)	Isolated Yield (%)
1	0.5	1	32
2	1.05	1	34
3	2.1	1	54
4	2.1	0.5	34
5	2.1	2	41

With the optimum conditions, 2.1 equivalents of sulfuric acid and 1 M acrylonitrile, in hand, the synthesis of *N*-pulegone acrylamide was scaled up in factors of 5 to 190 g. The yields stayed comparable at a moderate 50 % (Table 15).

Table 15: Scale Up of N-Pulegone Acrylamide Synthesis
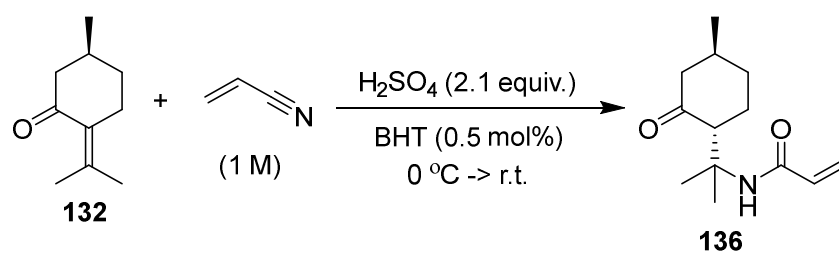
Entry	Scale (mmol)	Scale (g)	Yield (%)
1	10	1.5	54
2	50	7.6	58
3	250	38.0	50
4	1.25	190.0	48

Unlike the other four monomers, it was necessary for *N*-pulegone acrylamide to be purified *via* column chromatography rather than facile filtration. However, this novel renewable monomer was still synthesised in a simple, one-step reaction with a high atom economy and propensity for industrial scale up.

2.3 Further Diversification of Monomers

With five renewable monomers successfully synthesised *via* a facile, one-step Ritter reaction, our attention turned to potential further diversifications of these monomers, allowing for designer products with potentially tuneable properties. Excluding, *N*-isobornyl acrylamide, all the renewable Ritter monomers, and both of the Overman monomers, have extra exploitable functionalities which can be modified to suit a larger range of future applications. For the purposes of showcasing the potentially wide diversification of these monomers, *N*-carveol acrylamide was chosen as the subject of these investigations. *N*-Carveol acrylamide was chosen as previous polymerisations of carveol acrylate[67] within the group demonstrated a poor conversion and propensity for uncontrolled polymeric branching due to its exocyclic alkene.

2.3.1 Synthesis of *N,N'*-Carveol Bisacrylamide

The *N,N'*-carveol bisacrylamide formed originally as a side product was also of interest due to its potential as a renewable crosslinker and alternative to *N,N'*-methylenebis(acrylamide). *N,N'*-carveol bisacrylamide was determined to form due to overreaction of the Ritter reaction on carveol. There was a trend noticed where higher equivalents of acid resulted in higher yields of the carveol bisacrylamide. Therefore, just over two equivalents of sulfuric acid was charged compared with the 25 mol% of the mono-acrylamide synthesis to give a moderate yield, 62 %, of the carveol bisacrylamide (Scheme 71).
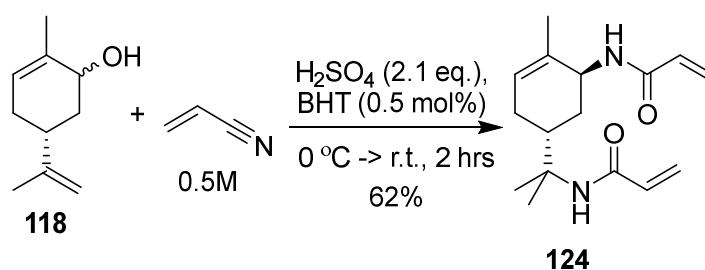
Scheme 71 : Optimised Condition for the Synthesis of N,N'-Carveol Bisacrylamide

To form the bisacrylamide, the exocyclic alkene was protonated to form a tertiary carbocation. Acrylonitrile nucleophilically attacks the carbocation to form a nitrilium ion. This is hydrated upon work up to form the bisacrylamide (Scheme 72).
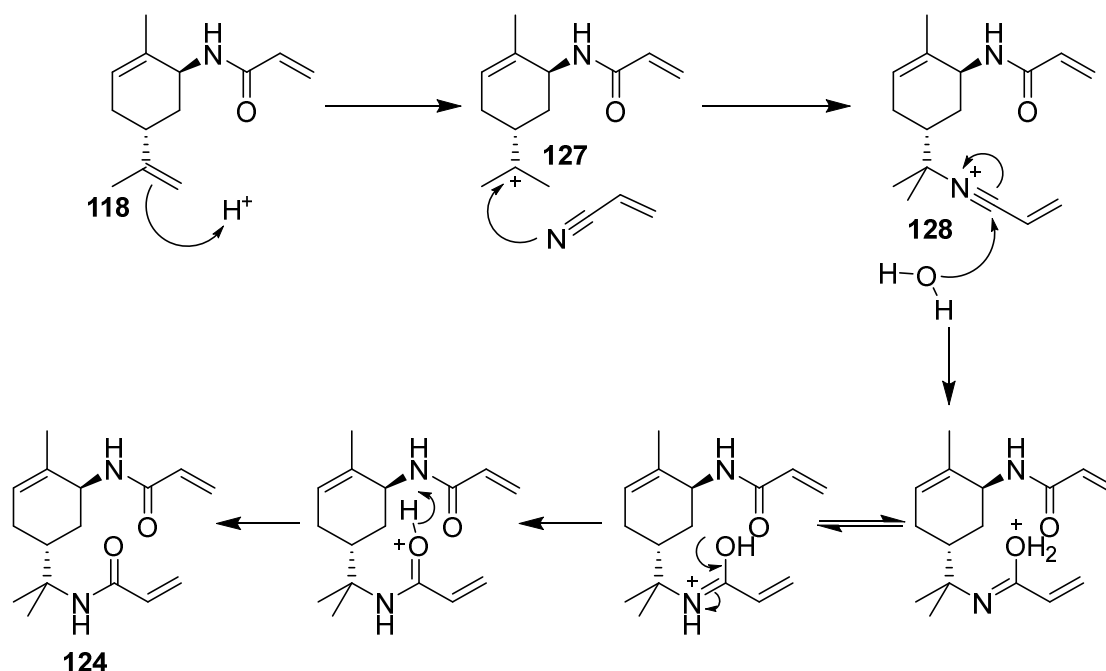
Scheme 72 : Mechanism of the Synthesis of N,N'-Carveol Bisacrylamide

Similarly to *N*-carveol acrylamide, *N,N'*-carveol bisacrylamide was easily purified *via* filtration after the reaction was quenched and showed excellent long term stability.

2.3.2 Thiol-ene Click Reaction

The exocyclic alkene on carveol also lends itself to click reactions such as thiol-ene click chemistry. The exocyclic alkene on limonene has been successfully reacted with various thiols using thiol-ene click chemistry by Meier and co-workers to form terpene mono- and disulfides (Scheme 73).[64] Alves *et al.* in 2014 similarly modified dihydromyrcenol with cysteamine hydrochloride and 3-mercaptopropionic acid.[140] The reactions by Meier and co-workers were conducted under vacuum (200mbar) in a carousel reaction station[TM] RR98072 and gave very good yields, up to 85 % for the terpene monosulfides.
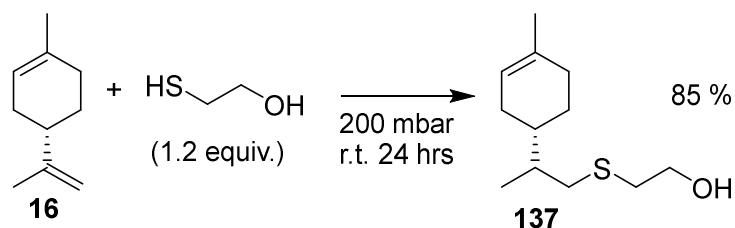
Scheme 73: Synthesis of Carveol 2-Mercaptoethanol by Meier and co-workers[64]

This procedure was closely replicated using Schlenk tube chemistry to demonstrate the potential of using thiol-ene click chemistry as high-pressure reactors were not available. The facile addition of thiol with varying pendant functionalities allows for the addition of diverse pendant groups, tuning the properties of any corresponding polyacrylamides. The reaction proceeded with a moderate 45 % yield due to low conversion and over addition of the mercaptoethanol (Scheme 74).
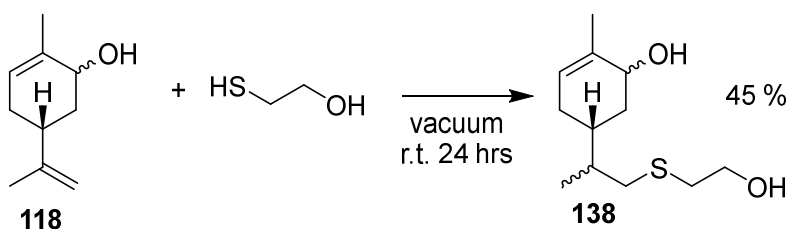
Scheme 74: Schlenk Tube Synthesis of Carveol 2-Mercaptoethanol

Longer reaction times and higher reaction temperatures resulted in poly(carveol) whereas the addition of a solvent resulted in lower conversions. This carveol 2-mercaptoethanol or other terpene sulfides can then potentially be reacted further in the Ritter reaction to form the corresponding acrylamides.

2.3.3 Double Epoxidation

Polymers containing epoxides are highly desirable and often used in coatings as the epoxides can readily undergo post-polymerisation functionalisation. The exocyclic and

endocyclic alkenes on *N*-carveol acrylamide were targeted selectively for epoxidation. After forming *N*-carveol acrylamide (**121**) from the Ritter reaction, the Prilezhaev epoxidation was used to form the bisepoxide acrylamide (**139**) in a moderate 51 % yield (Scheme 75).
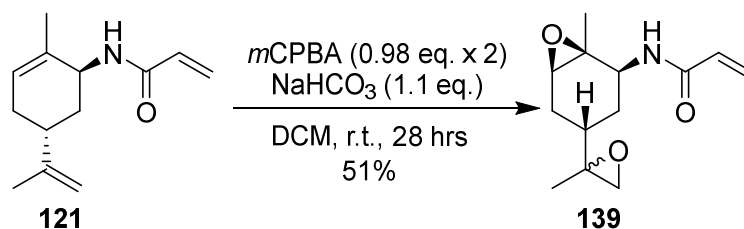
Scheme 75: Synthesis Route for the formation of N-Carveol Bisepoxide Acrylamide

*m*CPBA chemoselectively epoxidised the electron rich alkenes with retention of stereochemistry ignoring the electron deficient acrylamide. The endocyclic alkene initially underwent epoxidation to rapidly form the monoepoxide **140** in 2 hours, this was confirmed through isolation and analysis of the monoepoxide **140**. The stereochemistry was proposed due to the *J* values and coupling interactions within a range of NMR techniques (^{1}H, ^{13}C, COSY, HSQC, HMBC). The endocyclic epoxide forming stereoselectively, potentially due to hydrogen bonding of the amide to *m*CPBA directing the mCBPA to attack from the same face. Before the slow epoxidation of the exocyclic alkene in 16 hours results in the formation of the bisepoxide acrylamide (**139**). On the other hand, no diastereomeric selectivity was seen for the exocyclic alkene resulting in a 1:1 mixture of the two epimers.

122
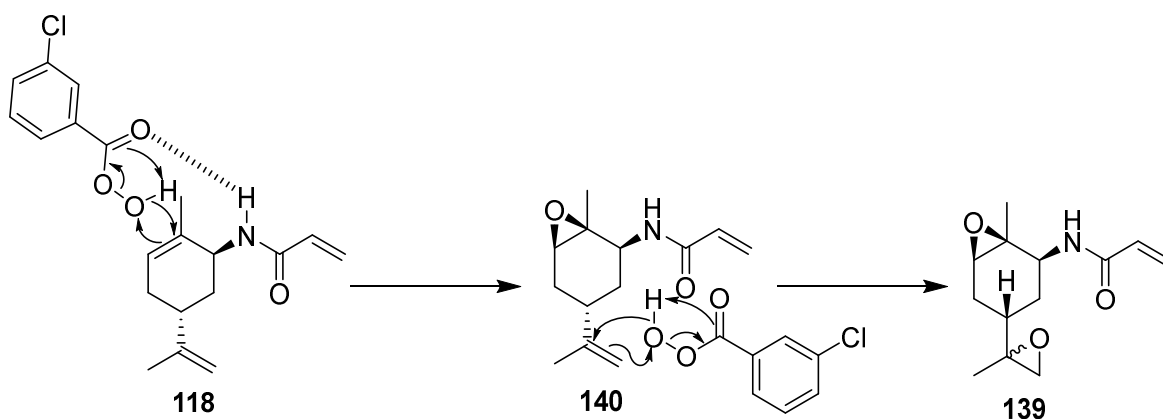
Scheme 76 : Mechanism for the Epoxidation of N-Carveol Acrylamide

A brief optimisation study was carried out and the amount of stoichiometric *m*CPBA was increased marginally to ensure the reagent was in excess, this increased the yield significantly from 51 % to 75 % (Table 16 Entry 2). Next, the scale of the reaction was increased from 0.98 mmol to 9.7 mmol which successfully increased the yield further to 84 % (Table 16 Entry 3). Finally when the reagents were charged at 0 °C rather than room temperature, the yield increased to 96 % (Table 16 Entry 4). This gave an overall yield of 94 % over the two steps from the natural product carveol. Scaling this reaction up to 50 mmol gave a comparable yield; however when the reaction was scaled up again by a factor of 5 no product was observed (Table 16 Entry 6). This was likely due to process limitations as the addition of *m*CPBA to reaction mixture was difficult on a large scale and slow addition is necessary. Switching the addition of the reagents around by slowly adding *N*-carveol acrylamide to the *m*CPBA-containing reaction mixture gave an improved yield of 72 %, however this was still a significant drop from the optimum yield (Table 16 Entry 7).

Table 16 : Optimisation of N-Carveol Bisepoxide Acrylamide Synthesis
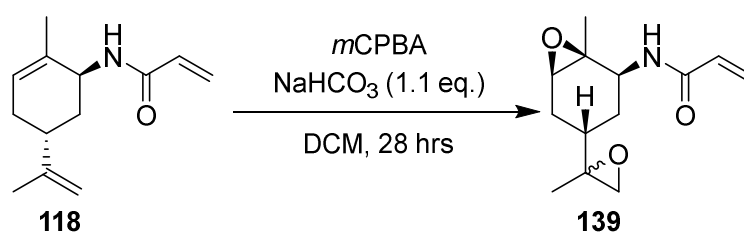
Entry	Scale (mmol)	mCPBA (equiv.)	Charging Temp. (°C)	Isolated Yield (%)
1	1	1.96	20	51
2	1	2.06	20	75
3	10	2.1	20	84
4	10	2.1	0	96
5	50	2.1	0	96
6	250	2.1	0	0
7	250	2.1	0	72*

*Order of reagent addition swapped, acrylamide added to solution of mCPBA and NaHCO$_3$ in DCM

As well as decreased yields and problematic process procedure on a larger scale, pure mCPBA is potentially explosive due to shock sensitivity. This means although high yielding, this synthesis is unlikely to be viable on an industrial scale and an alternate pathways was explored. The bisepoxide acrylamide (**139**) was synthesised using the more sustainable, industrial viable Oxone® epoxidation, in a comparable 90 % yield (Scheme 77).
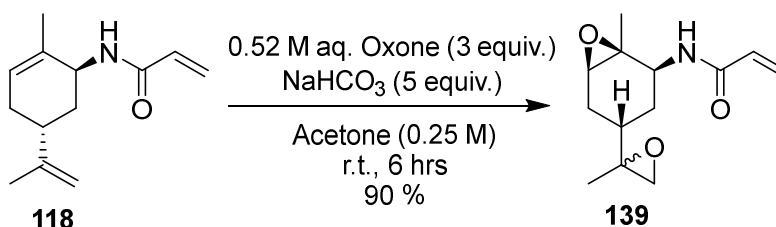
Scheme 77: Greener Synthesis of N-Carveol Bisepoxide Acrylamide

This alternate pathway removes the use of carcinogenic DCM and potentially explosive *m*CPBA for safe reagents; potassium sulfate salts, sodium bicarbonate and acetone. The reaction time is also reduced by a factor of 4. Using this method the overall yield of the synthesis of *N*-carveol bisacrylamide **139** from the natural product, carveol **118**, was a very good 87 %.

All three one-step modifications using a range of synthetic methods have demonstrated the potentially vast array of novel renewable acrylamides from natural waste material potentially allowing for targeted applications in the future.

2.4 Conclusion

In conclusion, five novel acrylamide monomers; *N*-isobornyl acrylamide (**108**), *N-trans* sobrerol acrylamide (**115**), *N*-carveol acrylamide (**123**), *N*-carvone acrylamide (**131**) and *N*-pulegone acrylamide (**133**), have been synthesised using Ritter reaction from monoterpenes and monoterpenoids in 54 - 97 % yields. The sustainable synthesis of *N*-isobornyl acrylamide has been investigated further with the aim of using only low hazard materials and heterogeneous catalysts, however further optimisation is needed to boost the yields of these alternative Ritter reactions. As the Ritter reaction is already used on an industrial scale, the synthesis of all the monomers were optimised and scaled up to hundred-gram reactions showing the potential for industrial synthesis of these novel monomers.
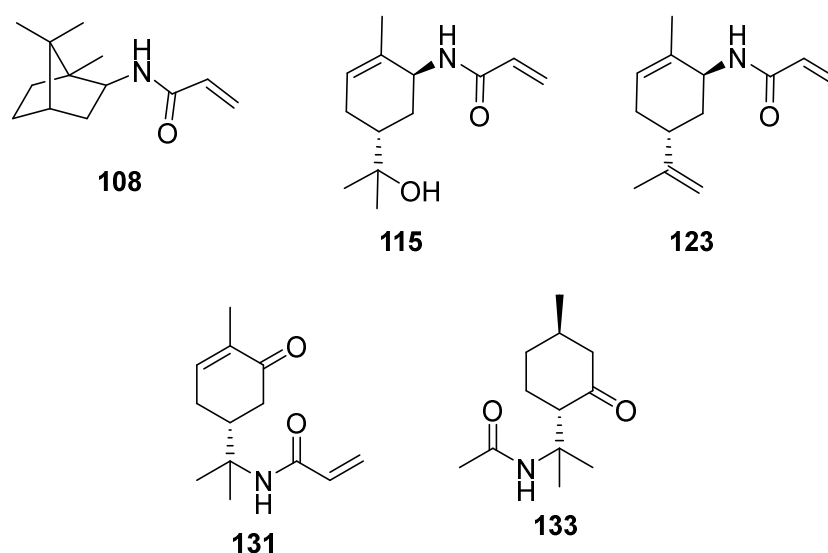
Figure 33: Acrylamide Monomers

Further synthetic modifications of *N*-carveol acrylamide (**123**) demonstrated the potential for directed diversification and the ability to target desired properties within novel renewable polymers. *N*-carveol acrylamide (**123**) was chosen as previous polymerisations of carveol acrylate[67] within the group demonstrated a poor conversion and propensity for uncontrolled polymeric branching due to its exocyclic alkene. Almost all the renewable Ritter monomers, and both of the Overman monomers (excluding, *N*-isobornyl acrylamide), have extra exploitable functionalities which can be modified to suit any future applications. Three synthetic modifications, bisacrylamide formation, sulfide formation and epoxidation

were all successfully carried out to demonstrate the wide scope of these renewable monomers.
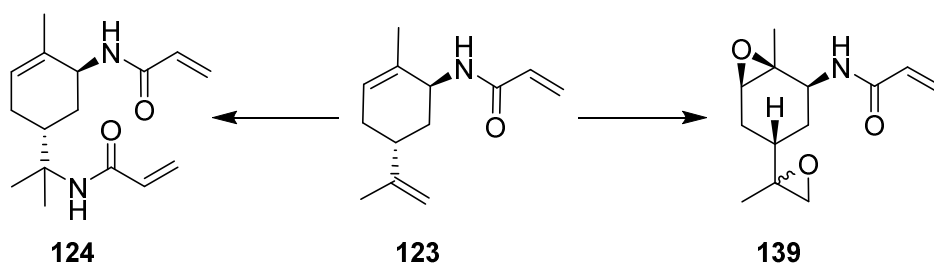
Scheme 78: Further Diversification of Acrylamide Monomers

3.0 Chapter 3: Polymer Synthesis

With a range of biobased acrylamides in hand, the polymerisation of these novel monomers was investigated. Since first being introduced in the 1950s, commercially available acrylamide monomers, such as acrylamide and *N*-isopropylacrylamide, have undergone polymerisation using a variety of techniques and initiators. As the majority of common acrylamide monomers are water-soluble, traditionally acrylamide polymerisations are carried out under aqueous conditions using water soluble thermal[141–144] or redox initiators.[79,145,146] Controlled living polymerisations[147] and inverse emulsion polymerisation[148–151] have also previously been used in the successful polymerisation of these commercially available monomers. The aim was to polymerise the novel biobased monomers synthesised in Chapter 2, screening and optimising a variety of techniques, to create a library of renewable polyacrylamides. In the first instance, free radical polymerisation was employed, as this has proved a facile and well-established method of acrylamide polymerisation.[152]

3.1 Thermally Initiated Homopolymerisations

There are numerous examples present in the literature where biobased acrylamide monomers (dopamine acrylamide, galactosyl acrylamide, guaiacol-based acrylamide) have undergone non-aqueous solution polymerisations with the thermal initiator 2,2'-azobis(2-methylpropionitrile), AIBN, in a range of different organic solvents.[89,90,94,95] As the biobased acrylamide monomers, synthesised in Chapter 2, are insoluble in water due to the high hydrocarbon content of the terpene moieties, thermally initiated solution polymerisations were initially investigated. This low aqueous compatibility is common in the literature among biobased acrylamides.[89,90,94,95]

3.1.1 Poly(*N*-Pinocarveol Acrylamide)

Polymerisation investigations began with *N*-pinocarveol acrylamide, **92,** which was successfully polymerised using standard free radical polymerisation techniques with AIBN as the initiator (Scheme 79). Containing two terminal alkenes, the monomer crosslinked under polymerisation conditions to create an insoluble red material with a rubbery consistency.
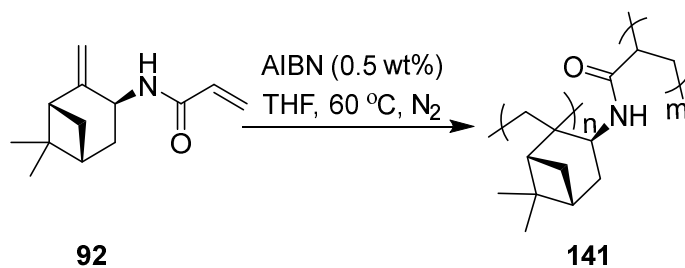
*Scheme 79: Polymerisation of Myrtenol-Derived Acrylamide **92***

Due to the insolubility of the polymer after crosslinking, the polymer conversion and its molecular weight were undetermined. However, this ability to crosslink is still an interesting property as few amide crosslinkers are commercially available or reported in the literature. The industry leading acrylamide crosslinker is the petroleum based *N,N′*-methylenebis(acrylamide). Crosslinking is important for coatings and flocculants to give structure to the material. Indeed PNIPAM, the industry leader for polyacrylamides, is used as a crosslinked 3D gel. Therefore, further investigation of the polymerisation of monomer **92** may prove to have potential use in these applications. Given the nature of this project, however, focus turned instead to the polymerisation of other terpene-based acrylamides which might prove easier to analyse.

3.1.2 Poly(*N*-Myrtenyl Acrylamide)

N-Myrtenylacrylamide **97** was polymerised using standard free radical techniques with the azo-initiator, AIBN, resulting in a good 83 % conversion by 400 MHZ ^{1}H NMR to poly(*N*-myrtenylacrylamide) **142** over the course of 22 hours (Scheme 80). Unlike poly(*N*-pinocarveol acrylamide) **142**, this polymer was found to be soluble in a range of organic solvents, indicating that despite containing two alkene moieties, it did not crosslink. This is likely due to the sterically hindered nature of the endocyclic alkene of **97**, as opposed to the acrylamide, which is exocyclic and therefore much more reactive. Analysis by GPC against a standard of PMMA gave a good M_n of 25.4 kDa with an unusually low polydispersity (Đ) of 1.07.
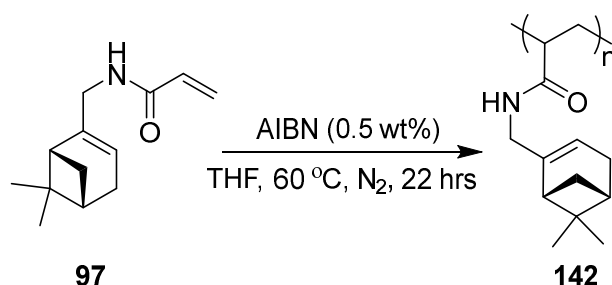
*Scheme 80 : Polymerisation of N-Myrtenylacrylamide **92***

Several reactions were then conducted to investigate the effect that different conditions might have on the molecular weight or other polymer properties. Repeating the polymerisation at an increased concentration gave an increased conversion but a lower molecular weight, 10.5 kDa, and a higher polydispersity of 2.32 (Table 17 Entry 2). The addition of a chain transfer agent, dodecanethiol, gave a similar Mn of 11.4 kDa (Table 17 Entry 3) and improved polydispersity, 1.23, compared to the uncontrolled polymerisation. A chain transfer agent, such as dodecanethiol, regulates the molecular weight, and therefore polydispersity, of propagating chains in the reaction by reacting with the free-radical site of a growing chain and interrupting chain growth. This radicalised chain transfer agent, then transfers the radical to another polymer or monomer. This imparts a level of control of the molecular weight of the polymer chains, lowering the polydispersity (Table 17 Entries 3 & 4).

131

Entry	Conc. (M)	DDM (wt%)	M_n[a] (kDa)	M_p (kDa)	M_w (kDa)	Polydispersity (Đ)	Conversion[b] (%)
1	1.6	-	25.4	19.3	29.6	1.16	83
2	2.4	-	10.5	13.3	24.4	2.32	>99
3	2.4	1	11.4	12.2	14	1.23	97
4	2.4	5	10.5	11.1	15.1	1.43	98

[a]Calculated from GPC calibrated with PMMA standard

[b]Calculated from ^{1}H NMR using the signals from the vinyl hydrogen (δ 5.61 ppm) of the unreacted monomer, and the nitrogen hydrogen (δ 5.36 ppm) of the polymer.

Unfortunately, the polymerisation of *N*-myrtenylacrylamide was not reliable, this was proposed to be due to a competing intramolecular radical cyclisation, forming a 5-*exo* membered ring through a kinetic pathway, terminating any propagating polymer chains and resulting in a low to negligible monomer conversion (Scheme 81). In the future, further investigations into the termination mechanism will be conducted through MALDI-MS analysis of the polymer end groups.
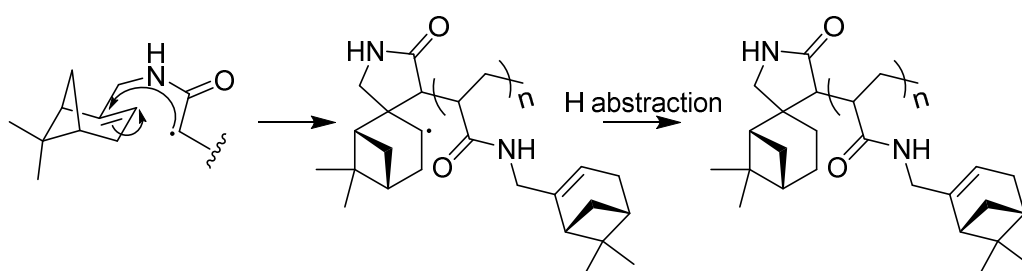
Scheme 81: Termination via Intramolecular Radical Cyclisation to form a Secondary Six-Membered Ring

Dynamic mechanical analysis of poly(*N*-myrtenyl acrylamide) with a Mn of 25.4 kDa (Table 17 Entry 1) gave a T_g of 91 °C (Figure 34). Comparatively, this is a lower glass transition temperature than the commercially produced poly(*N*-isopropyl acrylamide) which has a glass transition temperature of 155 °C suggesting the biobased material is a more flexible material than the commercial leader.
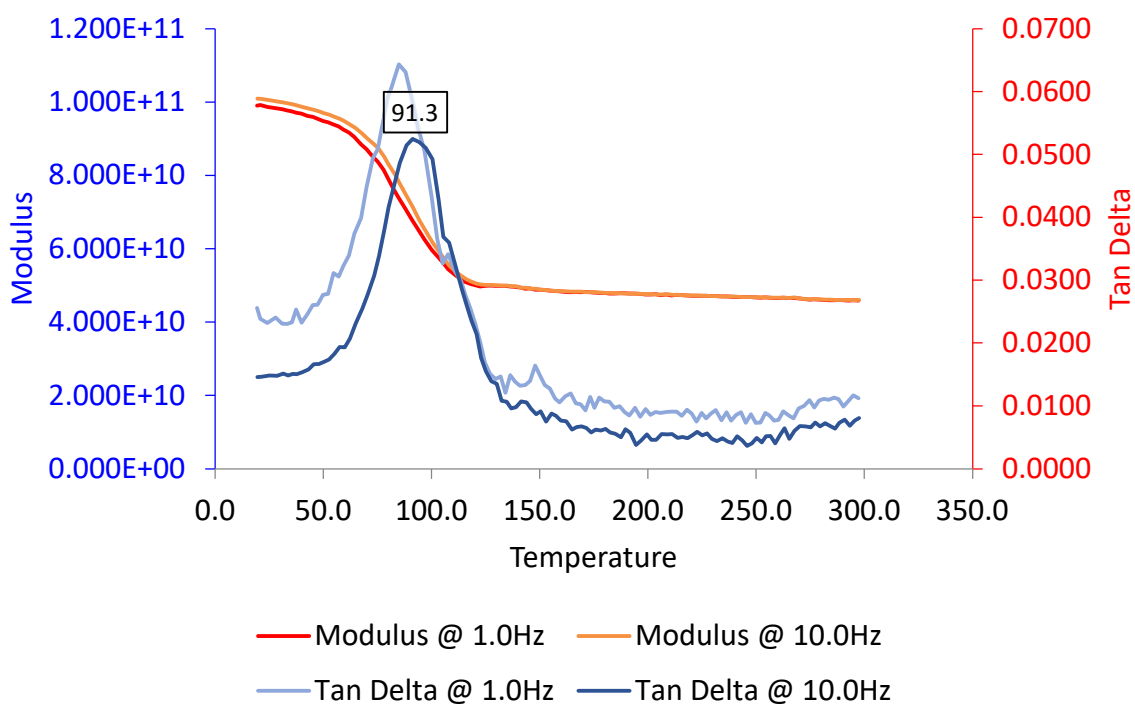
Figure 34: Dynamic Mechanical Analysis of Poly(N-Myrtenylacrylamide)

3.1.3 Poly(*N*-Isobornyl acrylamide)

N-Isobornyl acrylamide **108** was initially polymerised using standard free radical conditions, using 0.5 wt% AIBN as the radical initiator in THF at 60 °C for 22 hours (Scheme 82). The polymerisation was successful resulting in a high conversion (93 %) (Table 18 Entry 1).
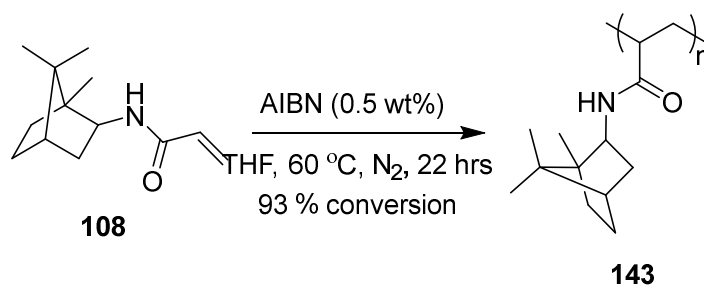
Scheme 82: Initial Polymerisation of N-Isobornyl Acrylamide **108**

However, only a relatively low molecular weight of 11.6 kDa (with a polydispersity of 1.46) was observed upon GPC analysis. To improve this, the polymerisation was repeated using a higher reaction concentration. This successfully resulted in higher molecular weights and conversion of 16.6 kDa and >99%, respectively (Table 18 Entry 2). Varying the amount of initiator can result in a change in molecular weight; usually decreasing the wt% of initiator increases the molecular weight.[153] However, in this case when the amount of AIBN was reduced to 0.25 wt% and 0.1 wt% (Table 18 Entry 3 & 4) no significant increase in molecular weight was observed. The addition of dodecanethiol as a chain transfer agent was found to result in a range of molecular weights, which decreased with the increasing concentration of dodecanethiol (Table 18 Entries 5-7). Using 1 wt% of the chain transfer agent gave an anomalous result, perhaps due to a procedural error (Table 18 Entry 6).

Table 18: Polymerisation of N-Isobornyl Acrylamide
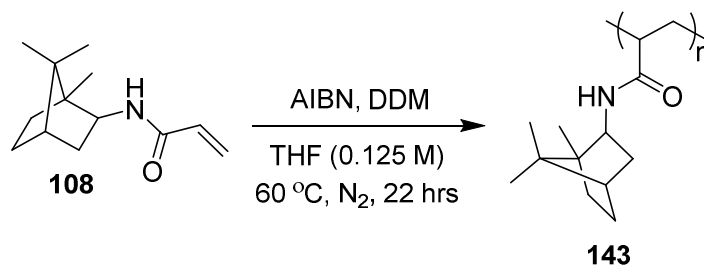
Entry	AIBN (wt%)	DDM (wt%)	M_n^a (kDa)	Mp (kDa)	M_w (kDa)	Polydispersity, Đ	Conversion[b] (%)
1	0.5	-	11.8	12.9	17.3	1.46	93
2[c]	0.5	-	16.6	25.2	30	1.81	>99
3	0.25	-	12.7	14.9	17.8	1.40	97
4	0.1	-	12.2	14.0	16.6	1.36	96
5	0.5	0.5	7.9	10	11.9	1.51	97
6	0.5	1	14.8	16	18.3	1.24	>99
7	0.5	5	6.5	9.3	9.2	1.41	>99

[a]Calculated from GPC calibrated with PMMA standard

[b]Calculated from NMR using the signals from the vinyl hydrogen (δ 5.49 ppm) of the unreacted monomer, and the α-amine hydrogen (δ 3.77 ppm) of the polymer.

[c] Effect of increased reaction concentration (0.3 M) investigated

Dynamic mechanical analysis of poly(*N*-isobornyl acrylamide) with molecular weight 16.6 kDa (Table 18 Entry 4) was conducted which gave a glass transition temperature of 189 °C (Figure 35).
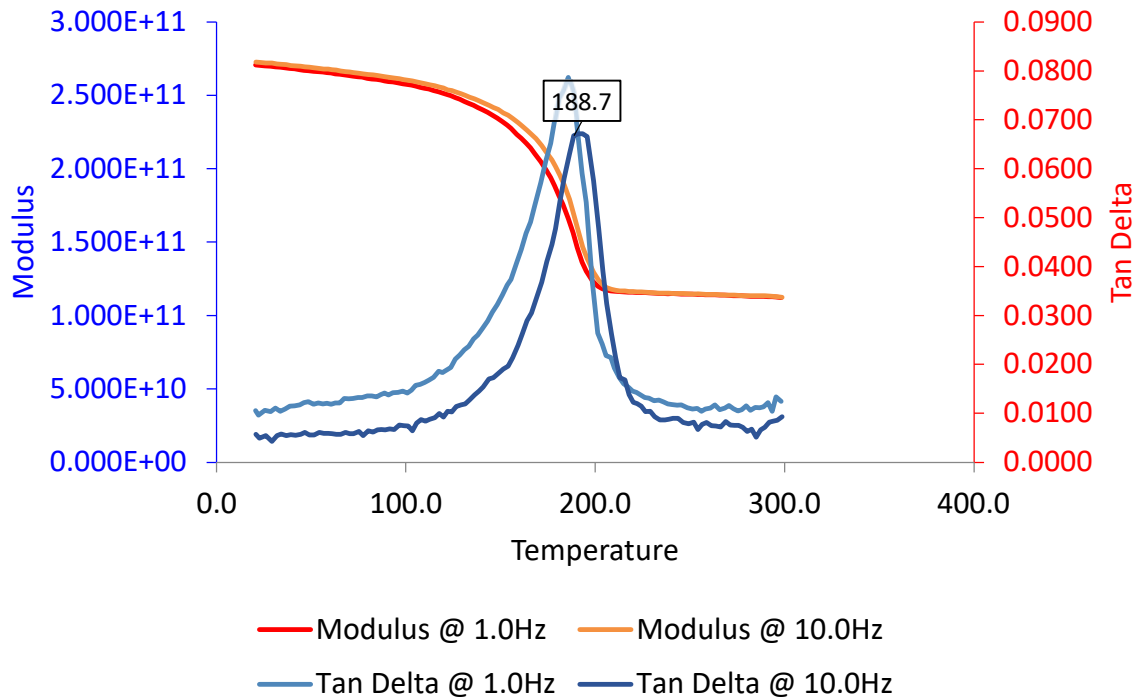
Figure 35: Dynamic Mechanical Analysis of Poly(N-Isobornyl Acrylamide)

Thermogravimetric analysis of poly(*N*-isobornyl acrylamide) gave a thermal decomposition temperature of 436 °C (Figure 36). This is over 200 °C above its glass transition temperature. This gives a large processing region, a useful characteristic in any future manufacturing processes as well as potential future uses in high temperature applications.
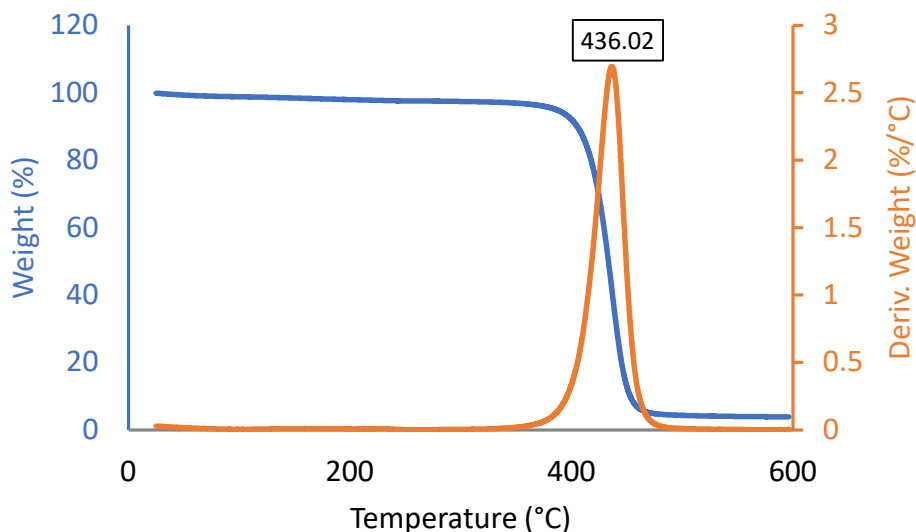
Figure 36: Thermogravimetric Analysis of Poly(N-Isobornyl Acrylamide)

Optimisation studies into the polymerisation of *N*-isobornyl acrylamide were carried out *via* a solvent screen. Polymerisation in cyclohexane (Table 19 Entry 2) gave comparable molecular weights compared to THF so the effect of a more polar solvent was investigated through the addition of 25 % v/v of *tert*-butanol. The addition of this polar solvent increased the molecular weight from 17 kDa to 25 KDa. Investigations into other similar polar protic solvents showed longer chain alcohols, in particular 1-pentanol (also known as amyl alcohol) to be the optimum solvent (Table 19 Entry 7). Using longer chain alcohols as the solvent allows for a higher active weight (i.e. polymer concentration) to be used within the polymerisation which resulted in higher molecular weights and a more commercially feasible polymerisation. In this case, longer chain alcohols are the optimum solvents due to the similar polarity and hydrogen bonding in space between the solvent, the monomer and the polymer.[154] Both the solvent and the solute have a non-polar region (hydrocarbon chain or terpene moiety) and a polar region (alcohol or amide moiety). Although a less exploited solvent, 1-pentanol is cheap and produced from biomass through alcoholic fermentation,[155] similar to ethanol, making it an ideal solvent choice for sustainable polymerisations. Unexpectedly, isopropanol gave a comparable yield to the polar aprotic solvents tetrahydrofuran and cyclohexanone due to low solubility of both the monomer and polymer

in isopropanol (Table 19 Entry 6). As such, pentanol was determined to be the most optimal solvent in terms of both solubility and sustainability.

Table 19: Investigation into the Optimum Polymerisation Solvent in the Synthesis of Poly(N-Isobornyl Acrylamide)
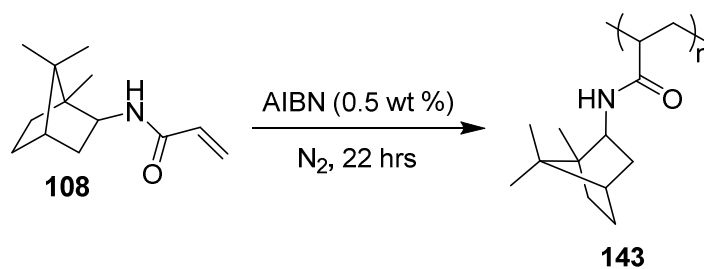
Entry	Solvent	M_n^a (kDa)	M_p (kDa)	M_w (kDa)	Polydispersity (Đ)	Conversion[b] (%)
1	THF	16.6	25.2	30.0	1.81	>99
2	Cyclohexanone	15.4	22.3	27.3	1.78	94
3	THF + 25% tBuOH	25.0	39.5	43.9	1.76	>99
4	Ethanol	37.3	54.8	64.8	1.74	99
5	Ethanol	32.3	53.1	59.5	1.84	98
6	Isopropanol	14.2	42.6	45.6	3.20	>99
7	Pentanol	62.3	99.3	126.8	2.04	>99

[a]Calculated from GPC calibrated with PMMA standard

[b]Calculated from NMR using the signals from the vinyl hydrogen (δ 5.49 ppm) of the unreacted monomer, and the α-amine hydrogen (δ 3.77 ppm) of the polymer.

With the optimum conditions for the highest molecular weights within thermal polymerisation of *N*-isobornyl acrylamide developed, the conversion of the monomer into polymer was measured over time using 400 MHz ^{1}H NMR anaylsis. The acrylamide alkene (a)

138

peak at 5.6 ppm and the polyacrylamide peak at 3.7 ppm represensting the hydrogen alpha to the nitrogen (b) were used as distinct markers of monomer depletion and polymer formation (Scheme 83).
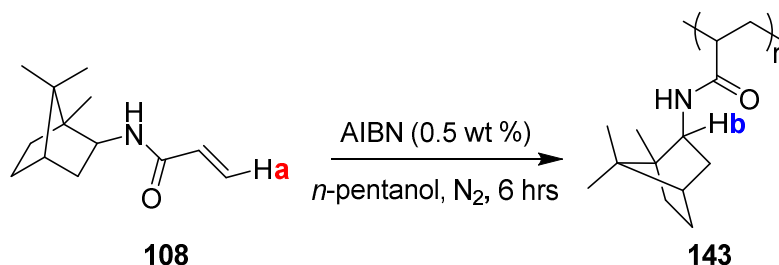
Scheme 83: 400 MHz ^1H NMR Monitored Synthesis of Poly(N-Isobornyl Acrylamide) in n-Pentanol

The results indicated the expected plot typical of chain growth polymerisations (Figure 37); increasing exponentially at first, followed by a slower plateau of chain growth as the number of collisons between free monomer and propagating chains decreases.[156–160] In pentanol, the polymerisation was completed (>99 % conversion) after 6 hours, reaching 93 % conversion after one hour. This is encouraging as the green solvent and short reaction time that denote these optimum conditions makes this polymerisation feasible on an industrial scale. Also, the facile polymerisation of *N*-isobornyl acrylamide would allow this monomer to be dropped directly into exisiting industrial processes as a replacement for other petroleum-based monomers.
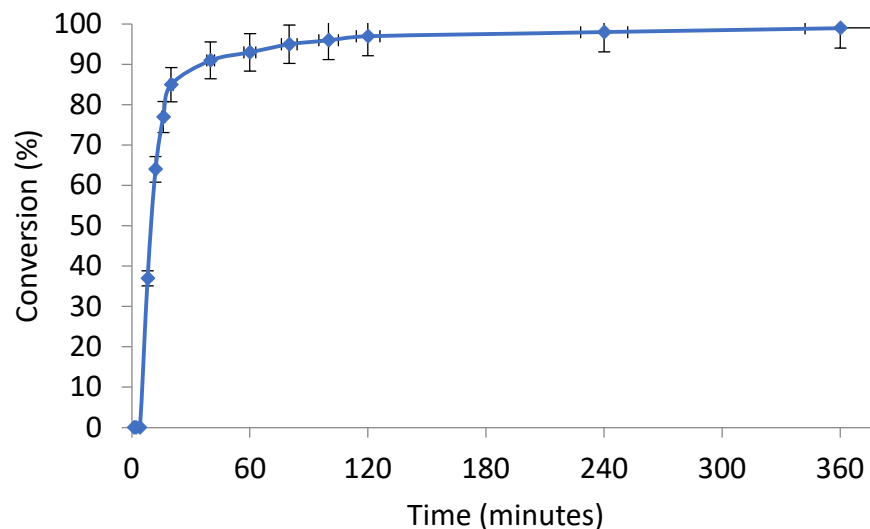
Figure 37: Conversion over Time for the Polymerisation of N-Isobornyl Acrylamide, measured using 400MHz ^1H NMR analysis

Dynamic mechanical analysis of the variety of molecular weights synthesis from the variety of conditions described in Table 18 and Table 19 gave a range of glass transition temperatures. Using these experimental values, a full analysis of how molecular weights affects the glass transition temperature for poly(*N*-isobornyl acrylamide) could be formulated using the Flory Fox equation. Plotting the experimental glass transition temperatures against the reciprocal of the Mn gave the limiting value of the glass transition temperature, $T_g \infty$, at around 208 °C and the constant, K, for poly(*N*-isobornyl acrylamide) as 1.2 x 10^5 g/mol (Figure 38). The limiting value of the glass transition temperature, 208 °C, is the highest glass transition temperature achievable for poly(*N*-isobornyl acrylamide). After a certain molecular weight, the number of entanglements along the polymer chains increases to the point that free movement is restricted irrespective of the temperature. This results in an upper limit to the glass transition temperature for any polymer, in this case is it 208 °C.

The experimental K value for poly(*N*-isobornyl acrylamide) is similar to the K value, 1.0 x 10^5 g/mol, for thermally polymerised polystyrene as reported by Flory and Fox in 1954.[161–163] The physical implications of K have been interpreted by several theories.[164] The most popular two are the chain rigidness theory and the free volume theory. The key point of the

chain rigidness theory is that the K value reflects the stiffness of the polymer chain.[165–168] Specifically, the more flexible the polymer, the smaller the K value and the influence of molecular weight on the glass transition temperature. Therefore a K value for poly(N-isobornyl acrylamide) which is similar to polystyrene would suggest a similar rigidity and strong molecular weight influence on the glass transition temperature. In addition, free volume theory states the chain ends contribute the most to the configurational entropy represented by the K value, as they have the most free volume within the polymer chain. This highlights the importance of initiator choice, as the ultimate chain end, with respect to these parameters.[161]

Figure showing a graph of T_g (°C) versus $1/M_n$ with a linear fit $y = -119183x + 208.04$
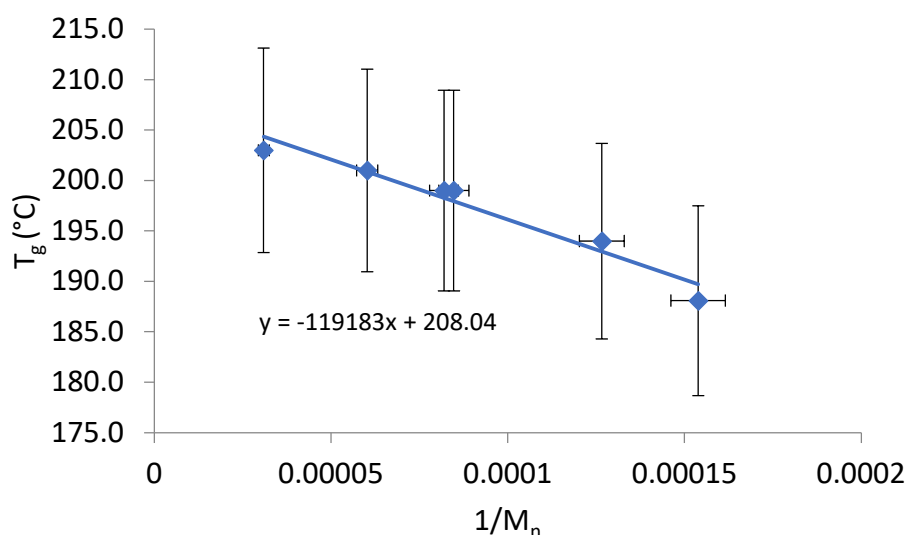
Figure 38: Graph showing Glass Transition Temperature versus Mn Reciprocal of Poly(N-Isobornyl Acrylamide)

Inputting these values into the Flory-Fox equation ($T_g = T_{g,\infty} - \dfrac{K}{M_n}$) gave the expected exponential curve of theoretical M_n values (Figure 39). The glass transition temperature increases exponentially with increasing molecular weight due to the free volume of the polymer chains in relation to the other polymer chains around it. Therefore, when the polymer has a low molecular weight, the polymer chains can move more freely, are more flexible and have a lower glass transition temperature. Using the K value derived from the experimental values, the data can be extrapolated to give a theoretical graph showcasing

the change in glass transition temperature over an extended molecular weight range. Using this graph allows for specific glass transition temperatures to be targeted, potentially enabling the material properties to be tuned by synthesising a particular molecular weight based upon this analysis.
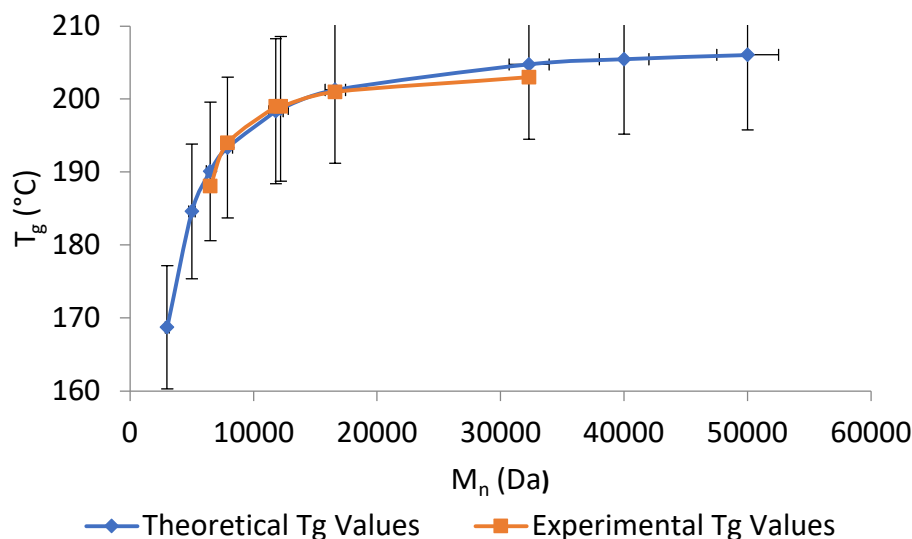
Figure 39: Experimental T_g's against the Theoretical T_g's for Poly(N-Isobornyl Acrylamide)

With the optimum conditions in hand, the homopolymerisation of *N*-isobornyl acrylamide was conducted on a large multigram scale (54 g) in industry *via* a semi-batch solution polymerisation with a monomer feed. Three different polymerisations were attempted with varying solvents and active weights (weight percentage of polymer in polymerisation) (Table 20). Initially due to availability, isopropanol was used instead of the optimum solvent, pentanol. 2,2'-Azodi(2-methylbutyronitrile), AMBN, was used instead of AIBN as these polymerisations were conducted in industry where AMBN is considered less hazardous. Polymerisations were conducted at 30 % and 22.5 % active weight as 30 % is Croda's ideal minimum active weight from an economic standpoint, however 22.5 % gave the optimum solubility of *N*-isobornyl acrylamide in isopropanol. The active weights were calculated from the varying amount of monomer in solution at the start of the polymerisation and then were checked at the end of the polymerisation *via* the weight difference before and after solvent removal. Both polymerisations, at 30 % and 22.5 % active weight, gave high

polydispersities with a range of molecular weights (Table 20 Entries 1 & 2) due to difficulties with the slow monomer addition *via* a pump. Switching to the optimum solvent, pentanol, at 30 % active weight, despite proving so successful in a batch process, unfortunately also gave high polydispersities in a semi batch process for the same reason (Table 20 Entry 3). The high polydispersities were proposed to be the result of low solubility of the monomer at 30 % active weight in both solvents at room temperature. If this polymerisation were to be commercially produced, more optimisation would be needed for large scale syntheses.

Table 20: Semi-Batch Polymerisation of Poly(N-Isobornyl Acrylamide)
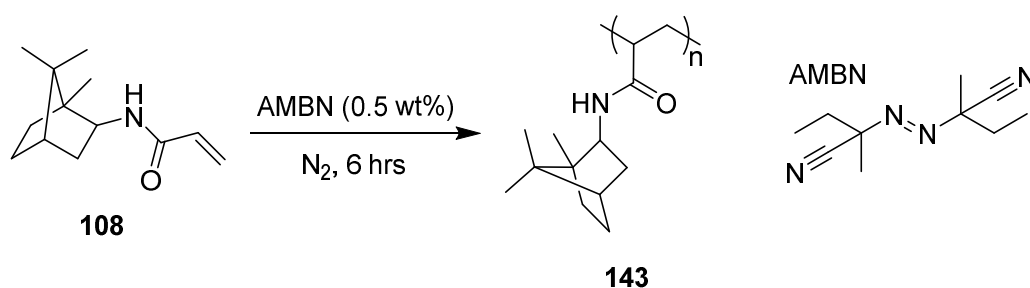
Entry	Solvent	Active Weight (%)	M_n^a (kDa)	M_p (kDa)	M_w (kDa)	Polydispersity, Đ
1	IPA	30	4.8	8.4	19.3	4.00
2	IPA	22.5	3.5	6.4	28.0	7.90
3	Pentanol	30	6.4	10.3	41.5	6.53

aCalculated from GPC calibrated with PMMA standard

143

3.1.4 Poly(*N-trans*-Sobrerol acrylamide)

N-trans-sobrerol acrylamide **121** was initially polymerised using standard free radical conditions successfully resulting in a >99 % conversion (Scheme 84). Analysis *via* GPC gave the M_n as 40 kDa with a polydispersity (Đ) of 1.21 (Table 21 Entry 1). This is a high molecular weight polymer with an unusually low polydispersity for an uncontrolled free radical polymerisation.
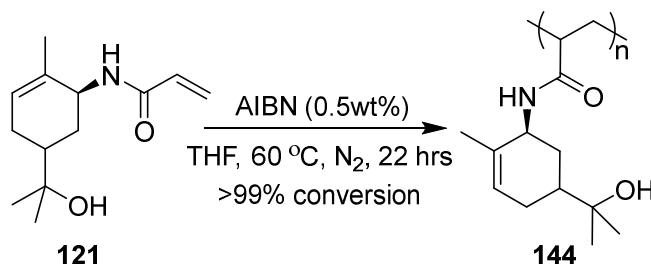
Scheme 84: Free Radical Polymerisation of N-trans-Sobrerol Acrylamide

Investigations into the effect of molecular weight on T_g were carried out using the chain transfer agent, dodecanethiol, to control molecular weight. The addition of 0.5 wt%, 1 wt% and 5 wt% successfully (Table 21 Entries 2, 3 and 4 respectively) controlled the polymerisation to create a range of molecular weights from 8.7 kDa to 28.7 kDa. Unusually low polydispersities were recorded for all four free radical polymerisations, at around 1.2, this suggests that the low polydispersity seen in the initial free radical polymerisation was due to the properties of the individual monomer rather than an anomaly. Ethanol, in the absence of a chain transfer agent, was also tested as a common green and sustainable solvent to replace tetrahydrofuran, resulting in comparable number average molecular weights and a slightly higher, but still acceptable, polydispersity (Table 21 Entry 5).

Table 21 : Polymerisation of N-trans-Sobrerol Acrylamide

Entry	Solvent	DDM (wt%)	M_n[a] (kDa)	M_p (kDa)	M_w (kDa)	Polydispersity, Đ	Conversion[b] (%)
1	THF	0	40.4	40.3	48.9	1.21	>99
2	THF	0.5	28.7	30.0	34.4	1.20	>99
3	THF	1	23.5	25.8	28.3	1.20	>99
4	THF	5	8.7	11.0	10.9	1.26	>99
5	Ethanol	0	40.2	53.0	60.6	1.51	>99

[a]Calculated from GPC calibrated with PMMA standard

[b]Calculated from NMR using the signals from the vinyl hydrogen (δ 6.03 ppm) of the unreacted monomer, and the α-amine hydrogen (δ 4.33 ppm) of the polymer.

Dynamic mechanical analysis of poly(*N-trans*-sobrerol acrylamide) with a molecular weight of 40.4 kDa (Table 21 Entry 1) gave a glass transition temperature of 202 °C (Figure 40). Interestingly, this glass transition temperature is similar to the previous poly(*N*-isobornyl acrylamide) despite their different structural characteristics. The high glass transition temperature of this polymer compared with commercially available polyacrylamides is potentially due to the additional tertiary alcohol moiety which increases hydrogen bonding between the side chains.[169] The increased energy needed to overcome this extra intermolecular bonding could result in the high glass transition temperature observed.

145
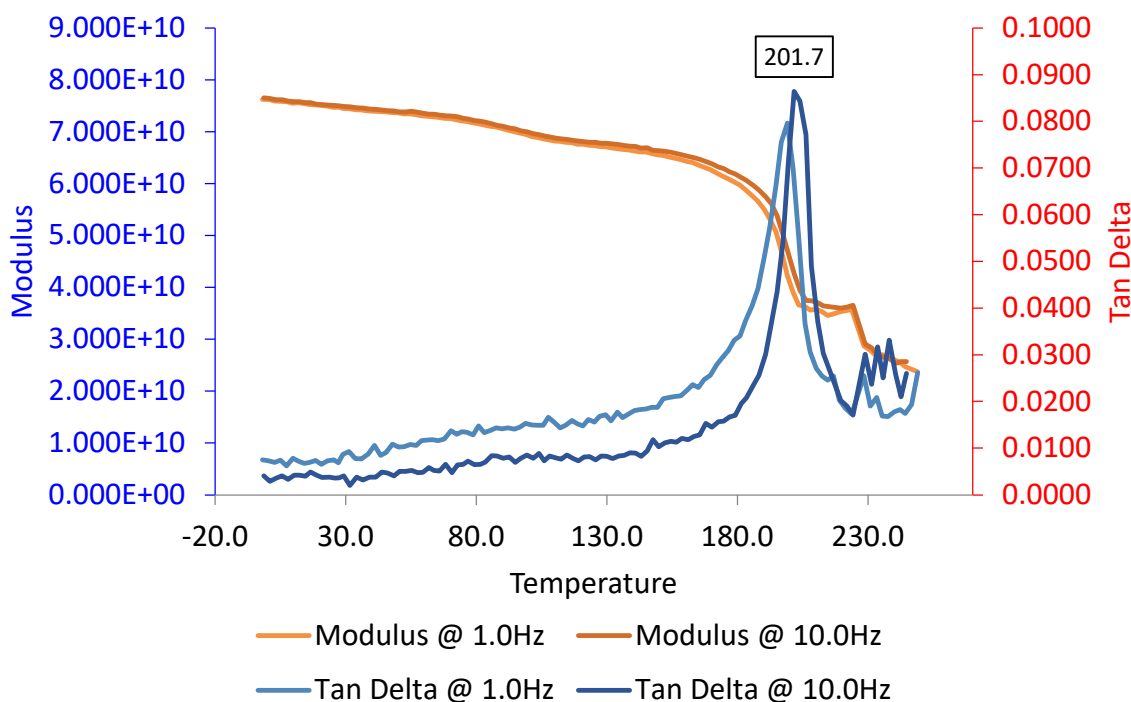
Figure 40: Dynamic Mechanical Analysis of Poly(N-trans-Sobrerol Acrylamide)

The glass transition temperatures were plotted against the reciprocal of the M_n to find the limiting vaule of the glass transition temperature, $T_{g, \infty}$, at around 207 °C and the constant, K, for poly(N-isobornyl acrylamide) as 2.0×10^5 g/mol (Figure 41). This K value is significantly higher than both the calculated K value for poly(N-isobornyl acrylamide), 1.2×10^5 g/mol, and the literature reported K value for polystyrene, 1×10^5 g/mol.[163] As the initiators for both terpene-derived polymers were the same, the higher K value suggests poly(N-trans-sobrerol acrylamide) to be a very rigid polymer with a high molecular weight dependence on the glass transition temperature.
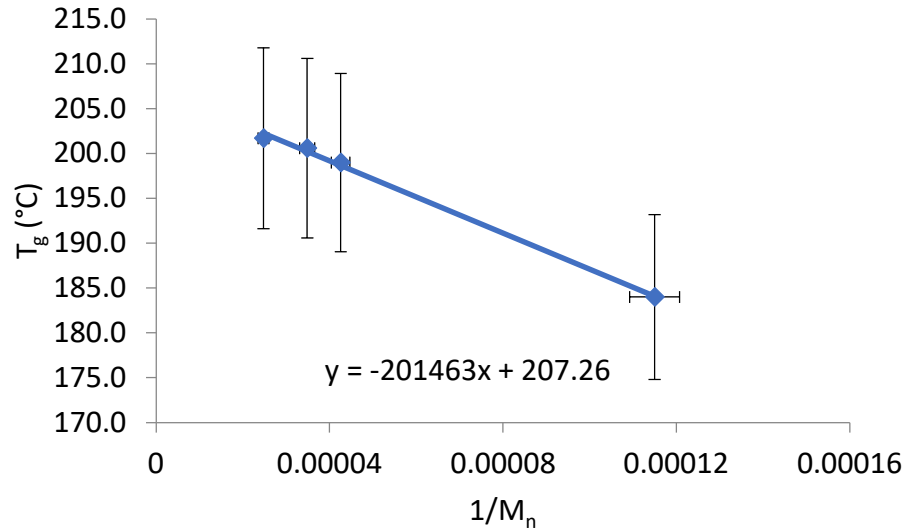
Figure 41: Graph showing Glass Transition Temperature versus M_n Reciprocal

Inputting these values into the Flory-Fox equation ($T_g = T_{g,\infty} - \frac{K}{M_n}$) gave the expected exponential curve of theoretical values. Using the K value derived from the experimental values, the data can be extrapolated to give a theoretical graph showcasing the change in glass transition temperature over an extended molecular weight range (Figure 42).
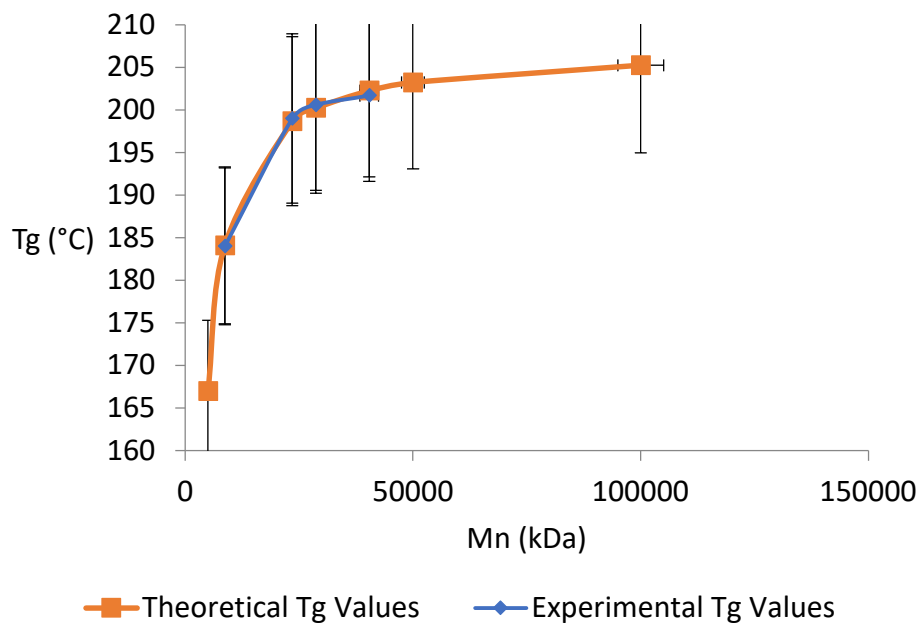
Figure 42: Experimental T_g's against Theoretical T_g's for Poly(N-trans-Sobrerol Acrylamide)

The homopolymerisation of *N-trans*-sobrerol acrylamide was also conducted on a large multi-gram scale (54 g) in industry *via* a semi-batch solution polymerisation with a monomer feed (Scheme 85).
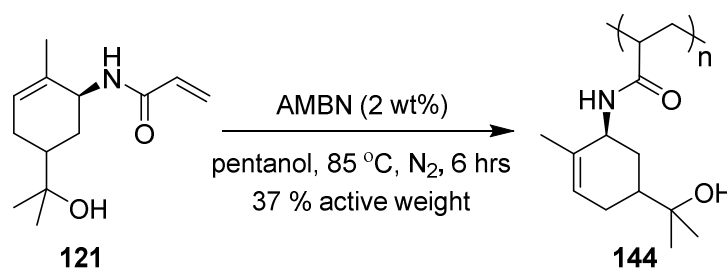
Scheme 85: Multi-gram Homopolymerisation of N-trans-Sobrerol Acrylamide

The polymerisation gave a low M_n of 10.6 kDa and a very high polydispersity of 4.03. The high polydispersity was due to the low solubility of the monomer, at 30 % active weight in

pentanol at room temperature. If this polymerisation was to be commercially produced, more optimisation on its large-scale synthesis would be required.

3.1.5 Poly(*N*-Carveol acrylamide)

N-Carveol acrylamide was polymerised using the same free radical conditions with AIBN as the initiator, as employed in previous polymerisations (Scheme 86). The polymerisation conversion by 400 MHz ^{1}H NMR was considerably lower than previously investigated polyacrylamides with a conversion of 45 %.
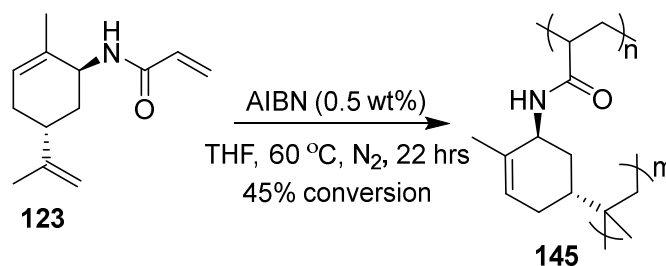
Scheme 86 : Polymerisation of N-Carveol Acrylamide

This was not unexpected due to the presence of the exocyclic alkene which has the potential for involvement causing branching in polymerisation. In 2016 Sainz *et al.*,[67] discussed previous investigations of renewable polyacrylates and polymethacrylates from similar terpene-based feedstocks, including carveol acrylate which also resulted in a low degree of polymerisation giving a conversion of only 5 % when the same conditions were used.

The low conversion is theorised to be due to the competing reactive alkenes. Radical formation on the exocyclic alkene has a faster reaction rate due to the positive induction effect of two alkyl groups. However, the high stability of the tertiary radical that forms results in a low propagation rate. Comparatively, the formation of a secondary radical on the acrylamide functionality has a slower reaction rate of formation due to the smaller positive induction, despite the extra stability from the electron withdrawing amide group. This decreased stability leads to increased reactivity towards chain propagation.[67]

Ultimately, these competing reaction centres result in a mixture of both functional groups across the backbone of the polymer and potentially some crosslinking or branching to form a graft macromolecule although the polymer still dissolved in all solvents for analysis so a

fully crosslinked polymer was never observed. This suggested that the polymer was a branched graft macromolecule. GPC analysis gave a very low polymer molecular weight of 3.2 kDa and DMA analysis gave a T_g of 105 °C.

Brief investigations into alternative solvents and initiators gave little improvement to the reaction conversion and subsequent polymer molecular weight (Table 22). In this case, tetrahydrofuran gave higher conversions than ethanol (Table 22 Entries 1 & 3). Increased reaction concentrations gave slightly higher molecular weights, as expected from collision theory (Table 22 Entries 1 & 2).

Table 22: Polymerisation of N-Carveol Acrylamide

Entry	Solvent	Conc. (M)	Temp. (°C)	M_n[a] (kDa)	M_p (kDa)	M_w (kDa)	Polydispersity (Đ)	Conversion[b] (%)
1	THF	0.17	60	1.9	2.1	2.9	1.51	66
2	THF	0.28	60	3.2	2.5	5.3	1.67	67
3	ethanol	0.67	75	2.5	2.5	3.6	1.43	50

[a]Calculated from GPC calibrated with PMMA standard

[b]Calculated from NMR using the signals from the vinyl hydrogen (δ 6.10 ppm) of the unreacted monomer, and the backbone (δ 6.25 ppm) of the polymer.

It was concluded that the low conversion of this polymer was due to the presence of the more reactive exocyclic alkene and the poor likelihood of any improvement means this

monomer is probably unsuitable for industrial use, so any further investigations into this polymer were suspended.

3.1.6 Poly(*N*-Carveol Bisepoxide Acrylamide)

The 1:1 epimeric mixture of *N*-carveol bisepoxide acrylamides was taken forward to polymerisation which was initially conducted under typical free radical conditions; 0.5 wt% AIBN in tetrahydrofuran (THF) at 60 °C for 22 hours (Scheme 87). The polymerisation resulted in a 94 % conversion, to form poly(*N*-carveol bisepoxide acrylamide). However, the molecular weight of the polymer was reasonably low at 5.9 kDa with a polydispersity (Đ) of 1.64 (Table 23 Entry 1). As the 1:1 mixture of epimers was used as the starting material, it is likely that a random co-polymer was formed as it is believed that the two diastereomers would have similar reactivity rates.
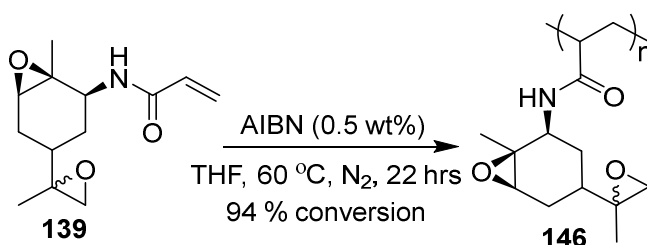
Scheme 87 : Polymerisation of N-Carveol Bisepoxide Acrylamide

Investigations were conducted into increasing the molecular weight of this polymer. Initially, decreasing the amount of initiator to 0.1 wt% (Table 23 Entry 2) was investigated, as in theory this would reduce the number of propagating polymer chains, resulting in longer chains. However, a lower average molecular weight (of just 4.9 kDa) was achieved due a loss of control from the lower initiator loading, resulting in a wider range of molecular weights as demonstrated by a higher polydispersity (Đ = 2.02). This lowered the average molecular weight and resulting in this unusual trend. The addition of a chain transfer agent, 0.5 wt% dodecanethiol (Table 23 Entry 3), gave a similar, low molecular weight but improved polydispersity of 1.57.

153

Table 23: Polymerisation of N-Carveol Bisepoxide Acrylamide

Entry	AIBN (wt%)	DDM (wt%)	M_n (kDa)[a]	M_p (kDa)	M_w (kDa)	Polydispersity, Đ	Conversion[b] (%)
1	0.5	0	5.9	10.6	9.6	1.64	94
2	0.1	0	4.9	11.1	9.8	2.02	>99
3	0.1	0.5	4.1	4.1	6.4	1.57	>99

[a]Calculated from GPC calibrated with PMMA standard

[b]Calculated from NMR using the signals from the vinyl hydrogen (δ 5.68 ppm) of the unreacted monomer, and the α-amine hydrogen (δ 4.38 ppm) of the polymer.

Next, investigations into alternative solvents were conducted. Cyclohexanone had been previously used within our group for the success polymerisation of a bisepoxide acrylate in high molecular weights and the addition of polar protic solvents have been successful in the polymerisation of other terpene-derived acrylamide monomers. Both investigative avenues were successful; increasing the molecular weight up to ~37 kDa (Table 24 Entry 6). The use of cyclohexanone, both as a co-solvent with tetrahydrofuran and on its own gave similar number average molecular weights of around 22-23 kDa with good polydispersities (Table 24 Entries 2 & 3). The addition of *tert*-butanol as a polar aprotic co-solvent to tetrahydrofuran gave a good molecular weight of 33 kDa (Table 24 Entry 4). This was matched when the solvent was swapped to the green, sustainable solvent, ethanol, which gave a molecular weight of 31 kDa and good polydispersity of 1.53 (Table 24 Entry 5). Repeating these conditions gave a comparable molecular weight and conversion demonstrating good reliability. Changing to polar solvents likely increased the molecular weights due to better solubility of the monomer and polymer in solution.

Table 24: Solvent Investigations for the Polymerisation of N-Carveol Bisepoxide Acrylamide

Entry	Solvent	M_n[a] (kDa)	M_p (kDa)	M_w (kDa)	Polydispersity, Đ	Conversion[b] (%)
1	THF	5.9	10.6	9.6	1.64	94
2	Cyclohexanone/THF	23.1	25.5	31.0	1.34	97
3	Cyclohexanone	22.1	26.1	32.0	1.45	>99
4	THF + 25% *t*BuOH	32.6	46.9	43.5	1.33	91
5	Ethanol	30.7	55.2	47.1	1.53	>99
6	Ethanol	36.7	42.1	41	1.12	>99

[a]Calculated from GPC calibrated with PMMA standard

[b]Calculated from NMR using the signals from the vinyl hydrogen (δ 5.68 ppm) of the unreacted monomer, and the α-amine hydrogen (δ 4.38 ppm) of the polymer.

Attempts to determine the glass transition temperatures for the varying molecular weight polymers were unsuccessful as the results varied both between samples and between reruns of the same samples (Figure 43). This was indicative of the polymer crosslinking upon heating *via* an epoxide ring open mechanism within the dynamic mechanical analysis instrument. This was confirmed visually by the swelling of the polymer material when solvent was added after a heating/cooling cycle.
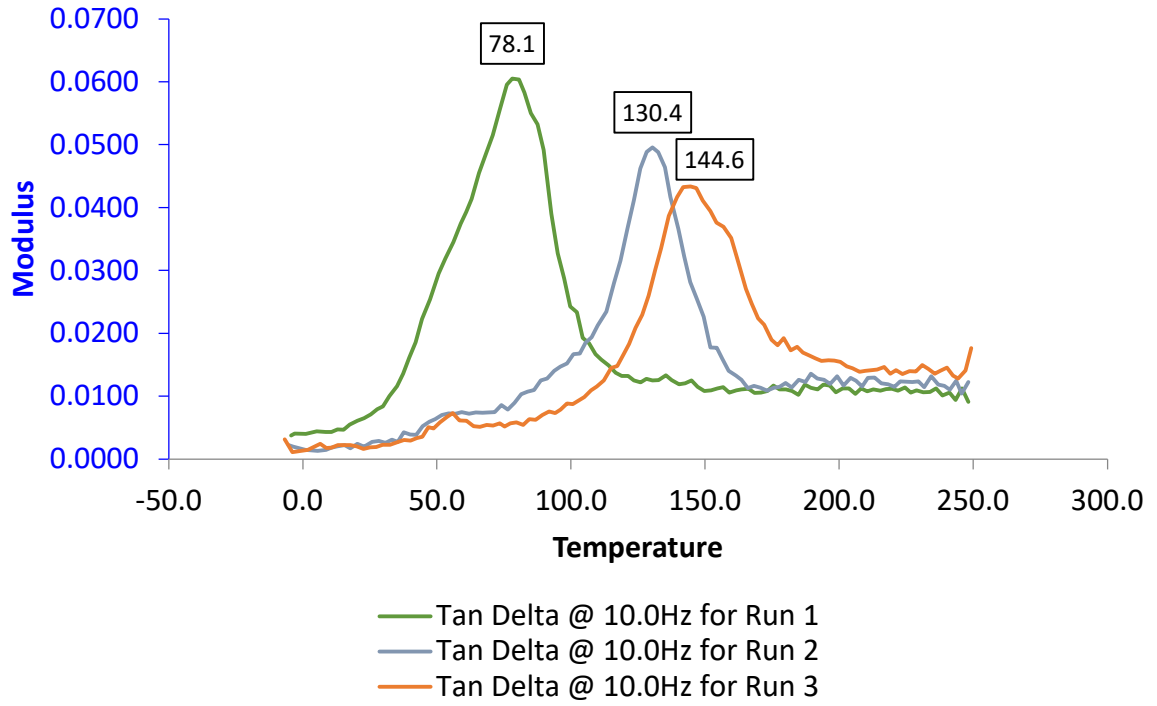
Figure 43: Dynamic Mechanical Analysis for Three Heating and Cooling Cycles of the Same Poly(N-Carveol Bisepoxide Acrylamide) Sample with an M_n of 32.6 kDa

3.1.7 Poly(*N*-Carvone Acrylamide)

N-Carvone acrylamide proved insoluble in tetrahydrofuran, therefore alternative solvents and initiators were investigated. As ethanol proved successful as a green solvent in the polymerisation of other terpene-derived acrylamides it was investigated first. The use of ethanol with 1 wt% AIBN gave poly(*N*-carvone acrylamide) with a M_n of 14 kDa and a good polydispersity of 1.40 (Table 25 Entry 1). The polymerisation stopped at a low conversion of 67 %, this was potentially due to the reactivity of the enone functionality towards radicals but not propagation causing a radical sink.[153] The use of a larger radical initiator, V88, gave no reaction with recovery of the starting monomer (Table 25 Entry 2). Switching the solvent to a non-polar aprotic solvent and adding a chain transfer agent, dodecanethiol, was a success. This was likely due to the chain transfer agent facilitating the movement of radicals within the reaction solution due to steric hindrance with the dodecanethiol favouring the more accessible acrylamide functionalities. The polymerisation proceeded with 94 % conversion resulting in a M_n of 11 kDa and a low polydispersity of 1.06 (Table 25 Entry 3).

Table 25: Syntheses of Poly(N-Carvone Acrylamide)
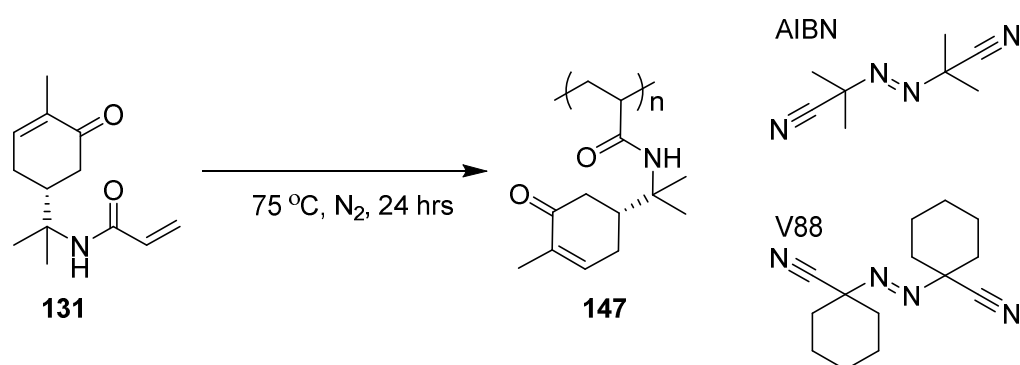
Entry	Solvent	Initiator	DDM (μL)	M_n^a (kDa)	M_p (kDa)	M_w (kDa)	Polydispersity, Đ	Conversion (%)
1	ethanol	AIBN	-	14.2	14.6	19.9	1.40	67
2	ethanol	V88	-	-	-	-	-	0
3	toluene	V88	5	10.7	8.7	11.3	1.06	94

[a]Calculated from GPC calibrated with PMMA standard

[b]Calculated from NMR using the signals from the vinyl hydrogen (δ 5.70 ppm) of the unreacted monomer, and the cyclohexyl hydrogens (δ 3.10 ppm) of the polymer.

The glass transition temperature of poly(*N*-carvone acrylamide) with a molecular weight of 10.7 kDa (Table 25 Entry 3) was determined to be 132 °C by dynamic mechanical analysis (Figure 44). This glass transition temperature sits in the middle of the previously characterised terpene-derived polyacrylamides. It is lower than poly(*N*-isobornyl acrylamide) (208 °C) and poly(*N*-*trans*-sobrerol acrylamide) (202 °C), likely due to the more flexible alkyl acrylamide pendant group compared with their more rigid α-cyclic acrylamide structures. It also has a higher glass transition temperature than poly(*N*-myrtenyl acrylamide) (91 °C) potentially due to the position of the enone functionality where it is able to participate in intermolecular hydrogen bonding between the polymer chains as a hydrogen bond acceptor.
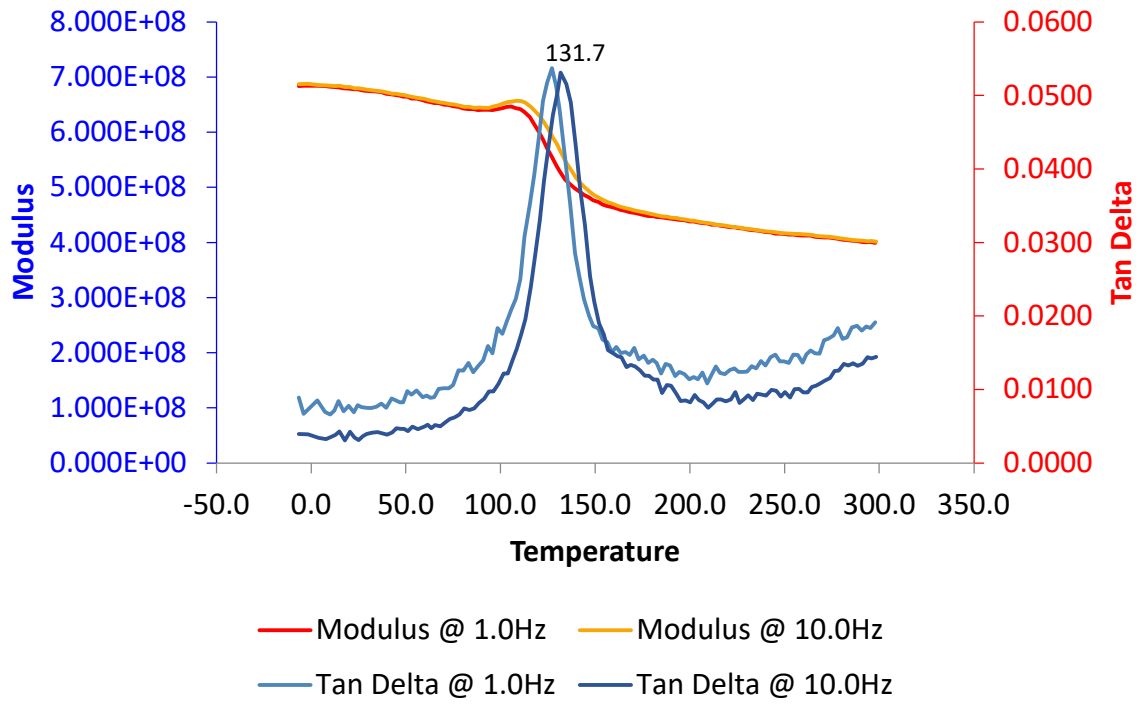
Figure 44: Dynamic Mechanical Analysis of Poly(N-Carvone Acrylamide)

3.1.8 Poly(*N*-Pulegone Acrylamide)

An initial free radical polymerisation of *N*-pulegone acrylamide in tetrahydrofuran, with AIBN as the radical initiator, gave poly(*N*-pulegone acrylamide) in a 99 % conversion with a M_n of 6.8 kDa and a polydispersity of 1.71 (Scheme 88).
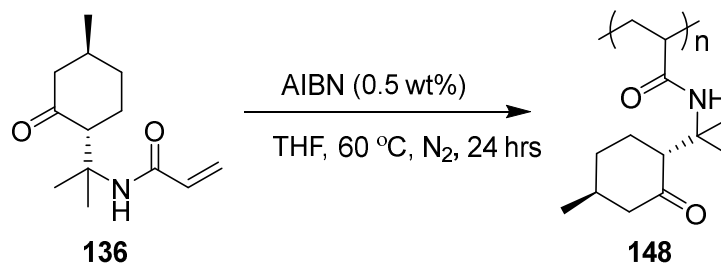
Scheme 88: Polymerisation of N-Pulegone Acrylamide

The molecular weight of poly(*N*-pulegone acrylamide) was low compared with the previous terpene-acrylamide polymerisations, therefore optimisation investigations were conducted. Polar protic solvents had proven to be successful in previous polymerisations, as such ethanol was chosen as the polymerisation solvent for an investigation into the optimum radical initiator. Initially, 0.5 wt % of AIBN in ethanol was attempted, however this resulted in complete recovery of the monomer. Switching the initiator to another azo-initiator V88 also gave 0 % conversion with recovery of the starting monomer (Table 26 Entry 1-2). Although the polymerisation of *N*-pulegone acrylamide in ethanol was looking unpromising, increasing the initiator loading was investigated with 1 wt% AIBN (Table 26 Entry 3). This gave a M_n of 14.8 kDa, over double that in tetrahydrofuran, and a good polydispersity of 1.43. Increasing the initiator loading of V88 gave a M_n of 6.2 kDa and a polydispersity of 1.85, comparable to the initial polymerisation in tetrahydrofuran (Table 26 Entry 4). In an effort to increase this further, a V88 initiator loading of 2 wt% was investigated (Table 26 Entry 5). However, this gave comparable results to the 1 wt% loading. Subsequently thermal peroxide initiators were investigated. *Tert*-butyl peroxybenzoate (TBPB) was used as the radical catalyst at 1 wt% to give a comparable result to that of AIBN (Table 26 Entry 6). Increasing the radical catalyst loading to 2 wt% lowered the molecular weight of the resulting polymer (Table 26 Entry 7) although improved polydispersity. This is likely due to

the increased number of radical initiators reacting with more monomers which go on to propagate into a larger number of smaller polymer chains. A second thermal peroxide initiator, *tert*-butyl hydroperoxide (TBHP), was investigated (Table 26 Entry 8). However, unlike the previous peroxide initiator, this reaction resulted in no conversion and recovery of the starting monomer after 24 hours.

Table 26: Investigations into Optimum Thermal Initiator for the Polymerisation of N-Pulegone Acrylamide
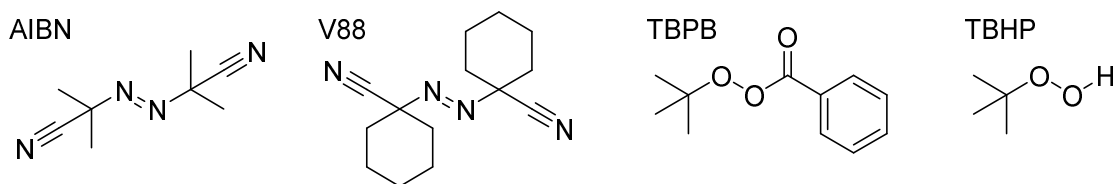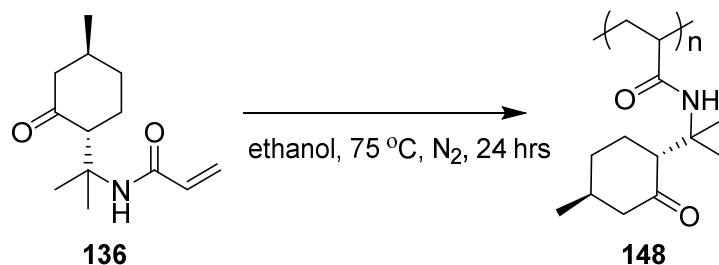
Entry	Initiator	Wt%	$M_n{}^a$ (kDa)	M_p (kDa)	M_w (kDa)	Polydispersity, Đ	Conversion[b] (%)
1	AIBN	0.5	-	-	-	-	0
2	V88	0.5	-	-	-	-	0
3	AIBN	1	14.1	17.4	20.2	1.43	86
4	V88	1	6.2	9.7	11.4	1.85	84
5	V88	2	6.3	9.6	10.9	1.74	89
6	TBPB	1	15.7	19	22.2	1.42	81
7	TBPB	2	10.2	9.6	12.6	1.24	96
8	TBHP	1	-	-	-	-	0

[a]Calculated from GPC calibrated with PMMA standard

[b]Calculated from NMR using the signals from the vinyl hydrogen (δ 5.55 ppm) of the unreacted monomer, and the α-methyl hydrogen (δ 1.88 ppm) of the polymer.

Two initiators, one azo-initiator, V88, and one peroxide initiator, TBPB, were used to investigate the polymerisation in pentanol, a previously successful solvent for terpene-derived acrylamide polymerisations. In both cases, although the conversions were slightly higher than those conducted in THF, the molecular weights were lower and polydispersities higher. This would suggest that, for the polymerisation of *N*-pulegone acrylamide, ethanol is the optimum green solvent choice.

Table 27: Polymerisation of N-Pulegone Acrylamide in Pentanol
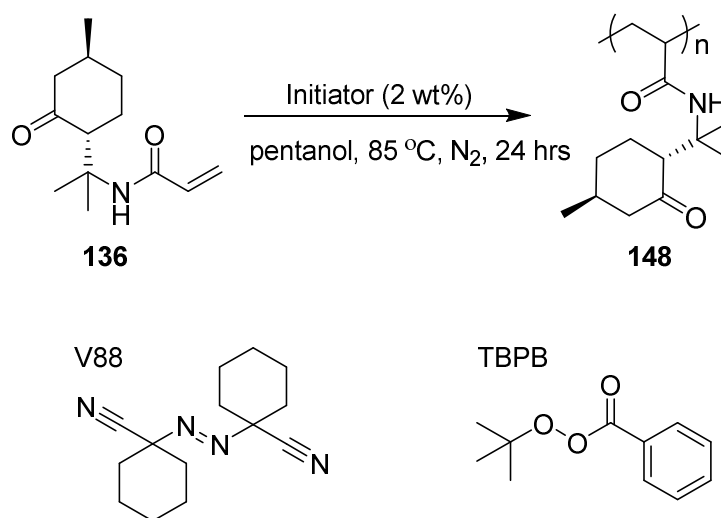
Entry	Initiator	M_n^a (kDa)	M_p (kDa)	M_w (kDa)	Polydispersity (Đ)	Conversion[b] (%)
1	V88	5.5	8.8	10.4	1.91	92
2	TBPB	6.9	7.2	9.3	1.34	99

[a]Calculated from GPC calibrated with PMMA standard

[b]Calculated from NMR using the signals from the vinyl hydrogen (δ 5.55 ppm) of the unreacted monomer, and the α-methyl hydrogen (δ 1.88 ppm) of the polymer.

Dynamic mechanical analysis of the polymer with the M_n of 6.9 kDa (Table 27 Entry 2) gave a glass transition temperature of 92 °C (Figure 45). Interestingly, this low glass transition temperature is comparable to that of poly(*N*-myrtenyl acrylamide), and lower than commercially available polyacrylamides. The low glass transition temperature could be due

to the extra flexibility of the polymer side chains, due to the extra rotatable carbon between the polymer chain and the structured terpene ring.
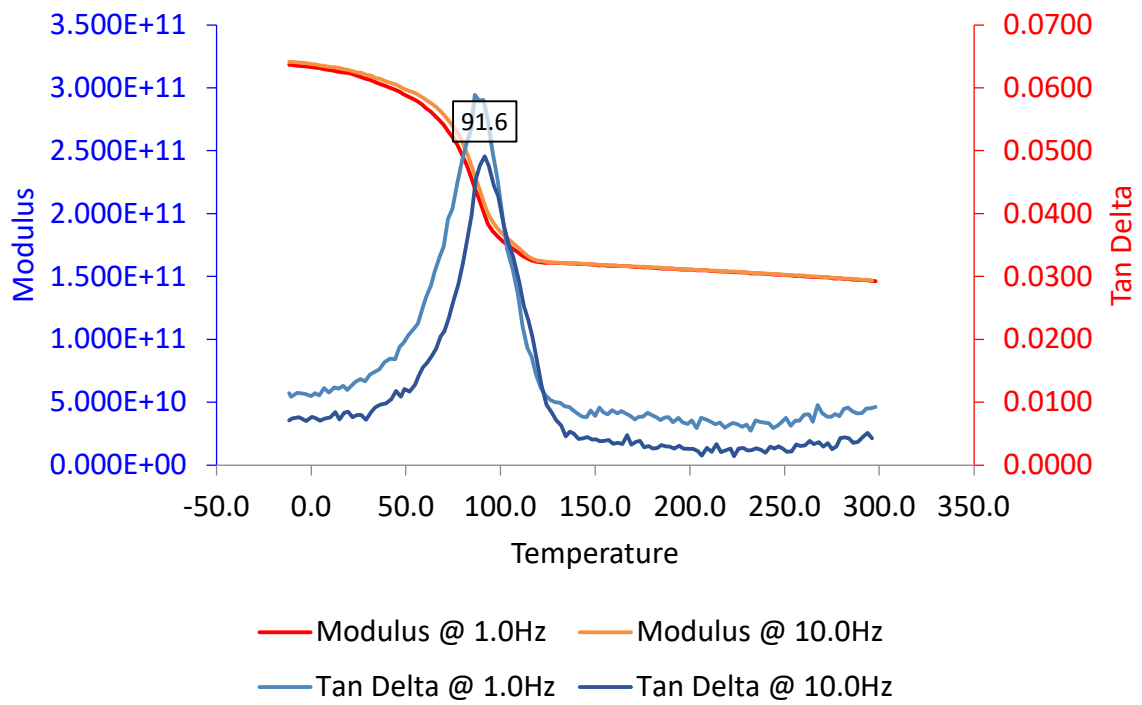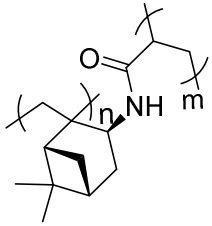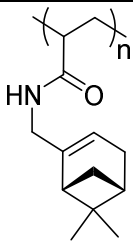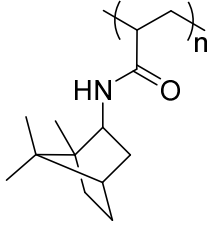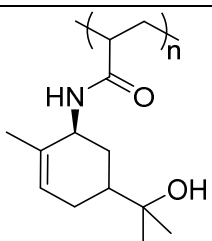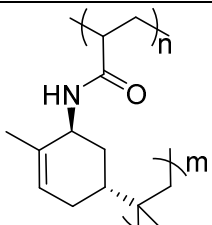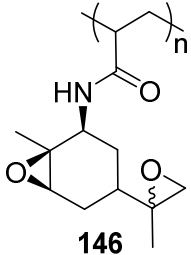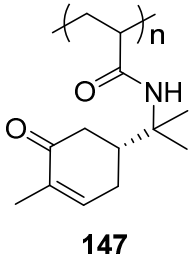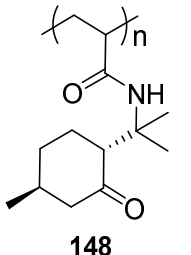
Figure 45: Dynamic Mechanical Analysis of Poly(N-Pulegone Acrylamide)

3.1.9 Summary of Terpene Derived Homopolymers by Free Radical Polymerisation

Poly(terpene)	Initiator	Solvent	Conversion[a] (%)	M_n[b] (kDa)	Polydispersity (Đ)	T_g (°C)
141	AIBN	THF	N/A - Polymer crosslinked			
142	AIBN	THF	>99	25.4	1.07	91
143	AIBN	Pentanol	>99	62.3	2.04	208
144	AIBN	THF	>99	40.4	1.21	202
145	AIBN	THF	67	3.2	1.67	N/A

165

146	AIBN	Ethanol	>99	36.7	1.12	N/A
147	AIBN	Ethanol	67	14.2	1.40	130
148	TPBP	Ethanol	96	10.2	1.24	92

[a]Calculated from NMR

[b]Calculated from GPC calibrated with PMMA standard

3.2 Thermally Initiated Random Co-polymerisations

Uniting characteristics of two or more chemically distinct homopolymers into one renewable co-polymer *via* covalent bonds allows for the combination of multiple desirable characteristics for designer applications and are ideal targets for innovation.[45] Investigations into the synthesis of a library of random copolymers will use commercially available co-monomers alongside the novel terpene-derived acrylamide monomers (described in chapter 2) to facilitate comparisons between the properties of varying mole fractions of the terpene moieties with biobased copolymers.

N-Vinyl pyrrolidone and *N*-isobornyl acrylamide were used for initial investigations into random co-polymerisations as co-polymers of *N*-vinyl pyrrolidone are already widely used in three markets in which Croda Plc. is already invested: personal care, crop care and adhesives.[170] Poly(*N*-vinyl pyrrolidone) is commercially successful due to its biological compatibility, low toxicity, film forming and adhesive characteristics, unusual complexing behaviour towards salts and acids coupled with thermal degradation in solution.[171] *N*-isobornyl acrylamide was targeted first from the terpene-based monomers due to its commercially appealing, one step synthesis from a readily available renewable chemical on a large scale.

3.2.1 Initiator Investigations

Initially a range of initiators (2 wt%) were investigated for the semi-batch co-polymerisation of *N*-vinyl pyrrolidone and *N*-isobornyl acrylamide (75:25) in isopropanol (IPA). The monomer ratio (75:25) was chosen due to solubility issues of *N*-isobornyl acrylamide in isopropanol and the commercial preference at Croda to run polymerisation at 30 % active weight (i.e. wt% polymer concentration). Two azo initiators, azobisisobutyronitrile (AIBN) and 2,2'-azodi(2-methylbutyronitrile) (AMBN), an inorganic sulfate initiator, ammonium persulfate (APS) and a peroxide initiator, *tert*-butyl peroxybenzoate (TBPB) were all investigated (Table 28).

Table 28: Random Co-polymerisation of N-Isobornyl Acrylamide and N-Vinyl Pyrrolidone[a]
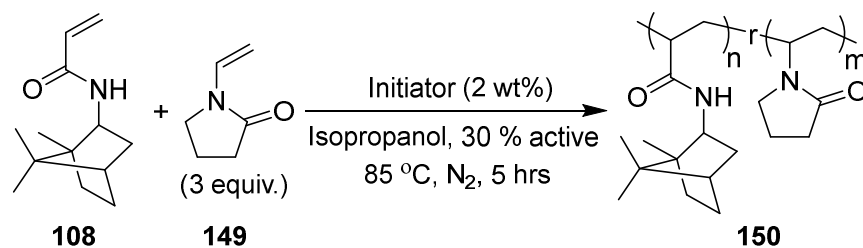
Entry	Initiator	M_n^a (kDa)	M_w (kDa)	Polydispersity, Đ
1	AIBN	1.6	4.5	2.8
2	AMBN	1.5	4.0	2.7
3	APS	1.3	2.8	2.2
4	TBPB	2.1	3.7	1.8

[a]5 hour reaction with a 3 hour monomer and initiator feed

[b]Calculated from GPC calibrated with PMMA standard

The molecular weights and polydispersities achieved by the azo initiators were comparable however; AIBN was only sparingly soluble in isopropanol and had to be added in aliquots (Table 28 Entries 1 & 2). Unsurprisingly, the inorganic initiator APS was insoluble in isopropanol and had to be added in aliquots which negatively affected the molecular weight. During the reaction with APS, a film formed on top of the reaction solution due to the insolubility of the polymer in isopropanol, which when analysed had a M_n of 1.3 kDa and a polydispersity of 2.2. This was a significantly higher molecular weight than the polymer chains left in solution suggesting that the solubility of the polymer reduced as the molecular

weight increased (Table 28 Entry 3). TBPB had the highest molecular weights and the best polydispersity in solution, however a white precipitate formed during the polymerisation. When analysed, this gave a M_n of 2.1 kDa and a polydispersity of 1.8 (Table 28 Entry 4). The consistently low molecular weights in solution suggest the co-polymer is insoluble in isopropanol after a certain molecular weight causing unfavourable precipitation, in turn resulting in high dispersities. Therefore, a solvent screen for the co-polymerisations was investigated next.

3.2.2 Solvent investigations

For semi-batch solution polymerisations at Croda Hull, standard polymerisation conditions for the solution polymerisation of acrylics are >80 °C and at least 30 % active weight (weight percent of monomer in the total reaction mass). From solvent investigations during the homopolymerisations of the terpene-derived acrylamides, it was determined that polar protic solvents such as ethanol consistently gave the highest molecular weights. However, with a boiling point of only 78 °C, an alternative high boiling solvent was desired. *n*-Pentanol was also previously investigated during the homopolymerisations of the terpene-derived acrylamides. With a boiling point of 138 °C, *n*-Pentanol was successfully used in the homopolymerisation of *N*-isobornyl acrylamide resulting in high molecular weights, low polydispersities and a short reaction time of 6 hours, ideal for an industrial shift. Similarly, to ethanol and isopropanol, pentanol is a renewable solvent that can be produced by alcoholic fermentation of biomass feed stocks. As such, the semi-batch co-polymerisation of *N*-vinyl pyrrolidinone and *N*-isobornyl acrylamide in a 1:1 ratio was conducted and compared against isopropanol as the solvent. *N*-isobornyl acrylamide, alongside the other acrylamide monomers was more soluble in pentanol than isopropanol and therefore a more equal ratio of comonomers could be used. The use of pentanol as the solvent doubled the M_n compared to isopropanol, although with a higher polydispersity (Table 29 Entry 2). Despite this increase in polydispersity, it was concluded that *n*-pentanol was a suitable solvent with which to conduct further polymerisations.

169

Table 29: Comparing the Effect of Different Solvents on the Random Co-polymerisation of N-Isobornyl Acrylamide and N-Vinyl Pyrrolidinone
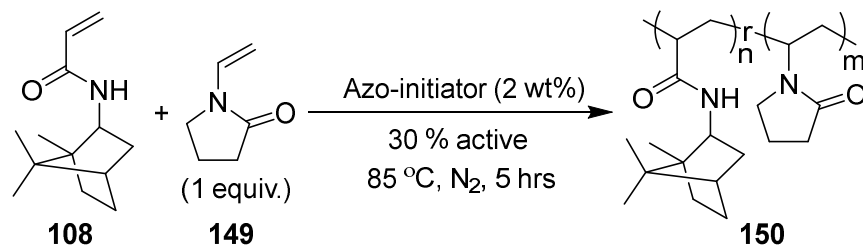
Entry	Solvent	Price[a] (£)	M_n[b] (kDa)	M_w (kDa)	Đ
1	isopropanol	196	1.5	3.4	2.24
2	*n*-pentanol	198	3.8	19.4	5.04

[a]price for 20kg from Sigma-Aldrich on 21/08/2019

[b]Calculated from GPC calibrated with PMMA standards

3.2.3 Co-monomer Investigations

With the first terpene-derived co-polymer now in hand, attention turned to expanding the co-polymer library with other commercially available monomers. Along with *N*-vinyl pyrrolidone, three other monomers were chosen for investigations into semi-batch solution co-polymerisations; allyl alcohol, PEG acrylate and stearyl methacrylate (Figure 46). Each co-monomer was chosen because of their varying structures, polymeric characteristics and use in target markets.
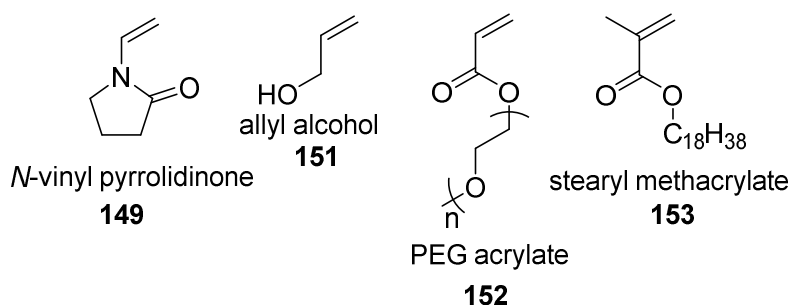
Figure 46: Commercially Available Vinyl Co-monomers

Poly(allyl alcohol) (PAA) has attracted interest within the literature due to its formal equivalence to hydroxy-functionalized polypropylene. It is aimed to maintain the favourable physical and chemical properties of polypropylene but with improved adhesive characteristics.[172] Currently, allyl alcohol is most often found commercially as a co-polymer with other olefinic monomers such as styrene, with incorporation of allyl alcohol typically <10% for polymers greater than 5 kDa due to the low reactivity of its vinyl functionality.[173] Applications of these allyl alcohol co-polymers include coatings for transportation, maintenance and general metals applications as the high hydroxyl functionality contributes to good adhesion and chemical and abrasion resistance in the final coating.[174,175]

Poly(ethylene glycol) is biologically inert, flexible, hydrophilic and features low polymer-water interfacial energy values, resistance to protein adsorption and cell adhesion. This polymer and the acrylate with pendant PEG moieties, PEG acrylate, is typically used as a hydrophilic block in the formation of block co-polymers and is currently used in health care, personal care and as an enhanced oil recovery additive.[176–178]

171

Poly(stearyl methacrylate) has good chemical resistance, hydrophobicity, good flexibility, high impact strength, low shrinkage, adhesion and weatherability. It has been used in automotive and industrial coatings, as viscosity modifiers and as pour point depressant in oil and lubricants applications.[179–181]

3.2.4 *N*-Isobornyl Acrylamide Random Copolymers

These commercially available monomers were successfully copolymerised in a 1:1 ratio with three different terpene-derived acrylamides, starting with *N*-isobornyl acrylamide. Conversion was determined as complete when no monomer peak was observed *via* GPC. As previously reported, *N*-isobornyl acrylamide gave a high polydispersity of polymer chain lengths when co-polymerised with *N*-vinyl pyrrolidone (Table 30 Entry 1). A comparable result was seen when allyl alcohol was used in the co-polymerisation (Table 30 Entry 2). This was not unexpected due to the predicted differing reactivity of the vinyl monomers compared to the acrylamides. The co-polymerisation of *N*-isobornyl acrylamide with PEG acrylate resulted in the formation of a white precipitate. When analysed by GPC, the remaining solution gave a low M_n of 6 kDa and a good polydispersity of 1.41 (Table 30 Entry 3). The white precipitate gave a higher M_n of 18.7 kDa and a higher polydispersity of 2.68 Đ, suggesting that poly(*N*-isobornyl acrylamide-*co*-PEG acrylate) was not soluble in pentanol after a certain molecular weight threshold, and alternate solvents would need to be investigated in the future to optimise the co-polymerisation for any large scale production of this polymer. The co-polymerisation of stearyl methacrylate and *N*-isobornyl acrylamide gave a good M_n of 19 kDa and a high polydispersity of 2.54 Đ (Table 30 Entry 4), though considerably lower than that of the vinyl copolymers. This can be attributed to the closer similarities in structure and reactivity of the acrylamide and methacrylate moieties of *N*-isobornyl acrylamide and stearyl methacrylate, respectively. Active weight (i.e. wt% polymer concentration) was determined by comparing the dry isolated polymer weight against the weight of the polymer reaction mixture.

Table 30: N-Isobornyl Acrylamide Random Co-polymerisations

R₁ = H, CH₃

R₂ =

150   **154**   **155**   **156**
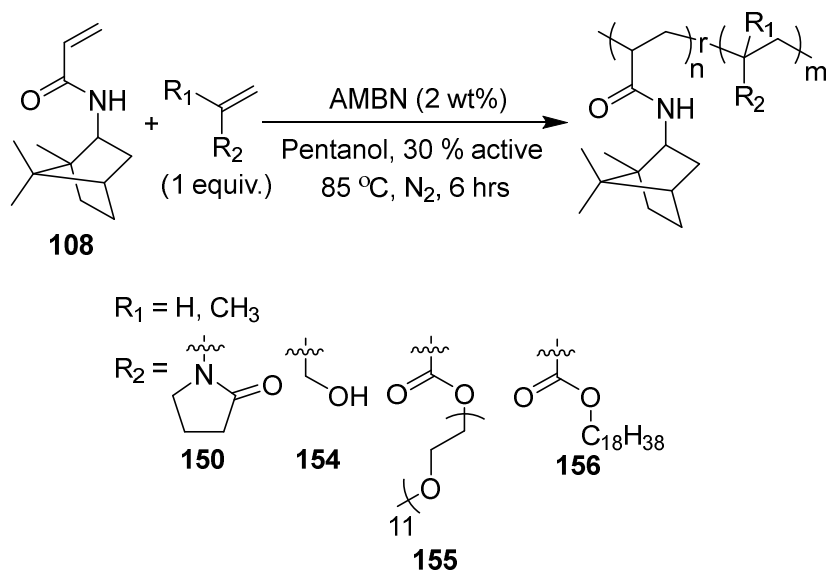
Entry	Co-monomer	$M_n{}^a$ (kDa)	M_w (kDa)	Polydispersity, Đ	Active Weight (%)
1	*N*-vinyl pyrrolidone	3.8	19.4	5.04	18
2	Allyl alcohol	3.4	19.0	5.63	11
3	PEG acrylate	6.0	8.5	1.41	23
4	Stearyl methacrylate	19.0	48.3	2.54	34

ªCalculated from GPC calibrated with PMMA standard

As the co-polymer with the highest degree of polymerisation, investigations into varying the ratio of *N*-isobornyl acrylamide to stearyl methacrylate were conducted, in order to probe the different polymer properties that might result. The ratio of *N*-isobornyl acrylamide: stearyl methacrylate was increased from 1:1 to 2:1 then 3:1 to create a larger library of co-monomers for applications testing and to distinguish the effect of monomer concentrations on the control and degree of polymerisation.

Table 31: Random Copolymerisation of N-Isobornyl Acrylamide (X) and Stearyl Methacrylate (Y) in Varying Ratios
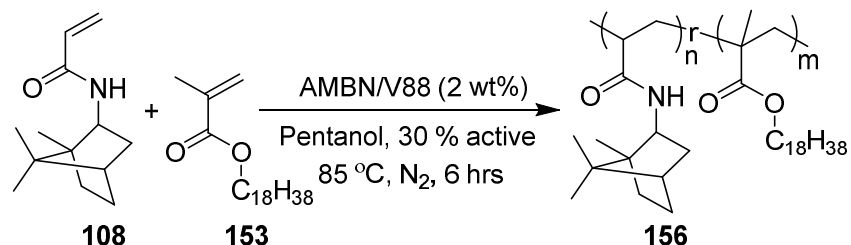
Entry	Ratio of X:Y	M_n^a (kDa)	M_p (kDa)	M_w (kDa)	Polydispersity, Đ
1	1:1	19.0	41.8	48.3	2.54
2	2:1	18.6	27.8	36.2	1.95
3	3:1	19.7	27.8	50.1	2.53

[a]Calculated from GPC calibrated with PMMA standard

3.2.5 *N-trans*-Sobrerol Acrylamide Random Copolymers

Next, the four commercially available co-monomers (*N*-vinyl pyrrolidone, allyl alcohol, PEG acrylate and stearyl methacrylate) were co-polymerised in a 1:1 ratio with *N-trans*-sobrerol acrylamide. The results were successful: overall, the co-polymerisations of *N-trans*-sobrerol acrylamide followed the same pattern of results but with slightly higher molecular weights and lower polydispersities than the respective co-polymerisations with *N*-isobornyl acrylamide. This was not entirely unexpected as *N-trans*-sobrerol acrylamide performed better in all comparable homopolymerisations as well. Similarly to *N*-isobornyl acrylamide, the co-polymerisation of *N-trans*-sobrerol acrylamide and *N*-vinyl pyrrolidone gave a low M_n polymer of 4.5 kDa and high polydispersity of 2.21 (Table 32 Entry 1). Co-polymerisation with allyl alcohol gave a comparable M_n, 5.5 kDa, and a very high polydispersity of 3.81 (Table 32 Entry 2). Co-polymerisation of *N-trans*-sobrerol acrylamide with PEG acrylate gave a good M_n of 9.1 kDa and polydispersity of 1.77 compared to the previous two copolymers (Table 32 Entry 3). Similarly, to *N*-isobornyl acrylamide, co-polymerisation of *N-trans*-

sobrerol acrylamide and stearyl methacrylate gave the highest M_n, 22.3 kDa, of all the co-polymerisations although with a high polydispersity of 2.48 (Table 32 Entry 4).

Table 32: N-trans-Sobrerol Acrylamide Random Co-polymerisations
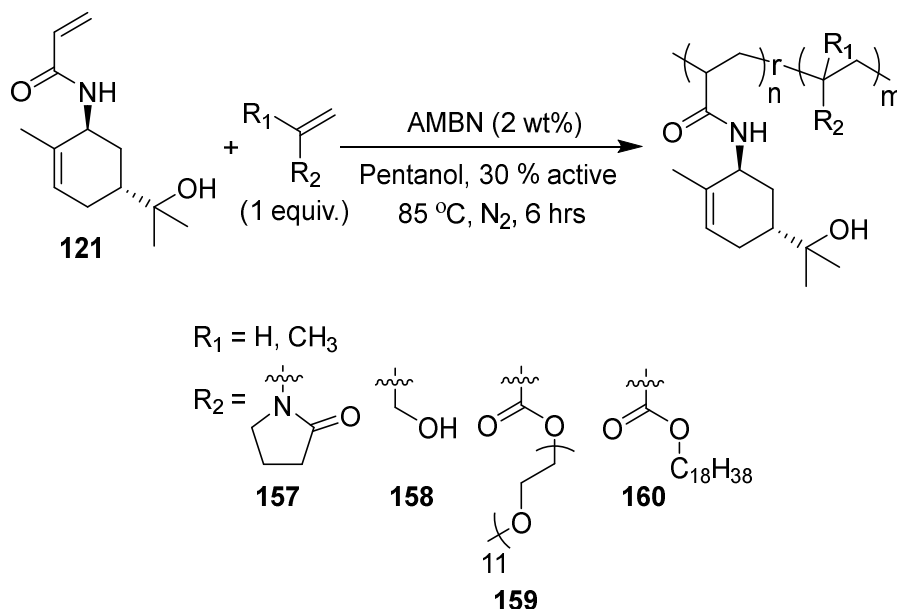
Entry	Co-monomer	M_n^a (kDa)	M_w (kDa)	Polydispersity, Đ	Active Weight (%)
1	*N*-vinyl pyrrolidone	4.5	9.8	2.21	35
2	Allyl alcohol	5.5	20.8	3.82	20
3	PEG acrylate	9.1	16.1	1.77	31
4	Stearyl methacrylate	22.3	55.4	2.48	31

^{a}Calculated from GPC calibrated with PMMA standard

The co-polymerisation of *N-trans*-sobrerol acrylamide and PEG acrylate ($M_n \approx 480$) was investigated further to expand the library of biobased copolymers (Table 33). This random co-polymer was of interest particularly due to the interesting properties that may arise from the opposing hydrophobic and hydrophilic natures of *N-trans*-sobrerol acrylamide and PEG acrylate, respectively. A range of monomer ratios, 3:1, 3:2, 1:1 and 2:1 were synthesised

and the degree of polymerisation calculated from the average number of monomeric units for molecule.

Table 33: Random Co-polymerisation of N-trans-Sobrerol Acrylamide (X) and PEG Acrylate (Y) in Varying Ratios
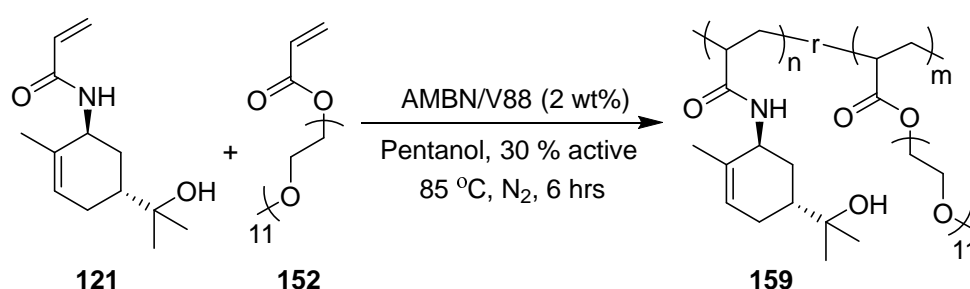
Entry	Ratio of X:Y	M_n^a (kDa)	M_w (kDa)	Polydispersity, Đ
1	3:1	24.6	62.6	2.55
2	3:2	19.1	47.9	2.51
3	1:1	9.1	16.1	1.77
4	1:2	12.1	30.6	2.52

^{a}Calculated from GPC calibrated with PMMA standard

3.2.6 *N*-Pulegone Acrylamide Random Co-polymerisations

Finally, the co-polymerisations of *N*-pulegone acrylamide with the four previously mentioned commercially available co-monomers were conducted. As AMBN was not commercially available at the time, another azo initiator, V88 was used. Polymerisation of *N*-pulegone acrylamide with *N*-vinyl pyrrolidone gave a moderate M_n of 6.9 kDa and a good polydispersity of 1.42 (Table 34 Entry 1). Co-polymerisation with allyl alcohol gave the lowest M_n of 4.1 kDa with a good polydisperisity of 1.54 (Table 34 Entry 2). Co-polymerisation of *N*-pulegone acrylamide with PEG acrylate using the azo-initiator V88 was unsuccessful resulting in incomplete conversion of either monomer. The reason for this is still unknown. However, switching to the peroxy-initiator TBPB gave a good M_n of 12.9 kDa and a good polydispersity of 1.56 (Table 34 Entry 3). Again, co-polymerisation of stearyl

176

methacrylate with the terpene-derived monomer gave the highest M_n, 17.6 kDa of the co-polymerisations, although the polydispersity was also the highest at 2.15 (Table 34 Entry 4). This was presumed to be due to a closer reactivity profile between the two monomers.

Table 34: N-Pulegone Acrylamide Co-polymerisations

$R_1 = H, CH_3$

$R_2 =$ **161** **162** **163** **164**
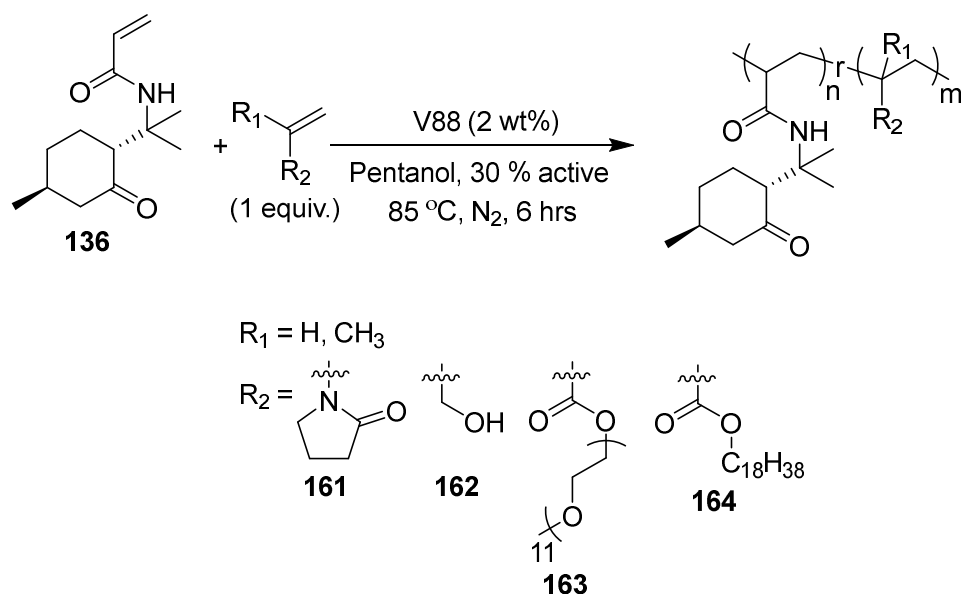
Entry	Co-monomer	$M_n{}^a$ (kDa)	M_w (kDa)	Polydispersity, Đ
1	*N*-vinyl pyrrolidone	6.9	9.9	1.42
2	Allyl alcohol	4.1	6.3	1.54
3[b]	PEG acrylate	12.9	20.2	1.56
4	Stearyl methacrylate	20.0	27.7	1.39

[a]Calculated from GPC calibrated with PMMA standard

[b]TBPB used as initiator

3.3 Redox Initiated Emulsion Polymerisation

Emulsion polymerisations are often used for the polymerisation of vinyl monomers such as vinyl acetate, meth(acrylates) and acrylamides. Compared to a standard free radical polymerisation, emulsion polymerisations often have faster reaction rates, higher molecular weights and greater control over heat dissipation. Sarkar and co-workers have reported the successful emulsion homo- and co-polymerisations of myrcene with dibutyl itaconate and alkyl acrylates,[44,50,51] and as such, investigations were conducted into using emulsion polymerisations in the formation of novel terpene-derived polyacrylamides.

Emulsion polymerisations are conducted using both thermal and redox initiators, although, redox initiated polymerisations can generally be conducted using milder conditions due to their lower activation energies compared with the homolytic bond fission of thermal initiators.[182] In redox polymerisations, initiation occurs when a reducing agent and an oxidising agent produce a reactive species. This reactive species then decomposes to form a free radical which initiates the polymerisation.

3.3.1 Poly(Isobornyl Methacrylate)

Isobornyl methacrylate was chosen as a commercially available model reagent for the optimisation of semi-batch redox-initiated homopolymerisations of hydrophobic terpene-derived monomers, due to its structural similarities with *N*-isobornyl acrylamide and closer glass transition temperature to poly(*N*-isobornyl acrylamide). However, isobornyl methacrylate is a liquid, unlike the solid state of *N*-isobornyl acrylamide.

In 2006, Back and Schork reported the emulsion and mini-emulsion polymerisation of isobornyl acrylate.[183] For both polymerisation types they investigated thermal initiation using potassium persulfate and redox initiation using *t*-butyl hydroperoxide as the oxidant and a mixture of sodium formaldehyde sulfoxylate (SFS) and ferrous sulfate as the reductant. The effect of the concentration of the surfactant, sodium dodecyl sulfate (SDS), on the reaction progression was investigated. For both emulsion polymerisations, thermal and redox, a higher concentration of surfactant up to 30 mmol/L, decreased the lag time and increased the rate of reaction as the diffusion of monomers and propagation of polymer

178

chains within the smaller micelles were faster. In comparison to the thermal initiator, the redox polymerisation was conducted at a lower temperature and with a faster reaction rate.

In 2009, Kohut-Svelko and co-workers investigated the performance of different redox initiator couples to initiate the emulsion polymerisation of butyl acrylate at low temperatures (40 – 50 °C) in both batch and semi-batch polymerisations.[182] The redox systems investigated used persulfates or hydroperoxides as oxidants and ascorbic acid, sodium formaldehyde sulfoxylate (SFS), tetramethyl ethylene diamine (TMEDA), Bruggolite FF6 and FF7 and sodium metabisulfites as the reductants. The redox couple TBHP/Bruggolite FF7 gave the highest conversion (99 %) with the lowest induction time (4 minutes). SFS was the only other reductant to give full conversion when partnered with TBHP after an induction time of 9 minutes, ascorbic acid stalled after 85 % conversion and Bruggolite FF6 did not initiate the emulsion polymerisation at all. Changing the oxidant to H_2O_2 with FF7 as the reductant gave a comparable conversion, 96 %, and an induction time of 4 minutes. The effect of the iron chelate of ethylendiamine tetracetic acid (EDTA), a powerful activator for peroxide catalysed reactions, was investigated by lowering the catalyst loading. Using the H_2O_2/FF7 redox system as a basis, lower catalysts loadings were seen to decrease the overall conversion although no effect was seen on the initial induction time.

Based on the previous literature reported, peroxides; t-butyl hydroperoxide (TBHP) and t-butyl peroxybenzoate (TBPB) were used in this instance as the oxidant initiators and 2-hydroxy-2-sulfinatoacetic acid disodium salt (Bruggolite FF7) was used as the reducing initiator. Although previously untested in this emulsion system, TBPB as a less toxic alternative to TBHP, was employed in the organic solution redox system. Deionised water was used as the solvent and the surfactant was the commercial product Disponil FES 993 (30 % aqueous solution), a fatty alcohol polyglycol ether sulfate sodium salt, similar to SDS.

Table 35: Emulsion Polymerisation of Isobornyl Methacrylate
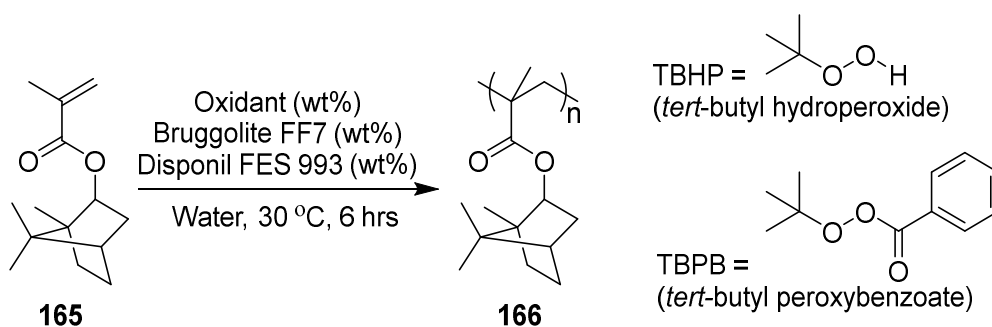
Entry	Oxidant	Initiator (wt%)	Disponil (wt%)	Active Weight (%)	M_n[a] (kDa)	M_w (kDa)	Polydispersity Đ
1[b]	TBHP	1	6	30	25.7	90.3	3.51
2[c]	TBHP	1	6	30	77.9	304.7	3.91
4	TBHP	1	6	20	20.8	43.3	2.20
5	TBHP	3	6	30	16.9	86.6	5.11
6	TBHP	3	4	30	8.9	88.7	10.34
7	TBPB	3	6	30	200.0	1231.4	6.16

[a]Calculated from GPC calibrated with PMMA standard

[b] Isobornyl methacrylate and TBHP (1 wt%) were added dropwise to emulsion containing Bruggolite FF7

[c] (1 wt%) of TBHP and Bruggolite FF7 were added dropwise to emulsion containing isobornyl methacrylate

Initially, an aqueous emulsion of isobornyl methacrylate and TBHP (1 wt%) was added dropwise over two hours to an aqueous solution of Disponil FES 993 and Bruggolite FF7 (1 wt%). After a further two hours, a white precipitate had formed giving an undesirable heterogeneous mixture. GPC analysis of the solid gave a good M_n of 26 kDa but a broad polydispersity of 3.51 (Table 35 Entry 1). To overcome this, the addition order was investigated. The same reagent ratios were used but aqueous solutions (1 wt%) of TBHP and Bruggolite FF7 were added dropwise, simultaneously, to an aqueous emulsion of isobornyl methacrylate (Table 35 Entry 2). After 90 minutes, the solution was too viscous to stir and after a further hold of two hours the mixture had fully solidified. GPC analysis gave a high M_n, 78 kDa, although similar to the previous experiment, poor reaction control (given by the

180

emulsion vesicle size distribution) was shown due to the high polydispersity at 3.91 (Table 35 Entry 2). Continuing with simultaneous monomer and initiator feeds, the active weight was reduced from 30 to 20 % to successfully achieved a homogeneous, if viscous, solution with a good M_n of 21 kDa and good polydispersity of 2.20 (Table 35 Entry 3). It was proposed previously that the hydrophobic polymer was precipitating at a particular molecular weight threshold. To control the molecular weight to ≤20 kDa and maintain a homogeneous solution with a higher active weight, the initiator concentrations were increased to 3 wt% from 1 wt%. These conditions gave a homogeneous, pourable solution with good M_n of 17 kDa although broad polydispersity at 5.11 (Table 35 Entry 4). Next, the volume of surfactant was investigated decreasing the weight percent of Disponil FES 993 from 6 to 4 wt%. This was unsuccessful giving both lower molecular weights and a very high polydispersity which corresponded with the visual analysis of an unstable emulsion, giving an uncontrolled polymerisation due to the reduced surfactant producing unstable micelles (Table 35 Entry 6). As TBHP is toxic an alternative, less harmful peroxide, TBPB was investigated. TBPB is water-insoluble so a pre-emulsion of water and Disponil FES 993 (30 %) was used to give a homogeneous aqueous initiator feed. After five hours, the polymerisation gave a high molecular weight polymer, M_n = 200 kDa, although with broad polydispersity (Đ = 6.16) and residual monomer was also detected by GPC (Table 35 Entry 7). This is proposed to be due to the low solubility of the initiator and its corresponding radical in water, reducing the number of polymer propagation sites within the emulsion, leading to high molecular weights and low conversions. In general, although the molecular weights on average are higher than the analogous semi-batch solution polymerisations, the polydispersities are broad suggesting poor control. This is proposed to be due to unstable or irregular micelles forming in the emulsion containing varying volumes of monomer and polymer leading to a wide variety of chain lengths. Nonetheless it was endeavoured to test the conditions from this investigation on the solid state terpene-derived acrylamides; *N*-isobornyl acrylamide and *N-trans*-sobrerol acrylamide, before investigations into optimisation of the surfactant conditions in these systems, in an effort to enhance the control of the polymerisation.

3.3.2 Polyacrylamides

The terpene-derived acrylamide monomers were polymerised using the optimum homogeneous emulsion polymerisation conditions determined using the isobornyl methacrylate monomer; 3 wt% TBHP, 6 wt% Disponil FES 993 (30 %) and 30 % active at 30 °C. In order to guarantee the consumption of all the starting acrylamide monomer after five hours, another 3 wt% TBHP, as a thermal initiator, was added after completion of the monomer addition and the reaction held at 90 °C for a further two hours. The emulsion polymerisation of *N*-isobornyl acrylamide gave a low M_n of 6.7 kDa and a good polydispersity of 1.85 (Scheme 89). The low molecular weight that was observed was likely due to the solid state of the hydrophobic monomer disrupting micelle formation, by instead forming aggregates.
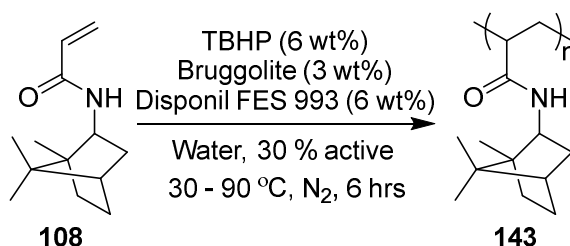
Scheme 89: Emulsion Polymerisation of N-Isobornyl Acrylamide

On the other hand, under the same conditions *N-trans*-sobrerol acrylamide gave a moderate M_n of 22 kDa which was in good agreement with the commercial test monomer, isobornyl methacrylate, although with a broad polydispersity of 3.08 (Scheme 90).
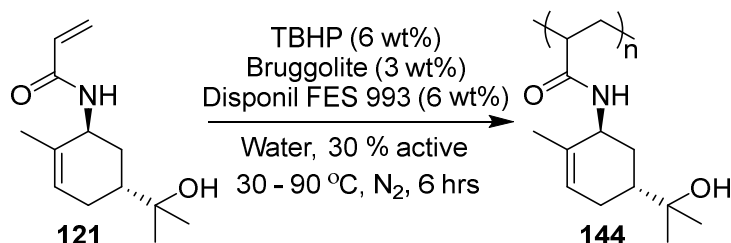
Scheme 90: Emulsion Polymerisation of N-trans-Sobrerol Acrylamide

182

During the polymerisations, the pre-emulsions of both monomer phases were unstable due to the solid state of the monomers and although initially giving a homogeneous mixture, over time it was found to separate out upon standing for a few hours. This, along with broad polydispersities shown during the polymerisations of isobornyl acrylate, prompted an investigation into a new surfactant system which might better suit the acrylamide monomers. Both an alternative ionic surfactant, sodium dodecyl sulfate (SDS) (also known as sodium lauryl sulfate), and a non-ionic surfactant, sorbitan oleate (commercial name Span® 80), were investigated. Unfortunately, polymerisations using each surfactant both individually or together, in varying ratios with redox and thermal initiators all gave no conversion and recovery of the starting material. The solid state of these hydrophobic, terpene-derived acrylamides meant that slow addition of the monomer phase was challenging. As emulsion polymerisations are traditionally conducted with liquid-state monomers, specifically oils, using this technique to polymerise terpene-derived polymers would require extensive future investigations into an optimisation of reaction conditions, methodology, and formulation, probably including the use of dispersants. This level of work was considered beyond the remit of this project, especially considering it was already determined that both homo- and co-polymers based on the acrylamides could be synthesised using other polymerisation techniques. Nonetheless, monomers that are able to undergo multiple, different polymerisation techniques are desirable for the versatility, and so it was endeavoured to investigate redox polymerisations in solution as the next alternative.

3.4 Redox Initiated Solution Polymerisation

Due to the solid state of the terpene-derived monomers and subsequent unfeasible heterogenous emulsion polymerisations. For this reason, alternative redox-initiated solution polymerisations were investigated as a possible alternative. However, as the majority of the redox initiators previously investigated are aqueous-based, their use in an organic solvent-based polymerisation of hydrophobic monomers required optimisation.

In 1998, a patent application was granted for the National Starch and Chemical Investment Holding Corporation for the free radical thermal polymerisations of vinyl polymers using water-soluble initiators in organic solvent media.[22] This was achieved by incorporating 2 - 18 wt% water into the reaction mixture to help solubilise the water insoluble monomers and polymeric systems. The polymerisations were generally conducted at 50 % active weight with a range of vinyl monomers including C1 - 18 acrylate or methacrylate esters or *N*-substituted acrylamide or methacrylamides or a mixture thereof. Thermal initiators were reacted at temperatures of 50 - 100 °C for 2 to 10 hours or until quantitative conversion was achieved. The patent reported an unexpected improvement in the efficiency of the reaction with higher conversion rates and lower residual monomer levels compared to standard reactions.

3.4.1 Poly(Isobornyl Methacrylate)

Based on the previous literature reported[182] and the results seen during the emulsion polymerisation investigations, *t*-butyl hydroperoxide (TBHP) and 2-hydroxy-2-sulfinatoacetic acid disodium salt (Bruggolite FF7) were used as the oxidant and reductant respectively. Again, isobornyl methacrylate was chosen as a commercially available model for the optimisation of a semi-batch homopolymerisation of the hydrophobic terpene-derived acrylamides.

Initially, two aqueous solutions of initiator were simultaneously added dropwise to isobornyl methacrylate dissolved in deoxygenated pentanol. However, as the aqueous monomer feeds were charged dropwise to the vessel, increasing volumes of polymers were observed to precipitate until a single piece of unusable solid remained (Table 36 Entry 1). The precipitation was presumed to be due to the hydrophobicity of the polymer interacting

with the level of water in the reaction, so in subsequent reactions, the amount of water in relation to the overall reaction was lowered from 12 to 6 wt%. The molecular weights achieved in the first reaction were very high, however as increasing molecular weight appears proportional to increased polymer hydrophobicity, the initiator concentration was also increased to 6 wt% in the second reaction in an effort to lower the molecular weight slightly and improve solubility of the polymer chains (Table 36 Entry 2). The resulting volume was not enough for dropwise addition over 3 hours through the pump so the water and organic-insoluble Bruggolite FF7 were charged directly to the vessel at the start. TBHP was dissolved in pentanol rather than water and added dropwise using the same addition rate as previously. However, although the molecular weight and polydispersity had improved as the polymer stayed in solution for longer, a clear gel-like precipitate was still observed at the end of the reaction. Therefore, in a third reaction, water was lowered to 3 wt%. This was charged along with the organic-insoluble Bruggolite FF7 at the start of the reaction and TBHP in pentanol was added over 3 hours to control the reaction. Unfortunately no polymerisation occurred, due to the precipitation of Bruggolite FF7 in the minimal water content inhibiting the formation of radicals (Table 36 Entry 3).

Table 36: Redox Polymerisation of Isobornyl Methacrylate using Bruggolite FF7
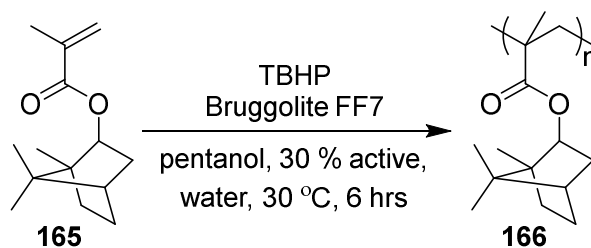
Entry	Initiator (wt%)	Water (wt%)	Final Appearance	M_n^a (kDa)	M_w (Da)	Đ
1	2	12	White Solid	130.1	290.7	2.24
2	6	6	Clear liquid with clear gel precipitate	292.2	353.4	1.21
3	6	3	Clear liquid	0	0	0

[a]Calculated from GPC calibrated with PMMA standard

Considering the solubility issues with the addition of water, an alternative organic soluble reductant was investigated. In the work by Kohut-Svelko and co-workers in 2009, ascorbic acid was investigated as a reductant in redox emulsions.[182] Also known as vitamin C, this naturally occurring reagent is a widely available non-hazardous substance. However, when this initiator was used in the literature, only an 85 % conversion was reported. This was thought to be a result of the initiators being charged as aliquots at the beginning of the reaction and as such it was proposed that the radicals formed were degrading before all the monomer had converted. Therefore, the semi-batch approach could mitigate this issue, if not, a further addition of the thermal initiator to remove any residual monomer would be employed. Initially, ascorbic acid was used in combination with TBHP at 30 °C for 6 hours (Table 37 Entry 1). This resulted in very high molecular weights and low polydispersity. As such, it was endeavoured to investigate the use of a less hazardous peroxide reagent as the oxidant initiator, *t*-butyl peroxybenzoate (TBPB). This, with the same conditions, again resulted in very high molecular weights, although a broader polydispersity of 2.23 (Table 37 Entry 2). The lower molecular weights seen with TBPB could be due to the formation of a more stable radical initiating more propagating polymer chains. Next the reaction

temperature was investigated as a possible means of improving the conversion. The reaction temperature was increased to 85 °C for two hours for the 'hold', i.e. after completion of the initiation addition at 30 °C (Table 37 Entry 3). This gave comparable results to the previous polymerisation conducted completely at 30 °C. The temperature during the addition of the initiators was then set to 50 °C (Table 37 Entry 4). This gave a significantly lower M_n than the other results, 30 kDa with broad polydispersity of 3.54. Increasing the hold temperature to 50 °C likely gave a lower molecular weight due a faster radical generation which initiated more propagating chains and increased the propagation rate uncontrollably leading to a broader polydispersity.

Table 37: Redox Polymerisation of Isobornyl Methacrylate using Ascorbic Acid
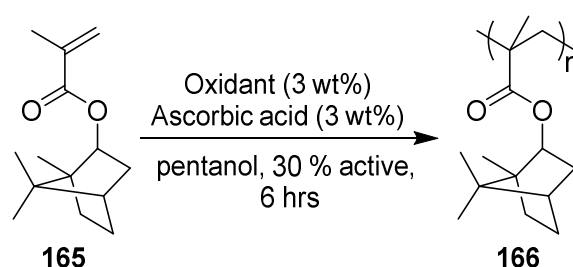
Entry	Oxidant	Initial Temp.[a] (°C)	Hold Temp.[b] (°C)	M_n[c] (kDa)	M_w (kDa)	Polydispersity, Đ
1	TBHP	30	30	593.6	792.5	1.34
2	TBPB	30	30	98.0	218.5	2.23
3	TBPB	30	85	104.8	211.2	2.01
4	TBPB	50	85	29.7	104.0	3.54

[a]Temperature during 4 hour initiator feed

[b]Temperature during 2 hour hold

[c]Calculated from GPC calibrated with PMMA standard

Analysing the varying levels of residual monomer after 6 hours *via* GPC gave an indication of conversion (Figure 47). Reaction conversion is important, as in general monomers are more hazardous than their respective polymers and high amounts of residual monomer would

likely fail industrial product specifications without further purification. The highest conversion is the polymerisation with TBPB at 50 °C with no discernible trace of monomer according to the GPC chromatogram. Although the polymerisation using TBHP in pentanol gave the highest molecular weights, it also gave one of the highest levels of residual monomer suggesting the formation of a very reactive but highly unstable radical producing only a few propagating chains. Not only did TBPB give low residual monomer levels, it is also a less harmful reagent than TBHP, therefore the optimised conditions of TBPB and ascorbic acid (Table 36 Entry 3) will be used to form homopolymers of *N*-isobornyl acrylamide, *N*-trans sobrerol acrylamide and *N*-pulegone acrylamide.
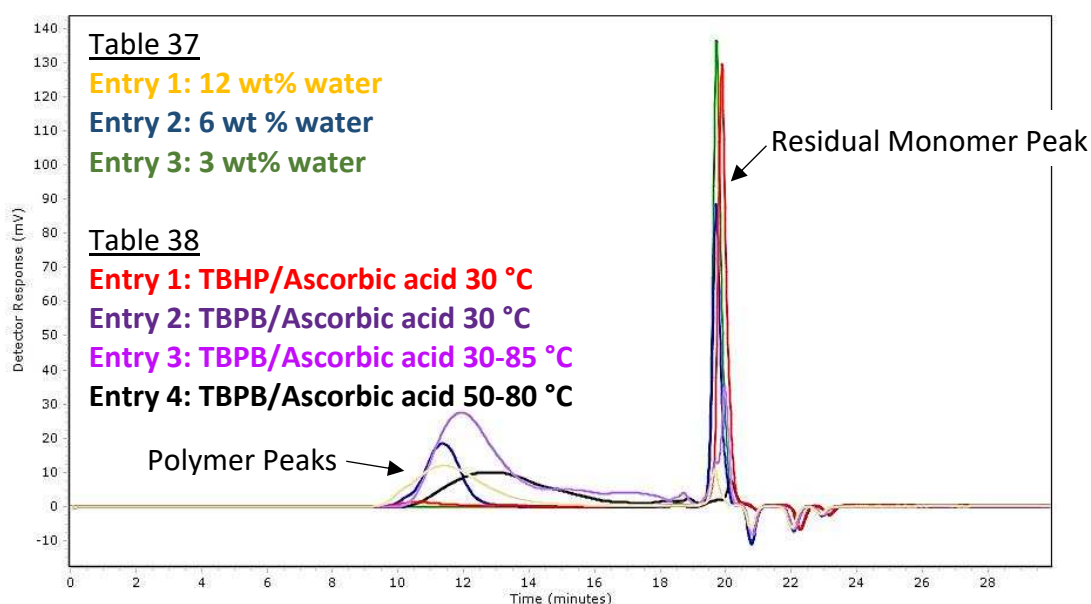
Figure 47: Overlaid GPC analysis of all Isobornyl Methacrylate Redox Polymerisation Optimisations

3.4.2 Polyacrylamides

After investigating a range of redox conditions on isobornyl methacrylate to determine the optimum initiators; TBPB and ascorbic acid at 6 wt% and 3 wt% respectively, our attention turned to implementing this knowledge for the redox-initiated polymerisations of terpene-derived polymers. As lower temperatures gave higher molecular weights in the screens with isobornyl methacrylate, the reaction was initially conducted at 40 °C during the addition of

the initiator and then left for 16 hours at 85 °C until full conversion was reached by NMR. Analysis gave a M_n of 33 kDa although broad polydispersity; 2.64 (Table 38 Entry 1). Increasing the temperature to 50 °C during the initiator addition period before increasing to 80 °C until full conversion was investigated next. This higher temperature for the initiator addition gave comparable molecular weights and polydispersity over a shorter reaction time; a potential pathway for industrial scale up (Table 38 Entry 2).

Table 38: Redox Polymerisation of N-Isobornyl Acrylamide
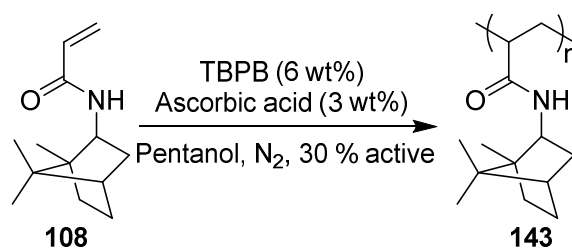
Entry	Initial Temp.[a] (°C)	Hold Temp.[b] (°C)	Time (hrs)	M_n[a] (kDa)	M_w (kDa)	Polydispersity, Đ
1	40	85	20	32.9	86.9	2.64
2	50	80	6	28.5	70.1	2.46

[a]Temperature during 4 hour initiator feed

[b]Temperature after completion of initiator feed

[c]Calculated from GPC calibrated with PMMA standard

Next, the redox-initiated polymerisation of *N-trans*-sobrerol acrylamide was investigated. Redox polymerisations are generally more environmentally friendly as the reactions require less energy than traditional thermal initiators. To investigate this, an initial investigation using the original, optimised conditions from isobornyl acrylate was unsuccessful, resulting in recovery of the *N-trans*-sobrerol acrylamide monomer starting material. Increasing the initial temperature to 40 °C, resulted in the successful formation of poly(*N-trans*-sobrerol acrylamide) albeit with a low M_n of 10 kDa and a broad polydispersity of 2.00 (Table 39

189

Entry 2). Increasing the temperature further to 50 °C during the addition of the initiators and 85 °C during the hold gave a good M_n of 29 kDa, though again with a broad polydispersity of 2.43 (Table 39 Entry 3). This suggests that the polymerisation of terpene-derived acrylamides, including *N-trans*-sobrerol acrylamide, have higher activation energies which need to be overcome through higher reaction temperatures before the reaction can occur.

Table 39: Redox Polymerisation of N-trans-Sobrerol Acrylamide
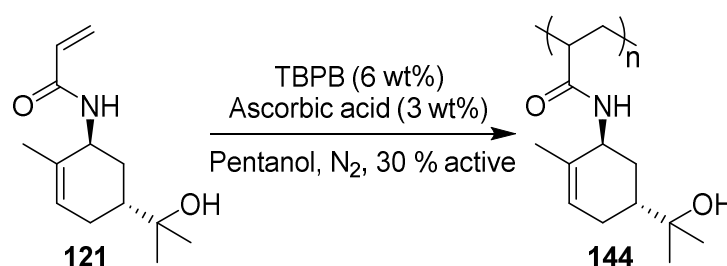
Entry	Initial Temp.[a] (°C)	Hold Temp.[b] (°C)	Time (hrs)	M_n[c] (kDa)	M_p (kDa)	M_w (kDa)	Polydispersity, Đ
1	30	30	20	No Conversion			
2	40	40	20	9.6	14.8	19.2	2.00
3	50	85	6	28.8	58.2	70	2.43

[a]Temperature during 4 hour initiator feed

[b]Temperature after completion of initiator feed

[c]Calculated from GPC calibrated with PMMA standard

Finally, the redox-initiated polymerisation of *N*-pulegone acrylamide was investigated. First the initiators were added at 40 °C, before increasing to 85 °C until full conversion was reached by NMR. This gave a good M_n of 36 kDa and a polydispersity of 1.99 (Table 40 Entry 1), which is significantly better than the results achieved by thermal initiated polymerisation

for this monomer.   Increasing the initiator addition temperature to 50 °C gave lower

molecular weights but a better polydispersity of 1.31 (Table 40 Entry 2).

Table 40: Redox Polymerisation of N-Pulegone Acrylamide
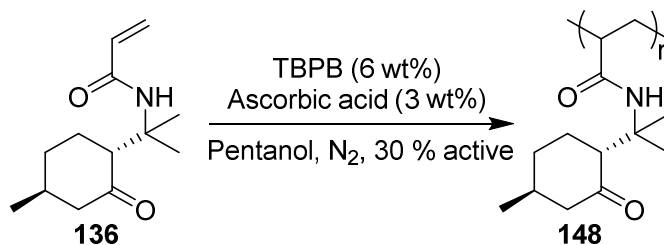
Entry	Initial Temp.[a] (°C)	Hold Temp.[b] (°C)	Time (hrs)	M_n[c] (kDa)	M_p (kDa)	M_w (kDa)	Polydispersity , Đ
1	40	85	20	35.5	62.9	70.5	1.99
2	50	85	6	24.6	18.7	32.3	1.31

[a]Temperature during 4 hour initiator feed

[b]Temperature after completion of initiator feed

[c]Calculated from GPC calibrated with PMMA standard

3.5 Conclusion

In conclusion, all the terpene-derived acrylamides were successfully polymerised using thermally initiated free radical conditions. In general, azo-initiators such as AIBN and AMBN and polar protic solvents such as ethanol and pentanol were found to be the optimum conditions. In the future, further investigations into end group analysis using MALDI-MS will be conducted. An investigation into the reaction kinetics showed these polymerisations matched the theorectical kinetics plots of a standard chain growth polymerisation. The green solvent and short reaction times of the optimised free radical polymerisation conditions makes the polymerisation of terpene-derived acrylamides feasible on an industrial scale and would allow these monomers to be dropped directly into exisiting industrial processes as potential replacements for other petroleum-based monomers. However, more optimisation of these semi-batch conditions would be required to optimise the molecular weights and dispersities of the samples. Glass transition temperatures for the various terpene-derived acrylamide homopolymers were determined by DMA, the wide range indicating these polymers may have potential applications ranging from resistant coatings to high temperature engineering applications.

The optimum thermally-initiated free radical polymerisation conditions were used to synthesise a library of copolymers consisting of a terpene-derived acrylamide and a commerically available co-monomer; *N*-vinyl pyrrolidone, allyl alcohol, PEG acrylate and stearyl methacrylate. The acrylate and methacrylate co-monomers resulted in terpene-derived co-polymers with higher molecular weights than the vinyl co-monomers due to the closer reactivities. However, as each of the commercial co-monomers was chosen for their specific polymer characteristics, all of the co-polymers synthesised will be carried forward for applications testing.

Along with thermally initiated free radical solution polymerisations, redox-initiated solution polymerisations and emulsion polymerisations were also investigated as potential alternative routes towards these acrylamide homopolymers. The use of redox initiators gave high molecular weights using less hazardous reagents than the free radical polymerisations. Switching to emulsion conditions resulted in low molecular weight polymers, however this polymerisation technique was determined to be uncontrolled and unreliable because the

terpene-derived monomers are solid. The thermally initiated solution polymerisations were found to give better performance than the redox initiated solution polymerisations and redox initiated emulsion polymerisation methods. The exception being *N*-pulegone acrylamide, which resulted in higher molecular weights and lower polydispersities when redox initiators were used within solution polymerisations.

4.0 Chapter 3: Physical Characteristics and Commercial Applications

One of the largest commercial uses for polyacrylamide is as a flocculant, to remove solids from liquids.[72] This process applies to water treatment, paper making and screen printing.[184] Above a certain concentration, polyacrylamide can have a dispersion and stabilising effect instead of flocculating. However, these are useful properties in other applications such as crop care formulations and soot dispersion in oil.[74]

Other commercially available, fossil fuel-derived polyacrylamides are also water soluble and found in other water-based applications such as personal care products and biomaterials, as well as flocculants in water treatment plants.[185] Cross-linked poly(*N*-isopropyl acrylamide), for example, forms a 3-D hydrogel that can be used in a variety of applications, from biomaterials to drug delivery to soil erosion control,[36–42] due to its ability to reversibly change its structure at a particular lower critical solution temperature (LCST) due to external temperature changes.[35]

Renewable polyacrylamides in the literature on the other hand, tend to be more hydrophobic due to their derivatisation from larger hydrocarbon-based natural products. Although, none have been commercialised so far, applications in biomaterials, adhesives and coatings have been suggested due to their extreme hydrophobicity, enhanced durability and good adhesion to a variety of substances.[89,95,186]

As the applications for both commercial and for renewable polyacrylamides have been wide ranging, a similarly diverse range of properties (viscosity, water contact angle, solubility) and applications (viscosity modifiers, dispersants, foaming agents and emulsifiers) were tested for the terpene-derived polyacrylamides. This scattered approach will help define the competitive characteristics of the terpene-derived polyacrylamides so that further optimisation towards a commercial application and manufacture will be economically viable in the future.

4.1 Viscosity

Viscosity is a physical parameter which is measured throughout industry to gain insight into different materials and their behaviours. It is a measure of the internal friction of a fluid (the resistance which a fluid shows when being deformed) which can be measured by density and shear flow. The density (mass per unit volume) and shear of some of the homopolymer and co-polymer solutions in *n*-pentanol were tested on an Anton Paar Stabinger Viscometer SVM 3001 at 20, 40 and 80 °C giving a range of viscosities. For comparison, *n*-pentanol has a density of 0.811 g/cm^3. Polymer solutions are usually non-Newtonian liquids, which means that their apparent viscosity (η)[1] depends in the applied shear rate and increases rapidly with molecular weight. When the same homopolymers of different molecular weights were compared, the polymer solutions with higher molecular weights were more viscous with higher densities and lower shear rates (Table 41 Entries 1-6 & 19-24). The viscosity of a polymer is always larger than that of its corresponding monomer and increases rapidly with increasing molecular weight due to entanglement and intermolecular forces between the polymer chains. Interestingly, the *N-trans*-sobrerol acrylamides homo- and co-polymers were more viscous across the board when compared directly to their equivalent *N*-isobornyl acrylamide homo- and copolymers (Table 41 Entries 19-24). This is likely due to additional hydrogen bonding through the tertiary alcohol which increases the density and requires a higher shear stress (energy) to move the polymer solution. The shear stress divided by the shear rate (at any given rate of shear) is known as the apparent viscosity.

The observed shear thinning of the polymer solutions as the temperature increases from 20

$$\eta = \frac{\tau}{\dot{\gamma}}$$

Equation 2: Relationship between Shear and Apparent Viscosity

°C to 80 °C is caused by disentanglement of the polymer chains during flow. Polymers with sufficiently high molecular weight are always entangled and randomly oriented when at rest.[187] When sheared, they begin to disentangle and align which causes the viscosity to

196

drop. The degree of disentanglement depends on the shear rate. At sufficiently high shear rates the polymers will be completely disentangled and fully aligned. In this regime, the viscosity of the polymer solution will be independent of the shear rate i.e. the polymer will behave like a Newtonian liquid again.

Rheological measurements such as these provide important information about the flow and creep properties of polymeric materials. This information might aid in optimising the processing conditions and finding potential applications for these biobased polyacrylamides.

When comparing the homopolymers and their corresponding copolymers directly, both homopolymers were more viscous than their corresponding copolymers. This decrease in viscosity is also proposed to be due to the hydrogen bonding as the randomly interspersed comonomers decreases the number of hydrogen bonds between the polymer side chains as the number of hydrogen bond acceptors and donators decreases. The allyl alcohol copolymers were the least viscous with the lowest densities and highest shear rates.

Table 41: Density and Shearing of Terpene-Derived Polyacrylamides in n-*Pentanol*

Entry	Sample	Temp. (°C)	Kin. Density (mm²/s)	Dyn. Density (mPa·s)	Density (g/cm³)	Shear Rate (1/s)	Shear Stress (Pa)
1	Poly(IBAA)	20	45.591	39.752	0.872	214.8	8.5
2	M_n=6kDa	40	19.680	16.862	0.857	379.2	6.4
3		80	5.978	4.734	0.792	673.7	3.2
4	Poly(IBAA)	20	227.640	199.940	0.878	50.5	10.1
5	M_n=29kDa	40	84.983	73.362	0.863	118.5	8.7
6		80	21.625	17.975	0.831	324.9	5.8
7	Poly(IBAA-*co*-NVP)	20	16.362	14.412	0.881	441.7	6.4
8		40	10.321	8.934	0.866	547.8	4.9
9		80	7.254	6.050	0.881	608.6	3.4
10	Poly(IBAA-*co*-AA)	20	8.826	7.505	0.850	618.1	4.6
11		40	4.944	4.128	0.835	748.5	3.1
12		80	2.044	1.621	0.793	900.0	1.5
13	Poly(IBAA-*co*-PEGA)	20	17.819	15.822	0.884	417.3	6.6
14		40	10.148	8.819	0.869	551.3	4.9
15		80	4.677	3.913	0.837	721.4	2.8
16	Poly(IBAA-*co*-SM)	20	14.730	12.476	0.847	480.4	6.0
17		40	7.969	6.628	0.831	628.8	4.2
18		80	3.154	2.435	0.772	827.6	2.0

Entry	Sample	Temp. (°C)	Kin. Density (mm²/s)	Dyn. Density (mPa·s)	Density (g/cm³)	Shear Rate (1/s)	Shear Stress (Pa)
19	Poly(TSAA)	20	4534.500	4096.100	0.903	2.6	10.5
20	M_n=11kDa	40	938.770	834.520	0.889	11.5	9.6
21		80	103.210	88.661	0.859	86.3	7.6
22	Poly(TSAA)	20	8449.000	7626.500	0.903	1.4	10.5
23	M_n=29kDa	40	1455.500	1292.000	0.888	7.5	9.6
24		80	129.600	111.200	0.85800	69.9	7.8
25	Poly(TSAA-co-NVP)	20	3576.600	3232.900	0.904	3.3	10.5
26		40	1250.200	1112.500	0.890	8.7	9.7
27		80	262.170	225.570	0.860	35.6	8.0
28	Poly(TSAA-co-AA)	20	90.984	79.824	0.877	118.4	9.5
29		40	36.358	31.372	0.863	242.4	7.6
30		80	8.994	7.486	0.832	550.7	4.1
31	Poly(TSAA-co-PEGA)	20	107.730	96.509	0.896	99.8	9.6
32		40	48.936	43.116	0.881	187.5	8.1
33		80	15.248	12.965	0.850	404.0	5.2
34	Poly(TSAA-co-SM)	20	222.340	193.730	0.871	52.0	10.1
35		40	86.815	74.410	0.857	117.0	8.7
36		80	22.169	18.336	0.827	320.4	5.9

IBAA = *N*-isobornyl acrylamide, NVP = *N*-vinyl pyrrolidinone, AA = allyl alcohol, PEGA = PEG acrylate, SM = stearyl methacrylate and TSAA = *N-trans* sobrerol acrylamide.

One industry which relies heavily on viscosity properties is the oil and lubricants sector. The choice of viscosity for lubricants is a compromise, too low and the lubricant film will not appear on the engine surfaces and they will contact causing wear. If it is too high the engine will struggle to pump the oil and the parts will struggle to move because of internal friction within the oil. A lot of energy will be lost because the fluid is too thick. Fluid manufactures can improve the viscosity index of base oil by using a polymer additive to form multi-grade viscosity oils. These modifiers are usually temperature sensitive where at low temperatures, the polymer chains in the modifiers contract or fold, therefore having little effect on viscosity. At higher temperatures, these polymer modifiers then expand, helping to increase viscosity and therefore decrease the overall change in fluidity maintaining the desired oil properties.[188]

The viscosity index has been calculated according to industry standards ASTM D2270 and ISO 2909 protocols. As the free temperatures, 40 °C and 80 °C, were used instead of the standard 40 °C and 100 °C, ASTM D341 was applied before calculating the viscosity index. The viscosity index for the biobased polyacrylamides were compared to single grade and multi-grade motor oil from the Society of Automotive Engineers (SAE).[189] In theory, the greater the viscosity index, the smaller the change in fluid viscosity for a given change in temperature.

The viscosity index for the commercially available SAE oils ranged from 105 to 175 (Figure 48). The two biobased polymers that have viscosity indexes within that range are poly(*N*-isobornyl acrylamide), with a M_n of 29 kDa, and poly(*N*-*trans*-sobrerol acrylamide-*co*-stearyl methacrylate) (Figure 48).

Co-polymerisation with *N*-vinyl pyrrolidone or PEG acrylate increased the viscosity indexes of the biobased polyacrylamides with poly(*N*-isobornyl acrylamide-*co*-*N*-vinyl pyrrolidone) giving an unusually high result of 743. While most examples of viscosity modifiers in the literature pertain to the introduction of basic nitrogen-containing moieties, neutral dispersant viscosity modifiers, including *N*-vinyl pyrrolidone, are also used with the aim of imparting dispersing properties to thickening additives for oils and increasing the effectiveness of additives in crude oils.[190] The rest of the polymer solution gave an average

viscosity index of 90 apart from poly(*N*-isobornyl acrylamide-*co*-allyl alcohol) which gave an unusually low viscosity index of 19.
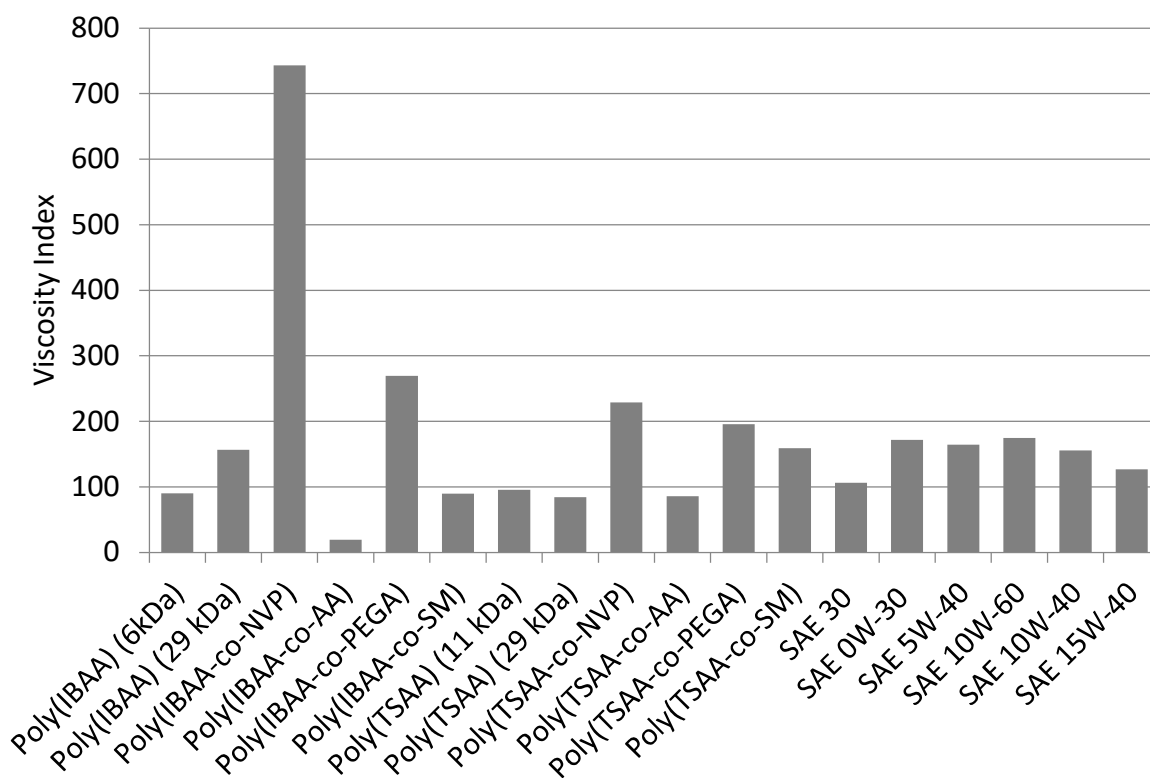
Figure 48: Viscosity Index of Biobased Polyacrylamides and SAE oils

4.2 Total Amine Value

The total amine value is a measure of the polymer's basicity and is defined by the number of milligrams of potassium hydroxide equivalent to the basicity of 1 g of sample. The total amine value was calculated using a direct titration of the amides with an alcoholic solution of hydrochloric acid (0.2 N) with bromophenol blue indicator gave a result of 0 for both homopolymers, poly(*N*-isobornyl acrylamide) and poly(*N*-*trans*-sobrerol acrylamide). This indicates that, as expected, the terpene-derived acrylamides have no effect on pH without additional amine functionalities.

201

4.3 Non-Aqueous Dispersants

With the application of oil soluble dispersants in mind, the homopolymers and copolymers were all tested for solubility in mineral oil by eye at a concentration of 10 mg/mL. It was observed that all of the poly(*N*-isobornyl acrylamide) polymers and poly(*N-trans*-sobrerol acrylamide-*co*-stearyl methacrylate) were visually soluble in mineral oil. For comparison, poly(*N*-vinyl pyrrolidone), poly(allyl alcohol), poly(PEG acrylate) are usually lipophobic due to their high polarity functionalities, whereas poly(stearyl methacrylate) is usually lipophilic due to its long, non-polar hydrocarbon chains. The other poly(*N-trans*-sobrerol acrylamide) polymers were not, due to the higher polarity, lower lipophilicity, of the *N-trans*-sobrerol acrylamide moiety compared to the *N*-isobornyl acrylamide moiety, leaving an insoluble gel-like precipitate.

Table 42: Solubility of Biobased Polyacrylamides in Mineral Oil

Entry	Polymer	Soluble	Aesthetics
1	Poly(*N*-isobornyl acrylamide)	Yes	Cloudy
2	Poly(*N*-isobornyl acrylamide-*co*-*N*-vinyl pyrrolidone)	Yes	Clear
3	Poly(*N*-isobornyl acrylamide-*co*-allyl alcohol)	Yes	Clear
4	Poly(*N*-isobornyl acrylamide-*co*-PEG acrylate)	Yes	Clear

5	Poly(*N*-isobornyl acrylamide-*co*-stearyl methacrylate)	Yes	Cloudy
6	Poly(*N-trans* sobrerol acrylamide)	No	Cloudy
7	Poly(*N-trans* sobrerol acrylamide-*co-N*-vinyl pyrrolidone)	No	Cloudy
8	Poly(*N-trans* sobrerol acrylamide-*co*-allyl alcohol)	No	Cloudy
9	Poly(*N-trans* sobrerol acrylamide-*co*-PEG acrylate)	No	Cloudy
10	Poly(*N-trans* sobrerol acrylamide-*co*-stearyl methacrylate)	Yes	Clear

4.4 Soot dispersants

Formulated lube oils contain various additives. One of the most important groups comprises of non-aqueous soot dispersants. These are mainly oil soluble polymers or copolymers which can be used for both mineral and synthetic base oil types with the purpose of

dispersing soot contamination developed from general use so that there is no impact on oil viscosity or engine performance. In general, the lower the viscosity, the better pumping efficiency around the engine, although additional viscosity modifier can be added to improve this.

As well as measuring the viscosity at different torques and temperatures to mimic the day-to-day running of the engine in different conditions and vehicles, the effect over time was also measured to assess whether the dispersant effect degrades over time. This also gives some insight into the stability of the soot-dispersant agglomerations. Yubase® is an automotive and industrial specialty oil and was used as a control to compare the differences in viscosity.

Poly(*N*-isobornyl acrylamide) and its copolymers along with poly(*N*-*trans*-sobrerol acrylamide-*co*-stearyl methacrylate) as long chain polyacrylates and polymethacrylates have had previous success as additives for pour point depressants, dispersing wax in oil. The samples were formulated with 3 wt% of the polymer dispersant in an engine oil which is typical of commercial formulations. The exceptions are poly(*N*-isobornyl acrylamide and poly(*N*-isobornyl acrylamide-*co*-*N*-vinyl pyrrolidone) which were investigated at a higher weight loading.

Initially, all of polymers were investigated against torque. Poly(*N*-isobornyl acrylamide), poly(*N*-isobornyl acrylamide-*co*-*N*-vinyl pyrrolidone), poly(*N*-isobornyl acrylamide-*co*-allyl alcohol) and poly(*N*-isobornyl acrylamide-*co*-PEG acrylate) were all similar to the blank sample (soot contaminated Yubase® with no dispersant additive) suggesting that these polymers have no impact on the viscosity and the soot particles were agglomerating increasing the viscosity. Poly(*N*-isobornyl acrylamide-*co*-stearyl methacrylate) seemed to have a slight impact on the viscosity, maintaining a lower viscosity than the blank sample and matching the uncontaminated Yubase® oil at higher torques. However, the most promising result was from poly(*N*-*trans*-sobrerol-*co*-stearyl methacrylate) which matched the viscosity of the uncontaminated Yubase® oil irrespective of torque and soot contamination (Figure 49). Practically, this means that addition of this polymer to an engine would reduce the impact of soot contamination and allow the engine to run with a superior performance for longer.
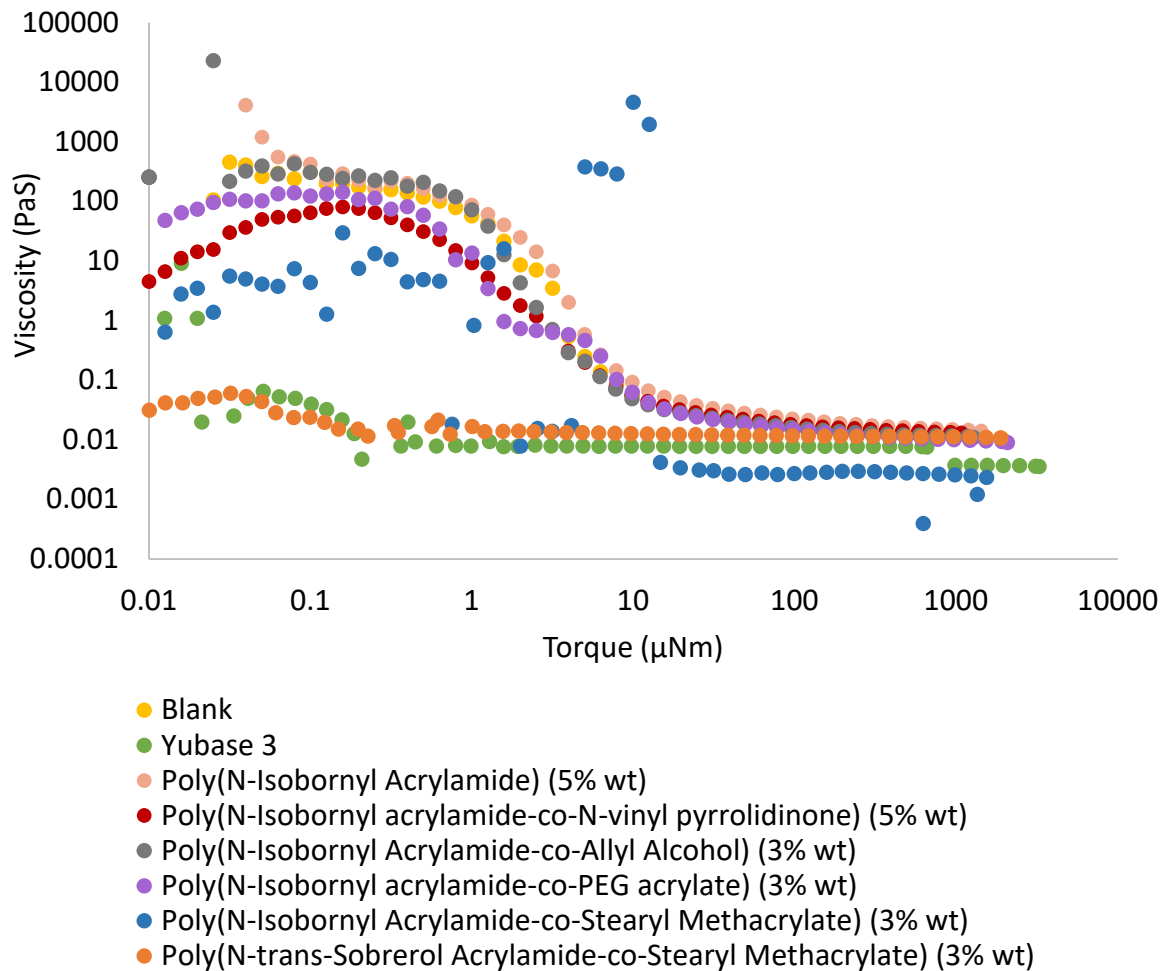
Figure 49: Effect of Terpene-Derived Polyacrylamides as Non-Aqueous Dispersants on Viscosity versus Torque for Soot Contaminated Oil

Rerunning the two best samples, poly(*N*-isobornyl acrylamide-*co*-stearyl methacrylate) and poly(*N-trans*-sobrerol acrylamide-*co*-stearyl methacrylate) samples again against the blank (soot contaminated Yubase®) and Yubase® only sample for reliability confirmed that these terpene-stearyl methacrylate copolymers were having a positive effect by dispersing the soot contaminate negating its impact on viscosity, theoretically improving engine performance (Figure 50).
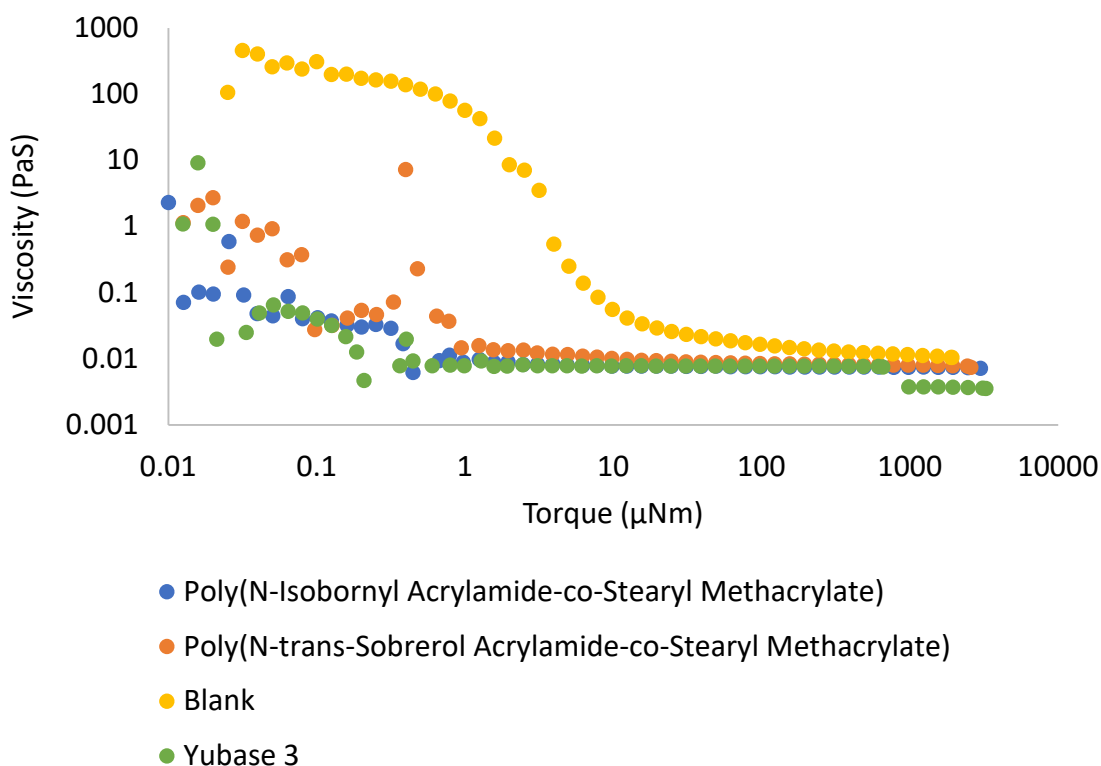
Figure 50: Direct Comparison of Terpene-Stearyl Methacrylate Copolymers with Soot Contaminated Yubase Oil

These samples were stored for a week to assess any degradation effects before being analysed at room temperature and at 40 °C. It was difficult to determine a trend in the viscosity at lower torques at room temperature with the stearyl methacrylate copolymers seemingly improving the viscosity slightly by dispersing the soot agglomerates. At around 0.5 µNm the viscosity trend for the stearyl methacrylate copolymers levels out and matches the viscosity trend for Yubase® Oil, showing a significant improvement from the blank sample (Figure 51). At 40 °C the trendlines were smoother and showed a distinct viscosity improvement when the stearyl methacrylate polymers were used as additives (Figure 52). In particular, poly(*N-trans*-sobrerol acrylamide-*co*-stearyl methacrylate) matched the viscosity profile of Yubase® oil showing excellent dispersant properties even after a week's storage.
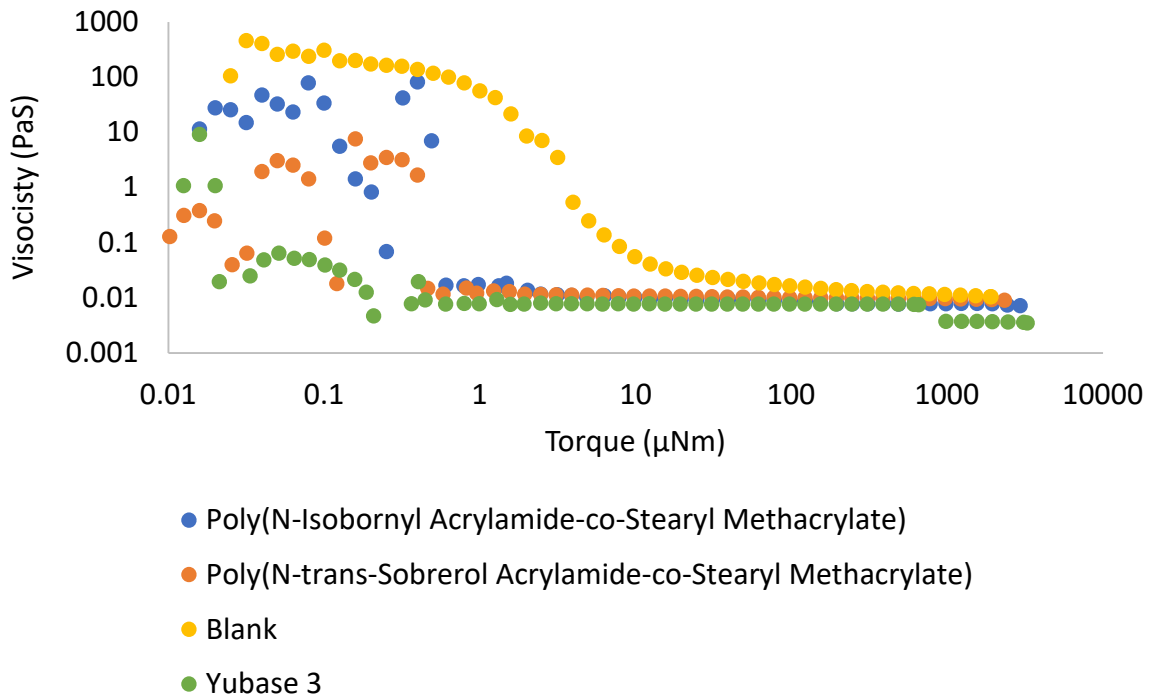
Figure 51: Direct Comparison at Room Temperature of Terpene-Stearyl Methacrylate Copolymers with Soot Contaminated Yubase® Oil after 1 Week of Storage
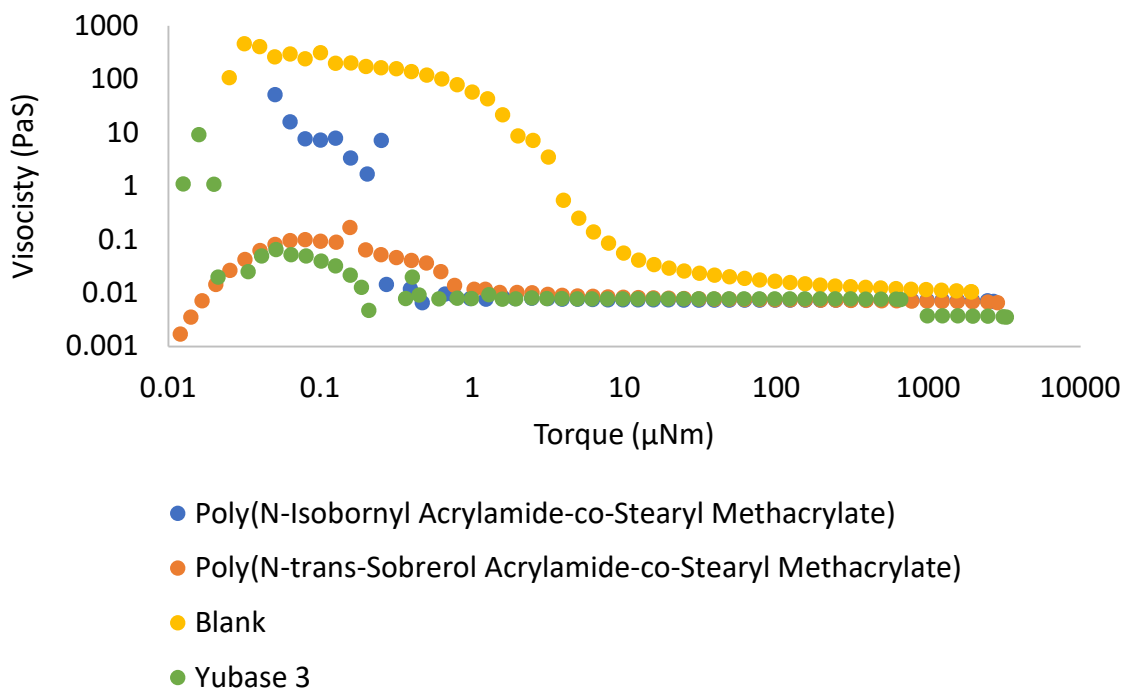
Figure 52: Direct Comparison at 40 °C of Terpene-Stearyl Methacrylate Copolymers with Soot Contaminated Yubase® Oil after 1 Week of Storage

The samples were then left for a further week, equalling two weeks ageing in total. Again, the samples were analysed at room temperature and 40 °C. At room temperature, both the stearyl methacrylate copolymers matched the viscosity profile of Yubase® with the blank control soot contaminated sample showing significantly higher viscosities at lower torques. A similar graph was seen when the samples were run at 40 °C, however, the viscosity of the sample with poly(*N-trans*-sobrerol acrylamide-*co*-stearyl methacrylate) was initially high, closer to the viscosity of the blank sample suggesting that some degradation may have occurred. After 0.5 µNm, the viscosity of the poly(*N-trans*-sobrerol acrylamide-*co*-stearyl methacrylate) sample matched the poly(*N*-isobornyl acrylamide-*co*-stearyl methacrylate) and Yubase® (Figure 54).

Poly(N-Isobornyl Acrylamide-co-Stearyl Methacrylate)

Poly(N-trans-Sobrerol Acrylamide-co-Stearyl Methacrylate)

Blank
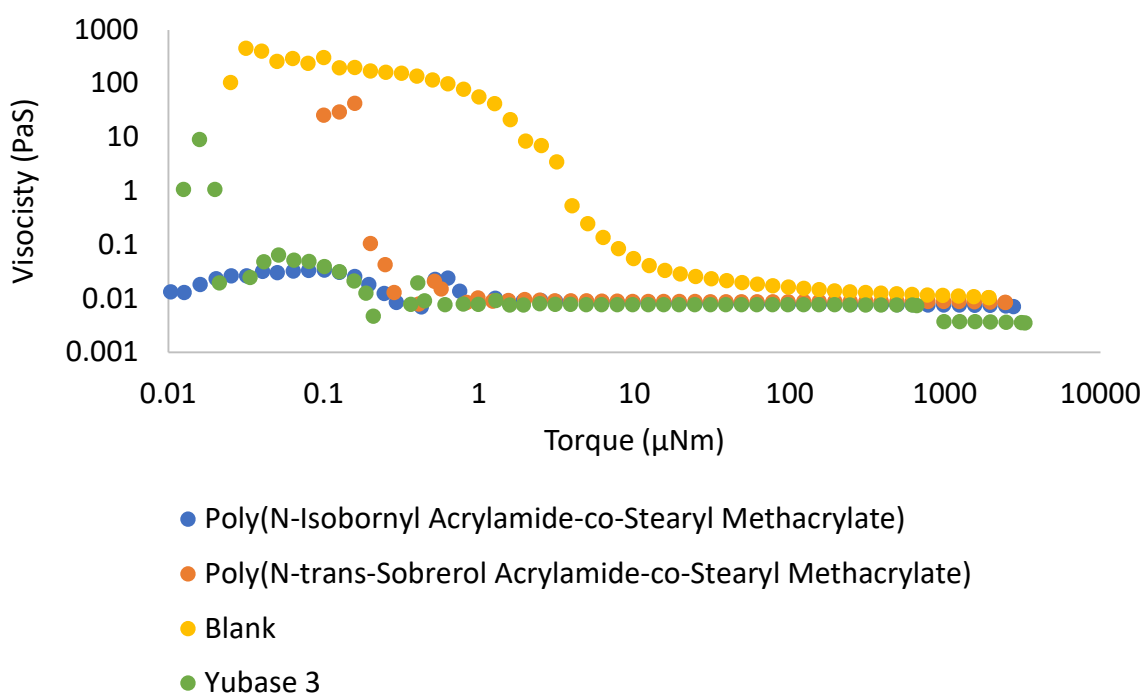
Yubase 3

Figure 53: Direct Comparison at Room Temperature of Terpene-Stearyl Methacrylate Copolymers with Soot Contaminated Yubase® Oil after 2 Weeks of Storage
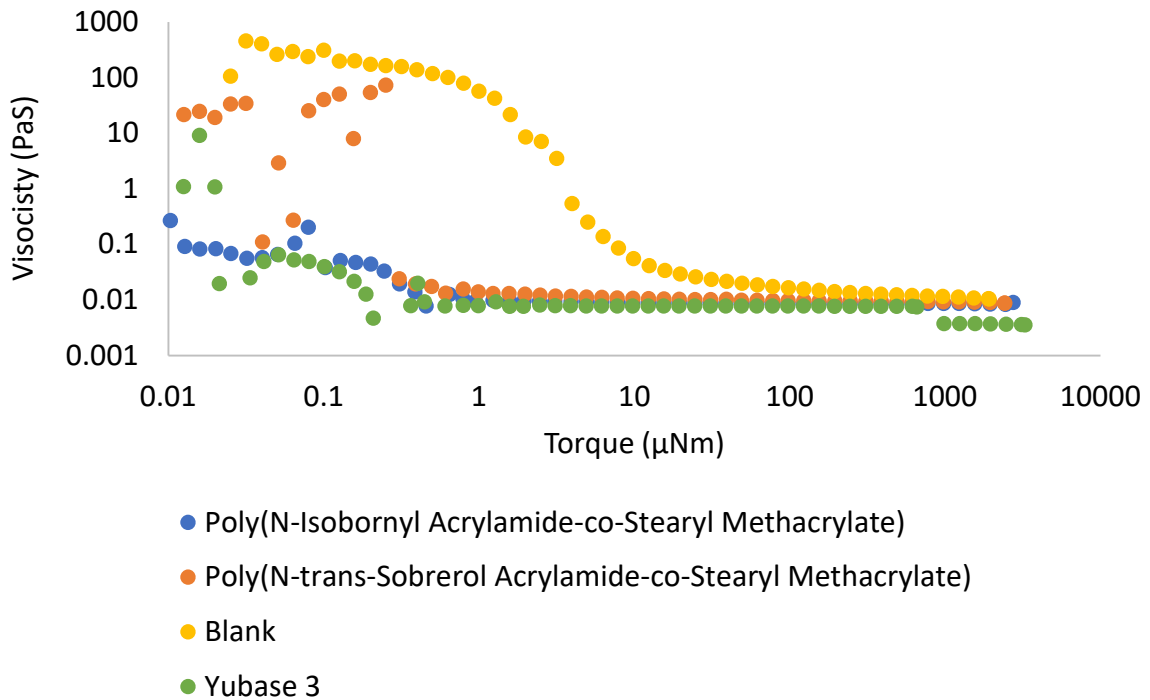
Figure 54: Direct Comparison at 40 °C of Terpene-Stearyl Methacrylate Copolymers with Soot Contaminated Yubase® Oil after 2 Weeks of Storage

The ageing effect was compared at different torques and temperatures to measure the effect of degradation on the novel dispersants. First, the viscosities at 100 µNm across the two weeks were compared. The stearyl methacrylate copolymer samples both at room temperature and at 40 °C showed good stability maintaining a similar viscosity to the uncontaminated Yubase® oil sample (Figure 55). In comparison, the blank sample containing soot contaminated Yubase® oil with no dispersant, had a significantly higher viscosity. This suggests that the terpene-derived, stearyl methacrylate copolymers are successfully acting as non-aqueous dispersants reducing the agglomeration effect of soot contamination in the sample to negligible effects. This is important practically, because the oil and lubricants used in engines are subjected to a diverse range of maintenance and the good age stability will ensure maximum performance over the product's lifetime.
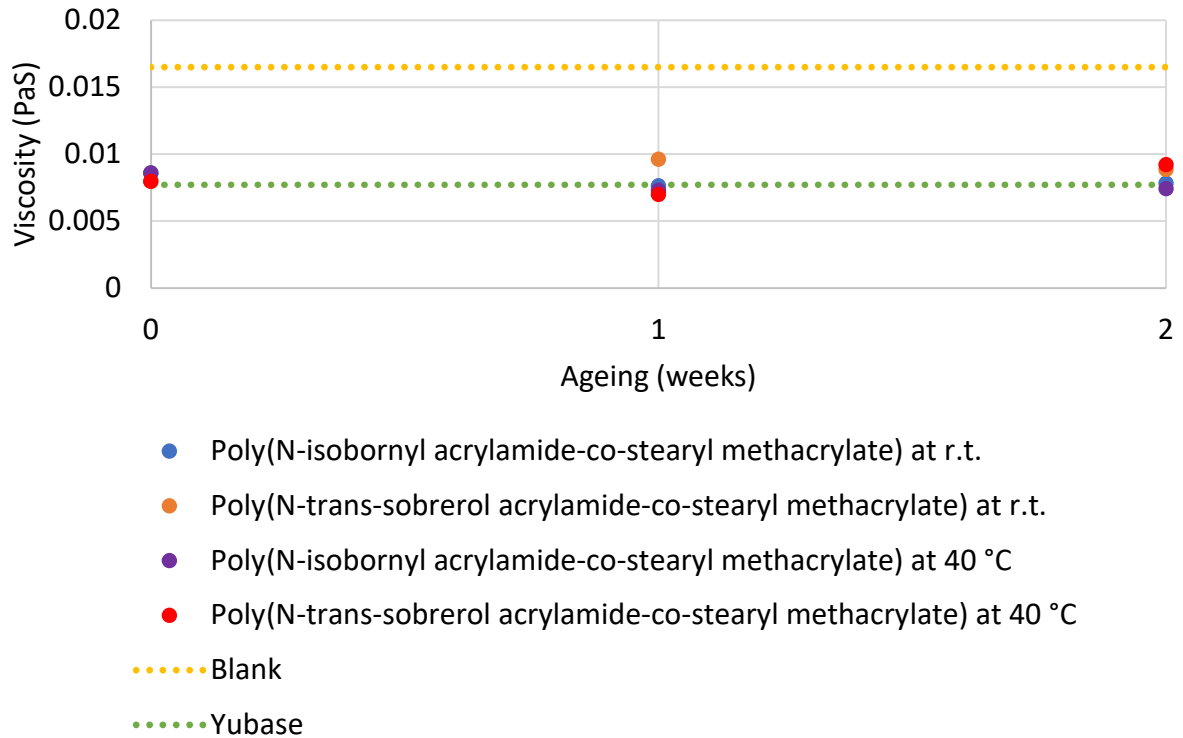
Figure 55: The Impact of Degradation on the Stearyl Methacrylate Copolymers when the Torque is 100 µNm

When the viscosities at 1000 µNm were compared over the two week ageing period, the stearyl methacrylate copolymers retained a similar viscosity suggesting that no degradation has occurred, or if it has, the effect of that degradation had no impact on its performance as a dispersant (Figure 56). At this higher torque, the stearyl methacrylate copolymers seemed to have a smaller effect on the viscosity, with the viscosity only reduced slightly compared with the contaminated Yubase®. However, there still seems to be some dispersant effect seen and at higher torques, the soot contaminated viscosity is closer in general to the uncontaminated sample, so this 'poorer' result may have little impact on the practical applications of this material in engines.
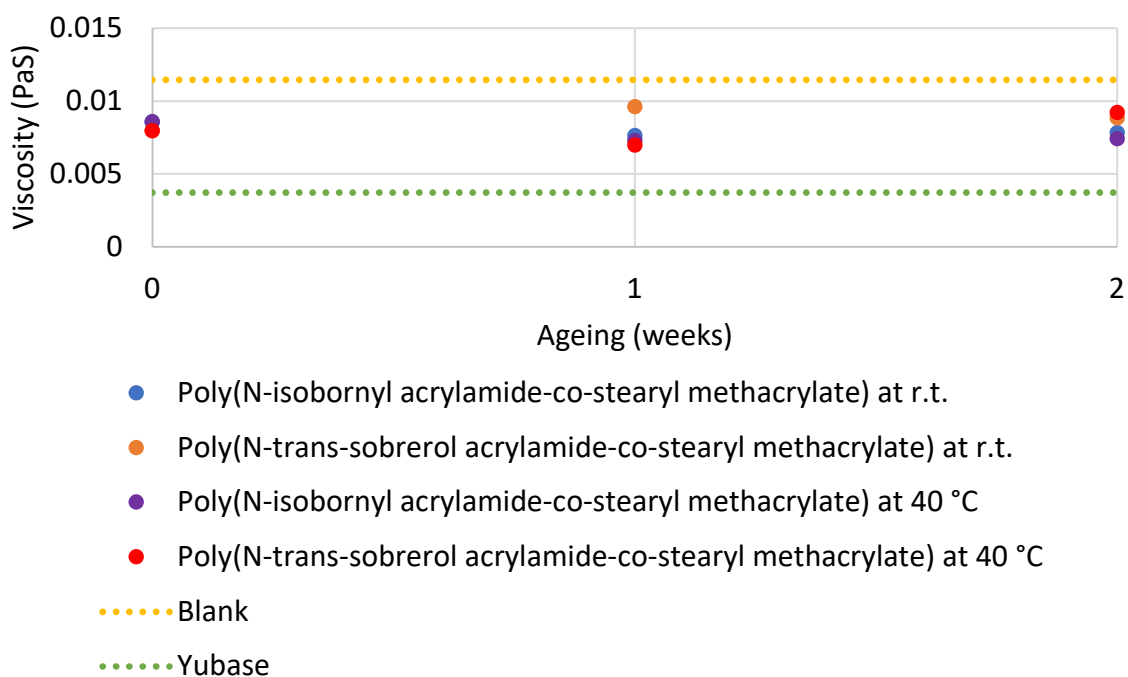
Figure 56: The Impact of Degradation on the Stearyl Methacrylate Copolymers when the Torque is 1000 µNm

4.5 Agricultural Dispersant

Non-aqueous dispersants are also used in crop care to disperse active ingredients such as pesticides or herbicides equally within the carrier emulsion solution. Crop protection products rarely consist of just a pure active ingredient. Instead, the active ingredient is usually formulated along with other materials which optimise the delivery of the active ingredient to the target. This allows more than one active ingredient to be used in the same formulation and creates products that are easier to handle, store and apply. The formulations ensure an even spread of the active ingredient over the crops, improving the bioavailability and reducing negative environmental effects enabling farmers to get the best yields for their crops.

A simplified oil dispersion formulation was used to measure the capabilities of the *N*-isobornyl acrylamide and *N-trans*-sobrerol acrylamide homopolymers and copolymers as non-aqueous dispersants for the insecticide, Imidacloprid (Figure 57).

211
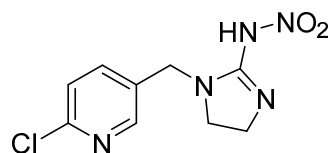
Figure 57: Imidacloprid

The simplified formulation contained a high loading of Imidacloprid, 20 wt %, along with Radia™ 7961 (a methylated seed oil) as the oil continuous phase, Atlas™ G1086 as the oil emulsifier and Tween™ 24 as the co-emulsifier/adjuvant.

Table 43: Simplified Crop Care Formulation

Function	(g/L)	wt%
Insecticide	10	20
Oil continuous phase	29	58
Oil emulsifier	5.5	11
Non-aqueous dispersant	1.1	2.2
Co-emulsifier/adjuvant	4.4	8.8

Atlox™ 4914 was used as the control to compare stability and API dispersancy. Initially the oil phase was mixed until homogeneous, and then the insecticide Imidacloprid was added. The mixture was vortexed for 10 minutes before it was heated to 54 °C for 2 hours. 5 mL of the mixture was added to 95 mL of tap water, mixed well to form an emulsion, and left for 30 minutes where upon the sediment was measured. This demonstrates the stability of the formulation as practically, the customers of pesticides, herbicides and fungicide formulations will not have the capabilities to remix their large volume of solution to ensure

212

even coverage of the active ingredient over their crops. Only the homopolymers and copolymers soluble in the Radia™ 7961 oil were investigated.

From this basic visual test the terpene derived homopolymers and copolymers; poly(*N*-isobornyl acrylamide), poly(*N-trans*-sobrerol acrylamide) and poly(*N-trans*-sobrerol acrylamide-*co*-allyl alcohol) performed comparably to the control dispersant, Atlox™ 4914. Poly(*N*-isobornyl acrylamide-*co-N*-vinyl pyrrolidone) performed better than the control with the least amount of sediment observed. Overall, the *N*-isobornyl acrylamide polymers performed slightly better than the *N-trans*-sobrerol acrylamide polymers. This is suggested to be due to the cage-like structure of the *N*-isobornyl acrylamide. The copolymers with stearyl methacrylate were the worst, unsurprising as the optimum non-aqueous dispersants are often surfactants and the stearyl methacrylate copolymers have two hydrophobic monomers.

Table 44: Sediment test for Terpene-derived Dispersants in Crop Care Formulations

Entry	Polymer Dispersant	Sediment (mm)
1	Atlox™ 4914	3
2	Poly(*N*-isobornyl acrylamide)	3
3	Poly(*N*-isobornyl acrylamide-*co-N*-vinyl pyrrolidone)	2
4	Poly(N-isobornyl acrylamide-*co*-allyl alcohol)	5
5	Poly(*N*-isobornyl acrylamide-*co*-stearyl methacrylate)	4
6	Poly(*N-trans*-sobrerol acrylamide)	3
7	Poly(*N-trans*-sobrerol acrylamide-*co*-allyl alcohol)	3
8	Poly(*N-trans*-sobrerol acrylamide-*co*-stearyl methacrylate)	5

4.6 Aqueous Dispersant

All the homopolymers and copolymers were tested for water-solubility with only the PEG acrylate co-polymers demonstrating hydrophilicity. Poly(*N*-isobornyl acrylamide-*co*-PEG acrylate) was then diluted to 5, 10 and 20 mg/mL solutions for aqueous carbon dispersancy testing.

Figure 58: 5, 10 and 20 mg/mL Aqueous Solutions of Poly(N-Isobornyl Acrylamide-co-PEG Acrylate) Respectively

Activated carbon has been of interest in the battery market due to its porous structure which dictates its high capacity and excellent cycling capabilities whilst boasting low costs and renewable precursors. To ensure uniform suspension of the activated carbon, a dispersant with binding properties is used to ensure an even spread of the activated carbon and good attachment to the electrode surface (in this case aluminium foil was used). One standard additive is PVDF (poly(vinylidene fluoride)).

The 5 mg/ml, 10 mg/ml and 20 mg/ml aqueous polymer solutions were combined with 5 wt% (0.1 g of activated carbon in 2 g solution) activated carbon. A control formulation which contained no polymer dispersant resulted in the activated carbon sedimenting.

A 5 wt% (0.1 g of activated carbon in 2 g poly(*N*-isobornyl acrylamide-*co*-PEG acrylate) aqueous solution) activated carbon, dispersant aqueous solution was prepared. Control with no dispersant left the activated carbon in lumps.

Figure 59: Activated Carbon-Dispersed Aqueous Solution on Aluminium Foil

With the dispersant present, the carbon was dispersed effectively however the viscosity was observed to be too high to be useful in battery applications. Unusually, as the dispersant concentration was increased the viscosity increased. This shear-thickening was proposed to be due to the formation of polymer nanoparticles in the aqueous dispersant solution. In the future, the ratio of monomers and its effect on the viscosity could be investigated.

The activated carbon-dispersed 5, 10 and 20 mg/mL poly(*N*-isobornyl acrylamide-*co*-PEG acrylate) solutions were evenly spread across aluminium foil and left to dry in air (Figure 60). Aluminium foil was used to mimic the electrode surface and test the binding and dispersant properties of poly(*N*-isobornyl acrylamide-*co*-PEG acrylate) for durability and even coverage of the activated carbon. As observed in the photos, use of poly(*N*-isobornyl acrylamide-*co*-PEG acrylate) as an aqueous dispersant gave a uniform coverage of the activated carbon across the aluminium surface, however the material was susceptible to cracking suggesting poor durability.

Activated carbon-dispersed aqueous solution of 5 mg/mL poly(*N*-isobornyl acrylamide-*co*-PEG acrylate) on aluminium foil

Activated carbon-dispersed aqueous solution of 10 mg/mL poly(*N*-isobornyl acrylamide-*co*-PEG acrylate) on aluminium foil

Activated carbon-dispersed aqueous solution of 20 mg/mL poly(*N*-isobornyl acrylamide-*co*-PEG acrylate) on aluminium foil
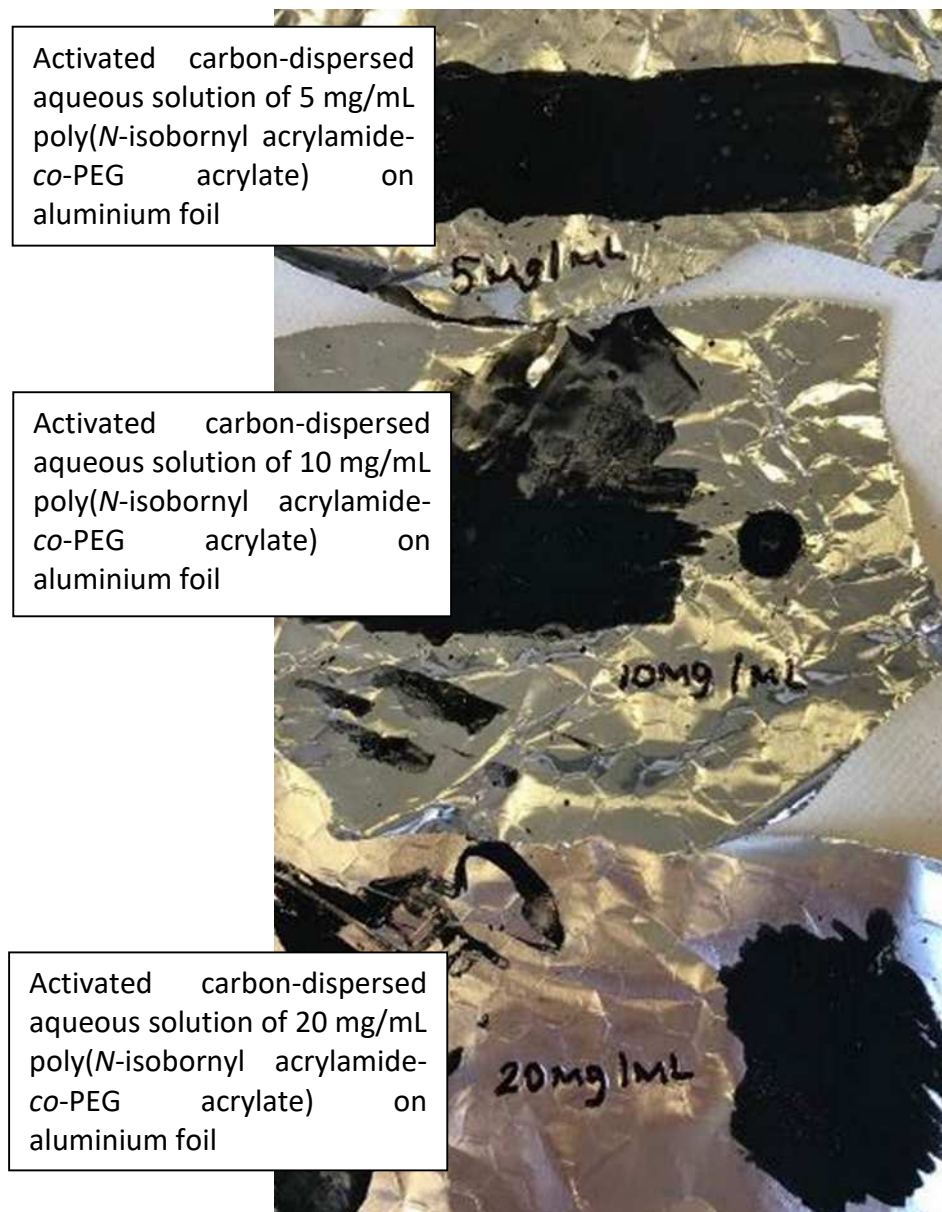
Figure 60: Activated Carbon-Dispersed 5, 10 and 20 mg/mL Polymer Solutions on Aluminium Foil

4.7 Particle Sizing

The possible self-assembly of polymer nanoparticles in aqueous media was investigated using particle size testing on different concentrations of the aqueous poly(*N*-isobornyl acrylamide-*co*-PEG acrylate) solutions using the Malvern Zetasizer Nano Spec021 at 25 °C. Despite the increase in concentration the average particle diameter remained at around 180 nm up to 5 mg/mL with reproducible results. The self-assembly of poly(*N*-isobornyl

acrylamide-*co*-PEG acrylate) is likely due to the hydrophobic hydrocarbon terpene moiety being encapsulated by the hydrophilic PEG acrylate chains stabilising the polymer structure and allowing good solubility of the material in water. On the other hand, poly(*N-trans*-sobrerol acrylamide-*co*-PEG acrylate) did not give a particle size curve in a 10 mg/mL aqueous solution suggesting a lack of nanoparticle formation. The tertiary alcohol functionality on *N-trans*-sobrerol acrylamide could partake in hydrogen bonding, potentially disrupting any self-assembly.

*Table 45: Particle Size Analysis of Poly(*N*-Isobornyl Acrylamide-*co*-PEG Acrylate) in Water*

Concentration (mg/mL)	Average Particle Diameter (± 0.1 nm)			
	Repeat 1	Repeat 2	Repeat 3	Average
10	441.9	433.8	458.5	444.7
5	178.8	180.0	178.9	179.2
2.5	215.0	214.7	211.7	213.8
1	112.3	112.0	113.9	112.7

In general the trend is, as the concentration of poly(*N*-isobornyl acrylamide-*co*-PEG acrylate) increases the average particle size increases (Figure 61). However, interestingly at 5 mg/mL the average particle diameter decreases instead suggesting the polymer nanoparticles potentially self-assembling at the optimum hydrophilic/hydrophobic ratio.
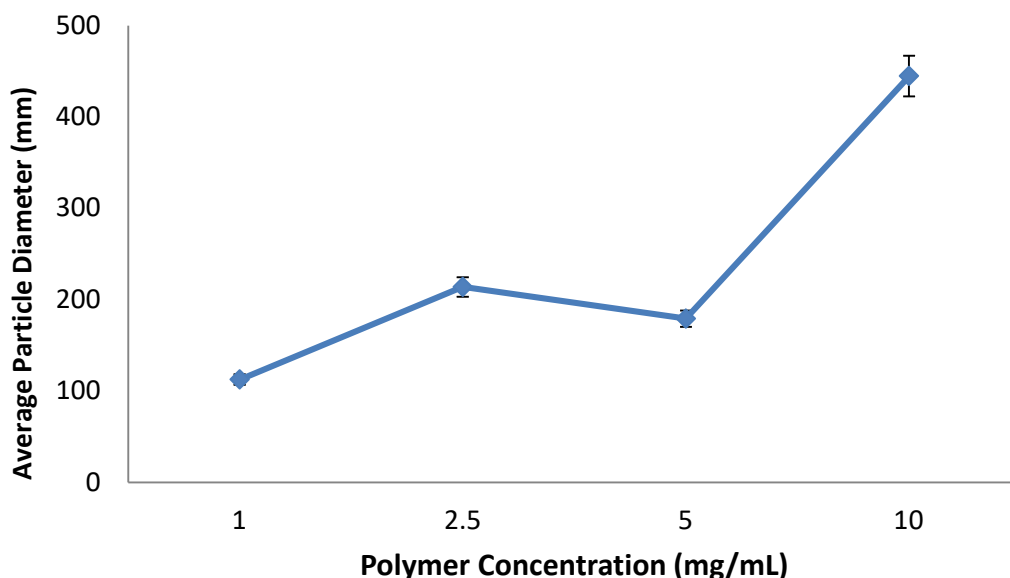
Figure 61: Average Particle Diameter versus Polymer Concentration

4.8   Foaming

Foaming agents are used in home and personal care products such as soaps, detergents and shampoos to create a foam or lather when mixed with air and water. The most common foaming agent is the surfactant, sodium laureth sulfate. Foam can be both an advantage and disadvantage to cleaning products. In dishwasher or washing machine products, a large amount of foam can decrease the cleaning performance of a formulation. In glass cleaning applications, a stable foam can require more water to be removed and can lead to unaesthetic spotting/streakiness. Therefore, it is important to have low or no foaming for these applications. However, consumers often associate foam with detergency and quality. Highly stable, small bubble foams can add a nice aesthetic to a home or personal care product such as washing up liquid, shampoos, bubble bath. Foam can also increase the surface area in contact with the active ingredient which maximises the use of cleaning additives in the formulation.

Here, three repeats of 1 wt% aqueous solutions of poly(*N*-isobornyl acrylamide-*co*-PEG acrylate) and poly(*N-trans*-sobrerol acrylamide-*co*-PEG acrylate) were run on a SITA foam former 2000. The mixer was run at 1200 rpm for 20 secs for 20 continuous measurements then held for 10 minutes with measurements every 20 secs to determine foam height and

stability. The average of the three repeats was found and the data visualised through graphs.

Rapidly spinning 250 mL of the 1 wt% aqueous solution of poly(*N*-isobornyl acrylamide-*co*-PEG acrylate) caused the mixture to double in height due to the wet, stable foam produced, this height then only slightly decreased over the 20 minute hold (Figure 62).

Poly(*N-trans*-sobrerol acrylamide-*co*-PEG acrylate) produced a less stable foam with the foam height reaching 200 mL before decaying at a rapid rate and then stabilising somewhat (Figure 62). The higher stability of the poly(*N*-isobornyl acrylamide-*co*-PEG acrylate) compared to poly(*N-trans*-sobrerol acrylamide-*co*-PEG acrylate) could be due to its better surfactant properties with more distinct lipophilic and hydrophilic regions within the polymer. This analysis of the foam build and decay of both polymers will allow these materials to be considered as additives for future foaming applications by customers.
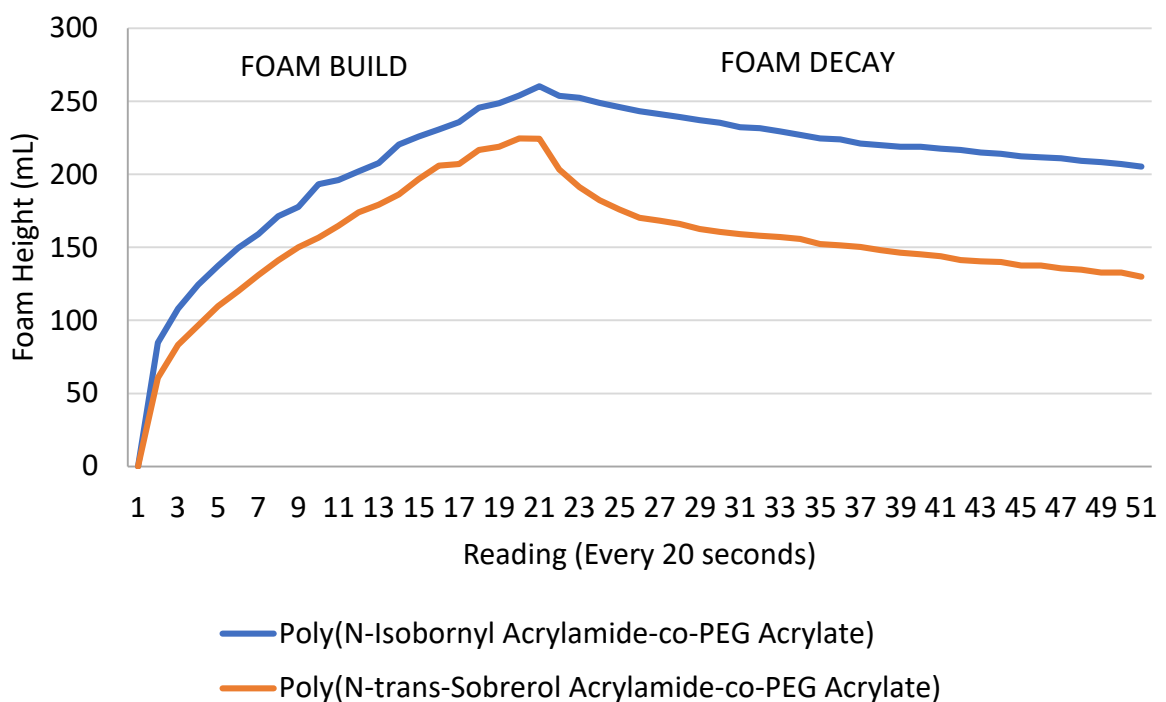
Figure 62: Foam Build and Decay of Poly(N-Isobornyl Acrylamide-co-PEG Acrylate) and Poly(N-trans-Sobrerol Acrylamide-co-PEG Acrylate)

4.9 Emulsifiers

Emulsifiers are used in formulations in many different industries such as personal care, coatings and crop care.[191] They combine hydrophobic active ingredients with water-based products to allow for effective delivery of properties in a form that is required by the application. Oil-in-water emulsions (o/w) contain a low concentration of oil and are used in products such as moisturisers. Water-in-oil emulsions (w/o) contain a low concentration of water and are found in applications such as omega 3 fish oil tablets or deep-sea oil mining.[191]

Polymeric emulsifiers are surfactants so the copolymers combining hydrophobic terpene monomers and hydrophilic commercial monomers were expected to be most likely to succeed. The emulsifications were prepared using the following simplified recipe, both oil in water (o/w) and water in oil (w/o) emulsifications were investigated. In both formulations, 5 wt% of the polymeric emulsifier was used with 15 wt% of the lower concentration medium (Table 46).

Table 46: Formulations for Oil in Water (o/w) and Water in Oil (w/o) Emulsions

Formulation Ingredient	o/w (wt%)	w/o (wt%)
Deionised water	80	15
Mineral Oil	15	80
Emulsifier	5	5

The emulsions were all mixed by shaking for 30 seconds then left to stand for at least two hours before the level of separation was visually assessed. Most of the oil in water emulsion formulations using terpene-derived homo- and copolmyers resulted in full separation of the water and oil layers (Figure 63).
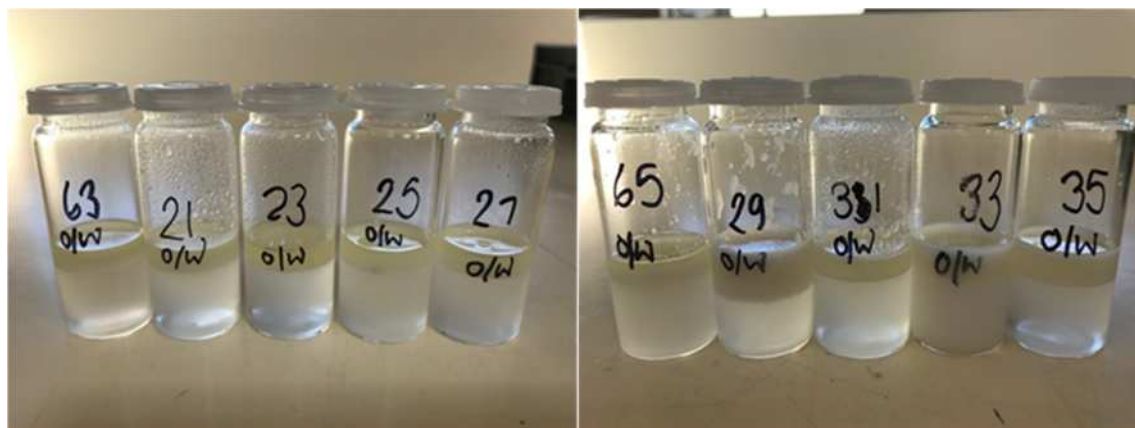
Number	Polymer
63	Poly(*N*-isobornyl acrylamide)
21	Poly(*N*-isobornyl acrylamide-*co*-*N*-vinyl pyrrolidinone)
23	Poly(*N*-isobornyl acrylamide-*co*-allyl alcohol)
25	Poly(*N*-isobornyl acrylamide-*co*-PEG acrylate)
27	Poly(*N*-isobornyl acrylamide-*co*-stearyl methacrylate)
65	Poly(*N*-*trans*-sobrerol acrylamide)
29	Poly(*N*-*trans*-sobrerol acrylamide-*co*-*N*-vinyl pyrrolidinone)
31	Poly(*N*-*trans*-sobrerol acrylamide-*co*-allyl alcohol)
33	Poly(*N*-*trans*-sobrerol acrylamide-*co*-PEG acrylate)
35	Poly(*N*-*trans*-sobrerol acrylamide-*co*-stearyl methacrylate)

Figure 63: Oil in Water Emulsion Investigations with Number Key

The best result was using poly(*N-trans*-sobrerol acrylamide-*co*-PEG acrylate) (vial 33), as although some separation occurred there was still a stable creaming of the oil and water layers (Figure 64).

221

Figure 64: Poly(N-trans-Sobrerol Acrylamide-co-PEG Acrylate) as an Emulsifier

This result could be further investigated in the future by increasing the molecular weight of the PEG chain (the current PEG acrylate monomer has an M_n of 480) or by increasing the ratio of PEG acrylate to *N-trans*-sobrerol acrylamide monomer, starting with a 3:1 or 3:2 ratio respectively. For this potential novel oil in water emulsifier the HLB (hydrophilic-lipophilic balance) value was calculated at 14.3, within the 8-16 range expected for other oil in water emulsifiers.

Again, visually all of the water in oil emulsion formulations using terpene-derived homo- and copolmyers resulted in full separation of the water and oil layers with some of the formulations resulting in precipitation of the polymer (Figure 65).
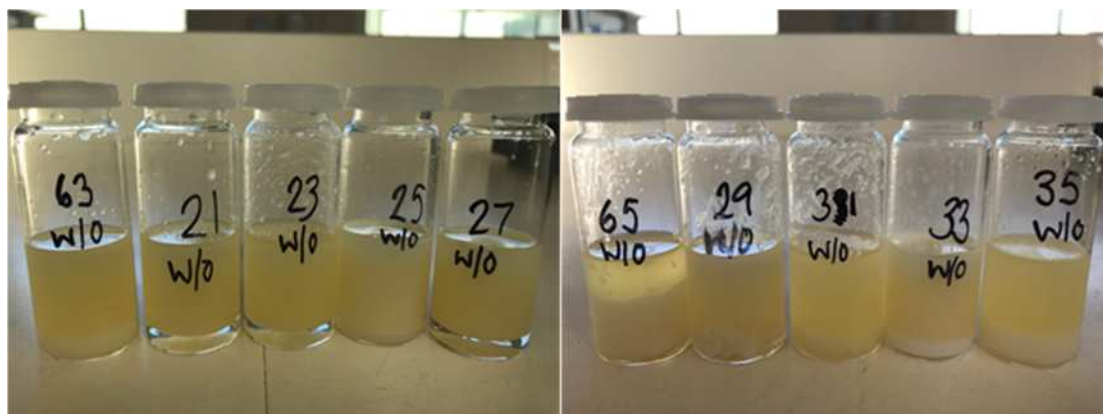
Figure 65: Water in Oil Emulsion Investigations

The coagulation of some of the polymers including, poly(*N-trans*-sobrerol acrylamide-*co-N*-vinyl pyrrolidone), within the water-in-oil emulsion formulations was interesting as one application for commercially available polyacrylamides is as a flocculant. However, as this coagulation was only seen in this oil/water mix and the polymer is insoluble in water, it is unlikely that an application can be found for it.
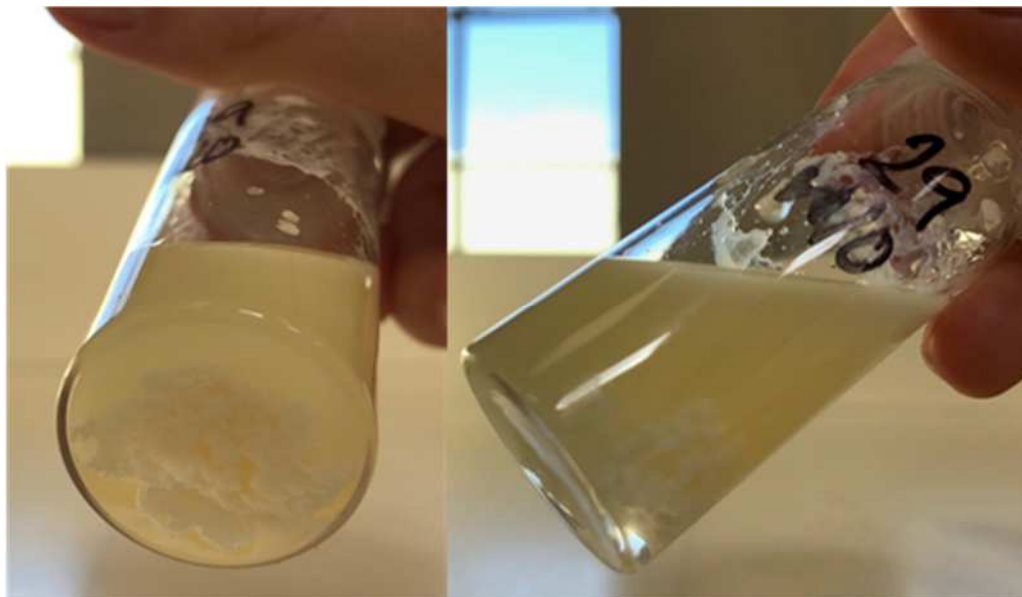
Figure 66: Coagulation of Poly(N-trans-Sobrerol Acrylamide-co-N-Vinyl Pyrrolidone) in an Water in Oil Mix

Although emulsification had not been fully achieved in mineral oil, the emulsifications of other oils were also investigated. The range of oils included vegetable oil, sunflower oil, soyabean oil, mineral oil (due to the lower concentration than previously investigated), rapeseed oil and Radia™ 7961 (a methylated seed oil). Poly(*N*-isobornyl acrylamide-*co*-PEG acrylate) in *n*-pentanol was incorporated separately into each different oil at 2 wt% inclusion level to test for compatibility (20 g scale). Visual observations of the samples were taken after one hour of mixing on rolling machine, where upon it was seen that the polymer was soluble in all the different types of oil. The emulsification test involved taking 5 mL of the oil-emulsifier blend and diluting it into 95 mL of tap water and mixing before observing the levels of separation after 30 minutes and 2 hours. However, at this low concentration, none

of the oil emulsified showing clear separation back into the two layers after 2 hours (Figure 67).
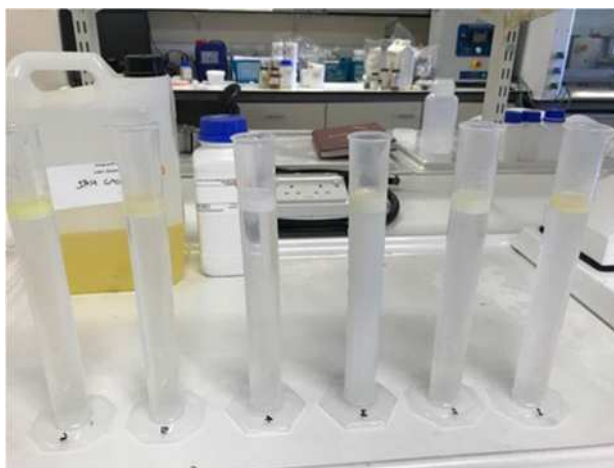
Figure 67: Emulsification Investigations using a Range of Different Oils

4.10 Water contact angle
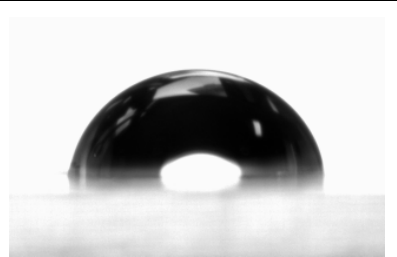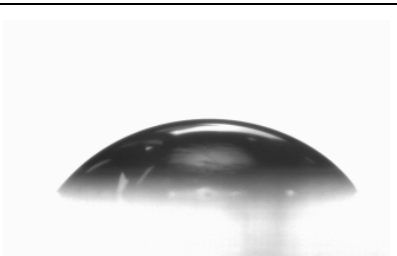
Water contact angles of all the water-insoluble homopolymers and copolymers were investigated to determine hydrophobicity. For a material to be hydrophobic, the water contact angle must be $\theta > 90°$, superhydrophobicity is classified as $\theta > 150°$. Hydrophobic coatings are used in applications such as car cleaning, waterproof clothing, and self-cleaning windows. Perfluorinated polymers are often used as waterproofing agents, however they are unsustainable environmentally persistent chemicals, therefore sustainable alternatives are required.
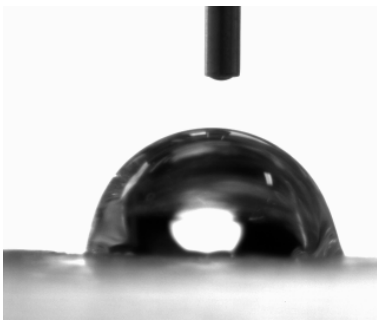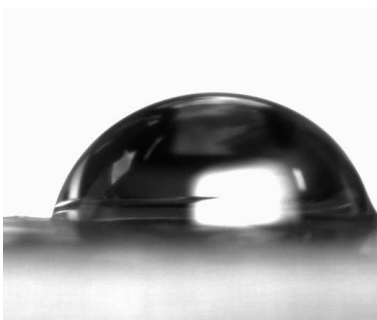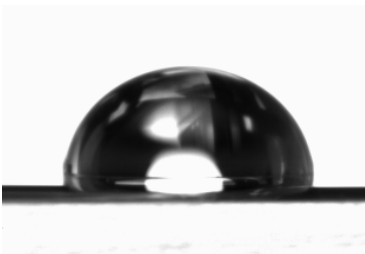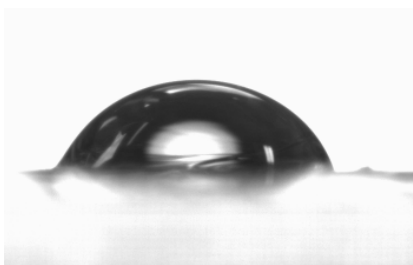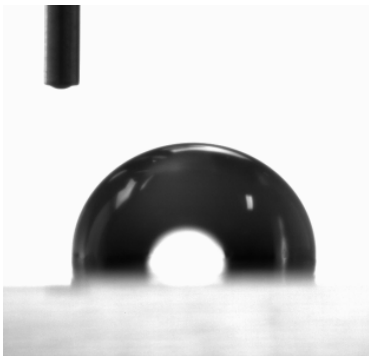
To measure the water contact angles, the polymer/pentanol solutions were dropped onto a glass microscope slide and dried in the oven at 40 °C for 4 hours to create a film. The *N-trans*-sobrerol acrylamide polymers formed a film exceedingly well, however as the solution underneath remained in a liquid state, the initial result was a rough surface which would have distorted any water contact angle measurement. Repeating process several times to produced useable samples. The PEG acrylate copolymers were not reported as they are known to be hydrophilic.

Out of the ten materials tested, three had hydrophobic properties; poly(*N*-isobornyl acrylamide-*co*-allyl alcohol) and poly(*N-trans*-sobrerol acrylamide-*co*-stearyl methacrylate) had water contact angles of 90° and poly(*N-trans*-sobrerol acrylamide-*co*-*N*-vinyl pyrrolidinone) had a water contact angle of 87°. Interestingly, when the effect of molecular weight on hydrophobicity was investigated with both of the homopolymers, poly(*N*-isobornyl acrylamide) and poly(*N-trans*-sobrerol acrylamide), both gave comparable results for both molecular weights, and indeed the hydrophobicity between the terpene-derived homopolymers was also similar. Overall, in this case, there did not seem to be much correlation between hydrophobicity and the structure of the polymer.

Further investigations into these three hydrophobic polymers could lead to applications into high impact, waterproof protective screens for electronics or rain fasteners in within crop care formulations depending on their durability and film forming properties, respectively.

Table 47: Analysis of Polymer Water Contact Angles

Entry	Sample	Picture	Average (°)[a]	Hydrophobic (Yes/No)
1	Poly(*N*-isobornyl acrylamide) M_n = 6 kDa		68.9	No
2	Poly(*N*-isobornyl acrylamide) M_n = 29 kDa		63.4	No
3	Poly(*N*-isobornyl acrylamide-*co*-*N*-vinyl pyrrolidinone)		71.5	No
4	Poly(*N*-isobornyl acrylamide-*co*-allyl alcohol)		90.0	Yes
5	Poly(*N*-isobornyl acrylamide-*co*-stearyl methacrylate)		51.4	No

6	Poly(*N-trans*-sobrerol acrylamide) Mn = 11 kDa		72.8	No
7	Poly(*N-trans*-sobrerol acrylamide) Mn = 29 kDa		72.3	No
8	Poly(*N-trans*-sobrerol acrylamide-*co-N*-vinyl pyrrolidinone)		86.5	No
9	Poly(*N-trans*-sobrerol acrylamide-*co*-allyl alcohol)		67.6	No
10	Poly(*N-trans*-sobrerol acrylamide-*co*-stearyl methacrylate)		91.3	Yes

[a]Average of both left and right tangents from two repeats

4.11 Conclusion

In summary, a wide range of applications were investigated for the homopolymers and copolymers of *N*-isobornyl acrylamide and *N-trans*-sobrerol acrylamide. Initially, the viscosity properties of the polymers in solution were characterised in full and their applicability as viscosity index modifiers investigated. Poly(*N*-isobornyl acrylamide), with a M_n of 29 kDa, and poly(*N-trans*-sobrerol acrylamide-*co*-stearyl methacrylate) were found to have good viscosity index modifier properties. Poly(*N*-isobornyl acrylamide-*co*-stearyl methacrylate) and poly(*N-trans*-sobrerol acrylamide-*co*-stearyl methacrylate) demonstrated good non-aqueous dispersant properties in oil for applications in soot dispersants. Demonstrating both good viscosity index modification and non-aqueous dispersant properties, the commercial manufacture and formulation of poly(*N-trans*-sobrerol acrylamide-*co*-stearyl methacrylate) will be further investigated as a product within the oil and lubricants industry.

Whilst investigating non-aqueous dispersant properties in crop care applications for pesticide dispersants, poly(*N*-isobornyl acrylamide), poly(*N-trans*-sobrerol acrylamide) and poly(*N-trans*-sobrerol acrylamide-*co*-allyl alcohol) performed comparably and poly(*N*-isobornyl acrylamide-*co*-N-vinyl pyrrolidone) performed better than the control commercial non-aqueous dispersant, Atlox^{TM} 4914. All four of these will be taken forward in the future for more extensive applications testing as part of a full commercial formulation.

As the only two water-soluble polymers poly(*N*-isobornyl acrylamide-*co*-PEG acrylate) and poly(*N-trans*-sobrerol acrylamide-*co*-PEG acrylate) were investigated for applications into aqueous dispersants for carbon batteries, foaming agents and emulsifiers due to the mix of hydrophobic acrylamide monomers and hydrophilic PEG acrylate. Although the materials performed adequately, they did not outperform current commercial products and further investigations into use within these applications are not warranted at this time.

Coatings made from poly(*N*-isobornyl acrylamide-*co*-allyl alcohol), poly(*N-trans*-sobrerol acrylamide-*co*-stearyl methacrylate) and poly(*N-trans*-sobrerol acrylamide-*co*-N-vinyl pyrrolidinone) showed hydrophobic properties. Further investigations into combing this property with the high glass transition temperatures of the terpene-derived polyacrylamides and their non-aqueous dispersants characteristics this could be investigated with

228

applications into high impact, waterproof protective screens for electronics or rain fasteners in within crop care formulations.

5.0 Conclusions and Further Work

The aim of this project has been successfully met. A library of renewable homopolyacrylamides were synthesised in good to excellent yields on a multigram scale in three steps or less which contained a renewable content of 75 % in line with Croda's carbon positive goal and the 12th United Nations Sustainable Development Goal. Thermally initiated solution polymerisations were found to give better performance than the redox initiated solution polymerisations and redox initiated emulsion polymerisation methods, although the methodology of low energy redox polymerisations using green initiators such as ascorbic acid and hydrogen peroxide will be investigated further in the future.

The green solvent and short reaction times of the optimised thermal free radical polymerisation conditions makes the polymerisation of terpene-derived acrylamides feasible on an industrial scale and would allow these monomers to be dropped directly into exisiting industrial processes as potential replacements for other petroleum-based monomers. However, more optimisation of these semi-batch conditions would be required to optimise the molecular weights and dispersities of the samples. The a range of glass transition temperatures were collected for the various terpene-derived acrylamide homopolymers, indicating these polymers may have potential applications ranging from resistant coatings to high temperature engineering applications.

The library was extended with the synthesis of a range of copolymers consisting of a terpene-derived acrylamide and a commerically available co-monomer; *N*-vinyl pyrrolidone, allyl alcohol, PEG acrylate and stearyl methacrylate. The acrylate and methacrylate co-monomers resulted in terpene-derived co-polymers with higher molecular weights than the vinyl co-monomers due to the closer reactivities.

The synthesis of the monomers using the Ritter reaction from monoterpenes and monoterpenoids has been shown to be sustainable, economical and robust for easy commercialisation on an industrial scale. The investigation into the sustainable synthesis of *N*-isobornyl acrylamide will continued with the aim of using only low hazard materials and recyclable heterogeneous catalysts. Further synthetic modifications of *N*-carveol acrylamide

231

demonstrated the potential for directed diversification and the ability to target desired properties within novel renewable polymers.

Finally, the properties of the polymers tested for potential applications in collaboration with Croda Europe Ltd. Poly(N-isobornyl acrylamide), with a M_n of 29 kDa, and poly(N-*trans*-sobrerol acrylamide-*co*-stearyl methacrylate) were found to have good viscosity index modifier properties. Poly(N-isobornyl acrylamide-*co*-stearyl methacrylate) and poly(N-*trans*-sobrerol acrylamide-*co*-stearyl methacrylate) demonstrated good non-aqueous dispersant properties in oil for applications in soot dispersants. Demonstrating both good viscosity index modification and non-aqueous dispersant properties, the commercial manufacture and formulation of poly(N-*trans*-sobrerol acrylamide-*co*-stearyl methacrylate) will be further investigated as a product within the oil and lubricants industry.

Whilst investigating non-aqueous dispersant properties in crop care applications for pesticide dispersants, poly(N-isobornyl acrylamide), poly(N-*trans*-sobrerol acrylamide) and poly(N-*trans*-sobrerol acrylamide-co-allyl alcohol) performed comparably and poly(N-isobornyl acrylamide-*co*-N-vinyl pyrrolidone) performed better than the control commercial non-aqueous dispersant, Atlox^{TM} 4914. All four of these will be taken forward in the future for more extensive applications testing as part of a full commercial formulation.

Coatings made from poly(N-isobornyl acrylamide-*co*-allyl alcohol), poly(N-*trans*-sobrerol acrylamide-*co*-stearyl methacrylate) and poly(N-*trans*-sobrerol acrylamide-*co*-N-vinyl pyrrolidinone) showed hydrophobic properties. Further investigations into combing this property with the high glass transition temperatures of the terpene-derived polyacrylamides and their non-aqueous dispersants characteristics this could be investigated with applications into high impact, waterproof protective screens for electronics or rain fasteners in within crop care formulations.

6.0   Experimental

6.1   General Experimental Data

Materials. Unless stated otherwise, all reactions were carried out under an atmosphere of argon and stirred magnetically. Cooling to 0 °C was effected using an ice-water bath. Cooling to -78 °C in freeze, pump, thaw was effected using liquid nitrogen. Degassing was achieved by purging nitrogen through the appropriate solution for 30 min. The term petroleum ether refers to the fraction with boiling point between 40 and 60 °C. Commercially available solvents and reagents were used as supplied and water was deionised before use. The transaminase enzymes ATA-113 and ATA-256 were supplied by codexis.

Reaction monitoring. Reactions were monitored using thin layer chromatography on Merck TLC silica gel 60 F254 pre-coated aluminium sheets with fluorescent indicator. Sheets were visualised using ultra-violet light (254 nm) and/or potassium permanganate solution or vanillin dip, as appropriate. Flash column chromatography was performed using Fluorochem silica gel 60, 40–63 µm, unless otherwise noted.

NMR. Bruker CHMNMR400 and CHMNMR500 spectrometers were used to record all ^{1}H and ^{13}C NMR spectra of dilute solutions of the appropriate compound in the indicated deuterated solvent. All chemical shifts (δ) were analysed using MestreNova software and reported in parts per million (ppm) relative to residual solvent peaks. All chemical shifts are reported relative to chloroform ($δ_H$ = 7.27 ppm, $δ_C$ = 77.0 ppm) as the internal standard on the δ scale. Coupling constants (J) are reported in Hertz and are reported after averaging. The multiplicity of a ^{1}H NMR signal is designated by one of the following abbreviations: s = singlet, d = doublet, t = triplet, q = quartet, p = quintet, sept = septet, m = multiplet, br = broad, app = apparent. The "multiplicities" of ^{13}C NMR signals were assigned using a DEPT sequence. Where appropriate, assignments were aided using COSY, HMQC and HMBC spectra.

Infra-Red. Infra-red spectra were recorded using a Bruker Tensor 27 FT-IR spectrometer using an ATR attachment, analysed using OPUS software and their peaks quoted as v_{max} in cm^{-1}. High resolution mass spectra were obtained using a Bruker MicroTOF mass

spectrometer operating in electrospray positive ionisation (ESI positive) or electrospray negative ionisation (ESI negative).

Dynamic mechanical analysis. Dynamic mechanical analysis (DMA) was used to determine the T_g of the polymers. Measurements were performed on a Triton Technologies DMA (now Mettler Toledo DMA1) using the powder pocket accessory. The sample (40 mg ± 5 mg) was weighed into a powder pocket. Samples were measured at 1 and 10 Hz in single cantilever bending geometry between 0 – 300 °C or -20 - 250 °C depending on the region of interest. The value of the T_g was taken as the peak of the tan delta (tan δ) curve.

Gel Permeation Chromatography. Size exclusion chromatography (SEC) was performed in THF (HPLC grade, Fisher Scientific) as eluent at room temperature using two Agilent PL-gel mixed-D columns in series with a flow rate of 1 mL min^{-1}. A multi-angle light scattering (MALS) detector, along with a differential refractometer (DRI), were used for sample detection. The differential index of refraction value of a PMMA standard was used to calculate the polymer molecular weight and dispersity.Size exclusion chromatography (SEC) was performed using an Agilent 1260 Infinity Series HPLC (Agilent Technologies, USA) in THF (HPLC grade, Fisher Scientific) as eluent at room temperature using two Agilent PL-gel mixed-C columns in series with a flow rate of 1 mL min^{-1}. A differential refractometer (DRI), was used for sample detection.

Thermogravimetric analysis. Thermal gravimetric analysis (TGA) was performed using a TA Instruments Q500 TGA with platinum crucibles over a temperature range of 30 to 500 °C (10 °C min^{-1} ramp) in N_2. Data was analysed using TA universal analysis software

Viscosity. Viscosity was measured using an Anton Paar Stabinger Viscometer SVM 3001 at 20, 40 and 80 °C. Samples of polymer solutions were injected directly into the machine.

Dynamic Light Scattering. Polymer particle sizes within 1, 2.5, 5 and 10 mg/mL aqueous poly(*N*-isobornyl acrylamide-*co*-PEG acrylate) solutions were measured using the Malvern Zetasizer Nano Spec021 at 25 °C. Data was analysed using compatible Zetasizer software.

Foaming. 1 wt% aqueous solutions of poly(*N*-isobornyl acrylamide-*co*-PEG acrylate) and poly(*N*-*trans*-sobrerol acrylamide-*co*-PEG acrylate) were run on a SITA foam former 2000. The mixer was run at 1200 rpm for 20 secs for 20 continuous measurements then held for

234

10 minutes with measurements every 20 secs to determine foam height and stability. The experiment was run three times for each sample and an average found. The data was analysed and visualised through graphs on Microsoft Excel.

235

6.2 Compound Experimental Data

6.3 Monomer Synthesis

6.3.1 (6,6-Dimethylbicyclo[3.1.1]hept-2-en-2-yl)methyl 2,2,2-trichloroacetimidate[103] (89)
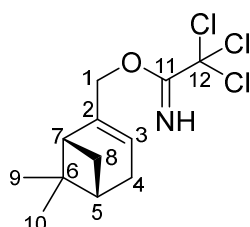
Myrtenol (1.6 mL, 10 mmol) was dissolved in DCM (40 mL) and the mixture was cooled to 0 °C. DBU (1.8 mL, 12 mmol) and trichloroacetonitrile (1.5 mL, 15 mmol) were added sequentially. The reaction mixture was stirred at room temperature for 2 hours. The reaction mixture was filtered under reduced pressure through a silica plug, washed with DCM (3 mL) and the solvent was removed under reduced pressure to give trichloroacetimidate 8**9** as a yellow oil (2.73 g, 9.2 mmol, 92 %). Product used without further purification.

R$_f$ = 0.63 (5% ethyl acetate in petrol); **IR v$_{max}$** (cm^{-1}) 3365 (NH), 3240, 3108, 2986, 2918, 1691, 1662 (C=NH), 1615 (C=C); **δ$_H$** (400 MHz, CDCl$_3$) 8.25 (1H, br, NH), 5.68 (1H, app sept, J = 1.5 Hz, 3-H), 4.68 (2H, m, 1-H$_2$), 2.42 (1H, app dt, J = 8.7, 5.6 Hz, 4-H$_a$), 2.32 (2H, m, 4-H$_2$), 2.23 (1H, app td, J = 5.6, 1.5 Hz, 7-H), 2.13 (1H, m, 5-H), 1.30 (3H, s, 9-H$_3$), 1.23 (1H, d, J = 8.7 Hz, 8-H$_b$), 0.87 (3H, s, 10-H$_3$); **δ$_C$** (101 MHz, CDCl3) 162.8 (C11), 142.6 (C2), 122.2 (C3), 71.7 (C1), 43.5 (C7), 40.7 (C5), 38.1 (C6), 31.5 (C4), 31.3 (C8), 26.2 (C9), 21.1 (C10) (C12 not observed, masked by CDCl$_3$ peak).

6.3.2 2,2,2-Trichloro-*N*-(6,6-dimethyl-2-methylenebicyclo[3.1.1]heptan-3-yl)acetamide[103] (90)
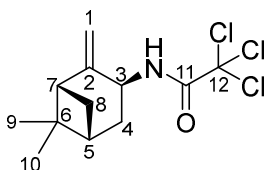
Trichloroacetimidate **89** (2.73 g, 9.20 mmol) was dissolved in xylene (92 mL). The solution was degassed by bubbling argon through for 30 minutes. The solution was then heated to 140°C over 1 hour and left to heat at reflux for 16 hours. The solution was cooled to room temperature before the solvent was removed under reduced pressure to give the product trichloroacetamide **90** as red oil (2.70 g, 9.11 mmol, 99 %). Product used without further purification.

R$_f$ = 0.68 (20% ethyl acetate in petrol). **IR v$_{max}$** (cm^{-1}) 3428, 3333 (NH), 2920, 2870, 1698 (C=O); **δ$_H$** (400 MHz, CDCl$_3$) 5.06 (1H, app t, J = 1.2 Hz, 1-H$_a$), 4.94 (1H, app t, J = 1.2 Hz, 1-H$_b$), 4.69 (1H, ddd, J = 9.5, 7.3, 2.0 Hz, 3-H), 2.57 (3H, m, 8-H$_a$, 7-H, 4-H$_a$), 2.08 (1H, m, 5-H), 1.81 (1H, m, 4-H$_b$), 1.30 (3H, s, 9-H$_3$), 1.19 (1H, d, J = 10.1 Hz, 8-H$_b$), 0.79 (3H, s, 10-H$_3$); **δ$_C$** (101 MHz, CDCl$_3$) 160.9 (C2), 151.9 (C11), 112.9 (C1), 51.2 (C7), 46.9 (C3), 40.1 (C5), 33.8 (C4), 29.8 (C8), 25.8 (C9), 22.1 (C10) (C12 not observed, masked by CDCl$_3$ peak); **HRMS** (ESI positive): Calculated for C$_{12}$H$_{17}$Cl$_3$NO [M+H]$^+$ 296.0370 obtained 296.0363.

6.3.3 6,6-Dimethyl-2-methylenebicyclo[3.1.1]heptan-3-amine (91)
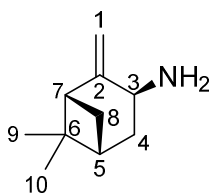
Trichloroacetamide **90** (382.1 mg, 1 mmol) was dissolved in dichloromethane (0.55 mL) and ethanol (1.07 mL). Aqueous NaOH (5M, 0.68 mL) was added and the reaction mixture heated to 50 °C and left stirring at reflux for 4 hours. After which water (5 mL) was added and the solution stirred for 5 minutes. The aqueous layer was extracted with dichloromethane (3 x 5 mL) before the combined organics were dried over anhydrous sodium sulfate and filtered. The solvent was removed under reduced pressure to give amine **91** as red oil (144 mg, 0.96 mmol, 96%). Product used without further purification.

IR v$_{max}$ (cm^{-1}) 2922, 2868, 1643; **δ$_H$** (400 MHz, CDCl$_3$) 4.86 (1H, app t, J = 1.3 Hz, 1-H$_a$), 4.74 (1H, app t, J = 1.4 Hz, 1-H$_b$), 3.71 (1H, m, 3-H), 2.51 (1H, t, J = 5.7 Hz, 7-H), 2.42 (1H, app dtd, J = 9.9, 5.7, 2.0 Hz, 8-H$_a$), 2.32 (1H, m, 4-H$_a$), 2.02 (1H, m, 5-H), 1.57 (1H, ddd, J = 14.1, 3.8, 2.1 Hz, 4-H$_b$), 1.48 (1H, d, J = 9.9 Hz, 8-H$_b$), 1.26 (3H, s, 9-H$_3$), 0.69 (3H, s, 10-H$_3$); **δ$_C$** (101 MHz, CDCl$_3$) 157.8 (C2), 109.2 (C1), 51.6 (C7), 46.9 (C3), 40.6 (C5), 40.0 (C6), 35.4 (C4), 28.9 (C8), 25.9 (C9), 21.9 (C10); **HRMS** (ESI positive): Calculated for C$_{10}$H$_{18}$N [M+H]$^+$ 152.1434 obtained 152.1437.

6.3.4 *N*-(6,6-Dimethyl-2-methylenebicyclo[3.1.1]heptan-3-yl)acrylamide (92)
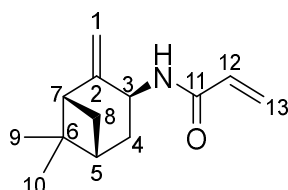
Acrylic acid (0.05 mL, 0.726 mmol) was added dropwise to HATU (502 mg, 1.32 mmol) dissolved in DMF (5 mL) whilst stirring. DIEA (0.4 mL, 1.98 mmol) was added dropwise. Amine **91** (100 mg, 0.66 mmol) in DMF (3 mL then 2 mL wash) was added dropwise. The solution was left stirring for 16 hours. Water (10 mL) was added and the organic layer was washed with water (10 mL x 2) before the combined aqueous layers were extracted with ethyl acetate (10 mL x 2). The combined organic layers were dried over anhydrous sodium sulfate and filtered. The solvent was removed under reduced pressure. Purification using column chromatography (50% ethyl acetate in petrol) gave acrylamide **92** as a red amorphous solid (68 mg, 0.33 mmol, 50%).

R$_f$ = 0.66 (50% ethyl acetate in petrol). **IR v$_{max}$** (cm^{-1}) 3274, 3074, 2973, 2920, 2868, 1652; **[α]$_D$$^{24.0}$** +23.63° (c 0.80, CHCl$_3$); **δ$_H$** (400 MHz, CDCl$_3$) 6.32 (1H, dd, *J* = 17.0, 1.5 Hz, 13-H$_a$), 6.11 (1H, dd, *J* = 17.0, 10.2 Hz, 12-H), 5.66 (1H, dd, *J* = 10.2, 1.5 Hz, 13-H$_b$), 5.01 (1H, app t, *J* = 1.5 Hz, 1-H$_a$), 4.88 (1H, app t, *J* = 1.5 Hz, 1-H$_b$), 4.83 (1H, m, 3-H), 2.59-2.50 (3H, m, 7-H, 8-H$_a$, 4-H$_a$), 2.08-2.04 (1H, m, 5-H), 1.82-1.77 (1H, m, 4-H$_b$), 1.29 (3H, s, 9-H$_3$), 1.20 (1H, d, *J* = 10.1 Hz, 8-H$_b$), 0.80 (3H, s, 10-H$_3$); **δ$_C$** (101 MHz, CDCl$_3$) 164.6 (C2), 153.5 (11), 131.0 (C12), 126.3 (C13), 111.9 (C1), 51.4 (C7), 45 (C3), 40.42 (C5), 40.02 (C6), 34.79 (C4), 29.88 (C8), 25.88 (C9), 22.09 (C10); **HRMS** (ESI positive): Calculated for C$_{13}$H$_{20}$NO [M+H]$^+$ 206.1539 obtained 206.1533, calculated for C$_{13}$H$_{19}$NONa [M+Na]$^+$ 228.1364 obtained 228.1357.

6.3.5 Pinocarveol[131] (93)
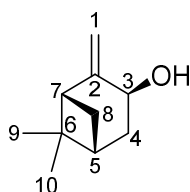
Diethylamine (6.85 mL, 32.9 mmol) was dissolved in diethyl ether (200 mL) and cooled to 0 °C. *n*-BuLi (2.5 M in hexane, 27.6 mL, 69.0 mmol) was added dropwise over 20 minutes. After stirring for 5 minutes, α-pinene oxide (10.4 mL, 66.0 mmol) in diethyl ether (40 mL) was added dropwise over 10 minutes. The mixture was heated to reflux and left stirring for 6 hours. After reaction completion, the reaction mixture was cooled to -20 °C before water (100 mL) was added whilst stirring quickly. The organic phase is separated and washed with aqueous HCl (1 M, 100 mL), then water (100 mL), then saturated aqueous sodium hydrogen carbonate (100 mL) then water (100 mL). The combined aqueous phases are then extracted with diethyl ether (3 x 50 mL). The combined organic phases are dried over anhydrous sodium sulfate, filtered and the solvent removed under reduced pressure. Purification using column chromatography (20% ethyl acetate in petrol) gave pinocarveol **93** as a pale yellow oil (9.23 g, 61 mmol, 92%).

R$_f$ = 0.24 (20% ethyl acetate in petrol). **IR v$_{max}$** (cm^{-1}) 3373, 3070, 2973, 2917, 2868, 2309, 1707, 1645; **δ$_H$** (400 MHz, CDCl$_3$)) 5.00 (1H, app t, *J* = 1.2 Hz, 1-H$_a$), 4.82 (1H, app t, *J* = 1.1 Hz, 1-H$_b$), 4.42 (1H, m, 3-H), 2.52 (1H, app t, *J* = 5.5 Hz, 5-H), 2.39 (1H, app dtd, *J* = 9.9, 5.5, 2.0 Hz, 8-H$_a$), 2.24 (1H, app ddt, *J* = 14.6, 7.7, 2.0 Hz, 4-H$_a$), 2.01 (1H, m, 7-H), 1.85 (1H, ddd, *J* = 14.6, 4.2, 1.0 Hz, 4-H$_b$), 1.72 (1H, d, *J* = 9.9 Hz, 8-H$_b$), 1.28 (3H, s, 9-H$_3$), 0.65 (3H, s, 10-H$_3$); **δ$_C$** (101 MHz, CDCl$_3$) 156.1 (C2), 111.4 (C1), 67.0 (C3), 50.6 (C7), 40.4 (C6), 39.9 (C5), 34.5 (C8), 27.9 (C4), 25.9 (C9), 21.9 (C10). Too small to detect by HRMS.

6.3.6 6,6-Dimethyl-2-methylenebicyclo[3.1.1]heptan-3-yl 2,2,2-trichloroacetimidate (94)
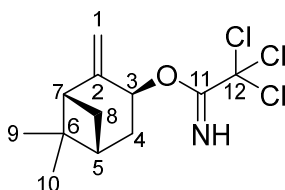
Pinocarveol **93** (9.23 g, 60.0 mol) was dissolved in DCM (230 mL) and stirring started. After cooling to 0 °C, DBU (10.75 mL, 72.0 mmol) was added dropwise and then after a few minutes stirring trichloroacetonitrile (9.00 mL, 90.0 mmol) was also added dropwise at 0 °C. The reaction mixture was allowed to warm up to room temperature and was left stirring for 2 hours. After which the solvent was removed under reduced pressure. Xylene (100 mL), petrol (100 mL) and water (300 mL) were added. The mixture was filtered through a celite® plug. The layers were separated and the organic layer washed with water (3 x 100 mL). The solvent was removed under reduced pressure and the crude flushed through a second celite plug using petrol. The solvent was removed under reduced pressure to give trichloroacetimidate **94** as a red oil (16.14 g, 54.0 mmol, 91%). Product used without further purification.

IR v_{max} (cm^{-1}) 3344, 2972, 2924, 2869, 2325, 2112, 1735, 1656; **δ_H** (400 MHz, CDCl$_3$) 8.46 (1H, br, NH), 5.86-5.83 (1H, m, 3-H), 5.28 (1H, app t, J = 1.3 Hz, 1-H$_a$), 5.06 (1H, app t, J = 1.3 Hz, 1-H$_b$), 2.77 (1H, t, J = 5.5 Hz, 7-H), 2.67-2.58 (2H, m, 4-H$_a$ and 8-H$_a$), 2.25-2.22 (1H, m, 5-H), 2.19-2.14 (1H, m, 4-H$_b$), 1.81 (1H, d, J = 10.1 Hz, 8-H$_b$), 1.40 (3H, s, 9-H$_3$), 0.82 (3H, s, 10-H$_3$); **δ_C** (101 MHz, CDCl$_3$) 162.2 (C11), 149.4 (C2), 115.0 (C1), 73.9 (C3), 50.7 (C7), 40.6 (C6), 39.5 (C5), 32.5 (C4), 29.0 (C7), 27.8 (C8), 26.0 (C9), 22.04 (C10) (C12 not observed, masked by CDCl$_3$ peak).

6.3.7 2,2,2-Trichloro-*N*-((6,6-dimethylbicyclo[3.1.1]hept-2-en-2-yl)methyl)acetamide] (95)
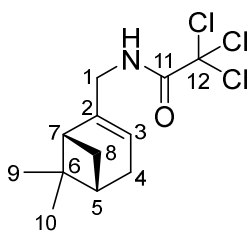
Trichloroacetimidate **94** (475 mg, 1.6 mmol) was dissolved in xylene (16 mL) and the solution was degassed by bubbling through argon for 10 minutes. The solution was then heated to 140 °C and left to reflux for 3 hours. The solution was then cooled and stirring stopped and left overnight before the solvent was removed under reduced pressure to give trichloroacetamide **95** as a red oil (475 mg, 1.6 mmol, 99%). Product used without further purification.

IR ν$_{max}$ (cm^{-1}) 2925, 2852, 1735, 1673; **δ$_H$** (400 MHz, CDCl$_3$) 6.66 (1H, br, NH), 5.55 (1H, tt, *J* = 3.1, 1.5 Hz, 3-H), 3.91 (2H, m, 1-H$_2$), 2.49-2.44 (1H, m, 8-H$_a$), 2.39-2.36 (2H, m, 4-H$_2$), 2.18-2.15 (1H, m, 5-H), 2.15-2.11 (1H, m, 7-H), 1.34 (3H, s, 9-H$_3$), 1.23 (1H, d, *J* = 8.8 Hz, 8-H$_b$), 0.90 (3H, s, 10-H$_3$); **δ$_C$** (101 MHz, CDCl$_3$) 161.8 (C11), 143.0 (C2), 120.3 (C3), 46.0 (C1), 44.0 (C5), 40.7 (C7), 38.1 (C6), 31.5 (C4), 31.2 (C8), 26.1 (C9), 21.2 (C10) (C12 not observed, masked by CDCl$_3$ peak); **HRMS** (ESI positive): Calculated for C$_{12}$H$_{17}$^{35}Cl$_3$NO [M+H]$^+$ 296.0370 obtained 296.0358.

6.3.8 (6,6-Dimethylbicyclo[3.1.1]hept-2-en-2-yl)methanamine (96)
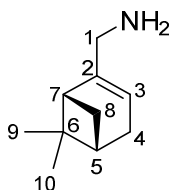
Trichloroacetamide **95** (499 mg, 1.68 mmol) was dissolved in dichloromethane (1 mL) and ethanol (2 mL). Aqueous NaOH (5M, 1.2 mL) was added and the reaction heated to 50 °C. The reaction mixture was left stirring at reflux for 4 hours. After 4 hours, water (10 mL) was added and dichloromethane (10 mL) were added. The organic layer was washed with water (10 mL x 3). Then the aqueous layers were extracted with dichloromethane (10 mL). the combined organics were dried over anhydrous sodium sulfate, filtered and the solvent removed under reduced pressure to give amine **96** as a red oil (213 mg, 1.41 mmol, 84%). Product used without further purification.

IR v_{max} (cm^{-1}) 2912, 2832, 1651. **δ_H** (400 MHz, CDCl$_3$) 5.35 (1H, app sept, J = 3.0, 1.5 Hz, 3-H), 3.17 (2H, app dd, J = 6.0, 1.9 Hz, 1-H$_2$), 2.41 (1H, ddd, J = 8.5, 5.6, 5.6 Hz, 8-H$_a$), 2.30-2.19 (2H, m, 4-H$_2$), 2.14-2.10 (1H, m, 7-H), 2.10-2.05 (1H, m, 5-H), 1.31 (3H, s, 9-H$_3$), 1.19 (1H, d, J = 8.5 Hz, 8-H$_b$), 0.85 (3H, s, 10-H$_3$). **δ_C** (101 MHz, CDCl$_3$) 149.6 (C2), 115.4 (C3), 47.2 (C1), 44.4 (C5), 41.0 (C7), 38.0 (C6), 31.7 (C4), 31.1 (C8), 26.2 (C9), 21.1 (C10). **HRMS** (ESI positive): Calculated for C$_{10}$H$_{18}$N [M+H]$^+$ 152.1434 obtained 152.1437.

6.3.9 *N*-((6,6-Dimethylbicyclo[3.1.1]hept-2-en-2-yl)methyl)acrylamide (97)
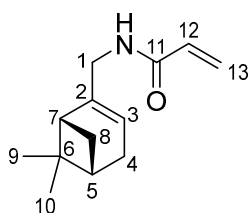
Amine **96** (1.52 g, 10.0 mmol) was dissolved in DCM (78 mL) and cooled to 0 °C. Triethylamine (2.80 mL, 20.0 mmol) was added dropwise. Acryloyl chloride (1.20 mL, 15.0 mmol) was added dropwise. The mixture was allowed to warm to room temperature and left stirring for 24 hours. The reaction was quenched with saturated aqueous sodium bicarbonate. The aqueous layer was extracted with DCM (100 mL). The organic layer was washed with water (3 x 100 mL), dried over anhydrous magnesium sulphate, filtered and the solvent removed under reduced pressure. Purification using column chromatography (30% ethyl acetate in petrol) gave acrylamide **97** as a yellow oil in (1.15 g, 5.6 mmol, 56%).

R$_f$ = 0.5 (50% ethyl acetate in petrol) ; **IR v$_{max}$** (cm^{-1}) 3293 (N-H), 2918, 1666 (C=O), 1503, 1382; **[α]$_D^{24.3}$** (c 0.80, CHCl$_3$) 27.35; **δ$_H$** (400 MHz, CDCl$_3$) 6.29 (1H, dd, *J* = 17.0, 1.5 Hz, 13-H$_a$), 6.12 (1H, dd, *J* = 17.0, 10.2 Hz, 12-H), 5.65 (1H, dd, *J* = 10.2, 1.5 Hz, 13-H$_b$), 5.64-5.55 (1H, br, NH), 5.42 (1H, dd, *J* = 1.5 Hz, 3-H), 3.93-3.82 (2H, m, 1-H$_2$), 2.40 (1H, ddd, *J* = 8.6, 5.6, 5.6 Hz, 8-H$_a$), 2.30-2.24 (2H, m, 4-H$_2$), 2.14-2.10 (1H, m, 5-H), 2.10-2.06 (1H, m, 7-H), 1.29 (3H, s, 9-H$_3$), 1.17 (1H, d, *J* = 8.6 Hz, 8-H$_b$), 0.84 (3H, s, 10-H$_3$); **δ$_C$** (101 MHz, CDCl$_3$) 165.4 (C11), 144.4 (C2), 130.9 (C13), 126.4 (C12), 118.8 (C3), 44.2 (C1), 44.1 (C5), 40.7 (C7), 38.0 (C6), 31.6 (C4), 31.1 (C8), 26.1 (C9), 21.1 (C10); **HRMS** (ESI positive): Calculated for C$_{13}$H$_{20}$NO [M+H]$^+$ 206.1539 obtained 206.1541, calculated for C$_{26}$H$_{39}$N$_2$O$_2$ [2M+H]$^+$ 411.3006 obtained 411.3008.

6.3.10 *N*-((1S,4S)-1,7,7-trimethylbicyclo[2.2.1]heptan-2-yl)acrylamide (108)
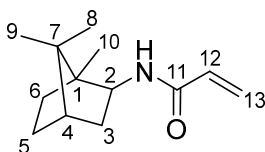
Camphene (34.06 g, 0.25 mmol) and BHT (275.0 mg, 0.5 mol%) were dissolved in acrylonitrile (250.0 mL) and stirring started. The solution was cooled to 0 °C and sulfuric acid (27.0 mL, 0.5 mol) was added dropwise over 2 hours. The solution was allowed to warm to room temperature and stirred for 4 hours. Saturated aqueous NaHCO$_3$ was added until pH 4 was reached upon which a cream solid precipitated. The solid was filtered under reduced pressure and dried to give acrylamide **108** as a white solid (41.91 g, 0.20 mol, 81 % yield).

m.p. = 139-140 °C; **IR** ν_{max} (cm^{-1}) 3329, 2950, 2877, 1667, 1623, 1535, 1458, 1410, 1239; **[α]$_D^{20.0}$** (c 0.80, CHCl$_3$) 5.37 ; **δ$_H$** (400 MHz, CDCl$_3$) 6.26 (1H, dd, J = 16.9, 1.5 Hz, 13-H$_a$), 6.08 (1H, dd, J = 16.9, 10.2 Hz, 12-H), 5.64 (1H, dd, J = 10.3, 1.5 Hz, 13-H$_b$), 5.47 (1H, s, NH), 4.02 (1H, td, J = 9.0, 5.0 Hz, 2-H), 1.92 (1H, dd, J = 13.3, 9.1 Hz, 3-H$_a$), 1.80 – 1.76 (1H, m, 5-H$_a$), 1.76 – 1.69 (1H, m, 4-H), 1.67 – 1.54 (2H, m, 3-H$_b$ and 6-H$_a$), 1.34 (1H, ddd, J = 12.6, 9.2, 3.6 Hz, 6-H$_b$), 1.20 (1H, ddd, J = 12.0, 9.3, 4.2 Hz, 5-H$_b$), 0.95 (3H, s, 8-H$_3$), 0.88 (3H, s, 10-H$_3$), 0.87 (3H, s, 9-H$_3$). **δ$_C$** (101 MHz, CDCl$_3$) 164.8 (C11), 131.3 (C12), 126.0 (C13), 56.8 (C2), 48.7 (C7), 47.2 (C1), 44.9 (C4), 39.2 (C3), 36.0 (C6), 27.0 (C5), 20.3 (C8), 20.3 (C9), 11.7 (C10); **HRMS** (ESI positive): Calculated for C$_{13}$H$_{22}$NO [M+H]$^+$ 208.1657 obtained 208.1696, calculated for C$_{13}$H$_{21}$NONa [M+Na]$^+$ 230.1521 obtained 230.1515.

6.3.11 α-Pinene Oxide[129] (52)
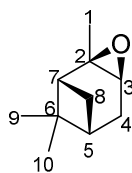
Both *m*CPBA (70-75%, 35.4 g, 150 mmol) and sodium hydrogen carbonate (16.0 g, 191 mmol) were dissolved in DCM (370 mL) and cooled to 0 °C. 1S-(-)-α-pinene (23 mL, 147 mmol) was dissolved in DCM (30 mL) and added dropwise over 50 minutes maintaining a temperature below 5 °C. The reaction mixture was left stirring at 0 °C for 1 hour. Sodium sulphite (16.35 g in 163.5 mL of water) was added. The reaction was stirred for a further 30 minutes. The organic layer was separated, washed with water three times, dried over MgSO$_4$, filtered and the solvent removed under reduced pressure to give α-pinene oxide **52** as a pale yellow oil (20.0 g, 131 mmol, 89%).

δ_H (400 MHz, CDCl$_3$) 3.09 (1H, dd, *J* = 4.2, 1.4 Hz, 3-H), 2.10 (4H, m, 4-H$_2$, 7-H, 8-H$_a$), 1.76-1.71 (1H, m, 5-H), 1.63 (1H, d, J = 8.7 Hz, 8-Hb), 1.36 (3H, s, 1-H3), 1.31 (3H, s, 9-H3), 0.95 (3H, s, 10-H3) ; δ_c (101 MHz, CDCl$_3$) 60.3 (C2), 56.9 (C3), 45.1 (C7), 40.5 (C6), 39.7 (C5), 27.6 (C4), 26.7 (C9), 25.9 (C8), 22.4 (C1), 20.2 (C10).[192,193]

6.3.12 *trans*-Sobrerol[129] (53)
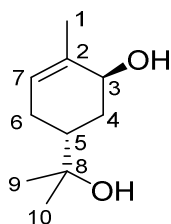
Carbon dioxide was bubbled through water (880 mL) for 30 minutes. (-)-α-Pinene oxide (500.0 g, 3.3 mol) was added in 50 mL aliquots over 60 minutes whilst vigorously stirring. The reaction was cooled to 0 °C. The reaction mixture was left vigorously stirring for 24 hours. The reaction was filtered and the white amorphous solid washed with minimum DCM. The filtrate was concentrated under reduced pressure and the solid washed with minimum DCM. The combined solids were used without further purification to give *trans*-sobrerol **53** (358.5 g, 2.1 mol, 63 %).

IR v_{max} (cm^{-1}) 3319, 3006, 2973, 2960, 2933, 2886, 2838, 1651 ; **δ_H** (400 MHz, CDCl$_3$) 5.59 (1H, dd, J = 5.4, 1.4 Hz, 3-H), 4.05 (1H, dd, J = 3.8, 2.2 Hz, 7-H), 2.20 – 2.09 (1H, m, 4-H$_a$), 2.04 (1H, dd, J = 13.4, 2.1 Hz, 6-H$_a$), 1.81 (3H, q, J = 1.5 Hz, 1-H$_3$), 1.78 (1H, m, 4-H$_b$) 1.76 (1H, m, 5-H), 1.42 (1H, td, J = 13.4, 3.8 Hz, 6-H$_b$), 1.23 (3H, s, 9-H$_3$), 1.19 (3H, s, 10-H$_3$) ; **δ_C** (101 MHz, CDCl$_3$) 134.4 (C2), 125.3 (C3), 72.3 (C8), 68.6 (C7), 38.8 (C5), 32.7 (C6), 27.8 (C9), 27.2 (C4), 26.2 (C10), 20.9 (C1) ; **HRMS** (ESI negative): Calculated for C$_{10}$H$_{16}$O [M+Na-2H] 191.1054 obtained 190.9287.[193]

6.3.13 *N*-(2-(5-Hydroxy-4-methylcyclohex-3-en-1-yl)propan-2-yl)acrylamide (121)
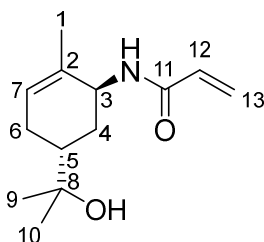
Both BHT (11 mg, 0.5 mol%) and *trans*-sobrerol (1.70 g, 10 mmol) were dissolved in acrylonitrile (100 mL). The reaction mixture was cooled to 0 °C and concentrated H_2SO_4 (98%, 0.53 mL, 10 mol%) was added dropwise. The solution was left stirring for 24 hours. Water (80 mL) was added before the aqueous layer was extracted with ethyl acetate (3 x 15 mL). The organic layers were combined and washed with water (3 x 20 mL), dried over anhydrous magnesium sulfate, filtered and the solvent removed under reduced pressure. The pale yellow solid was washed with ethyl acetate to give acrylamide **121** as a white solid (1.85 g, 8.3 mmol, 83%).

m.p. = 153-154 °C; **IR v_{max}** (cm^{-1}) 3349 (O-H), 3248 (N-H), 3042 (C=CH), 2968, 2929, 1657 (C=O), 1618, 1531; $[\alpha]_D^{24.1}$ +2.51° (c 0.80, CHCl$_3$); **δ_H** (400 MHz, CDCl$_3$) 6.31 (1H, dd, *J* = 17.0, 1.4 Hz, 13-H$_a$), 6.10 (1H, dd, *J* = 17.0, 10.2 Hz, 12-H), 5.67 (1H, dd, *J* = 10.2, 1.4 Hz, 13-H$_b$), 5.65 – 5.57 (1H, m, 3-H), 5.60 (1H, d, *J* = 8.4 Hz, NH), 4.56-4.52 (1H, m, 7-H), 2.20-2.12 (1H, m, 4-H$_a$), 2.03-1.99 (1H, m, 6-H$_a$), 1.89-1.80 (1H, m, 4-H$_b$), 1.72 (3H, m, 1-H$_3$), 1.58-1.50 (1H, m, 5-H), 1.48-1.44 (1H, m, 6-H$_b$), 1.20 (3H, s, 10-H$_3$), 1.19 (3H, s, 9-H$_3$) ; **δ_c** (101 MHz, CDCl$_3$) 165.0 (C11), 132.4 (C2), 131.0 (C12), 126.5 (C13), 126.2 (C3), 72.2 (C8), 48.0 (C7), 39.9 (C5), 30.3 (C6), 27.2 (C9/C10), 26.8 (C4), 20.9 (C1); **HRMS** (ESI positive): Calculated for C$_{13}$H$_{21}$NO$_2$Na [M+Na]$^+$ 246.1470 obtained 246.1464.

6.3.14 Pinol[130,193] (122)
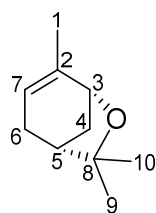
BHT (11 mg, 0.5 mol%) and *trans*-sobrerol (1.7 g, 10 mmol) were dissolved in acrylonitrile (20 mL) and the solution was vigorously stirred for 5 minutes. Concentrated H_2SO_4 (98%, 0.1 mL, 20 mol%) was added dropwise and the solution was left stirring under an argon atmosphere for 48 hours. Aqueous sodium hydroxide (1M, 25 mL) was added before the aqueous layer was extracted with ethyl acetate (3 x 15 mL). The organic layers were combined and dried over anhydrous magnesium sulfate, filtered and the solvent removed under reduced pressure. Purification using column chromatography (20% ethyl acetate in petrol, then 10% methanol in dichloromethane) gave pinol **122** as a pale yellow oil (0.30g, 2.0 mmol, 20%).

IR v_{max} (cm^{-1}) 3273, 2966, 2931, 2879, 2855, 1656; **δ_H** (400 MHz, CDCl$_3$) 5.18-5.14 (1H, m, 3-H), 4.01-3.87 (1H, m, 7-H), 2.24-2.14 (3H, m, 4-H$_2$ and 6-H$_a$), 2.12-2.06 (1H, m, 5-H), 1.81 (1H, d, *J* = 10.6 Hz, 6-H$_b$), 1.70-1.64 (3H, m, 1-H$_3$), 1.28 (3H, s, 9-H$_3$), 1.17 (3H, s, 10-H$_3$) ; **δ_C** (101 MHz, CDCl$_3$) 139.5 (C2), 120.2 (C3), 82.7 (C8), 76.6 (C7), 41.8 (C5), 34.6 (C6), 30.4 (C10), 30.4 (C4), 25.4 (C9), 21.4 (C1).[193]

6.3.15 *N*-((1S,5R)-2-methyl-5-(prop-1-en-2-yl)cyclohex-2-en-1-yl)acrylamide[138] (123)

1
2
7
3
H
N
11
12
13
6
5
4
O
8
10
9
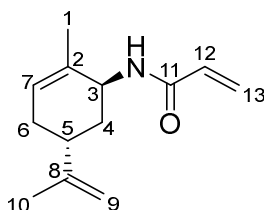
(-)-Carveol (1.6 mL, 10 mmol) was dissolved in acrylonitrile (20 mL). BHT (11 mg, 0.5 mol%) was added and stirring started. The reaction mixture was cooled to 0 °C. Sulfuric acid (0.13 mL, 2.5 mmol) was added dropwise. The reaction mixture was allowed to warm to room temperature and stirred at room temperature for 2 hours. Water (20 mL) and ethyl acetate were added and the organic layer washed with water (3 x 20 mL). The combined aqueous layers were extracted with ethyl acetate (2 x 20 mL). The combined organics were dried over anhydrous magnesium sulphate, filtered and the solvent removed under reduced pressure which gave acrylamide **123** as a colourless solid in (1.99 g, 9.7 mmol, 97%).

m.p. = 106-108 °C ; **R$_f$** = 0.15 (20% ethyl acetate in petrol) ; **IR v$_{max}$** (cm^{-1}) 3264 (N-H), 2916 (C-H), 1653 (C=O), 1618 (C=C), 1531, 1407, 1236; **[α]$_D^{20.5}$** (c 0.80, CHCl$_3$) -3.38 ; **δ$_H$** (400 MHz, CDCl$_3$) 6.30 (1H, dd, J = 16.9, 1.5 Hz, 13-H$_a$), 6.09 (1H, dd, J = 16.9, 10.3 Hz, 12-H), 5.67-5.56 (2H, m, 13-H$_b$ and 7-H), 5.64 – 5.50 (1H, br, NH), 4.75-4.71 (2H, m, 9-H$_2$), 4.52–4.49 (1H, m, 3-H), 2.19 – 2.07 (2H, m, 4-H$_a$ and 5-H), 1.98-1.92 (1H, m, 6-H$_a$), 1.91-1.85 (1H, m, 4-H$_b$), 1.72 (3H, m,1-H$_3$), 1.73 – 1.71 (3H, m, 10-H$_3$), 1.68-1.63 (1H, m, 6-H$_b$) ; **δ$_C$** (101 MHz, CDCl$_3$) 164.9 (C11), 148.6 (C2), 132.4 (C8), 131.0 (C12), 126.5 (C13), 126.3 (C7), 109.3 (C9), 47.9 (C3), 36.3 (C5), 34.0 (C6), 30.8 (C4), 20.9 (C10), 20.8 (C1) ; **HRMS** (ESI positive): Calculated for C$_{13}$H$_{20}$NO [M+H]$^+$ 206.1539 obtained 206.1538.

6.3.16 *N*-(2-(4-methyl-5-oxocyclohex-3-en-1-yl)propan-2-yl)acrylamide (131)
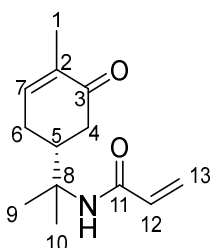
Carvone (1.6 mL, 10 mmol) and BHT (11 mg) were dissolved in acrylonitrile (10 mL) and cooled to 0 °C. Sulfuric acid (1.12 mL) was added dropwise. The reaction was left to warm to room temperature and stirred for 16 hours. The reaction was cooled to 0 °C, NaHCO$_3$ (sat. aq.) was added and the reaction stirred for 30 minutes. The solid was filtered under reduced pressure and dried to give *N*-carvone acrylamide **131** as a white solid (1.7 g, 7.7 mmol, 77 % yield).

IR ν$_{max}$ (cm^{-1}) 3253, 3063, 2964, 2936, 1673, 1651, 1626; **δ$_H$** (400 MHz, CDCl$_3$) 6.76 (1H, d, *J* = 6.1 Hz, 7-H), 6.24 (1H, d, *J* = 16.7 Hz, 13-H$_a$), 6.05 (1H, dd, *J* = 16.9, 10.2 Hz, 12-H), 5.62 (1H, d, *J* = 10.0 Hz, 13-H$_b$), 5.39 (1H, s, NH), 3.03 – 2.95 (1H, m, 5-H), 2.54 (1H, dd, *J* = 15.8, 3.9 Hz, 4-H$_a$), 2.42-2.35 (1H, m, 6-H$_a$), 2.21-2.13 (2H, m, 4-H$_b$, 6-H$_b$), 1.77 (3H, s, 1-H$_3$), 1.38 (6H, d, *J* = 3.4 Hz, 9-H$_3$, 10-H$_3$); **δ$_C$** (101 MHz, CDCl$_3$) 199.7 (C3), 164.8 (C11), 144.9 (C2), 135.4 (C7), 131.5 (C12), 126.3 (C13), 55.8 (C8), 41.3 (C5), 39.7 (C4), 27.6 (C6), 24.5 (C9), 24.2 (C10), 15.6 (C1). **HRMS** (ESI positive): Calculated for C$_{13}$H$_{19}$NO$_2$Na [M+Na]$^+$ 244.1313 obtained 244.1309.

6.3.17 *N*-(2-(4-methyl-2-oxocyclohexyl)propan-2-yl)acrylamide[139] (136)
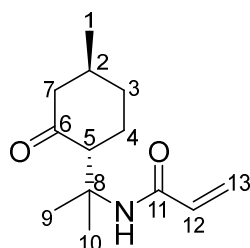
Pulegone (8 mL) and BHT (55 mg) were dissolved in acrylonitrile (50 mL) and the reaction mixture cooled to 0 C. Sulfuric acid (5.6 mL) was added dropwise. The reaction was allowed to warm to room temperature and stirred for 48 hours. The reaction was cooled to 0 °C and NaHCO$_3$ (sat. aq.) was added. Ethyl acetate added and the layers separated. The aqueous layers were extracted with ethyl acetate three times. The combined organics were dried over anhydrous NaSO$_4$, filtered, and the solvent removed under reduced pressure. Purification by column chromatography (0-30 % ethyl acetate in petrol) gave *N*-pulegone acrylamide **136** as a pale yellow solid (6.5 g, 29 mmol, 58 % yield).

IR v$_{max}$ (cm^{-1}) 3292, 2949, 2926, 2864, 1705, 1657; **δ$_H$** (400 MHz, CDCl$_3$) 6.19 (1H, d, J = 16.9 Hz, 13-H$_a$), 6.03 (1H, dd, J = 16.9, 10.1 Hz, 12-H), 5.89 (1H, s, NH), 5.57 (1H, d, J = 10.1 Hz, 13-H$_b$), 3.36 (1H, dd, J = 12.6, 5.1 Hz, 5-H), 2.30-2.25 (1H, m, 3-H$_a$), 2.20 − 2.01 (2H, m, 3-H$_b$, 6-H$_a$), 1.95 − 1.77 (2H, m, 2-H, 7-H$_a$), 1.58 − 1.36 (8H, m, 6-H$_b$, 7-H$_b$, 9-H$_3$, 10-H$_3$), 1.02 (3H, d, *J* = 6.4, 1-H$_3$); **δ$_C$** (101 MHz, CDCl$_3$) 211.9 (C4), 164.9 (C11), 132.1 (C12), 125.5 (C11), 55.0 (C5), 54.8 (C8), 51.7 (C3), 36.0 (C2), 34.1 (C7), 28.6 (C6), 25.6 (C9), 24.4 (C10), 22.3 (C1); **HRMS** (ESI positive): Calculated for C$_{13}$H$_{21}$NO$_2$Na [M+Na]$^+$ 246.1470 obtained 246.1462.

6.3.18 *N*-(2-(5-acrylamido-4-methylcyclohex-3-en-1-yl)propan-2-yl)acrylamide (124)
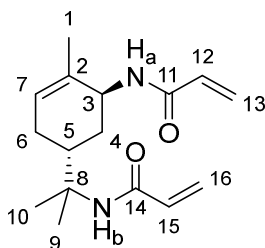
Carveol (1.6 mL, 10 mmol) was dissolved in acrylonitrile (20 mL). BHT (11 mg) was added and stirring started. The reaction mixture was cooled to 0 °C. Sulfuric acid (1.12 mL) was added dropwise. The reaction mixture was allowed to warm to room temperature stirred at room temperature for 2 hours. NaHCO$_3$ (sat aq.) and ethyl acetate were added and the organic layer separated. The aqueous layer was extracted with ethyl acetate twice. The combined organics were dried over anhydrous NaSO$_4$, filtered and the solvent removed under reduced pressure to give a cream solid. The solid was washed with ethyl acetate to give *N*-carveol bisacrylamide **124** as a white solid (1.7 g, 0.62 mmol, 62 % yield).

IR v$_{max}$ (cm^{-1}) 3277, 1655, 1615, 1530, 1405, 1247; **[α]$_D^{20.5}$** (c 0.80, CHCl$_3$) -10.82 ; **δ$_H$** (400 MHz, CDCl$_3$) 6.27 (1H, dd, J = 17.0, 1.5 Hz, 13-H$_a$), 6.19 (1H, dd, J = 16.8, 1.6 Hz, 16-H$_a$), 6.11 (1H, J = 17.0, 10.3 Hz, 12-H), 6.02 (1H, dd, J = 16.8, 10.1 Hz, 15-H), 5.83 (1H, d, J = 9.0 Hz, NH$_a$), 5.63 (1H, dd, J = 10.2, 1.5 Hz, 13-H$_b$), 5.61-5.59 (1H, m, 7-H), 5.57 (1H, dd, J = 10.1, 1.6 Hz, 16-H$_b$), 5.33 (1H, s, NH$_b$), 4.77-4.38 (1H, m, 3-H), 2.69 (1H, tdd, J = 13.6, 4.8, 2.1 Hz, 5-H), 2.13-1.98 (1H, m, 6-H$_a$), 1.85 (dq, J = 13.1, 2.1 Hz, 4-H$_a$), 1.79 (1H, ddt, J = 9.9, 4.9, 2.2 Hz, 6-H$_b$), 1.76-1.68 (3H, m, 1-H$_3$), 1.44 (1H, td, J = 13.2, 4.5 Hz, 4-H$_b$), 1.34 (3H, s, 9-H3), 1.27 (3H, s, 10-H3) ; δC (101 MHz, CDCl$_3$) 165.3 (C11), 164.8 (C14), 132.9 (C2), 131.7 (C15), 131.2 (C12), 126.1 (C13), 126.0 (C7 and C16), 56.4 (C8), 48.2 (C3), 34.6 (C5), 30.8 (C4), 27.0 (C6), 24.5 (C9), 24.0 (C10), 20.8 (C1); **HRMS** (ESI positive): Calculated for C$_{16}$H$_{25}$N$_2$O$_2$ [M+H]+ 277.1871 obtained 277.1909, calculated for [M+Na]+ 299.1735 obtained 299.1728.

6.3.19 (5R)-5-(1-((2-hydroxyethyl)thio)propan-2-yl)-2-methylcyclohex-2-en-1-ol (138)
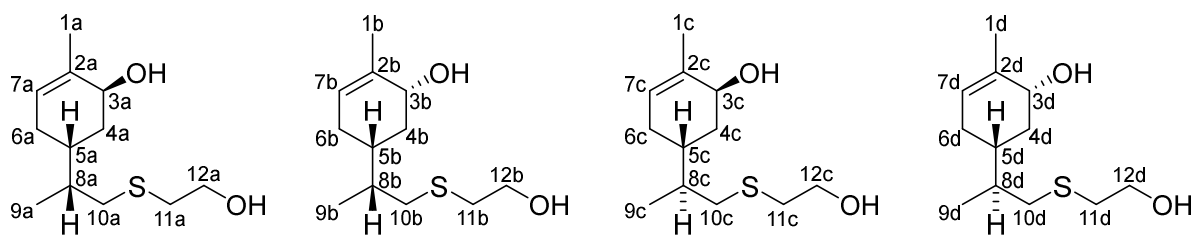
Carveol (1.6 mL, 10 mmol) and mercaptoethanol (0.8 mL) were degassed under vacuum using three freeze, pump, thaw cycles. The reaction was then left under vacuum and stirred at room temperature for 24 hours. The reaction mixture was purified via column chromatography (20-40 % ethyl acetate in petrol) to give thiol **138** (1:1:1:1) as a pale yellow oil (1 g, 4.5 mmol, 45 %).

IR ν_{max} (cm^{-1}) 3337.08, 2958.10, 2912.00, 2875, 1703, 1658; **δ_H** (400 MHz, CDCl$_3$) 5.55 (1H, dt, J = 5.2, 1.7 Hz, 7-H), 5.45 (1H, dt, J = 5.4, 1.8 Hz, 7-H), 4.27 – 4.09 (1H, m, 3-H), 3.98 (1H, d, J = 3.8 Hz, 3-H), 3.71 (2H, t, J = 6.1 Hz, 12-H$_2$), 2.81 – 2.69 (2H, m, 11-H), 2.67 – 2.53 (1H, m, 10-H), 2.48 – 2.33 (1H, m, 10-H), 2.20 – 1.55 (7H, m, 1-H$_3$, 5-H, 6-H$_2$, 8-H), 1.40 (1H, dtd, J = 26.3, 13.3, 3.9 Hz, 4-H), 1.31 – 1.12 (1H, m, 4-H), 1.06 – 0.88 (3H, m, 9-H$_3$); **δ_C** (101 MHz, CDCl$_3$) 136.6 (C2), 136.5 (C2), 134.6 (C2), 134.5 (C2), 125.4 (C7), 125.2 (C7), 123.8 (C7), 123.7 (C7), 71.0 (C3) , 71.0 (C3), 68.5 (C3), 68.4 (C3), 60.4 (C12), 37.6 (C10), 37.6 (C10), 37.5 (C10), 37.4 (C10), 37.2 (C8), 37.2 (C8), 37.0 (C8), 37.0 (C8), 37.0 (C2), 36.8 (C2), 36.0 (C2), 35.8 (C2), 35.8 (C4), 35.7 (C4), 35.6 (C4), 33.8 (C4), 31.6 (C5), 31.4 (C5), 29.9 (C6), 29.8 (C6), 27.6 (C6), 27.6 (C6), 20.9 (C1), 18.8 (C1), 16.0 (C9), 16.0 (C9), 15.7 (C9), 15.6 (C9); **HRMS** (ESI positive): Calculated for C$_{24}$H$_{44}$O$_4$S$_2$Na [2M+Na]+ 483.2573 obtained 483.2578.

6.3.1 *N*-((2S,4S)-1-methyl-4-((*R*)-2-methyloxiran-2-yl)-7-oxabicyclo[4.1.0]heptan-2-yl)acrylamide (139)
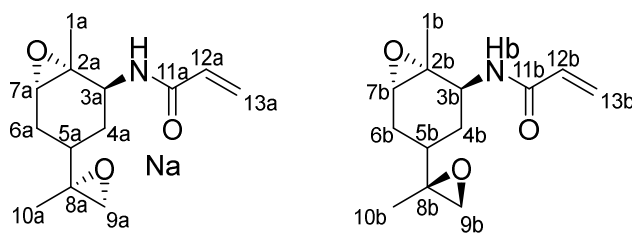
Acrylamide **139** (2.05 g, 10.0 mmol) and NaHCO$_3$ (0.92 g, 11.0 mmol) were dissolved in DCM (200 mL). The solution was cooled to 0 °C. *m*CPBA (70-75%, 2.54 g, 10.5 mmol) was dissolved in DCM (50 mL) and added dropwise to the solution whilst stirring. After 6 hours, the reaction was cooled to 0 °C and *m*CPBA (70-75%, 2.54 g, 10.5 mmol) dissolved in DCM (50 mL) was added dropwise. The reaction was left stirring at room temperature for 22 hours. The reaction was quenched with a solution of saturated aqueous Na$_2$SO$_3$. The organic layer was separated and washed three times with aqueous NaHCO$_3$ (5 %), dried over anhydrous MgSO$_4$, filtered and the solvent removed under reduced pressure to give *N*-carveol bisacrylamide **139** (1:1) as a colourless oil (2.27 g, 9.6 mmol, 96 %).

IR v$_{max}$ (cm^{-1}) 3293, 2973, 2925, 1657, 1625; **[α]$_D^{20.2}$** (c 0.80, CHCl$_3$) 0.95 ; **δ$_H$** (400 MHz, CDCl$_3$) 6.33 (2H, dd, J = 17.0, 1.4 Hz, 13-Ha$_a$ and 13-Hb$_a$), 6.13 (2H, ddd, J = 16.9, 10.2, 3.0 Hz, 12-Ha and 12-Hb), 6.08 (2H, d, J = 7.9 Hz, NHa and NHb), 5.68 (2H, apparent dt, J = 10.2, 1.3 Hz, 13-Ha$_b$ and 13-Hb$_b$), 4.48 (2H, m, 3-Ha and 3-Hb), 3.24 (2H, dt, J = 11.7, 2.1 Hz, 7-Ha and 7-Hb), 2.71 – 2.48 (4H, m, 9-Ha$_2$ and 9-Hb$_2$), 2.19 (2H, m, 6-Ha$_a$ and 6-Hb$_a$), 1.74 – 1.67 (2H, m, 4-Ha$_a$ and 4-Hb$_a$), 1.67 – 1.56 (2H, m, 6-Ha$_b$ and 6-Hb$_b$), 1.51 (2H, ddddd, J = 24.6, 11.4, 3.7, 2.2 Hz, 5-Ha and 5-Hb), 1.37 (3H, s, 1-Ha$_3$ or 1-Hb$_3$), 1.37 (3H, s, 1-Ha$_3$ or 1-Hb$_3$), 1.45-1.27 (2H, m, 4-Ha$_b$ and 4-Hb$_b$), 1.25 (3H, s, 10-Ha$_3$ or 10-Hb$_3$), 1.23 (3H, s, 10-Ha$_3$ or 10-Hb$_3$) ; **δ$_C$** (101 MHz, CDCl$_3$) 165.0 (C11a and C11b), 130.7 (C12a or C12b), 130.7 (C12a or C12b), 126.8 (C13a and C13b), 62.0 (C7a or C7b), 61.7 (C7a or C7b), 59.0 (C2a or C2b), 58.8 (C2a or C2b), 58.3 (C8a and C8b), 53.0 (C9a or C9b), 52.7 (C9a or C9b), 46.6 (C3a or C3b), 46.4 (C3a or C3b), 31.6 (C5a or C5b), 31.3 (C5a or C5b), 31.1 (C4a or C4b), 30.7 (C4a or C4b), 27.1 (C6a or C6b), 27.0 (C6a or C6b), 22.2 (C1a or C1b), 22.0 (C1a or C1b), 18.6 (C10a or C10b), 18.3 (C10a or C10b); **HRMS** (ESI positive): Calculated for C$_{13}$H$_{19}$NO$_3$Na [M+Na]$^+$ 260.1263 obtained 260.1262.

6.4 Polymer Synthesis

6.4.1 Poly(*N*-(6,6-dimethyl-2-methylenebicyclo[3.1.1]heptan-3-yl)acrylamide) (141)
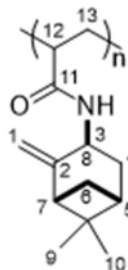
Acrylamide **95** (230 mg, 1.1 mmol) was dissolved in THF (0.4 mL). AIBN (1.2 mg, 0.5 wt%) was dissolved in THF (0.1 mL) and added to the reaction mixture. The reaction was degassed using five freeze, pump, thaw cycles and then filled with argon and sealed. The reaction mixture was heated to 60 °C and left stirring for 24 hours. After which the mixture was cooled to room temperature and added dropwise to hexane to give a red solid.

6.4.2 Poly((6,6-dimethylbicyclo[3.1.1]hept-2-en-2-yl)methyl)acrylamide (142)
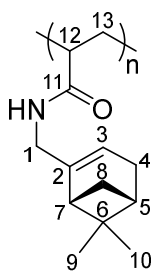
Acrylamide **100** (80 mg, 0.39 mmol) was gradually dissolved in THF (0.2 mL) over an hour. AIBN (0.8 mg, 1.0 wt%) was dissolved in THF (0.1 mL) and added to the reaction mixture. The reaction mixture was degassed using five freeze, pump, thaw cycles and then filled with argon and sealed. The reaction mixture was heated to 60 °C and left stirring for 24 hours. After which the mixture was cooled to room temperature to give polymer **102** (60% conversion). Polymer **102** was purified by dissolving in the minimum amount of THF, precipitated in methanol, filtered and dried at room temperature to give a yellow solid (82% conversion by ^{1}H NMR).

$δ_H$ (400 MHz, CDCl$_3$) 6.30 (br, 12-H, 13-H$_2$), 5.31 (br, NH, 3-H) 2.31 (br, 1-H$_2$, 4-H$_2$), 2.17 (br, 5-H$_2$), 1.97 (br, 7-H), 1.16 (br, 8-H$_2$), 0.77 (br, 9-H$_3$, 10-H$_3$).

Conditions	Conversion by 400 MHz ^{1}H NMR (%)	M_n (kDa)	M_p (kDa)	M_w (kDa)	Polydispersity (Mw/Mn)	T_g (°C)
1g monomer, THF, AIBN 0.5wt%	83	25.4	19.3	29.6	1.163	91.6
1g monomer, THF, AIBN 0.5wt%	>99	10.5	11.1	15.1	1.429	150.0
1g monomer, THF, AIBN 0.5wt%, DDM 5wt%	97	11.4	12.2	14	1.234	139.6
1g monomer, THF, AIBN 0.5wt%, DDM 1wt%	98	10.5	13.3	24.4	2.318	-

6.4.3 Poly(*N*-((1S,4S)-1,7,7-trimethylbicyclo[2.2.1]heptan-2-yl)acrylamide) (143)
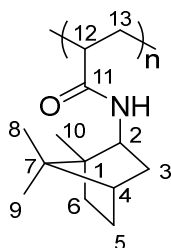
Isobornyl acrylamide (230 mg, 1.2 mmol) was dissolved in THF (2 mL). AIBN (1.2 mg, 0.5 wt%) was dissolved in THF (0.1 mL) and added to the reaction mixture. The reaction was degassed using five freeze, pump, thaw cycles and then filled with argon and sealed. The reaction mixture was heated to 60 °C and left stirring for 22 hours. After which the mixture was cooled to room temperature. The reaction mixture was added to methanol and the precipitate filtered to give poly(isobornyl acrylamide) as a white powder (93% conversion by ^{1}H NMR).

δ_H (400 MHz, CDCl$_3$) 6.26 (br, 12-H, 13-H$_2$), 3.77 (br, 2-H), 1.59 (br, 3-H$_2$), 1.43 (br, 4-H), 1.12 (br, 6-H$_2$), 1.01 (br, 5-H$_2$), 0.85 (br, 10-H$_3$)., 0.71 (br, 8-H$_3$, 9-H$_3$).

Conditions	Conversion by 400 MHz ^{1}H NMR (%)	M_n (kDa)	M_p (kDa)	M_w (kDa)	Polydispersity (Mw/Mn)	T_g (°C)	Decomp. Temp. (°C)
0.25g monomer, THF, AIBN 0.5 wt%	>99	11.1	15.4	17.4	1.562	-	-
1g monomer, THF, AIBN 0.5 wt%	93	11.8	12.9	17.3	1.463	203.3	436
1g monomer, THF, AIBN 0.5 wt%, DDM 0.5wt%	97	7.9	10	11.9	1.507	196.2	-
1g monomer, THF, AIBN 0.5 wt%, DDM 1wt%	>99	14.8	16	18.3	1.236	206.0	-
1g monomer, THF, AIBN 0.5 wt%, DDM 5wt%	>99	6.5	9.3	9.2	1.414	188.1	-
1g monomer, THF, AIBN 0.1 wt%	96	12.2	14	16.6	1.363	213.1	-
1g monomer, THF, AIBN 0.25 wt%	97	12.7	14.9	17.8	1.397	211.0	-
1g monomer, THF, AIBN 0.5wt% + 25% ^{t}BuOH	>99	25	39.5	43.9	1.758	-	-
1g monomer, cyclohexanone, AIBN 0.5 wt%	94	15.4	22.3	27.3	1.779	190.0	-

1g monomer, ethanol, AIBN 0.5 wt%	98	32.3	53.1	59.5	1.842	203.0	-
1g monomer, THF, AIBN 0.5wt%	>99	16.6	25.2	30	1.812	188.7	-
0.25g monomer, ethanol, AIBN 0.5wt%	98	32.3	53.1	59.5	1.84	-	-
5g monomer, ethanol, AIBN 0.5wt%	99	37.3	54.8	64.8	1.736	-	-
20g monomer, redox		32.9	64.8	86.9	2.638	-	-
1g monomer IPA	>99	14.2	42.6	45.6	3.202	-	-
1g monomer pentanol	>99	62.3	99.3	126.8	2.035	-	-
20g monomer, redox emulsion, TBPB 3wt%, Ascorbic acid 6wt%, 50 °C, Span80 6wt%	-	0	0	0	0	-	-
20g monomer, TBPB 3wt%, Ascorbic acid 6wt%, 50 °C, SDS 3wt%, Span80 3wt%	-	0	0	0	0	-	-
20g monomer TBPB 3wt%, Ascorbic acid 6wt%, 50 °C SDS 1.5 wt%, Span80 4.5 wt%	-	0	0	0	0	-	-
20g monomer, IPA, AIBN 2wt%, 85 °C, 30% active weight	-	4.8	8.4	19.23	4	-	-
20g monomer, IPA, AIBN 2wt%, 85 °C, 22.5% active weight	-	3.5	6.4	28	7.9	-	-
20g monomer, pentanol, AMBN 2wt%, 85 °C, 22% active weight	-	6.4	10.3	41.5	6.53	-	-
20g monomer, water, TBHP/Bruggolite 6wt%, 30-90 °C, 30% active weight	-	6.7	11.1	12.7	1.85	-	-
20g monomer, pentanol, TBPB/Ascorbic acid 6wt%, 50-80 °C, 30% active weight	-	28.5	54.9	70.1	2.46	-	-
20g monomer, pentanol, TBPB/Ascorbic acid 6wt%, 45-85 °C, 30% active weight	-	32.9	-	86.9	2.64	-	-

6.4.4 Poly(*N*-(2-(5-hydroxy-4-methylcyclohex-3-en-1-yl)propan-2-yl)acrylamide) (144)
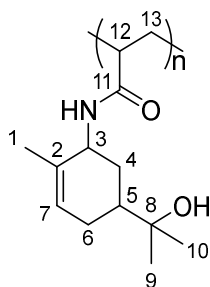
trans-Sobrerol acrylamide (745 mg, 3.36 mmol) was gradually dissolved in THF (12 mL) over an hour. AIBN (3.75 mg, 0.5 wt%) was added to the reaction mixture. The reaction mixture was degassed using three freeze, pump, thaw cycles and then filled with nitrogen and sealed. The reaction mixture was heated to 60°C and left stirring for 24 hours. After which the mixture was cooled to room temperature to give polymer. Poly(trans-sobrerol acrylamide) was purified by dissolving in the minimum amount of THF, precipitated in methanol (10 mL), filtered and dried at room temperature to give the poly(*trans*-sobrerol acrylamide) as a white powder (98% conversion by ^{1}H NMR).

δ_H (400 MHz, CDCl$_3$) 5.59 (br, 12-H, 13-H$_2$), 4.33 (br, 3-H, 7-H), 2.03 (br, 4-H$_2$, 6-H$_a$), 1.75 (br, 1-H$_3$), 1.69 (br, 5-H, 6-H$_b$), 1.16 (br, 9-H$_3$, 10-H$_3$).

Conditions	Conversion by 400 MHz ^{1}H NMR (%)	M_n (kDa)	M_p (kDa)	M_w (kDa)	Polydispersity (Mw/Mn)	T_g (°C)
0.25g monomer, THF, AIBN 0.5wt%	>99	19.9	22.1	27.1	1.362	-
0.25g monomer, THF, AIBN 0.5wt%	>99	40.4	40.3	48.9	1.21	201.7
1g monomer, THF, AIBN 0.5wt%, 0.5wt% DDM	>99	28.7	30	34.4	1.199	200.6
1g monomer, THF, AIBN 0.5wt%, 1wt% DDM	>99	23.5	25.8	28.3	1.204	199.0
1g monomer, THF, AIBN 0.5 wt%, 5wt% DDM	>99	8.7	11	10.9	1.255	184.1

1g monomer, AIBN 0.5wt%, ethanol	>99	40.2	53	60.6	1.506	-
20g monomer, pentanol, TBPB 6wt%, ascorbic acid 3wt%, 30 °C	>99	0	0	0	0	-
20g monomer, pentanol, TBPB 6wt%, ascorbic acid 3wt%, 40 °C	>99	9.6	14.8	19.2	1.998	-
5g monomer, THF, AIBN 0.5wt%	49	50.8	58.3	68.4	1.34	-
5g monomer, pentanol, AMBN 2wt%, 85 °C 37%, active weight	-	10.6	27.9	42.9	4.03	-
5g monomer, water, TBPB/Bruggolite 6wt%, 30-90 °C, 30% active weight	-	22.2	44.8	68.6	3.08	-
5g monomer, pentanol, TBPB/Ascorbic acid 6wt%, 50-85 °C, 30% active weight	-	28.8	58.2	70	2.43	-

6.4.5 Poly(*N*-((1S,5R)-2-methyl-5-(prop-1-en-2-yl)cyclohex-2-en-1-yl)acrylamide (145)
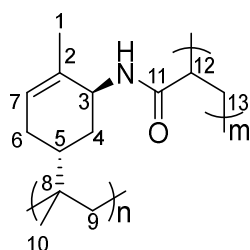
Carveol acrylamide (0.25 g, 1.2 mmol) was dissolved in THF (0.9 mL). AIBN (1.4 mg, 0.5 wt%) was dissolved in THF (0.1 mL) and added to the reaction mixture. Freeze, pump, thaw was used until no bubbles were observed. The reaction was heated to 60 °C and stirred for 22 hours. The solution was cooled to room temperature and added dropwise to water. The precipitate was filtered to give poly(carveol acrylamide) as a white powder (41% conversion by ^{1}H NMR).

δ_H (400 MHz, CDCl$_3$) 6.28 (m, 12-H$_a$), 6.10 (m, 13-H$_2$), 5.57 (br, 12-H$_b$), 4.67 (m, 9-H$_2$), 4.45 (m, 3-H), 2.09 (m, 4-H$_2$, 1-H$_3$), 1.84 (m, 5-H, 6-H$_b$), 1.59 (m, 10-H$_3$).

Conditions	Conversion by 400 MHZ ^{1}H NMR (%)	M_n (kDa)	M_p (kDa)	M_w (kDa)	Polydispersity (Mw/Mn)	T_g (°C)
0.25g monomer, THF, AIBN 0.5 wt%	66	1.9	2.1	2.9	1.509	-
0.25g monomer, THF, AIBN 0.5 wt%	67	3.2	2.5	5.3	1.672	105.4
1g monomer, ethanol, AIBN 0.5 wt%	50	2.5	2.5	3.6	1.429	-

6.4.1 Poly(*N*-((2S,4S)-1-methyl-4-((*R*)-2-methyloxiran-2-yl)-7-oxabicyclo[4.1.0]heptan-2-yl)acrylamide) (146)
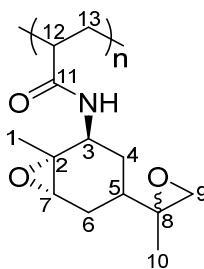
Bisepoxide acrylamide (230 mg, 1.1 mmol) was dissolved in THF (2 mL). AIBN (1.2 mg, 0.5 wt%) was dissolved in THF (0.1 mL) and added to the reaction mixture. The reaction was degassed using five freeze, pump, thaw cycles and then filled with argon and sealed. The reaction mixture was heated to 60 °C and left stirring for 22 hours. After which the mixture was cooled to room temperature. The reaction mixture was added dropwise to hexane and the precipitate filtered to give poly(bisepoxide acrylamide) as a white solid (94% conversion by ^{1}H NMR).

δ_H (400 MHz, CDCl$_3$) 6.77 (br, 12-H, 13-H$_2$), 4.38 (br, 3-H), 3.08 (br, 9-H$_2$), 2.37 (br, 7-H), 1.59 (br, 4-H$_2$), 1.30 (br, 1-H$_3$), 1.19 (br, 5-H$_2$, 6-H$_2$, 10-H$_3$).

Conditions	Conversion by 400 MHz ^{1}H NMR (%)	M_n (kDa)	M_p (kDa)	M_w (kDa)	Polydispersity (Mw/Mn)
0.25g monomer, THF, AIBN 0.5 wt%	94	5.9	10.6	9.6	1.639
1g monomer, THF, AIBN 0.1wt%	>99	4.9	11.1	9.8	2.015
1g monomer, THF, AIBN 0.1wt%, DDM 0.5 wt%	>99	4.1	4.1	6.4	1.565
1g monomer, cyclohexanone/THF (1:1), AIBN 0.5wt%	97	23.1	25.5	31	1.341
1g monomer, THF +25% ^{t}BuOH, AIBN 0.5wt%	-	7.8	9.6	11.8	1.506
1g monomer, THF + 25% ^{t}BuOH, AIBN 0.5wt%	91	32.6	46.9	43.5	1.334
1g monomer, cyclohexanone, AIBN 0.5wt%	>99	22.1	26.1	32	1.449
1g monomer, ethanol, AIBN 0.5wt%	>99	30.7	55.2	47.1	1.531
4g monomer, ethanol, AIBN 0.5wt%	>99	36.7	42.1	41	1.117

6.4.2 Poly(2-methyl-*N*-(2-((*R*)-4-methyl-5-oxocyclohex-3-en-1-yl)propan-2-yl)butanamide) (147)
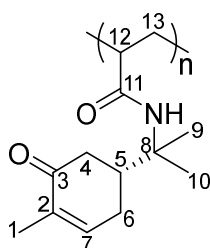
Carvone acrylamide (250 mg, 1.1 mmol), dodecanethiol (5 µL) and V88 (1.2 mg, 0.5 wt%) were dissolved in toluene (2 mL). The reaction was degassed using five freeze, pump, thaw cycles and then filled with argon and sealed. The reaction mixture was heated to 90 °C and left stirring for 24 hours. After which the mixture was cooled to room temperature. The reaction mixture was added dropwise to methanol and the precipitate filtered to give poly(carvone acrylamide) as a white solid (94% conversion by ^{1}H NMR).

δ_H (400 MHz, CDCl$_3$) 7.01 (br, 12-H, 13-H$_2$), 3.10 (m, 1-H$_3$, 4-H$_2$, 6-H$_2$, 7-H), 1.69 (m, 5-H,), 1.31 (m, 9-H$_3$, 10-H$_3$).

Conditions	Conversion by 400 MHz ^{1}H NMR (%)	M$_n$ (kDa)	M$_p$ (kDa)	M$_w$ (kDa)	Polydispersity (Mw/Mn)	T$_g$ (°C)
0.25g monomer, ethanol, V88 0.5wt%	0	0	0	0	0	-
0.25g monomer, toluene, V88 0.5 wt%, 5uL DDM	94	10.7	8.7	11.3	1.057	132
20g monomer, pentanol, redox, TBPB 6wt%, ascorbic acid 3wt%	0	0	0	0	0	-
20g monomer, pentanol, redox TBPB 12 wt%, ascorbic acid 6wt%	0	0	0	0	0	-
1g monomer, ethanol, V88 0.5wt%	0	0	0	0	1.192	-
1g monomer, ethanol, AIBN 1wt%	67	14.2	14.6	19.9	1.396	-

6.4.1 Poly(2-methyl-*N*-(2-((1R)-4-methyl-2-oxocyclohexyl)propan-2-yl)butanamide) (148)
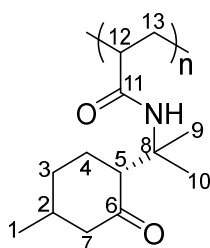
Pulegone acrylamide (1 g, 2.23 mmol) was dissolved in ethanol (2 mL). TBPB (10 mg, 1 wt%) was dissolved in toluene (1 mL) and added to the reaction mixture. The reaction was degassed using three freeze, pump, thaw cycles and then filled with argon and sealed. The reaction mixture was heated to 75 °C and left stirring for 24 hours. After which the mixture was cooled to room temperature. The reaction mixture was added dropwise to hexane and the precipitate filtered to give poly(pulegone acrylamide) as a yellow solid (96% conversion by ^{1}H NMR).

δ_H (400 MHz, CDCl$_3$) 6.73 (m, 12-H, 13-H$_2$), 2.30 (m, 1-H$_3$, 4-H$_2$, 6-H$_2$, 7-H) 1.88 (m, 2-H), 1.56 (m, 5-H, 9-H$_3$), 0.90 (m, 10-H$_3$).

Conditions	Conversion by 400 MHz ^{1}H NMR (%)	M_n (kDa)	M_p (kDa)	M_w (kDa)	Polydispersity (M_w/M_n)	T_g (°C)
0.25g monomer, THF, AIBN 0.5 wt%	>99	6.8	12	11.6	1.706	-
0.25g monomer, ethanol, AIBN 0.5wt%	-	0	0	0	0	-
20g monomer, redox 20hrs		35.5	62.9	70.5	1.987	-
0.5g monomer, ethanol, V88 0.5wt%	-	0.6	0.6	0.6	1.024	-
20g monomer, redox, 6hrs]		24.6	18.7	32.3	1.311	-
1g monomer, ethanol, AIBN 1wt%	86	14.1	17.4	20.2	1.431	-
1g monomer, ethanol, TBPB 1wt%	81	15.7	19	22.2	1.416	-
1g monomer, pentanol, V88 2wt%	92	5.5	8.8	10.4	1.906	-
1g monomer, ethanol, V88 2wt%	89	6.3	9.6	10.9	1.742	-
1g monomer, ethanol, V88	84	6.2	9.7	11.4	1.85	

1wt%						
1g monomer, ethanol, TBHP 1wt%		81	15.7	19.0	22.2	1.42	-
1g monomer, ethanol TBPB 2wt%		96	10.2	9.6	12.6	1.24	-
1g monomer, pentanol, TBPB 2wt%		99	6.9	7.2	9.3	1.34	91.6
20g monomer, pentanol, TBPB 6wt%, Ascorbic acid 3wt%, 50-85 °C, 30% active weight		-	24.6	18.7	32.3	1.311	-
20g monomer, pentanol, TBPB 6wt%, Ascorbic acid 3wt%, 40-85 °C, 30% active weight		-	35.5	62.9	70.5	1.99	-

7.0 References

(1)   Geyer, R.; Jambeck, J. R.; Law, K. L. *Sci. Adv.* **2017**, *3* (7), 25–29.

(2)   Thomsett, M. R.; Stockman, R. A.; Storr, T. E.; et al. *Green Mater.* **2016**, *4*, 115–134.

(3)   European Bioplastics nova-Institute. *Global production capacities of bioplastics 2018-2023 Bioplastics market data 2018*; **2018**.

(4)   New, T.; Economy, P.; The Ellen MacArthur Foundation. *Ellen MacArthur Found.* **2016**, 1–120.

(5)   Foundation, T. E. M.; The Ellen MacArthur Foundation. *Plastics-the facts 2017, An analysis of European plastics production, demand and waste data; 2017*; **2017**.

(6)   Zhu, Y.; Romain, C.; Williams, C. K. *Nature* **2016**, *540* (7633), 354–362.

(7)   Anastas, P. T.; Warner, J. C. *Green Chemistry: Theory and Practice*; Oxford University Press: New York, **1998**.

(8)   Erythropel, H. C.; Zimmerman, J. B.; De Winter, T. M.; et al. *Green Chemistry*. Royal Society of Chemistry **2018**, 1929–1961.

(9)   United Nations, United Nations 2030 Agenda for Sustainable Development, *United Nations* **2016**, 12–14.

(10)   Llevot, A.; Dannecker, P. K.; von Czapiewski, M.; et al. *Chem. - A Eur. J.* **2016**, *22*, 11510–11521.

(11)   Hillmyer, M. A. *Science (80-.).* **2017**, *358* (6365), 868–870.

(12)   Zhu, Y.; Romain, C.; Williams, C. K. *Nature* **2016**, *540* (7633), 354–362.

(13)   Miller, S. A. *ACS Macro Lett.* **2013**, *2* (6), 550–554.

(14)   McNaught, A. D.; Wilkinson, A. *Pure Appl. Chem.* **1996**, *68*, 2287–2311.

(15)   Fuss, R. W. (ISO). *Plastics -- Differential scanning calorimetry (DSC) -- Part 2: Determination of glass transition temperature and glass transition step height*; **2013**.

(16)   Fox, T. G.; Flory, P. J. *J. Appl. Phys.* **1950**, *21*, 581–591.

(17)Http://polymerdatabase.com/polymer%20chemistry/Chain%20versus%20Step%20Grow
       th.htmltle. Accessed 01/09/2020

(18)   Young, R. J. *Introduction to Polymers*; Chapman and Hall, **1987**.

(19)   Su, W.-F. In *Principles of Polymer Design and Synthesis*; Springer Berlin Heidelberg:
       Berlin, Heidelberg, **2013**; 137–183.

(20)   Gooch, J. W. *Encyclopedic Dictionary of Polymers*; Springer New York, **2011**.

(21)   Sahu, P.; Bhowmick, A. K. *Ind. Eng. Chem. Res.* **2019**, *58* (46), 20946–20960.

(22)   Chanadran, R. S.; Gallaway, G. Solution Polymerisation of Vinyl Monomers with Water
       Soluble Initiators in Substantially Non-Aqueous Media, **1998**.

(23)   Http://www.bpf.co.uk/plastipedia/polymers/polymer-bio-based-degradables.aspx.
       Accessed 01/09/2020.

(24)   Vert, M.; Doi, Y.; Hellwich, K.-H.; et al. *Pure Appl. Chem.* **2012**, *84* (2), 377–410.

(25)   marketsandmarkets.com. *Renewable Chemicals Market - Alcohols (Ethanol, Methanol), Biopolymers (Starch Blends, Regenerated Cellulose, PBS, Bio-PET, PLA, PHA, Bio-PE, and Others), Platform Chemicals & Others - Global Trends & Forecast to 2020*; **2015**.

(26)   *EU-Policy: Bioplastics in The Bio-Economy Ongoing Commercialization and Strong Political Support*; **2011**.

(27)   Future Market Insights. *Biopolymers Market: Global Industry Analysis and Opportunity Assessment 2017-2027*; **2017**.

(28)   Rudnik, E. In *Handbook of Biopolymers and Biodegradable Plastics: Properties, Processing and Applications*; **2012**.

(29)   Avérous, L. In *Handbook of Biopolymers and Biodegradable Plastics: Properties, Processing and Applications*; **2012**.

(30) Sin, L. T.; Rahmat, A. R.; Rahman, W. A. W. A. In *Handbook of Biopolymers and Biodegradable Plastics: Properties, Processing and Applications*; **2012**.

(31) Sin, L. T.; Rahmat, A. R.; Rahman, W. A. W. A. In *Handbook of Biopolymers and Biodegradable Plastics: Properties, Processing and Applications*; **2012**.

(32) Jiang, L.; Zhang, J. In *Handbook of Biopolymers and Biodegradable Plastics: Properties, Processing and Applications*; Elsevier Inc., **2013**; 109–128.

(33) Yao, K.; Tang, C. *Macromolecules* **2013**, *46*, 1689–1712.

(34) Breitmaier, E. *Terpenes: Flavors, Fragrances, Pharmaca, Pheromones*; **2006**.

(35) Gusevskaya, E. V. *ChemCatChem,* **2014**, *6*, 1506-1515.

(36) Wilbon, P. A.; Chu, F.; Tang, C. *Macromol. Rapid Commun.* **2013**, *34*, 8–37.

(37) Kamani, M. H.; Eş, I.; Lorenzo, J. M.; et al. *Green Chem.* **2019**, *21* (12), 3213–3231.

(38) Gandini, A.; Lacerda, T. M. *Progress in Polymer Science*. **2015,** *48*, 1-39.

(39) Mewalal, R.; Rai, D. K.; Kainer, D.; et al. *Trends Biotechnol.* **2017**, *35* (3), 227–240.

(40) Roberts, W. J.; Day, A. R. *J. Am. Chem. Soceity* **1950**, *72* (3), 1226–1230.

(41) Keszler, B.; Kennedy, J. P. In *Macromolecules: Synthesis, Order and Advanced Properties. Advances in Polymer Science*; Springer-Verlag, **1992**; 1–9.

(42) Satoh, K.; Sugiyama, H.; Kamigaito, M. *Green Chem.* **2006**, *8* (10), 878–882.

(43) Kukhta, N. A.; Vasilenko, I. V.; Kostjuk, S. V. *Green Chem.* **2011**, *13* (9), 2362–2364.

(44) Sarkar, P.; Bhowmick, A. K. *RSC Adv.* **2014**, *4* (106), 61343–61354.

(45) Holmberg, A. L.; Reno, K. H.; Wool, R. P.; et al. *Soft Matter* **2014**, *10* (38), 7405–7424.

(46) Lu, J.; Liang, H.; Li, A.; et al. *Eur. Polym. J.* **2004**, *40* (2), 397–402.

(47) Liang, H.; Lu, J. *J. Appl. Polym. Sci.* **2000**, *75* (5), 599–603.

(48) Li, A. L.; Wang, X. Y.; Liang, H.; et al. *React. Funct. Polym.* **2007**, *67* (5), 481–488.

(49)   Wang, Y.; Li, A. L.; Liang, H.; et al. *Eur. Polym. J.* **2006**, *42* (10), 2695–2702.

(50)   Sarkar, P.; Bhowmick, A. K. *ACS Sustain. Chem. Eng.* **2016**, *4* (4), 2129–2141.

(51)   Sarkar, P.; Bhowmick, A. K.; Bhowmick, A. K. *J. Polym. Sci., Part A Polym. Chem* **2017**, *55*, 2639–2649.

(52)   Thomsett, M. R.; Moore, J. C.; Buchard, A.; et al. *Green Chem.* **2019**, *21* (1), 149–156.

(53)   Winnacker, M.; Rieger, B. *ChemSusChem* **2015**, *8*, 2455–2471.

(54)   Gandini, A.; Lacerda, T. M. *Prog. Polym. Sci.* **2015**, *48*, 1–39.

(55)   Byrne, C. M.; Allen, S. D.; Lobkovsky, E. B.; et al. *J. Am. Chem. Soc.* **2004**, *126* (37), 11404–11405.

(56)   Hauenstein, O.; Agarwal, S.; Greiner, A. *Nat. Commun.* **2016**, *7*, 1–7.

(57)   Lowe, J. R.; Martello, M. T.; Tolman, W. B.; et al. *Polym. Chem.* **2011**, *2*, 702–708.

(58)   De Carvalho, C. C. C. R.; Da Fonseca, M. M. R. *Food Chem.* **2006**, *95* (3), 413–422.

(59)   Knight, S. C.; Schaller, C. P.; Tolman, W. B.; et al. *RSC Adv.* **2013**, *3*, 20399–20404.

(60)   Quilter, H. C.; Hutchby, M.; Davidson, M. G.; et al. *Polym. Chem.* **2017**, *8* (5), 833–837.

(61)   Winnacker, M.; Vagin, S.; Auer, V.; et al. *Macromol. Chem. Phys.* **2014**, *215*, 1654–1660.

(62)   Winnacker, M.; Sag, J. *Chem. Commun.* **2018**, *54*, 841–844.

(63)   Stockmann, P. N.; Pastoetter, D. L.; Woelbing, M.; et al. *Macromol. Rapid Commun.* **2019**, *1800903*, 1800903.

(64)   Firdaus, M.; Montero De Espinosa, L.; Meier, M. A. R. *Macromolecules* **2011**, *44*, 7253–7262.

(65)   Firdaus, M.; Meier, M. A. R. *Green Chem.* **2013**, *15* (2), 370–381.

(66)   Stockman, R.; Avery, S.; Alexander, C.; et al. *J. Mater. Chem. B* **2019**, *7*, 5222–5229.

(67)   Sainz, M. F.; Souto, J. A.; Regentova, D.; et al. *Polym. Chem.* **2016**, *7*, 2882–2887.

(68)   Lima, M. S.; Costa, C. S. M. F.; Coelho, J. F. J.; et al. *Green Chem.* **2018**, *20* (21), 4880–4890.

(69)   Stamm, A.; Tengdelius, M.; Schmidt, B.; et al. *Green Chem.* **2019**, *21* (10), 2720–2731.

(70)   Stamm, A.; Tengdelius, M.; Schmidt, B.; et al. *Green Chem.* **2019**, *21* (10), 2720–2731.

(71)   Droesbeke, M. A.; Du Prez, F. E. *ACS Sustain. Chem. Eng.,* **2019,** *7,* 11633–11639.

(72)   Owen, A. T.; Fawell, P. D.; Swift, J. D.; et al. *Int. J. Miner. Process.* **2002**, *67* (1–4), 123–144.

(73)   Lee, H. K.; Jong, W. L. *Journal of Polymer Research*. 1997, *4* (2), 119–128.

(74)   Xiong, B.; Loss, R. D.; Shields, D.; et al. *npj Clean Water* **2018**, *17,* 1-9.

(75)   Mohsin, M., Poster, Polyacrylamide for wastewater treatment, **2016**.

(76)   Bajpai, A. K.; Shukla, S. K.; Bhanu, S.; et al. *Prog. Polym. Sci.* **2008**, *33*, 1088–1118.

(77)   Ward, M. A.; Georgiou, T. K. *Polymers (Basel).* **2011**, *3*, 1215–1243.

(78)   Miller, D. J.; Dreyer, D. R.; Bielawski, C. W.; et al. **2017**, *564*, 662–4711.

(79)   Sabhapondit, A.; Borthakur, A.; Haque, I. *J. Appl. Polym. Sci.* **2003**, *87* (12), 1869–1878.

(80)   Sigma-Aldrich. Polymer Properties Thermal Transitions of Homopolymers: Tg and MP https://www3.nd.edu/~hgao/thermal_transitions_of_homopolymers.pdf.

(81)   Nguyen, H. T. H.; Qi, P.; Rostagno, M.; et al. *Journal of Materials Chemistry A*, **2018**, *6*, 9298–93311.

(82)   Marcincinova Benadillah, K.; Boustta, M.; Coudane, J.; et al. *Can the glass transition temperature of PLA polymers be increased?*, 764th ed.; Scholz, C., Gross, R. A., Eds.; ACS Symposium Series: Polymers from Renewable Resources: Biopolyesters and Biocatalysis, **2000**.

272

(83) Singha, N. R.; Mahapatra, M.; Karmakar, M.; et al. *Polym. Chem.* **2017**, *8* (44), 6750–6777.

(84) Kai, D.; Tan, M. J.; Chee, P. L.; et al. *Green Chem.* **2016**, *18* (5), 1175–1200.

(85) Liu, H.; Chung, H. *J. Polym. Sci. Part A Polym. Chem.* **2017**, *55* (21), 3515–3528.

(86) Cui, G.; Wang, X.; Xun, J.; et al. *Int. Biodeterior. Biodegrad.* **2017**, *123*, 269–275.

(87) Hufendiek, A.; Trouillet, V.; Meier, M. A. R.; et al. *Biomacromolecules* **2014**, *15* (7), 2563–2572.

(88) Sen, G.; Mishra, S.; Prasad Dey, K.; et al. *J. Appl. Polym. Sci.* **2014**, *131* (22), 1–9.

(89) Nishida, J.; Kobayashi, M.; Takahara, A. *J. Polym. Sci. Part A Polym. Chem.* **2013**, *51* (5), 1058–1065.

(90) Yang, J.; Bos, I.; Pranger, W.; et al. *J. Mater. Chem. A* **2016**, *4* (18), 6868–6877.

(91) Lamping, S.; Otremba, T.; Ravoo, B. J. *Angew. Chemie - Int. Ed.* **2018**, *57* (9), 2474–2478.

(92) Gang, F.; Yan, H.; Ma, C.; et al. *Chem. Commun.* **2019**, *55* (66), 9801–9804.

(93) Kim, M.; Chung, H. *Polym. Chem.* **2017**, *8* (40), 6300–6308.

(94) Li, J.; Zhang, Y.; Cai, C.; et al. *Biomater. Sci.* **2020**, *8* (1), 189–200.

(95) Liu, H.; Lepoittevin, B.; Roddier, C.; et al. *Polymer (Guildf).* **2011**, *52* (9), 1908–1916.

(96) Croda International Plc. *Croda Sustainability Report 2019*; **2019**.

(97) Overman, L. E. *J. Am. Chem. Soceity* **1974**, *96* (2), 597–599.

(98) Ritter, J. J.; Minieri, P. P. *J. Am. Chem. Soc.* **1948**, *70* (12), 4045–4048.

(99) Constable, D. J. C.; Dunn, P. J.; Hayler, J. D.; et al. *Green Chem.* **2007**, *9*, 411–420.

(100) Bryan, M. C.; Dunn, P. J.; Entwistle, D.; et al. *Green Chem.* **2018**, *20* (22), 5082–5103.

(101) Overman ', L. E. *J. Am. Chem. Soceity* **1976**, *98* (10), 2901–2910.

273

(102) Valeev, R. F.; Vostrikov, N. S.; Miftakhov, M. S. *ISSN Russ. J. Org. Chem. Zhurnal Org. Khimii* **2009**, *45* (6), 1070–4280.

(103) Csillag, K.; Németh, L.; Martinek, T. A.; et al. *Tetrahedron Asymmetry* **2012**, *23*, 144–150.

(104) Sabatini, M. T.; Boulton, L. T.; Sneddon, H. F.; et al. *Nat. Catal.* **2019**, *2* (1), 10–17.

(105) Hajjaj, B.; Shah, A.; Bell, S.; et al. *Synlett* **2016**, *27* (16), 2357–2361.

(106) Kurth, M. J.; Decker, O. H. W. **1985**, *3*, 5769–5775.

(107) Dangerfield, E. M.; Plunkett, C. H.; Win-Mason, A. L.; et al. *J. Org. Chem.* **2010**, *75* (16), 5470–5477.

(108) Green, A. P.; Turner, N. J.; O'Reilly, E. *Angew. Chemie - Int. Ed.* **2014**, *53* (40), 10714–10717.

(109) Jiménez-González, C.; Poechlauer, P.; Broxterman, Q. B.; et al. *Org. Process Res. Dev.* **2011**, *15* (4), 900–911.

(110) Gavrilescu, M.; Chisti, Y. *Biotechnol. Adv.* **2005**, *23* (7–8), 471–499.

(111) Schmid, A.; Hollmann, F.; Park, J. B.; et al. *Curr. Opin. Biotechnol.* **2002**, *13* (4), 359–366.

(112) Plaut, H.; Ritter, J. J.; Plaut, H. *J. Am. Chem. Soc* **1951**, *73* (9), 4076–4077.

(113) Guérinot, A.; Reymond, S.; Cossy, J. *European J. Org. Chem.* **2012**, *2012* (1), 19–28.

(114) Jiang, D.; He, T.; Ma, L.; et al. *RSC Adv.* **2014**, *4*, 64936–64946.

(115) Shakeri, M.-S.; Tajik, H.; Niknam, K. *J. Chem. Sci. Indian Acad. Sci.* **2012**, *124* (5), 1025–1032.

(116) Leiva, R.; Gazzarrini, S.; Esplugas, R.; et al. *Tetrahedron Lett.* **2015**, *56* (10), 1272–1275.

(117) Findik, S.; Gündüz, G. *J. Am. Oil Chem. Soc.* **1997**, *74* (9), 1145–1151.

274

(118) Wagner, G. *J. Russ. Phys. Chem. Soc.* **1899**, *31*, 690.

(119) Birladeanu, L. *J. Chem. Educ.* **2000**, *77* (7), 858.

(120) Meerwein, H. *Justus Liebig's Ann. der Chemie* **1914**, *405* (2), 129–175.

(121) Bishop, R. In *Comprehensive Organic Synthesis: Second Edition*; **2014**.

(122) Hanzawa, Y.; Kasashima, Y.; Tomono, K.; et al. *J. Oleo Sci.* **2012**, *61* (12), 715–721.

(123) Posevins, D.; Suta, K.; Turks, M. *European J. Org. Chem.* **2016**, *2016* (7), 1414–1419.

(124) Shifa, W.; Xincheng, Z.; Yu, T.; Yiqin Y.; Xu, X. Wen, G.; Yuxun, Z.; Haiyan, Y. Haochuang, L.; China, **2019**, CN109810011A.

(125) Schleyer, P. V. R.; Mainz, V. V; Strom, E. T. *Norbornyl Cation Isomers Still Fascinate*; American Chemical Soceity, **2015**.

(126) Das, B.; Majhi, A.; Banerjee, J.; et al. *J. Mol. Catal. A Chem.* **2006**, *260* (1–2), 32–34.

(127) Mokhtary, M.; Goodarzi, G. *Chinese Chem. Lett.* **2012**, *23* (3), 293–296.

(128) Thomsett, M. R.; Moore, J.; Monaghan, O. R.; et al. *Private Communication*.

(129) Xu, Z. B.; Qu, J. *Chem. - A Eur. J.* **2013**, *19* (1), 314–323.

(130) Bleier, D. B.; Elrod, M. J. *J. Phys. Chem. A* **2013**, *117* (20), 4223–4232.

(131) Costa, V. V.; Da Silva Rocha, K. A.; De Sousa, L. F.; et al. *J. Mol. Catal. A Chem.* **2011**.

(132) Rothenberg, G.; Yatziv, Y.; Sasson, Y. *Tetrahedron* **1998**, *54*, 593–598.

(133) Da Silva Rocha, K. A.; Hoehne, J. L.; Gusevskaya, E. V. *Chem. - A Eur. J.* **2008**, *14* (20), 6166–6172.

(134) Yaragorla, S.; Singh, G.; Lal Saini, P.; et al. *Tetrahedron Lett.* **2014**, *55* (33), 4657–4660.

(135) Da Silva Rocha, K. A.; Hoehne, J. L.; Gusevskaya, E. V. *Chem. - A Eur. J.* **2008**.

(136) Tundo, P.; Selva, M. *Acc. Chem. Res.* **2002**, *35* (9), 706–716.

(137) HMDB. Dimethyl Carbonate Data https://hmdb.ca/metabolites/HMDB0059844.

275

Accessed 01/09/2020.

(138) Nair, V.; Rajan, R.; Balagopal, L.; et al. *Tetrahedron Lett.* **2002**, *43* (49), 8971–8974.

(139) Kozlov, N. G.; Basalaeva, L. I.; Atazhanova, G. A.; et al. *Chem. Nat. Compd.* **2015**, *51* (3), 488–490.

(140) Alvès, M. H.; Sfeir, H.; Tranchant, J. F.; et al. *Biomacromolecules* **2014**, *15* (1), 242–251.

(141) Pojman, J. A.; Nagy, I. P.; Salterns, C. *J. Am Chem. Soc.* **1993**, *115* (23), 11044–11045.

(142) Asanuma, H.; Hishiya, T.; Ban, T.; et al. *J. Chem. Soc. Perkin Trans. 2* **1998**, 9, 1915–1918.

(143) Pojman, J. A.; Curtis, G.; Ilyashenko, V. M. **1996**, 3783–3784.

(144) Zhang, X.; Wang, X.; Li, L.; et al. *J. Appl. Polym. Sci.* **2015**, *132* (24), 1–7.

(145) Heskins, M.; Guillet, J. E. *J. Macromol. Sci. Part A -Chemistry J. MACROMOL. SC1.-CHEM* **1968**, *28* (8), 1441–1455.

(146) Dohi, H.; Nishida, Y.; Mizuno, M.; et al. **1999**, *7*, 2053–2062.

(147) Lloyd, D. J.; Nikolaou, V.; Collins, J.; et al. *Chem. Commun. (Camb).* **2016**, *52* (39), 6533–6536.

(148) Graillat, C.; Pichot, C.; Guyot, A.; et al. *J. Polym. Sci. Part A Polym. Chem.* **1986**, *24* (3), 427–449.

(149) Benda, D.; Republic, C.; Swparek, J. *Science (80-.).* **1997**, *33* (8), 1345–1352.

(150) Hernández-Barajas, J.; Hunkeler, D. J. *Polymer (Guildf).* **1997**, *38* (2), 437–447.

(151) Candau, F.; Leong, Y. S.; Fitch, R. M. *J. Polym. Sci.* **1985**, *23*, 193–214.

(152) Abdollahi, Z.; Gomes, V. *Chemeca Conf.* **2011**, Synthesis and Characterization of Polyacrylamide with Molar Structure. *Chemeca Conf.*, presentation.

(153) Newkirk, A. E., *J. Am. Chem. Soc.*, **1946**, *68*, 2467–2471.

(154) Hansen, C. M. *Hansen Solubility Parameters*; CRC Press, **2007**.

(155) Vinod Babu, V. B. M.; Madhu Murthy, M. M. K.; Amba Prasad Rao, G. *Renew. Sustain. Energy Rev.* **2017**, *78* (May), 1068–1088.

(156) Chmela, Š.; Fiedlerová, A.; Liptaj, T.; et al. *E-Polymers* **2018**, *18* (3), 205–216.

(157) Zhang, Y.; Han, L.; Ma, H.; et al. *Polymer (Guildf).* **2019**, *169* (February), 95–105.

(158) Fischer, E. J.; Storti, G.; Cuccato, D. *Processes,* **2017**, *5* (2), 23.

(159) Jašo, V.; Radičević, R.; Stoiljković, D. *J. Therm. Anal. Calorim.* **2010**, *101* (3), 1059–1063.

(160) Castagnet, T.; Aguirre, G.; Asua, J. M.; et al. *ACS Sustain. Chem. Eng.* **2020**, *8* (19), 7503–7512.

(161) Zhang, L.; Marsiglio, J. A.; Lan, T.; Torkelson, J. M., *Macromolecules,* **2016**, *49*, 2387–2398.

(162) Temperature, T. G. **2000**, 315–319.

(163) Fox, T. G.; Flory, P. J. *Journal of Applied Physics*, **1950,** *21*, 581-591.

(164) Huang, Y.; Liu, Y.; Muhammad, S.; et al. *React. Funct. Polym.* **2020**, *151*, 104566.

(165) Gibbs, J. H., *J. Chem Phys.*, **1956**, 2*5*, 185–186.

(166) Gibbs, J. H.; Dimarzio, E. A., *J. Chem Phys.*, **1958**, *28*, *373*-383

(167) Karplus, M.; Grant, M.; Carolina, N., *J. Polymer Sci.*, **1962**, *62*, 151–155.

(168) Pezzin, G.; Marghera, P. *European Polymer Journal*, **1970**, *6*, 1053-1061

(169) Van Der Sman, R. G. M. *J. Phys. Chem. B* **2013**, *117* (50), 16303–16313.

(170) Haaf, F.; Sanner, A.; Straub, F. *Polymer Journal*. **1985**, *17*, 143–152.

(171) Teodorescu, M.; Bercea, M. *Polym. - Plast. Technol. Eng.* **2015**, *54* (9), 923–943.

(172) Bae, C.; Hartwig, J. F.; Boaen Harris, N. K.; et al. *J. Am. Chem. Soc.* **2005**, *127* (2), 767–776.

277

(173) Larsen, M. B.; Wang, S. J.; Hillmyer, M. A. *J. Am. Chem. Soc.* **2018**, *140* (38), 11911–11915.

(174) Tobias, M.A., United States Patent [426,529]. **1983**.

(175) Shokal, E. C.; Devlin, P. A. US2940946A - Ally alcohol-vinyl aromatic copolymers, **1960**.

(176) Sundararajan, S.; Samui, A. B.; Kulkarni, P. S. *React. Funct. Polym.* **2018**, *130* (April), 43–50.

(177) Raffa, P.; Broekhuis, A. A.; Picchioni, F. *J. Appl. Polym. Sci.* **2016**, *133* (42), 1–8.

(178) Lutz, J. F. *J. Polym. Sci. Part A Polym. Chem.* **2008**, *46* (11), 3459–3470.

(179) Sabatini, V.; Pargoletti, E.; Longoni, M.; et al. *Appl. Surf. Sci.* **2019**, *488* (May), 213–220.

(180) Ahmed, M. R.; Mohammed, A. H. A.-K.; A.hamad, M. *IOSR J. Appl. Chem.* **2017**, *10* (04), 50–58.

(181) Jukic, A.; Vidovic, E.; Janovic, Z. *Chem. Technol. Fuels Oils* **2007**, *43* (5), 386–394.

(182) Kohut-Svelko, N.; Pirri, R.; Asua, J. M.; et al. *J. Polym. Sci. Part A Polym. Chem.* **2009**, *47* (11), 2917–2927.

(183) Back, A. J.; Schork, F. J. *J. Appl. Polym. Sci.* **2007**, *103* (2), 819–833.

(184) Guezennec, A.-G.; Michel, C.; Bru, K.; et al. *Research* **2015**, *22* (9), 6390-6406.

(185) Gandhi, A.; Paul, A.; Sen, S. O.; et al. *Asian J. Pharm. Sci.* **2015**, *10* (2), 99–107.

(186) Patil, N.; Jérôme, C.; Detrembleur, C. *Prog. Polym. Sci.* **2018**, *82*, 34–91.

(187) Stephanou, P. S.; Tsimouri, I. C.; Mavrantzas, V. G. *Macromolecules,* **2016**, *49*, 3161–3173.

(188) Wong, V. W.; Tung, S. C., *Friction*, **2016**, *4*, 1–28.

(189) Haycock, R. F.; Caines, A. J.; Hiller, J. *Automotive Lubricants Reference Book*, Third Edit.; Society of Automotive Engineers, **2014**.

278

(190) Sivokhin, A. P.; Kazantsev, O. A.; Shirshin, K. V.; et al. *Int. Polym. Sci. Technol.* **2015**, *43* (10), 11–16.

(191) Julian, D.; Mahdi, S. *Adv. Colloid Interface Sci.* **2018**, *251*, 55–79.

(192) Sigma-Aldrich. Analysis Matches Commercially Available Material.

(193) Bleier, D. B.; Elrod, M. J. Supporting Information, *J. Phys. Chem. A*, **2013**, *117*, 4223–4232.

8.0 Single Crystal Xray Diffraction Data and Refinement

Crystal Data	108	123
Formula	$C_{13}H_{21}NO$	$C_{13}H_{19}NO$
Formula Weight	207.31	205.29
Temperature/K	120(2)	120(2)
Crystal System	orthorhombic	monoclinic
Space Group	Pbca	$P2_1/n$
a	10.52509(17) Å	15.12366(18) Å
b	9.76026(13) Å	9.18216(8) Å
c	23.8446(4) Å	19.1357(2) Å
α	90°	90°
β	90°	112.8726(13)°
γ	90°	90°
v	2449.50(6)$Å^3$	2448.39(5)$Å^3$
Z	8	8
P_{calc}	1.124g/cm^3	1.114g/cm^3
μ	0.542/mm^{-1}	0.542/mm^{-1}
F	912.0	896.0
Crystal Size	0.475x0.114x0.053mm^3	0.245x0.055x0.04 mm^3
Diffractometre	SuperNova	SuperNova
Radiation	CuKα (λ=1.54184)	CuKα (λ=1.54184)
2θ (min - max)	7.414 to 149.22°	9.498 to 155.184°
Index ranges	-13≤h≤12,-12≤k≤12, -29≤l≤29	-19≤h≤19,-11≤k≤11, -24≤l≤24
Reflections collected	27623	79087
Independent reflections	2490 [R_{int}=0.0270, R_{sigma}=0.0101]	5157 [R_{int}=0.0586, R_{sigma}=0.0170]
Refinement method	Full-matrix least squares on F^2	Full-matrix least squares on F^2
Data/restraints/parameters	2490/0/142	5157/0/282
Goodness-of-fit on F^2	1.044	1.114

Final R indexes [I>=2σ(I)]	R_1=0.0494, wR_2=0.1301	R_1=0.0413, wR_2=0.1119
Final R indexes [all data]	R_1=0.0520, wR_2=0.1330	R_1=0.0444, wR_2=0.1153
Largest diff. peak/hole	0.45/-0.22 e$Å^{-3}$	0.21/-0.18 e$Å^{-3}$

Crystal Data	**53**	**121**
Formula	$C_{13}H_{21}O_2$	$C_{13}H_{21}NO_2$
Formula Weight	170.24	223.31
Temperature/K	120(2)	293(2)
Crystal System	monoclinic	monoclinic
Space Group	C2	P2$_1$/n
a	18.7679(3) Å	14.87130(10)Å
b	7.92820(10) Å	11.40500(10)Å
c	6.60160(10) Å	15.5355(2) Å
α	90°	90°
β	97.2010(10)°	96.7100(10)°
γ	90°	90°
v	974.54(2)$Å^3$	2616.88(4)$Å^3$
Z	5	9
P_{calc}	1.450g/cm^3	1.027g/cm^3
μ	0.779/mm^{-1}	0.596/mm^{-1}
F	470.0	809.0
Crystal Size	0.260x0.133x0.123mm^3	0.604x0.333x0.110mm^3
Diffractometre	SuperNova	SuperNova
Radiation	CuKα (λ=1.54184)	CuKα (λ=1.54184)
2θ (min - max)	9.5 to 144.656°	7.788 to 144.848°
Index ranges	-22≤h≤23,-9≤k≤9, -8≤l≤8	-18≤h≤17,-14≤k≤13, -18≤l≤19
Reflections collected	17073	20180
Independent reflections	1912 [R_{int}=0.0342, R_{sigma}=0.0153]	5130 [R_{int}=0.0186, R_{sigma}=0.0158]
Refinement method	Full-matrix least squares on	Full-matrix least squares on F^2

	F^2	
Data/restraints/parameters	1912/1/114	5130/0/297
Goodness-of-fit on F^2	1.117	1.067
Final R indexes [I>=2σ(I)]	R$_1$=0.0341, wR$_2$=0.0975	R$_1$=0.0454, wR$_2$=0.1379
Final R indexes [all data]	R$_1$=0.0345, wR$_2$=0.0980	R$_1$=0.0486, wR$_2$=0.1415
Largest diff. peak/hole	0.44/-0.30 eÅ^{-3}	0.80/-0.23 eÅ^{-3}

Crystal Data	**131**	**136**
Formula	C$_{13}$H$_{19}$NO$_2$	C$_{13}$H$_{21}$NO$_2$
Formula Weight	221.29	223.21
Temperature/K	120(10)	293(2)
Crystal System	monoclinic	monoclinic
Space Group	P2$_1$	P2$_1$
a	6.50000(10)Å	9.67210(10)Å
b	20.9029(2)Å	13.5074(2)Å
c	9.32210(10)Å	10.49440(10)Å
α	90°	90°
β	105.2620(10)°	104.2650(10)°
γ	90°	90°
v	1221.9(3)Å^3	1328.77(3)Å^3
Z	4	5
P$_{calc}$	1.203g/cm^3	1.396g/cm^3
μ	0.642/mm^{-1}	0.739/mm^{-1}
F	480.0	610.0
Crystal Size	0.427x0.147x0.065mm^3	0.689x0.260x0.113 mm^3
Diffractometre	SuperNova	SuperNova
Radiation	CuKα (λ=1.54184)	CuKα (λ=1.54184)
2θ (min - max)	8.46 to 144.67°	8.694 to 145.56°
Index ranges	-8≤h≤7,-25≤k≤25, -9≤l≤11	-11≤h≤10,-16≤k≤16, -13≤l≤13
Reflections collected	22662	19748

Independent reflections	4738 [R_{int}=0.0318, R_{sigma}=0.0235]	5187 [R_{int}=0.0312, R_{sigma}=0.0222]
Refinement method	Full-matrix least squares on F^2	Full-matrix least squares on F^2
Data/restraints/parameters	4738/1/311	5187/1/311
Goodness-of-fit on F^2	1.037	1.048
Final R indexes [I>=2σ(I)]	R_1=0.0302, wR_2=0.0793	R_1=0.0428, wR_2=0.1295
Final R indexes [all data]	R_1=0.0317, wR_2=0.0807	R_1=0.0434, wR_2=0.1305
Largest diff. peak/hole	0.24/-0.16 e$Å^{-3}$	0.39/-0.26 e$Å^{-3}$